

Neutrino-nucleus cross sections

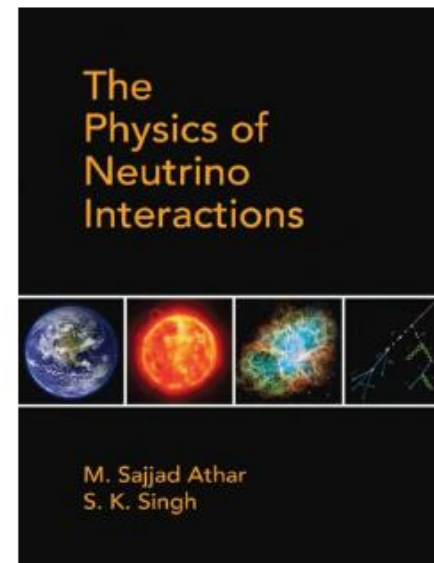
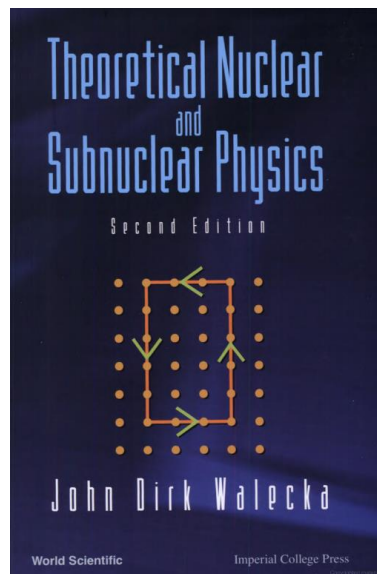
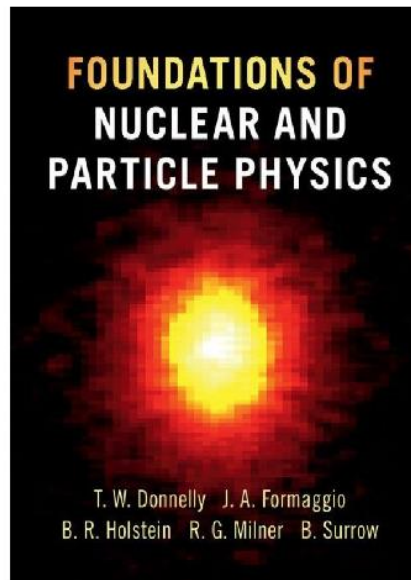
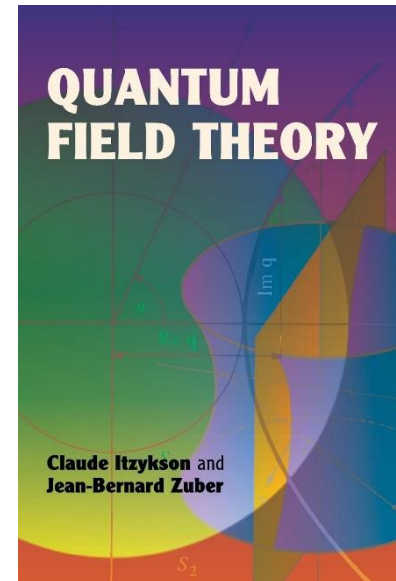
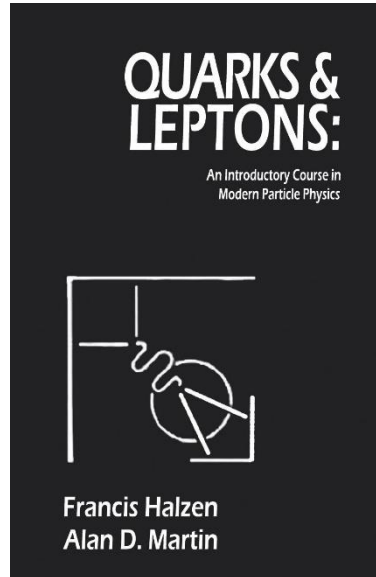
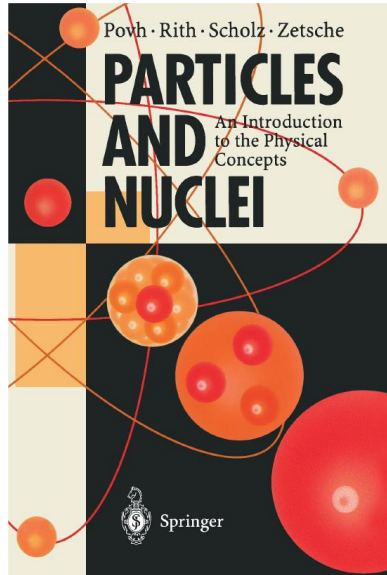
Marco Martini



Neutrino-nucleus cross sections -- Plan

- First lecture: generalities (theory and experiment)
- Second lecture: results and perspectives

Some Books



Some Review papers

[1305.7513.pdf \(arxiv.org\)](#)

REVIEWS OF MODERN PHYSICS, VOLUME 84, JULY–SEPTEMBER 2012

From eV to EeV: Neutrino cross sections across energy scales

J. A. Formaggio*

Laboratory for Nuclear Science Massachusetts Institute of Technology, Cambridge, Massachusetts 02139, USA

G. P. Zeller†

Fermi National Accelerator Laboratory, Batavia, Illinois 60510, USA

[1611.07770.pdf \(arxiv.org\)](#)

IOP Publishing

Journal of Physics G: Nuclear and Particle Physics

J. Phys. G: Nucl. Part. Phys. **45** (2018) 013001 (98pp)

<https://doi.org/10.1088/1361-6471/aa8bf7>

Topical Review

Neutrino–nucleus cross sections for oscillation experiments

Tepei Katori^{1,4,5} and Marco Martini^{2,3,4,5}

¹ School of Physics and Astronomy, Queen Mary University of London, London, United Kingdom

² ESNT, CEA, IRFU, Service de Physique Nucléaire, Université de Paris-Saclay, F-91191 Gif-sur-Yvette, France

³ Department of Physics and Astronomy, Ghent University, Proeftuinstraat 86, B-9000 Gent, Belgium

[1706.03621.pdf \(arxiv.org\)](#)

Progress in Particle and Nuclear Physics 100 (2018) 1–68



ELSEVIER

Contents lists available at ScienceDirect

Progress in Particle and Nuclear Physics

journal homepage: www.elsevier.com/locate/ppnp



Review

NuSTEC¹ White Paper: Status and challenges of neutrino–nucleus scattering

L. Alvarez-Ruso^a, M. Sajjad Athar^b, M.B. Barbaro^c, D. Cherdack^d, M.E. Christy^e, P. Coloma^f, T.W. Donnelly^g, S. Dytman^h, A. de Gouvêaⁱ, R.J. Hill^{j,f}, P. Huber^k, N. Jachowicz^l, T. Katori^m, A.S. Kronfeld^f, K. Mahnⁿ, M. Martini^o, J.G. Morfin^{f,*}, J. Nieves^a, G.N. Perdue^f, R. Petti^p, D.G. Richards^q, F. Sánchez^r, T. Sato^{s,t}, J.T. Sobczyk^u, G.P. Zeller^f



[2206.13792.pdf \(arxiv.org\)](#)

Neutrinos and their interactions with matter

M. Sajjad Athar^{a,*}, A. Fatima^a, S. K. Singh^a

^aDepartment of Physics, Aligarh Muslim University, Aligarh - 202002, India

Appetizer: Neutrino (interactions) (pre)history

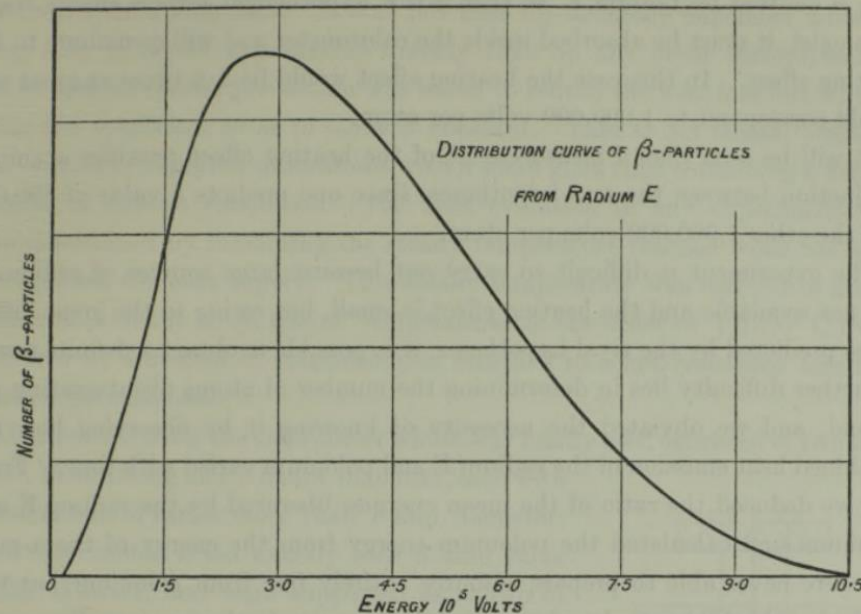
Nuclear Beta Decay

Electron energy spectrum in Nuclear Beta Decay is continuous (*J. Chadwick 1914*)

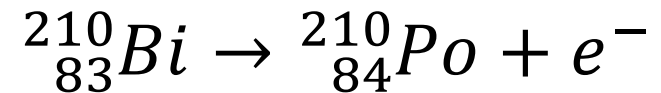
C. D. Ellis and W. A. Wooster (1927)

Average Energy of Disintegration of Radium E. 111

of the other atoms present, we conclude that the energy of disintegration is not a fixed characteristic quantity. To take the extreme cases, there are a few



[Historical papers \(in2p3.fr\)](http://in2p3.fr)




Two-body final state

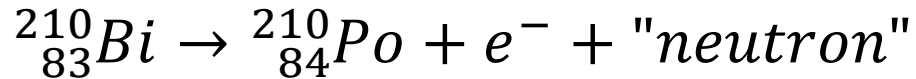


Electron should have a unique energy value

Puzzle

Niels Bohr  questioned the strict validity of energy conservation in subatomic processes

4 December 1930: Neutrino birth – W. Pauli letter



Original - Photocopy of PLC 0393
Abschrift/15.12.30 FM

Offener Brief an die Gruppe der Radioaktiven bei der
Gauvereins-Tagung zu Tübingen.

Abschrift

Physikalisches Institut
der Eidg. Technischen Hochschule
Zürich

Zürich, 4. Des. 1930
Gloriastrasse

Liebe Radioaktive Damen und Herren,

Wie der Ueberbringer dieser Zeilen, den ich halbvöllig
ansuhören bitte, Ihnen des näheren auseinandersetzen wird, bin ich
angesichts der "falschen" Statistik der N- und Li-6 Kerne, sowie
des kontinuierlichen beta-Spektrums auf einen verwerflichen Ausweg
verfallen um den "Wechselgats" (1) der Statistik und dem Energiesatz
zu retten. Nämlich die Möglichkeit, es könnten elektrisch neutrale
Teilchen, die ich Neutronen nennen will, in den Kernen existieren,
welche den Spin 1/2 haben und das Ausschliessungsprinzip befolgen und
sich mit Lichtgeschwindigkeit laufen. Die Masse der Neutronen
müsste von derselben Grössenordnung wie die Elektronenmasse sein und
jedenfalls nicht grösser als 0,01 Protonenmasse. Das kontinuierliche
beta-Spektrum wäre dann verständlich unter der Annahme, dass beim
beta-Zerfall mit dem Elektron jeweils noch ein Neutron existiert
würde, dertart, dass die Summe der Energien von Neutron und Elektron
konstant ist.

Man handelt es sich weiter darum, welche Kräfte auf die
Neutronen wirken. Das wahrscheinlichste Modell für das Neutron scheint
mir aus wellenmechanischen Gründen (näheres wies der Ueberbringer
dieser Zeilen) dieses zu sein, dass das ruhende Neutron ein
magnetischer Dipol von einem gewissen Moment μ ist. Die Experimente
verlören wohl, dass die ionisierende Wirkung eines solchen Neutrons
nicht grösser sein kann, als die eines gamma-Strahls und darf dann
 μ wohl nicht grösser sein als $e \cdot (10^{-13} \text{ cm})$.

Ich traue mich vorläufig, aber nicht, etwas über diese Idee
zu publizieren und wende mich erst vertrauensvoll an Euch, liebe
Radioaktive, mit der Frage, wie es um den experimentellen Nachweis
eines solchen Neutrons stünde, wenn dieses ein ebensolches oder etwa
kmal grösseres Durchdringungsvermögen besätsen würde, wie ein
gamma-Strahl.

Ich gebe zu, dass mein Ausweg vielleicht von vornherein
wenig wahrscheinlich erscheinen wird, weil man die Neutronen, wenn
sie existieren, wohl schon längst gesehen hätte. Aber nur wer wagt,
gemusst und der Ernst der Situation beim kontinuierliche beta-Spektrum
wird durch einen Ausspruch meines verstorbenen Vorgängers im Amt,
Herrn Debye, beleuchtet, der mir kürzlich in Brüssel gesagt hat:
"O, daran soll man am besten gar nicht denken, sowie an die neuen
Steuern." Darum soll man jeden Weg zur Rettung ernstlich diskutieren.-
Also, liebe Radioaktive, prüfet, und richtet.- Leider kann ich nicht
persönlich in Tübingen erscheinen, da ich infolge eines in der Nacht
vom 6. zum 7. Des. in Zürich stattfindenden Balles hier unabhörmlich
bin.- Mit vielen Grüssen an Euch, sowie an Herrn Back, Euer
untertänigster Diener

ges. W. Pauli

Dear Radioactive Ladies and Gentlemen!

As the bearer of these lines, to whom I graciously ask you to listen, will explain to you in more detail, because of the "wrong" statistics of the N- and Li-6 nuclei and the continuous beta spectrum, **I have hit upon a desperate remedy to save the "exchange theorem" (1) of statistics and the law of conservation of energy.** Namely, the **possibility that in the nuclei there could exist electrically neutral particles, which I will call neutrons** [now neutrinos], that have spin 1/2 and obey the exclusion principle...

The continuous beta spectrum would then make sense with the assumption that in beta decay, in addition to the electron, a neutron is emitted such that the sum of the energies of neutron and electron is constant...



But so far, I do not dare to publish anything about this idea, and trustfully turn first to you, dear radioactive ones, with the question of how likely it is to find experimental evidence for such a neutron...

I admit that my remedy may seem almost improbable because one probably would have seen those neutrons, if they exist, for a long time. But nothing ventured, nothing gained...

Thus, dear radioactive ones, scrutinize and judge.

Unfortunately, I cannot personally appear in Tübingen since I am indispensable here in Zürich because of a ball on the night from December 6 to 7.

Neutrino naming and the Fermi theory of Weak Interactions

To avoid confusion with the neutron, discovered in 1932 by J. Chadwick , E. Fermi  in his theory of weak interactions (1933-34) called this particle neutrino, meaning little neutron in Italian. This term was coined by E. Amaldi, one of the young members of Fermi's group (« I Ragazzi di Via Panisperna »).

An attempt to a β rays theory

E. Fermi, *Ricerca Scientifica* 4 (1933) 491

Tentativo di una teoria dell'emissione dei raggi "beta"

Nota del prof. ENRICO FERMI

Riassunto: Teoria della emissione dei raggi β delle sostanze radioattive, fondata sull'ipotesi che gli elettroni emessi dai nuclei non esistono prima della disintegrazione ma vengano formati, insieme ad un neutrino, in modo analogo alla formazione di un quanto di luce che accompagna un salto quantico di un atomo. Confronto della teoria con l'esperienza.

TENTATIVO DI UNA TEORIA DEI RAGGI β

Nota ⁽¹⁾ di ENRICO FERMI

Sunto. - Si propone una teoria quantitativa dell'emissione dei raggi β in cui si ammette l'esistenza del « neutrino » e si tratta l'emissione degli elettroni e dei neutrini da un nucleo all'atto della disintegrazione β con un procedimento simile a quello seguito nella teoria dell'irradiazione per descrivere l'emissione di un quanto di luce da un atomo eccitato. Vengono dedotte delle formule per la vita media e per la forma dello spettro continuo dei raggi β , e le si confrontano coi dati sperimentali.

E. Fermi, *Nuovo Cimento* 11 (1934) 1

Rejected from *Nature* for being 'too removed from reality'

$$(Z, A) \rightarrow (Z + 1, A) + e^- + \bar{\nu}_e$$

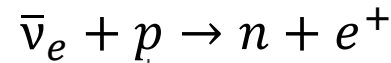
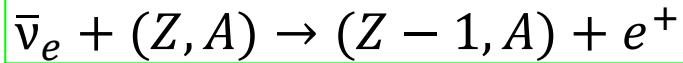
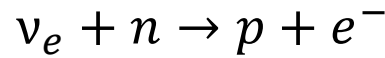
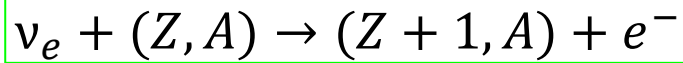
$$n \rightarrow p + e^- + \bar{\nu}_e$$

Theory of the emission of β rays by radioactive substances, based on the hypothesis that the electrons emitted by nuclei do not exist before the disintegration but are formed, together with a neutrino, in a way which is analogous to the formation of a quantum of light which accompany a quantum jump of an atom. Comparison of theory with experience

A quantitative theory of β -rays emission is proposed in which the existence of the «neutrino» is admitted; electrons and neutrinos emission from a nucleus at a β decay is treated with a procedure similar to the one followed for radiation theory to describe a light quantum emission by an excited atom. Formulae are derived for the mean life and for the distribution of the β -rays continuum spectrum, which are compared with experimental data.

[FB.dvi \(uniroma3.it\)](http://FB.dvi.uniroma3.it)

Neutrino interaction and neutrino detection



The "Neutrino", Nature 133 (1934) 532

The possibility of creating neutrinos necessarily implies the existence of annihilation processes. The most interesting amongst them would be the following: a neutrino hits a nucleus and a positive or negative electron is created while the neutrino disappears and the charge of the nucleus changes by 1.

The cross section σ for such processes for a neutrino of given energy may be estimated from the lifetime t of β -radiating nuclei giving neutrinos of the same energy. (This estimate is in accord with Fermi's model but is more general.) Dimensionally, the connexion will be

$$\sigma = A/t$$

where A has the dimension $\text{cm}^2 \text{ sec}$. The longest length and time which can possibly be involved are \hbar/mc and \hbar/mc^2 . Therefore

$$\sigma < \frac{\hbar^3}{m^3 c^4 t}$$

The longest length and time which can possibly be involved

```
hbarc = 197.3269804 #MeV fm
me = 0.51099895 # MeV
c = 299792458 #ms-1
t = 3*60 #s
hbarc**3*(10**-13)**3/(me**3*c*10**2*t) #cm2
1.0671026026257229e-44
```

For an energy of 2.3×10^6 volts, t is 3 minutes and therefore $\sigma < 10^{-44} \text{ cm}^2$ (corresponding to a penetrating power of 10^{16} km . in solid matter). It is therefore absolutely impossible to observe processes of this kind with the neutrinos created in nuclear transformations.

With increasing energy, σ increases (in Fermi's model³ for large energies as $(E/mc^2)^2$) but even if one assumes a very steep increase, it seems highly improbable that, even for cosmic ray energies, σ becomes large enough to allow the process to be observed.

If, therefore, the neutrino has no interaction with other particles besides the processes of creation and annihilation mentioned—and it is not necessary to assume interaction in order to explain the function of the neutrino in nuclear transformations—one can conclude that there is no practically possible way of observing the neutrino.

H. BETHE. 
R. PEIERLS.



Penetrating power: $10^{16} \text{ km} \approx 10^3 \text{ light-year}$

$\sigma \sim 10^{-44} \text{ cm}^2 \leftrightarrow$ Probability $\sim 10^{-18}$ to interact in a solid detector of 1m thickness

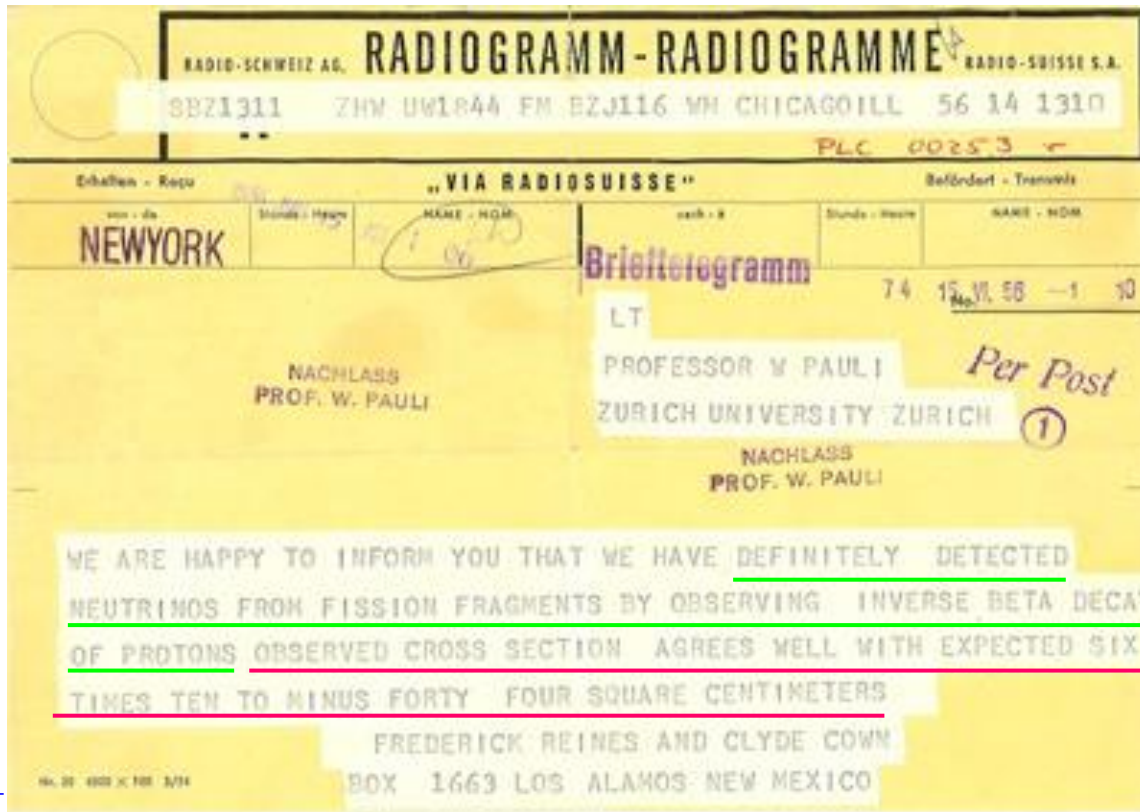
\leftrightarrow Probability $\sim 10^{-11}$ to interact inside the Earth along a trajectory passing through its center

For many years no one thought about how to detect the neutrinos

1956: C. Cowan and F. Reines detect (anti)neutrinos



- Antineutrinos were produced by the Savannah River nuclear reactor
- A typical reactor emits $\sim 2 \times 10^{20} \bar{\nu}_e/s$ per each GW of the thermal energy power ; $E_{\bar{\nu}} \sim MeV$



$$\bar{\nu}_e + p \rightarrow n + e^+$$

$$\sigma = 6 \times 10^{-44} \text{cm}^2$$

[Experimental discovery \(in2p3.fr\)](http://in2p3.fr)

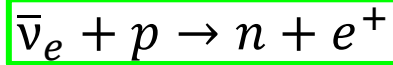
[Neutrinos detected at last! | timeline.web.cern.ch](http://timeline.web.cern.ch)

[Frederick Reines - Nobel Lecture \(nobelprize.org\)](http://nobelprize.org)

Frederick REINES and Clyde COWAN
 Box 1663, LOS ALAMOS, New Mexico
 Thanks for message. Everything comes to
 him who knows how to wait.
 Pauli

conclude that there is no practically possible way
 of observing the neutrino.
 Nature 133 (1934) 532
 H. BETHE.
 R. PEIERLS.
 Reines: I confronted Bethe, with this pronouncement
 some 20 years later and with his characteristic good
 humor he said, "Well you shouldn't believe
 everything you read in the papers."
 10

Example of (simple) evaluation of the cross section



P. Vogel and J. F. Beacom, Phys. Rev. D 60, 053003 (1999)

$$\begin{aligned}\sigma_{tot}^{(0)} &= \sigma_0 (f^2 + 3g^2) E_e^{(0)} p_e^{(0)} \\ &= 0.0952 \left(\frac{E_e^{(0)} p_e^{(0)}}{1 \text{ MeV}^2} \right) \times 10^{-42} \text{ cm}^2 \\ \sigma_0 &= \frac{G_F^2 \cos^2 \theta_C}{\pi} (1 + \Delta_{inner}^R)\end{aligned}$$

```
import numpy as np
```

```
import matplotlib.pyplot as plt
%matplotlib inline
```

```
GF = 1.16637*10**(-5) #GeV-2
cthc = 0.9746
hbarc = 197.3269804 #MeV fm
f = 1
g = 1.266
```

```
s0=hbarc**2*(10**(-13))**2*GF**2*(1/10**6)**2*cthc**2/np.pi*(1+0.024)
fact=s0*(f**2+3*g**2)
fact
```

```
9.525661986246197e-44
```

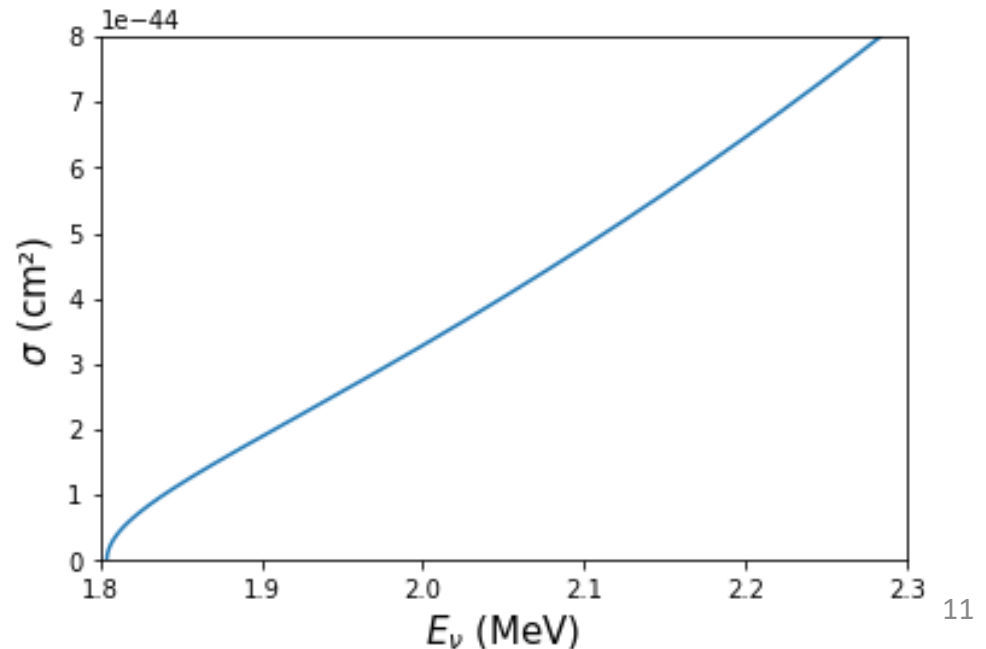
```
me = 0.51099895 # MeV
Mp = 938.27208816 # MeV
Mn = 939.56542052 # MeV
```

```
D = Mn-Mp
```

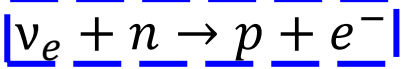
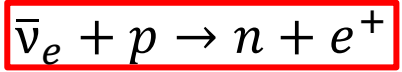
```
Enu = np.linspace(D+me, 2.3, 10000)
```

```
Ee = Enu-D
pe = np.sqrt(Ee**2-me**2)
```

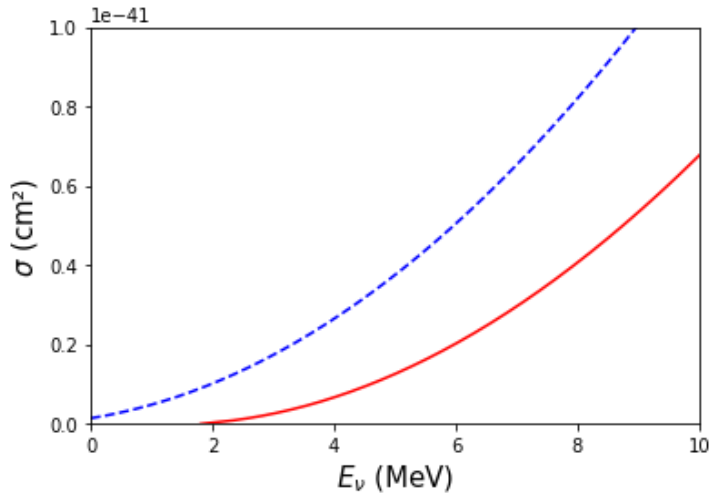
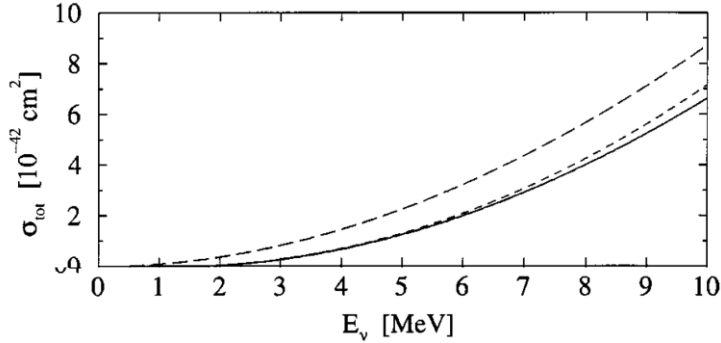
```
plt.plot(Enu, fact*Ee*pe)
plt.ylim(0, 8*10**-44)
plt.xlim(1.8, 2.3)
plt.xlabel(r'$E_{\nu}$ (MeV)', fontsize=15)
plt.ylabel(r'$\sigma$ (cm$^2$)', fontsize = 15);
```



Neutrino-nucleon (quasielastic) cross section at different ν energies

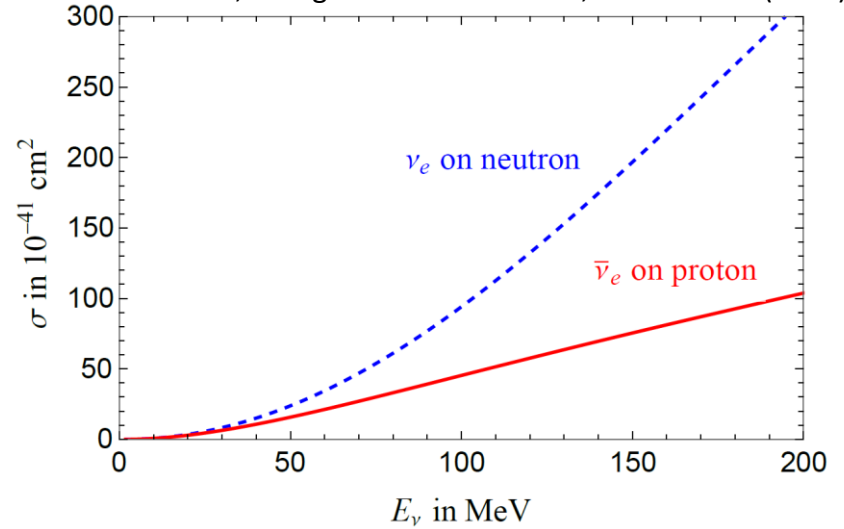


P. Vogel and J. F. Beacom, Phys. Rev. D 60, 053003 (1999)

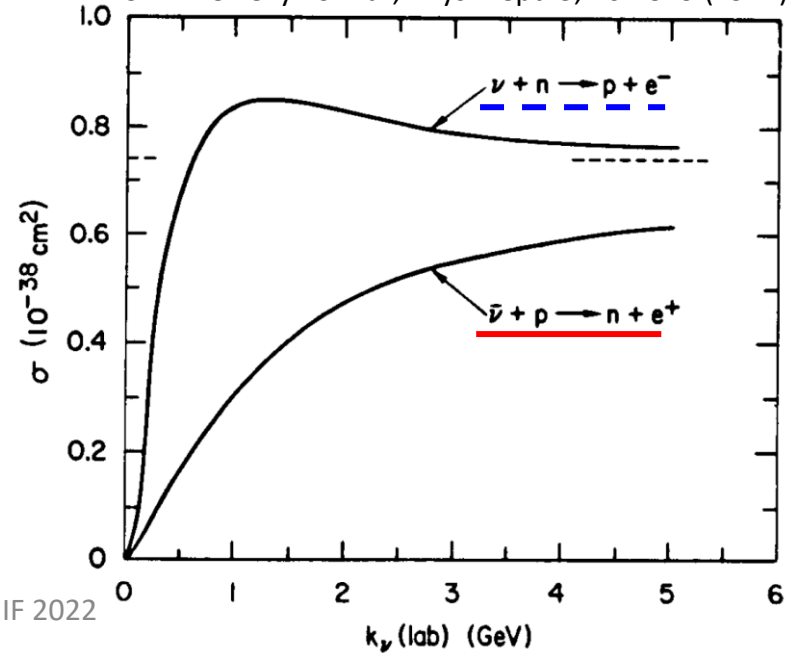


A. Strumia and F. Vissani, Phys. Lett. B 564, 42-54 (2003)

G. Ricciardi, N. Vignaroli and F. Vissani, JHEP 08 212 (2022)



C. H. Llewellyn Smith, Phys. Rept. 3, 261-379 (1972)



M. Martini, GIF 2022

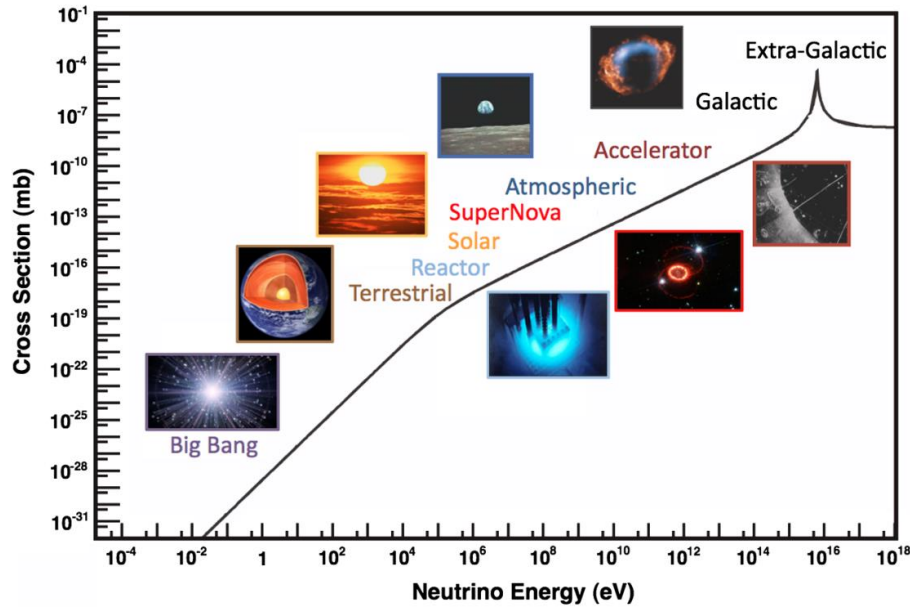
Supernova

Accelerator

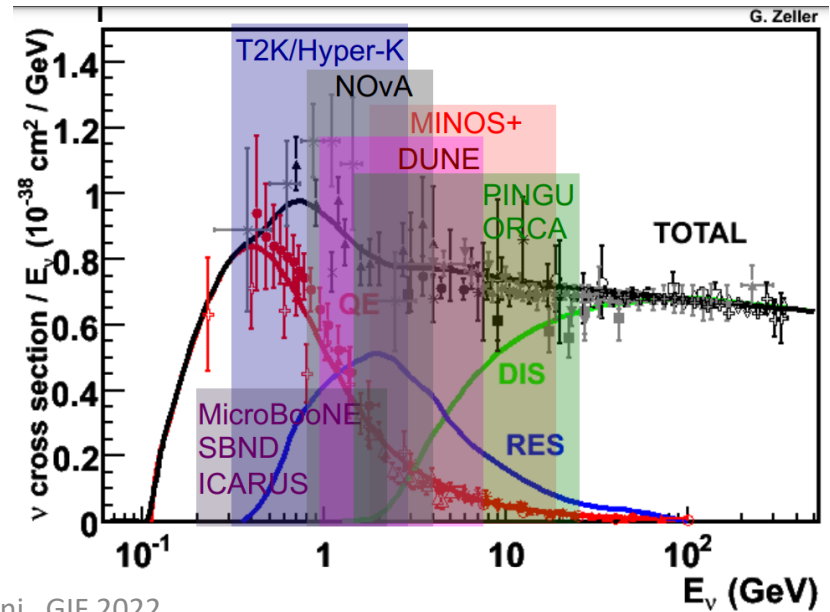
Reactor

From eV to EeV: Neutrino cross sections across energy scales

J. A. Formaggio, G. P. Zeller



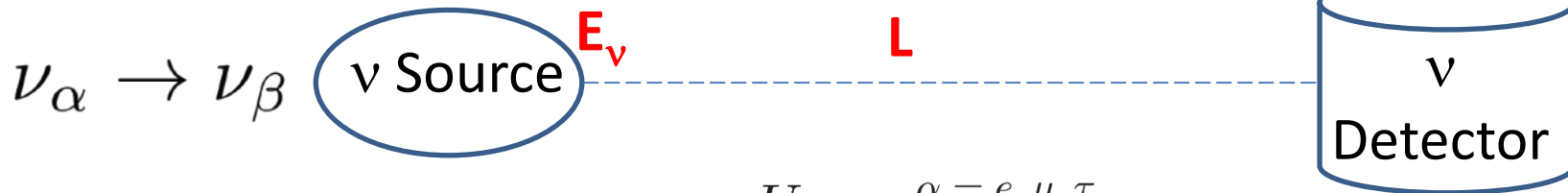
Accelerator



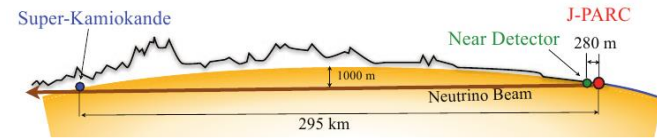
Neutrino-nucleus cross sections (for ν oscillation experiments \leftrightarrow at accelerator energies)

Generalities

Neutrino oscillation experiments



$$\nu_\alpha = U_{\alpha i} \nu_i \quad \begin{matrix} \alpha = e, \mu, \tau \\ i = 1, 2, 3 \end{matrix}$$



$$N_{\nu_\beta}(\overline{E_\nu}) \sim \int \Phi_{\nu_\alpha}(E_\nu) P_{\nu_\alpha \rightarrow \nu_\beta}(E_\nu, L, \{\Theta\}) \sigma_{\nu_\beta}(E_\nu) \epsilon_{\text{det.}} d(E_\nu, \overline{E_\nu}) dE_\nu$$

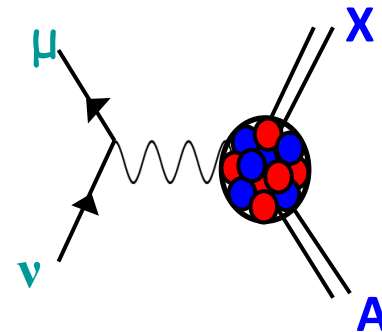
Reconstructed ν energy $\overline{E_\nu}$ (blue box)
 True ν energy E_ν (pink box)

Number of detected events



Modern accelerator-based neutrino oscillation experiments:

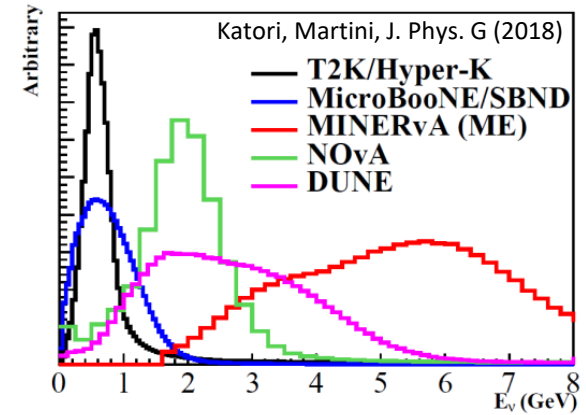
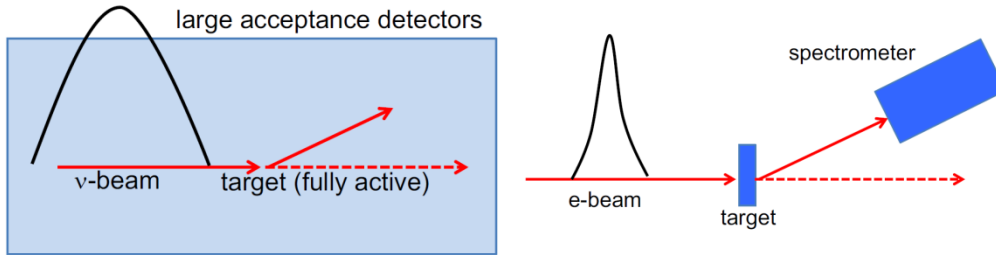
- The neutrino energy is reconstructed from the final states
- Nuclear targets (C, O, Ar, Fe...)



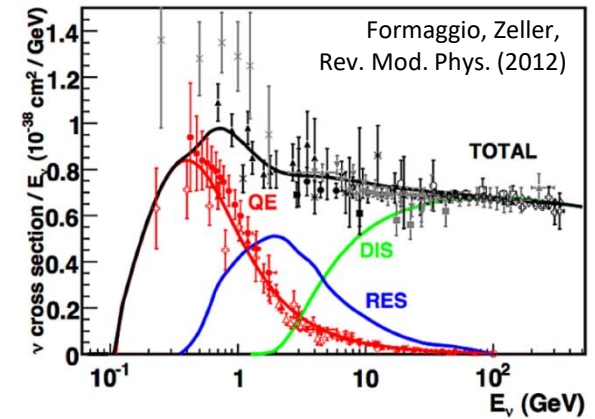
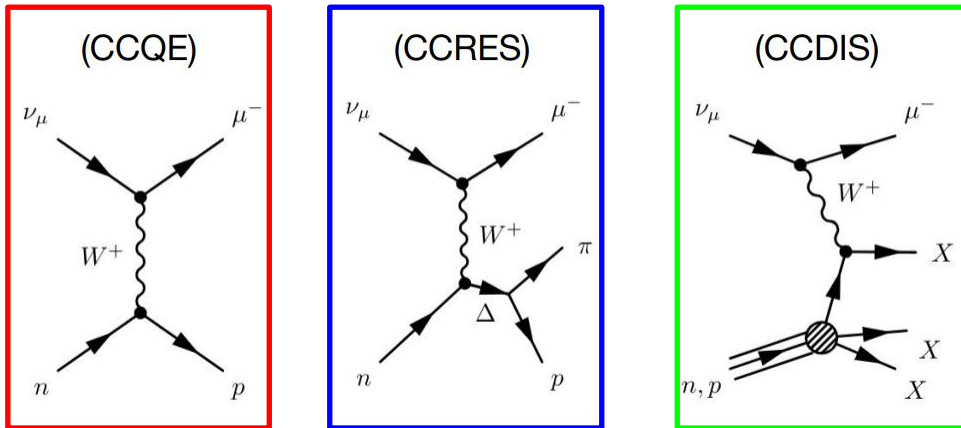
→ the knowledge of the neutrino-nucleus cross section is crucial

Some crucial points of the accelerator-based ν experiment

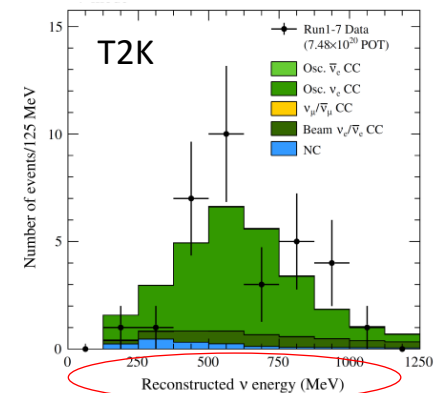
- Neutrino beams are not monochromatic (at difference with respect to electron beams)



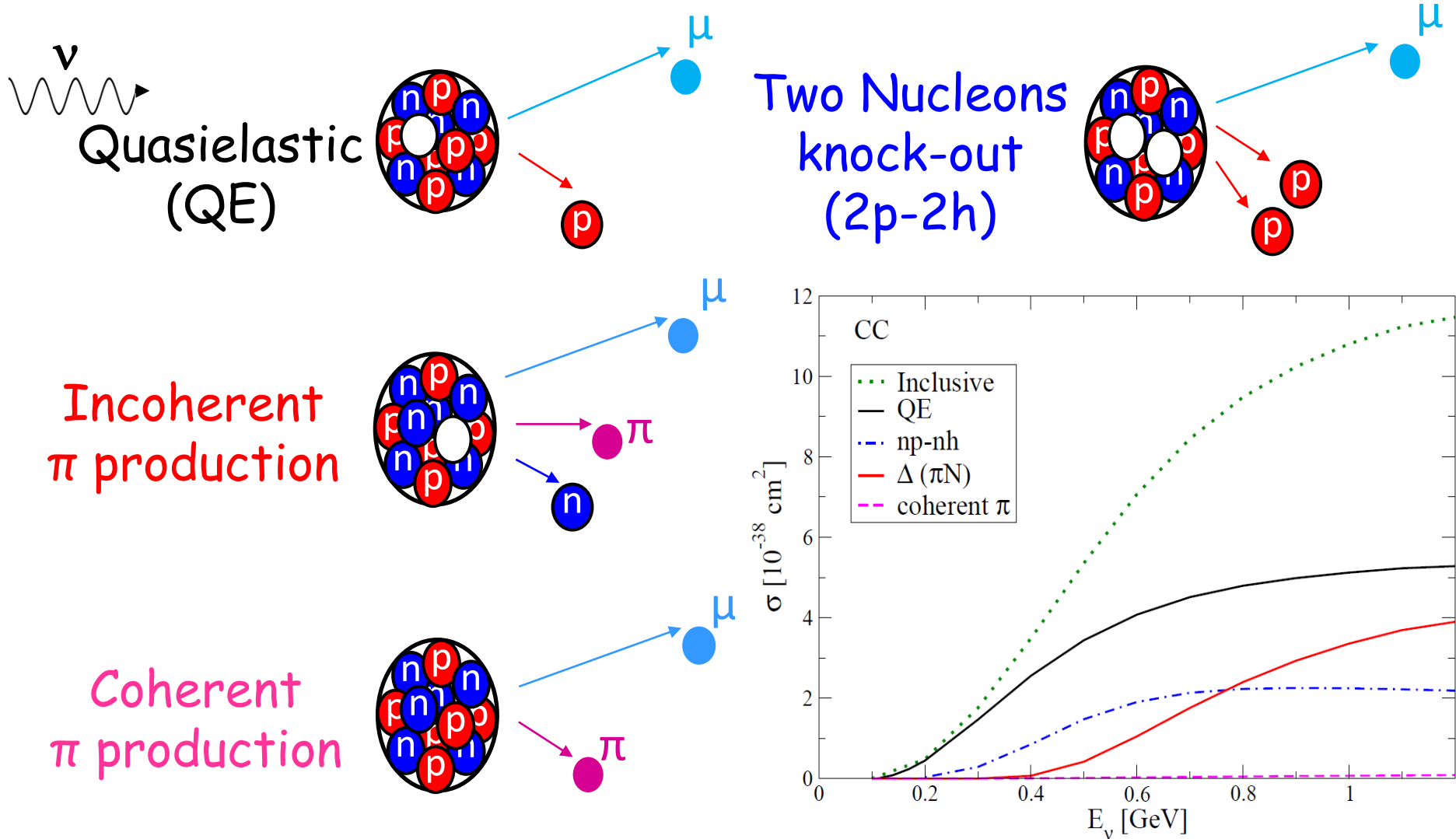
- Different reaction mechanisms contribute



- The neutrino energy is reconstructed from the final states of the reaction (often from CCQE events)



In these lectures: Neutrino - nucleus interaction @ $E_\nu \sim O(1 \text{ GeV})$

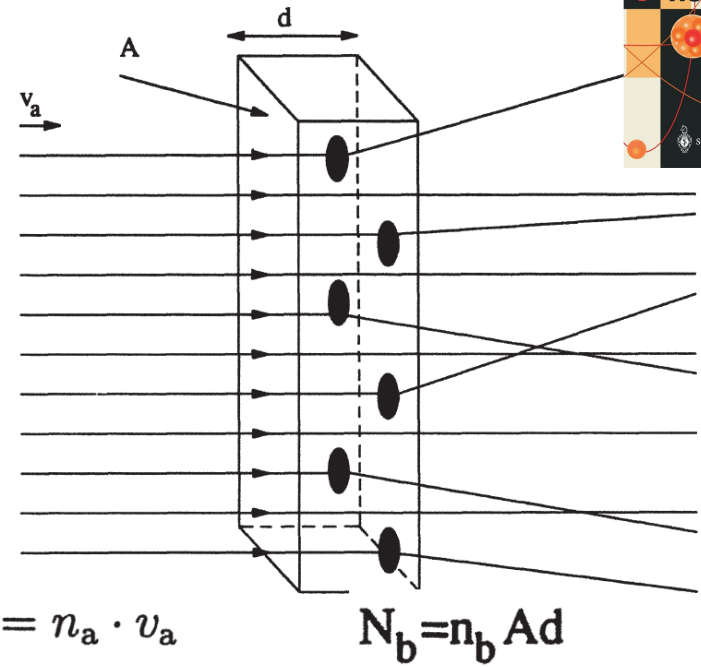


Different processes are entangled

Cross Section generalities - textbook definitions

- **Definition:** The **Cross Section** is a measure for the **probability** of a process to happen
- **Dimensions:** **Area**

$$a + b \rightarrow a' + b^*$$



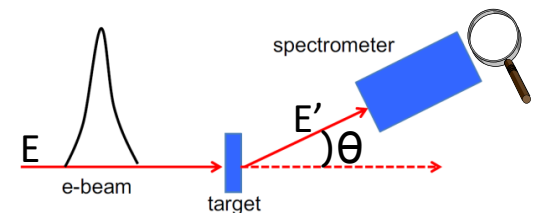
$$\sigma_b = \frac{\dot{N}}{\Phi_a \cdot N_b}$$

$$\Phi_a = \frac{\dot{N}_a}{A} = n_a \cdot v_a$$

$$N_b = n_b A d$$

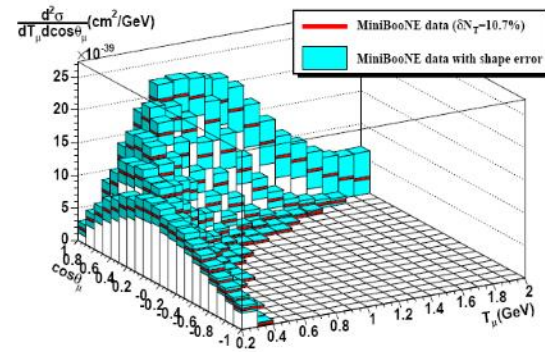
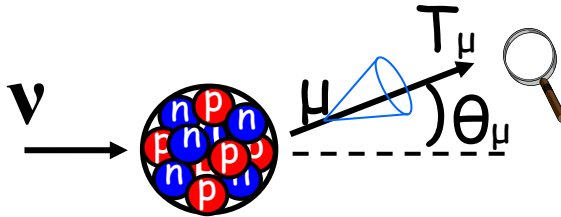
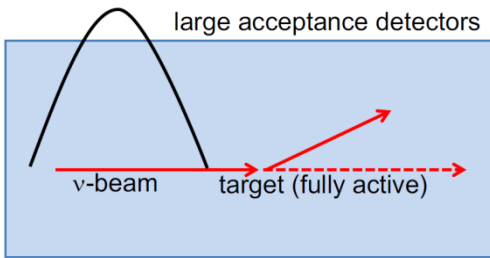
number of reactions per unit time

beam particles per unit time per unit area \times scattering centres



$$\sigma_{\text{tot}}(E) = \int_0^{E'_{\text{max}}} \int_{4\pi} \frac{d^2\sigma(E, E', \theta)}{d\Omega dE'} d\Omega dE'$$

Neutrino flux integrated double differential cross sections



Flux-integrated differential cross section is where theorists and experimentalists meet for ν interaction

Theory

$$\frac{d^2\sigma}{dT_l d\cos\theta} = \frac{1}{\int \Phi(E_\nu) dE_\nu} \int dE_\nu \left[\frac{d^2\sigma}{d\omega d\cos\theta} \right]_{\omega=E_\nu-E_l} \Phi(E_\nu)$$

Unfolding matrix to remove detector effects

Number of observed events

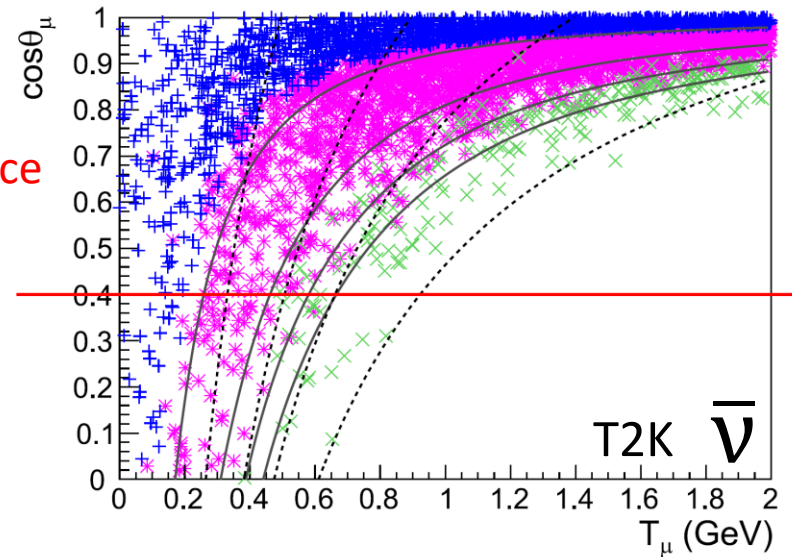
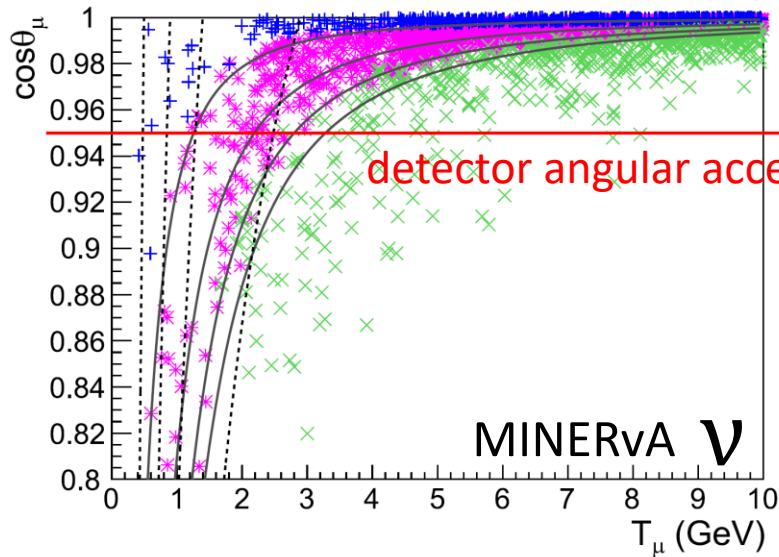
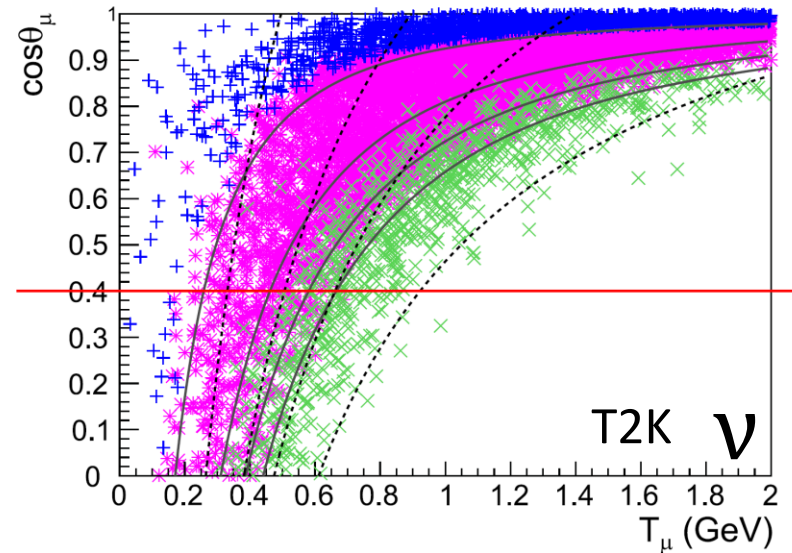
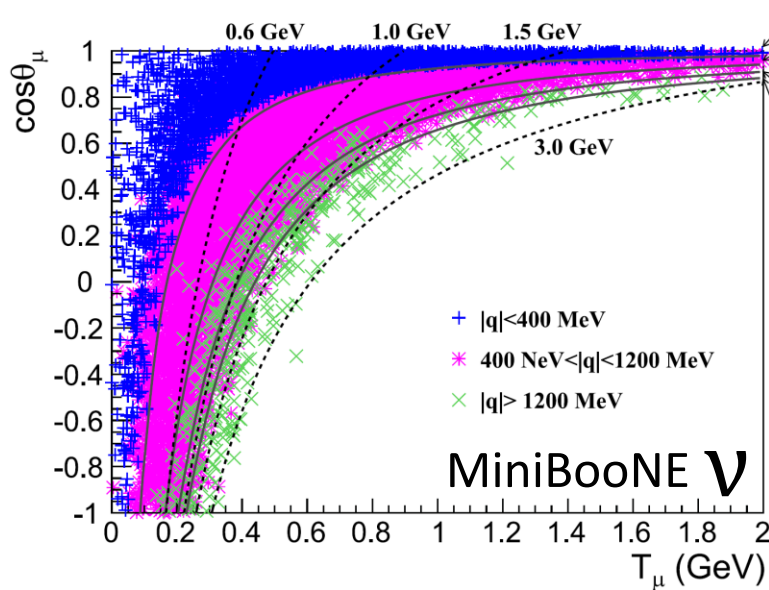
Background contribution

Experimental Definition

$$\left(\frac{d^2\sigma}{dT_l \cos\theta} \right)_i = \frac{\sum_j U_{ij} (d_j - b_j)}{\Phi \cdot T \cdot \epsilon_i \cdot (\Delta T_l, \Delta \cos\theta)_i}$$

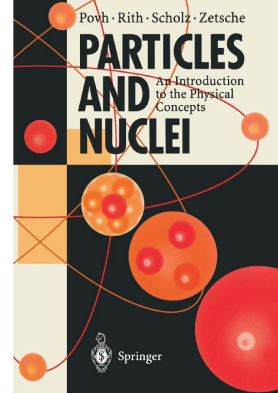
← Total integrated flux
↓ Number of target nucleons in the Fiducial Volume
↘ Efficiency
↘ Bin widths

$(\cos\theta_\mu, T_\mu)$ distributions of neutrino flux integrated CCQE generated events



Cross Section generalities - Theory

Quantum Mechanics (Time-dependent perturbation theory)



Reaction rate per target particle and per beam particle:

Fermi's golden rule

$$W = \frac{2\pi}{\hbar} |\mathcal{M}_{fi}|^2 \cdot \rho(E')$$

Transition matrix element

$$\mathcal{M}_{fi} = \langle \psi_f | \mathcal{H}_{\text{int}} | \psi_i \rangle$$

Density of final states

$$\rho(E') = \frac{dn(E')}{dE'} = \frac{V \cdot 4\pi p'^2}{v' \cdot (2\pi\hbar)^3}$$

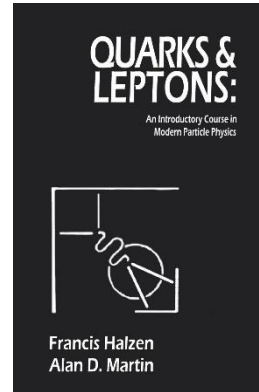
$$W = \frac{\dot{N}(E)}{N_b \cdot N_a} = \frac{\Phi_a \cdot N_b \cdot \sigma}{N_b \cdot N_a} = \frac{\sigma \cdot v_a}{V}$$

(see equations slide 18)

$$\sigma = \frac{2\pi}{\hbar \cdot v_a} |\mathcal{M}_{fi}|^2 \cdot \rho(E') \cdot V$$

Lorentz invariant general expression of differential Cross Section

$$d\sigma = \frac{|M|^2}{Flux} dQ$$



Scattering of 2 particles leading to N outgoing particles

$$p_1 + p_2 \rightarrow p_{f1} + p_{f2} + \dots + p_{fN}$$

$$d\sigma = \frac{(2\pi)^4}{4[(p_1 \cdot p_2)^2 - m_1^2 m_2^2]^{1/2}} \delta^4 \left(\sum_f p_f - \sum_i p_i \right) \left(\prod_f \frac{d^4 p_f}{(2\pi)^3} \delta(p_f^2 - m_f^2) \right) |\bar{M}|^2$$

Invariant flux
Lorentz invariant phase space factor dQ
Invariant squared amplitude averaged and summed over initial and final states

Standard Model of electroweak interaction

Electroweak interaction Lagrangian

$$\mathcal{L}_{\text{int}} = -e J_{\text{EM}}^\mu A_\mu - \frac{g}{2\sqrt{2}} \left(J_{\text{CC}}^\mu W_\mu^\dagger + \text{h. c.} \right) - \frac{g}{2 \cos \theta_W} J_{\text{NC}}^\mu Z_\mu$$

Feynman Rules

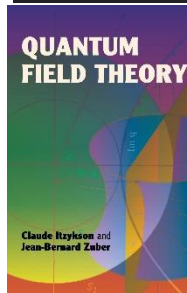
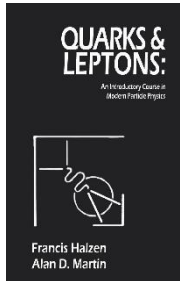
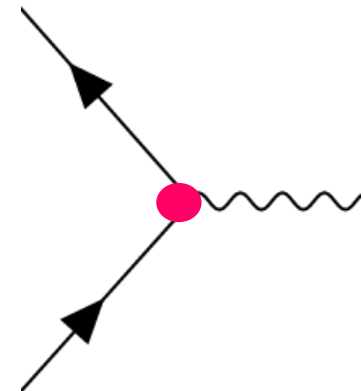
Gauge Bosons Propagators

- Photon (γ) $\frac{i}{q^2} (-g^{\mu\nu})$
- Massive vector bosons (W,Z) $\frac{i}{q^2 - M_V^2} \left(-g^{\mu\nu} + \frac{q^\mu q^\nu}{M_V^2} \right) \xrightarrow{|q^2| \ll M_V^2} \frac{i g^{\mu\nu}}{M_V^2}$

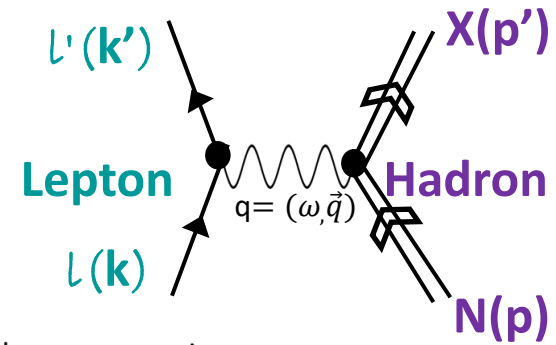


Fermion Vertices

- Electromagnetic $-ieQ_f \gamma_\mu$
 - $Q_{e^-} = -1, Q_{up} = 2/3, \dots$
- Weak (W exchange) $-i \frac{g}{\sqrt{2}} c \gamma_\mu \frac{1 - \gamma^5}{2}$
 - $c = 1$ for leptons
 - $c =$ Cabibbo-mixing matrix element for quarks



Electroweak transition matrix elements



Electromagnetic transition $\ell^- N \rightarrow \ell^- X$

$$-i\mathcal{M} = -\underbrace{(ie)^2 \bar{u}(k') \gamma_\mu u(k)}_{\text{e.m. lepton current}} \frac{-ig^{\mu\nu}}{q^2} \underbrace{\langle X(p'_f) | J_\nu(0) | N(p) \rangle}_{\text{hadronic current (Vector)}}$$

Charged current transition $\nu N \rightarrow \ell^- X$

$$-i\mathcal{M} = \left(\frac{-ig}{2\sqrt{2}} \right)^2 \underbrace{\cos \theta_C \bar{u}(k') \gamma_\mu (1 - \gamma^5) u(k)}_{\text{weak lepton current}} \frac{ig^{\mu\nu}}{M_W^2} \underbrace{\langle X(p'_f) | J_\nu(0) | N(p) \rangle}_{\text{hadronic current (Vector-Axial)}}$$

θ_C

Cabibbo angle

$$\frac{g^2}{8M_W^2} = \frac{G_F}{\sqrt{2}}$$

Fermi coupling constant

Invariant squared amplitude (and Cross Section) in terms of Leptonic and Hadronic tensors

$$|\bar{\mathcal{M}}|^2 = C_{\text{EM,CC,NC}}^2 L_{\mu\nu} W^{\mu\nu}$$

Leptonic tensor

Hadronic tensor

$$C_{\text{EM}} = \frac{e^2}{4\pi\alpha/q^2} \quad C_{\text{CC}} = G_F \cos \theta_C / \sqrt{2} \quad C_{\text{NC}} = G_F / \sqrt{2}$$
$$\alpha = 1/137 \quad G_F = 1.16637 \cdot 10^{-5} \text{ GeV}^{-2} \quad \cos \theta_C = 0.9746$$

$$d\sigma \propto L_{\mu\nu} W^{\mu\nu}$$

A universal structure, valid for any lepton and hadron and maintained at different energy scales

The leptonic tensor

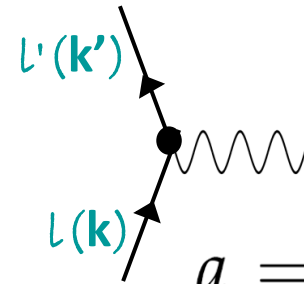
$$L_{\mu\nu} = \frac{1 + |a|}{2} \sum_{s_i} \sum_{s_f} j_\mu^\dagger j_\nu = \frac{1 + |a|}{2} \sum_{s_i} \sum_{s_f} \bar{u}(k) \tilde{l}_\mu u(k') \bar{u}(k') l_\nu u(k)$$

$$= \frac{1 + |a|}{2} \text{Tr} \left[(\not{k} + m_\ell) \tilde{l}_\mu (\not{k}' + m_{\ell'}) l_\nu \right]$$

Leptonic component of the electroweak current

$$j_\mu = \bar{u}(k') l_\mu u(k)$$

$$l_\mu = \gamma_\mu (1 - a\gamma^5) \quad \tilde{l}_\mu = \gamma_0 l_\mu^\dagger \gamma_0$$



$$\not{p} = \gamma_\mu p^\mu$$

$$a = 0 \text{ EM}$$

$$a = 1 (-1) \text{ CC and NC}$$

Electron scattering

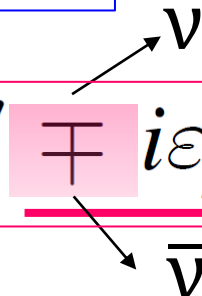
$$L_{\mu\nu} = k_\mu k'_\nu + k'_\mu k_\nu - g_{\mu\nu} (k \cdot k' - m_e^2)$$

$$g_{\mu\nu} = (+, -, -, -)$$

$$\epsilon_{0123} = +1$$

Neutrino scattering

$$L_{\mu\nu} = k_\mu k'_\nu + k_\nu k'_\mu - g_{\mu\nu} k \cdot k' \mp i\epsilon_{\mu\nu\alpha\beta} k^\alpha k'^\beta$$



The hadronic tensor

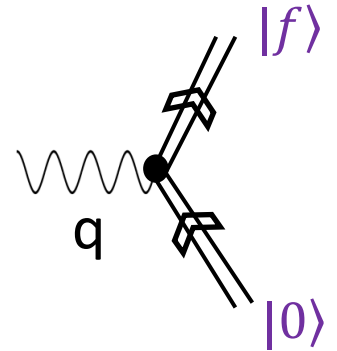
The hadronic tensor contains all the information on the target response

$$W^{\mu\nu} = \sum_f \langle 0 | J^{\mu\dagger}(q) | f \rangle \langle f | J^\nu(q) | 0 \rangle \delta^{(4)}(p_0 + q - p_f)$$

$|0\rangle$ hadronic initial state

$|f\rangle$ hadronic final state

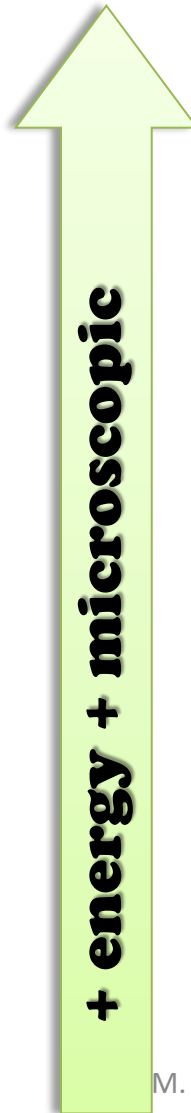
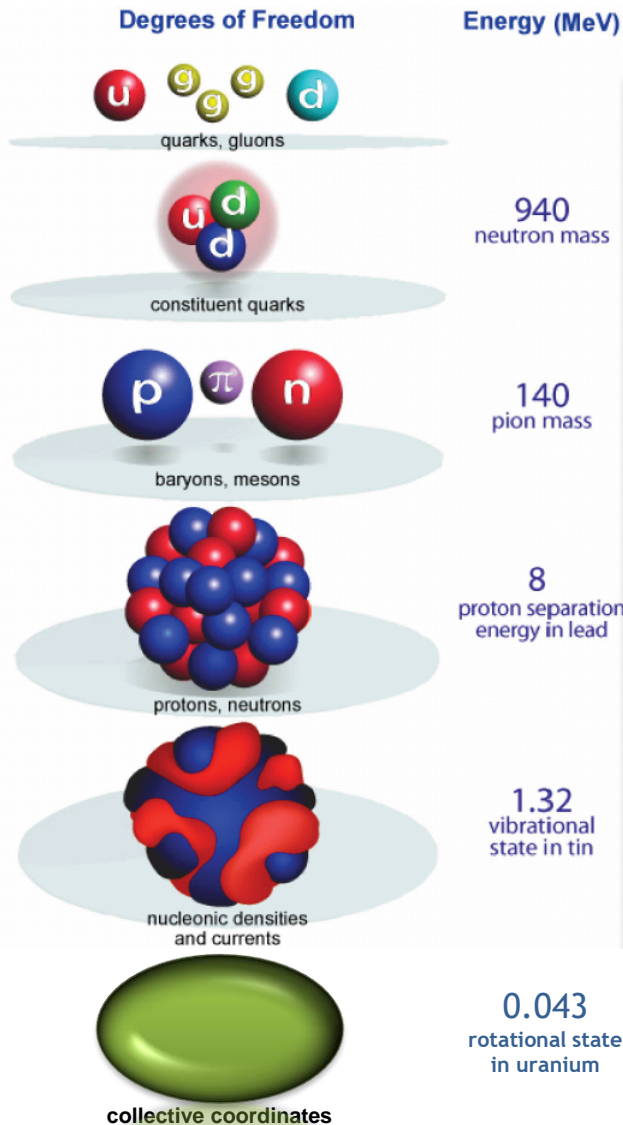
J^ν Hadronic component of the electroweak current



A general expression

- valid for different degrees of freedom (quark, nucleon, nucleon resonances, nucleus)
- valid for different currents (electromagnetic, weak; one-body, two-body,...)

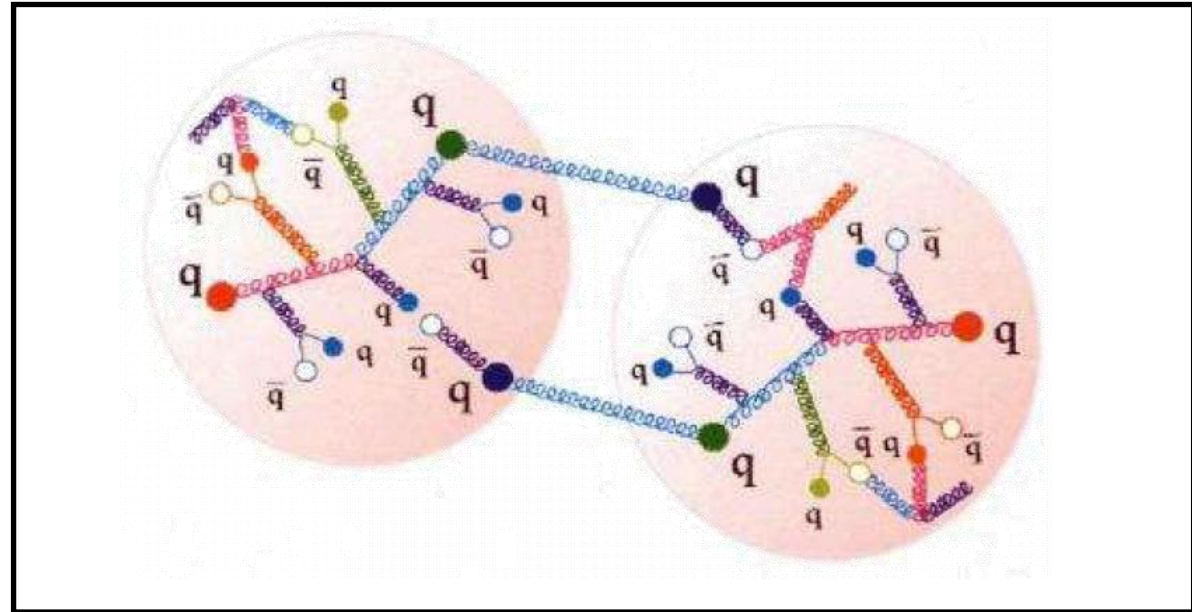
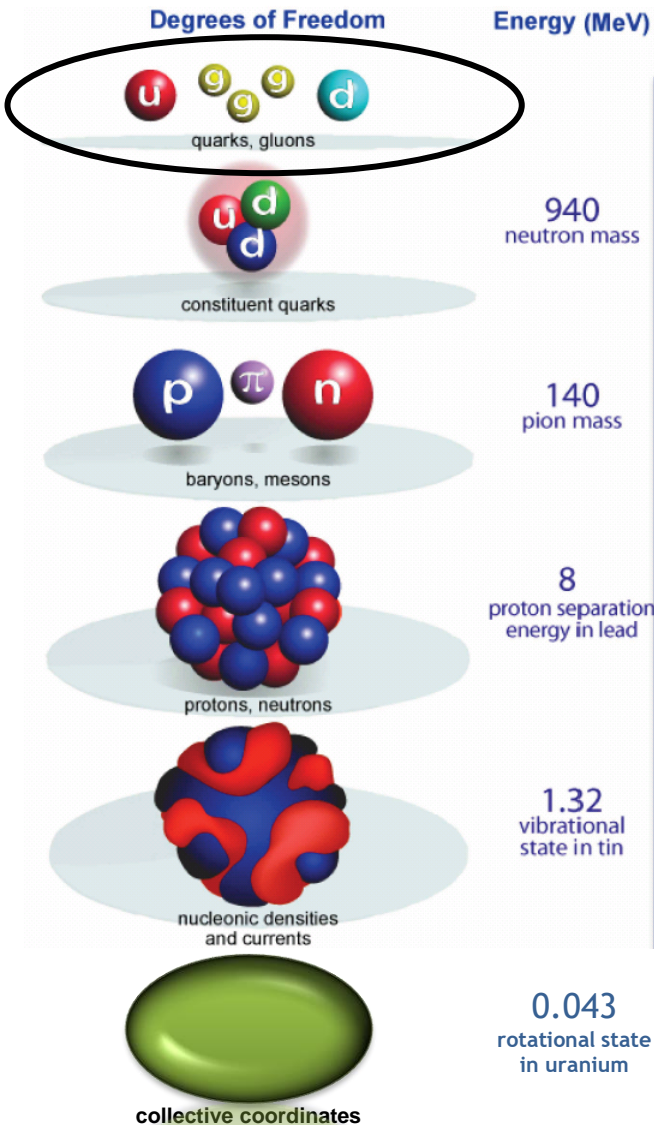
Parenthesis: Nuclear physics and strong interaction



QCD is non-perturbative at low energies

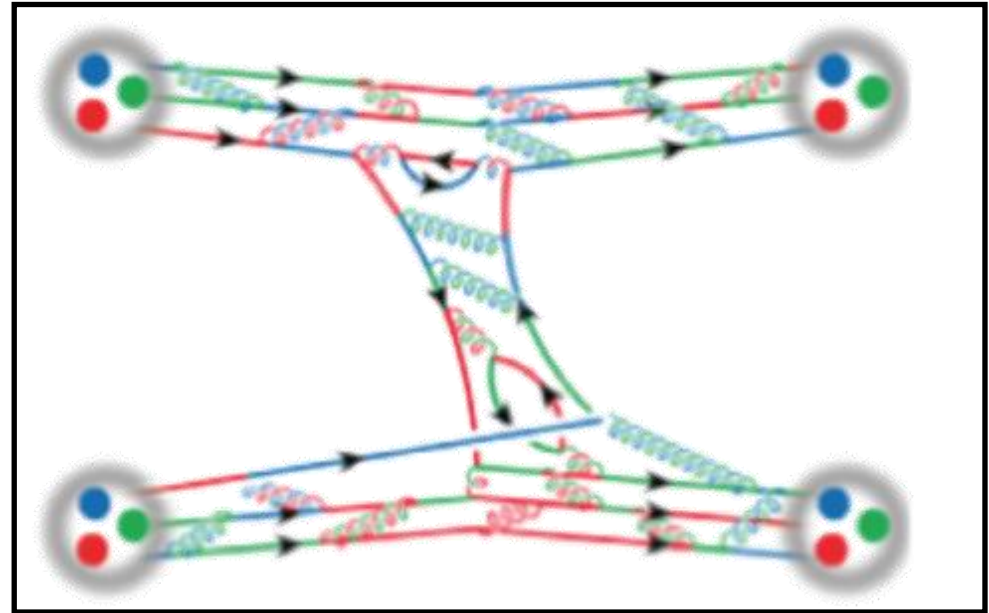
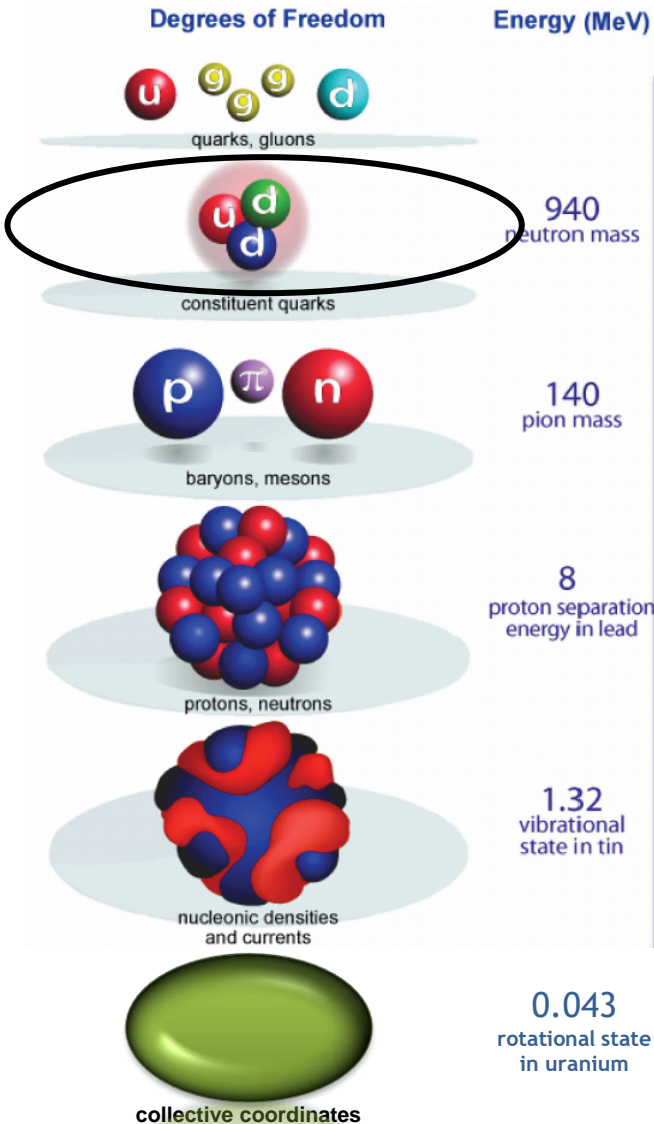
Currently there is no knowledge on how to use it directly in a system as complex as the atomic nucleus

Choice of appropriated Degrees of Freedom



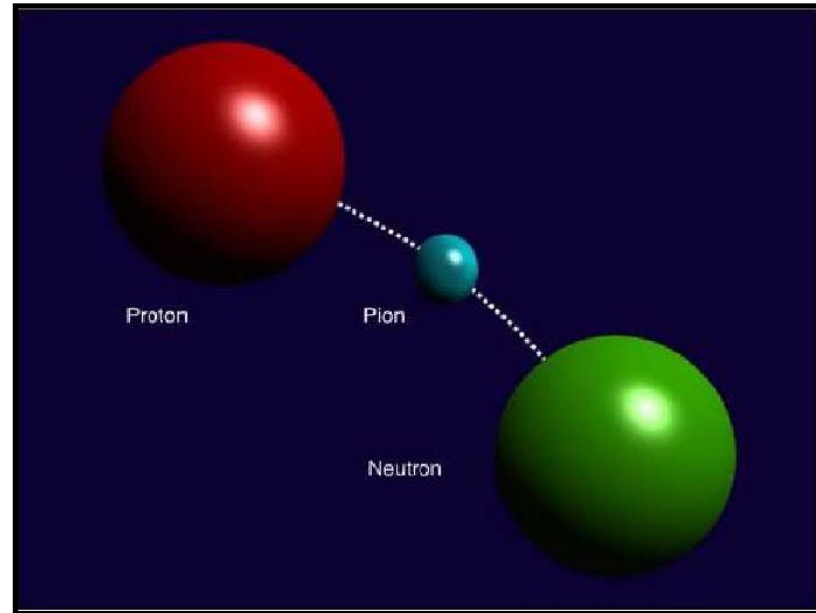
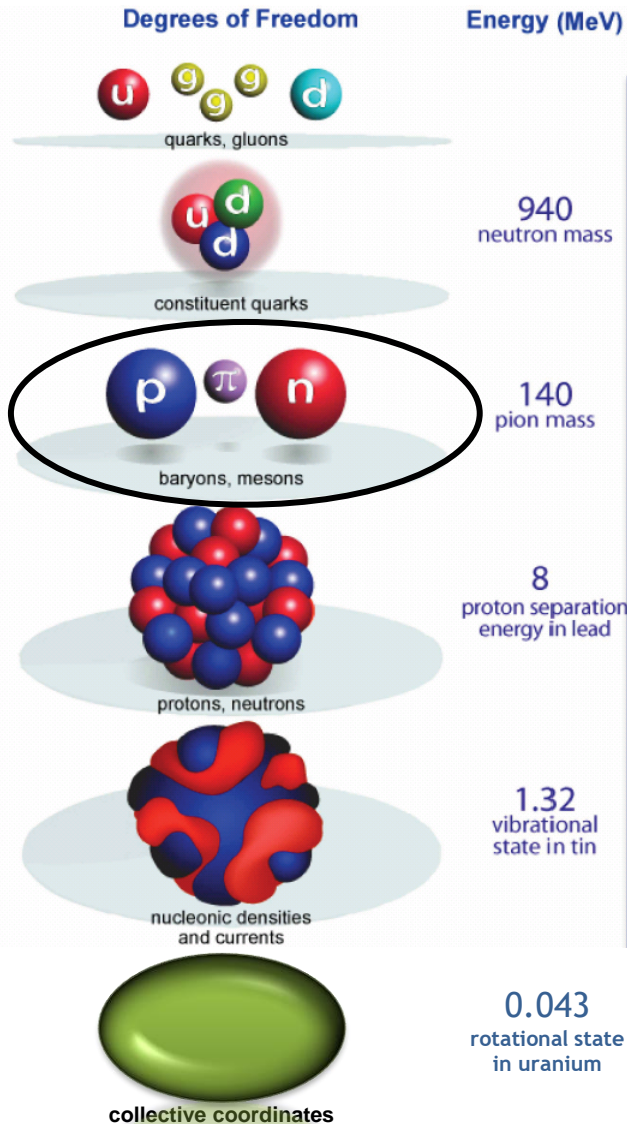
- DoF = quarks and gluons
- QCD

Choice of appropriated Degrees of Freedom



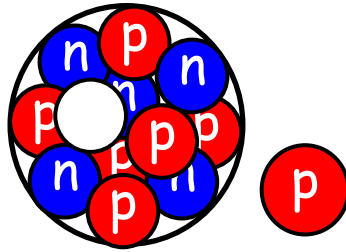
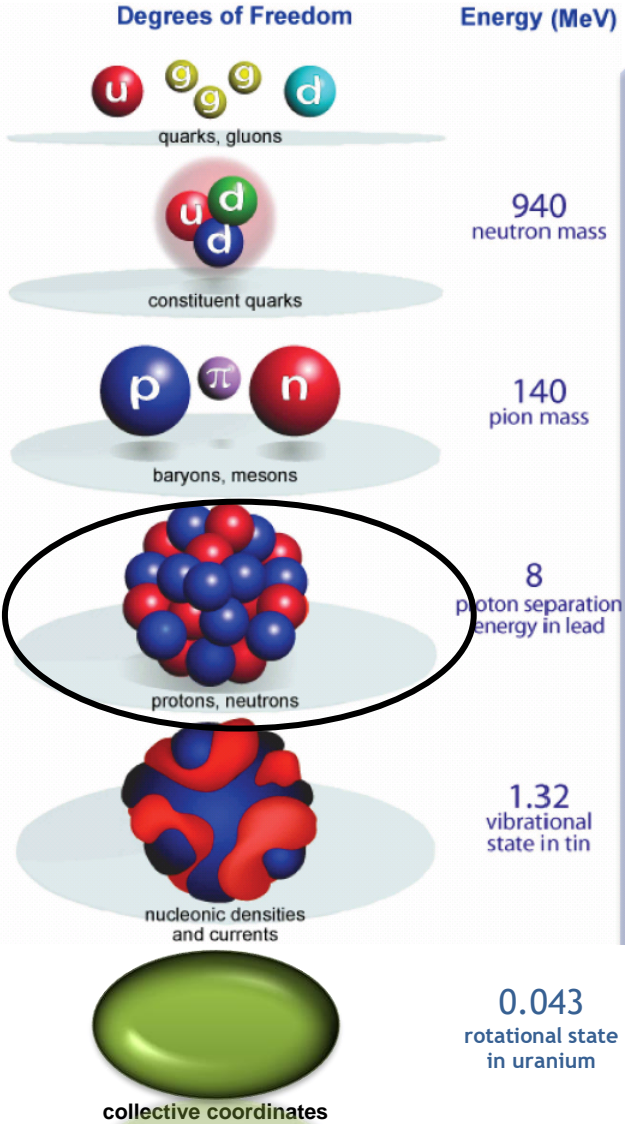
- DoF = valence quarks and gluons
- Low energy QCD, Effective Theories

Choice of appropriated Degrees of Freedom



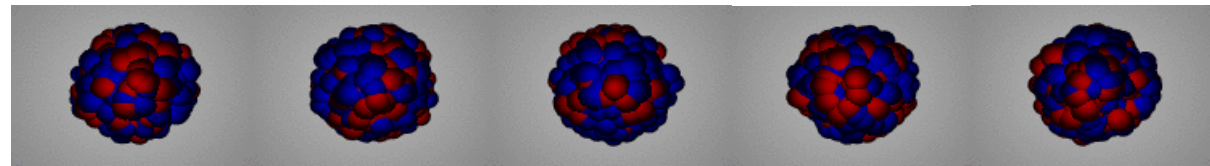
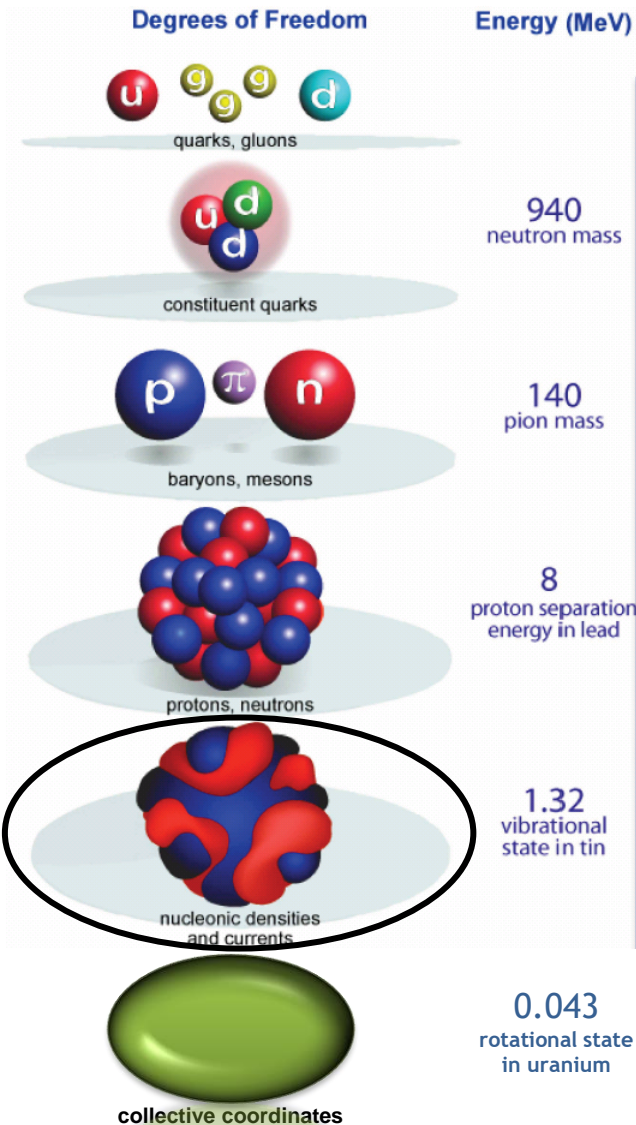
- DoF = baryons and mesons
- Effective Field Theories

Choice of appropriated Degrees of Freedom



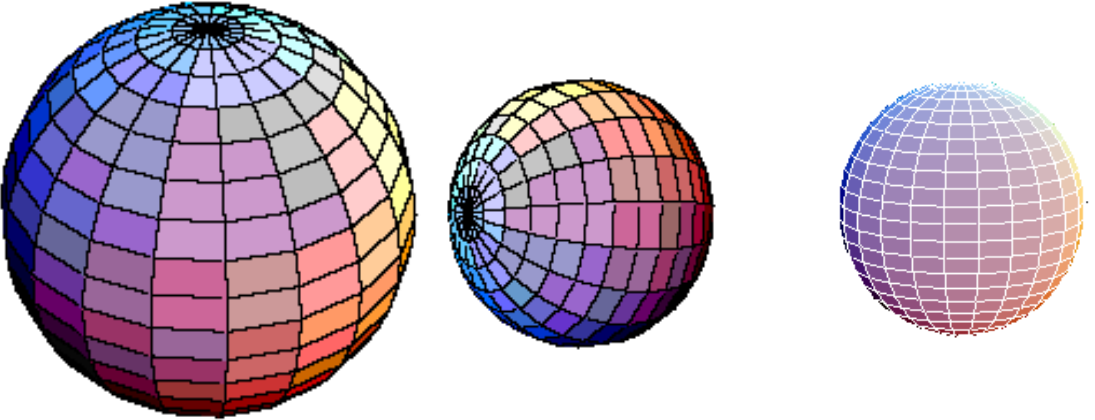
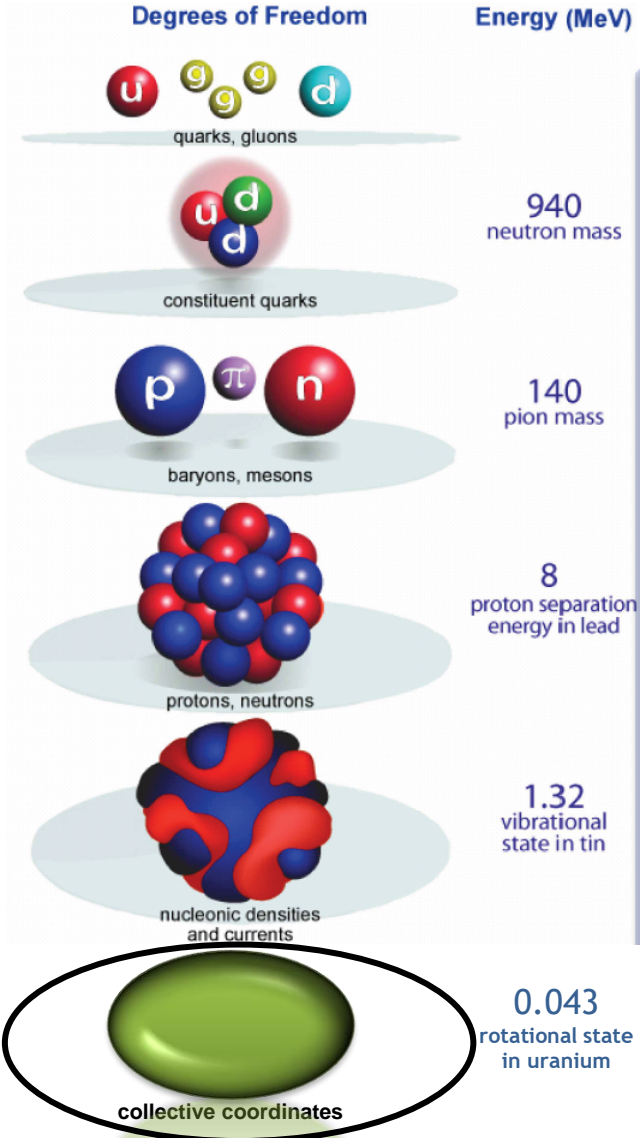
- DoF = Nucleons
- Nuclear Many Body Physics

Choice of appropriated Degrees of Freedom



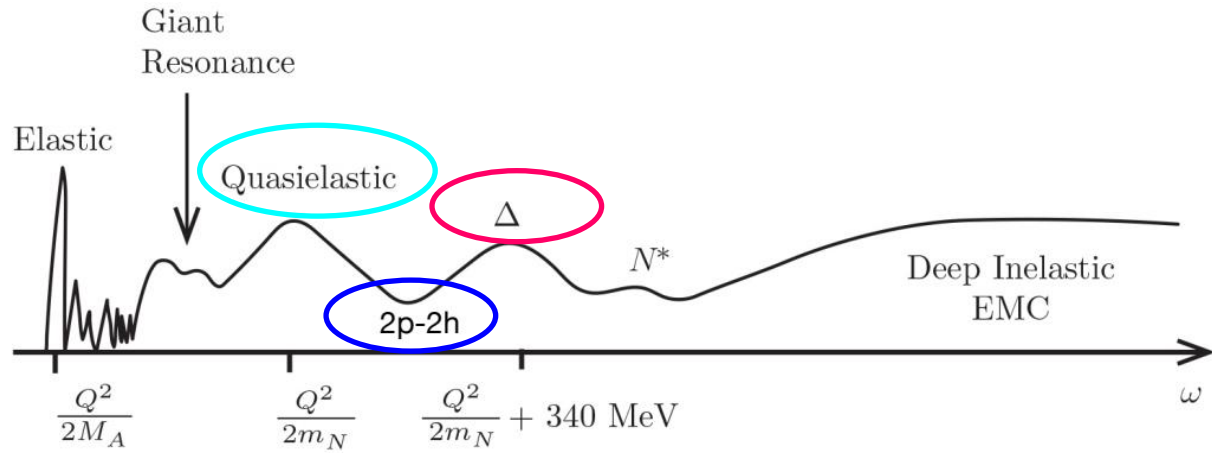
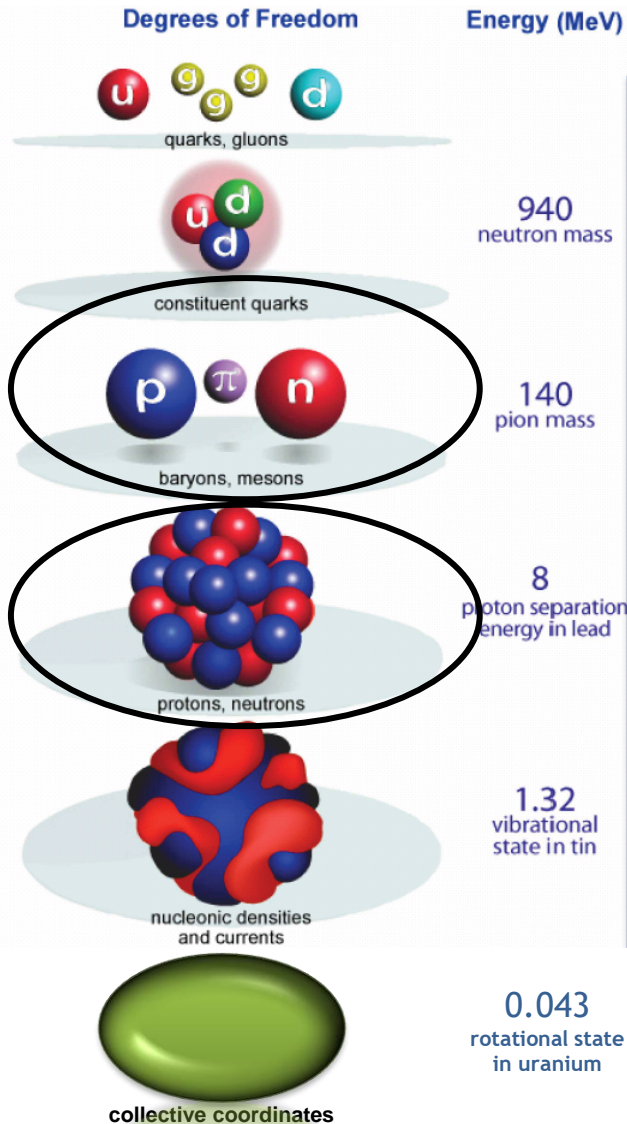
- DoF = nucleonic densities and currents
- Nuclear Many Body Physics

Choice of appropriated Degrees of Freedom

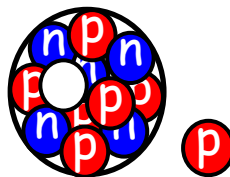
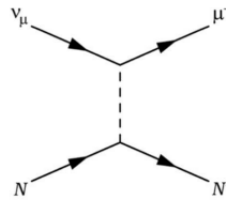


- DOF = collective coordinates
- Macroscopic models

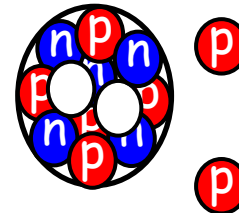
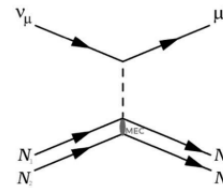
In the following:



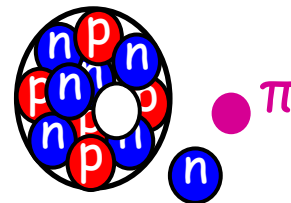
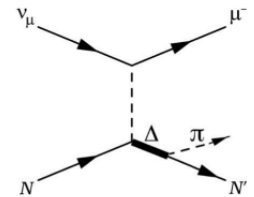
Quasielastic



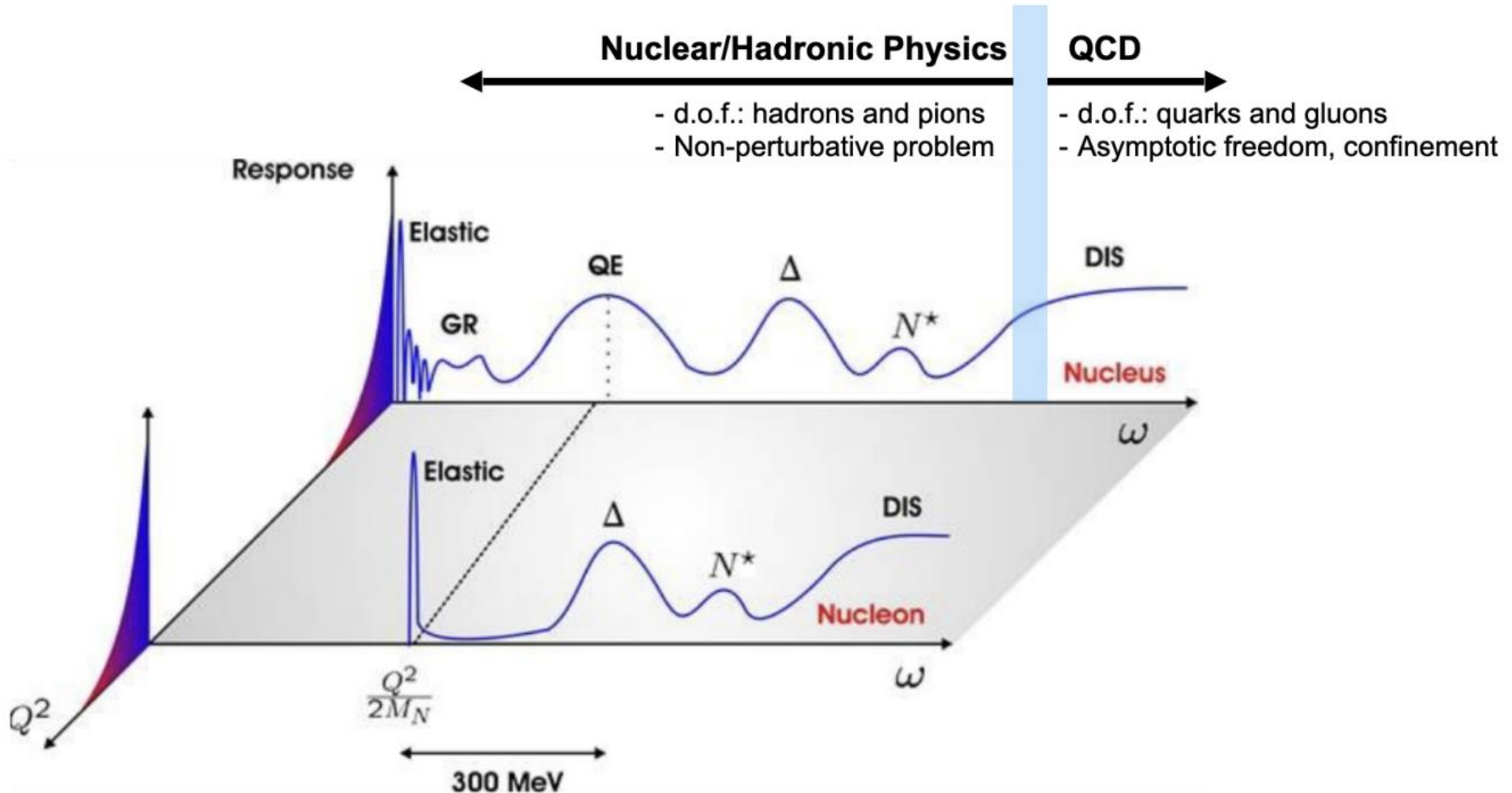
2p-2h



RES π production



Choice of appropriated Degrees of Freedom



The hadronic tensor

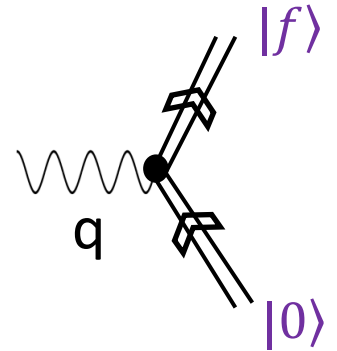
The hadronic tensor contains all the information on the target response

$$W^{\mu\nu} = \sum_f \langle 0 | J^{\mu\dagger}(q) | f \rangle \langle f | J^\nu(q) | 0 \rangle \delta^{(4)}(p_0 + q - p_f)$$

$|0\rangle$ hadronic initial state

$|f\rangle$ hadronic final state

J^ν Hadronic component of the electroweak current



A general expression

- valid for different degrees of freedom (quark, nucleon, nucleon resonances, nucleus)
- valid for different currents (electromagnetic, weak; one-body, two-body,...)

Let's start by considering the single nucleon electroweak current

The single nucleon electroweak current

Electromagnetic current - Electron scattering

$$J_{s's}^\mu(\mathbf{p}', \mathbf{p}) = \bar{u}_{s'}(\mathbf{p}') \left[F_1(Q^2) \gamma^\mu + F_2(Q^2) i \sigma^{\mu\nu} \frac{q_\nu}{2m_N} \right] u_s(\mathbf{p})$$

$$Q^2 = -q^2 \quad \sigma^{\mu\nu} = \frac{i}{2} [\gamma^\mu, \gamma^\nu]$$

Weak current – CC neutrino scattering

$$J^\mu = V^\mu - A^\mu \quad \text{Vector – Axial}$$

Vector $V_{s's}^\mu(\mathbf{p}', \mathbf{p}) = \bar{u}_{s'}(\mathbf{p}') \left[2F_1^V \gamma^\mu + 2F_2^V i \sigma^{\mu\nu} \frac{q_\nu}{2m_N} \right] u_s(\mathbf{p})$

Conserved Vector Current (CVC) $q_\alpha V^\alpha = 0$ and isospin symmetry $\Rightarrow F_i^V = F_i^p - F_i^n$

Axial $A_{s's}^\mu(\mathbf{p}', \mathbf{p}) = \bar{u}_{s'}(\mathbf{p}') \left[G_A \gamma^\mu \gamma_5 + G_P \frac{q^\mu}{2m_N} \gamma_5 \right] u_s(\mathbf{p})$

Partially Conserved Axial Current (PCAC) and pion-pole dominance $\Rightarrow G_P = \frac{4m_N^2}{m_\pi^2 + Q^2} G_A$

$q_\alpha A^\alpha = i(m_u + m_d) \bar{q}_u \gamma_5 q_d \rightarrow 0$

The nucleon form factors

The form factors are corrections to “point-like coupling”

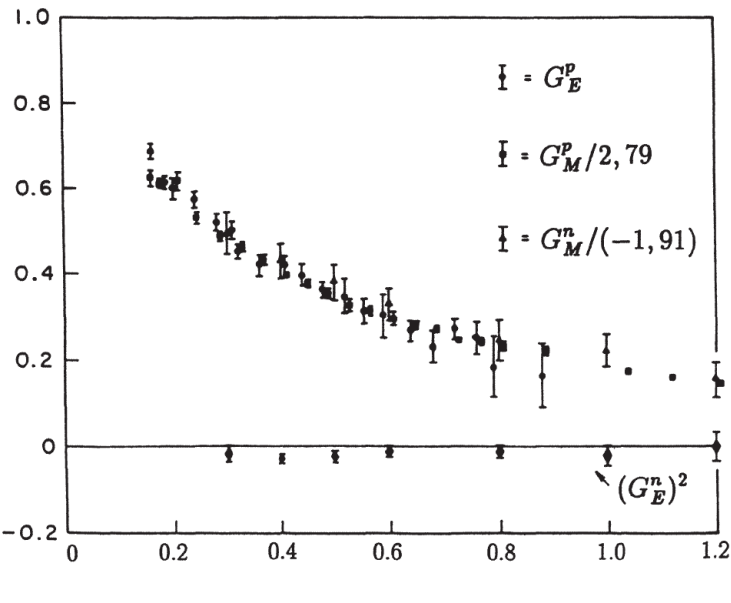
They reflect the fact that the nucleon has an internal structure and a finite size

F_1 and F_2 can be written as a combination of the Electric and Magnetic form factors G_E and G_M

$$F_1^{p,n} = \left[G_E^{p,n} + \frac{Q^2}{4m_N^2} G_M^{p,n} \right] \left[1 + \frac{Q^2}{4m_N^2} \right]^{-1} \quad F_2^{p,n} = [G_M^{p,n} - G_E^{p,n}] \left[1 + \frac{Q^2}{4m_N^2} \right]^{-1}$$

Electron-nucleon cross section

$$\left(\frac{d\sigma}{d\Omega} \right) = \left(\frac{d\sigma}{d\Omega} \right)_{\text{Mott}} \cdot \left[\frac{G_E^2(Q^2) + \tau G_M^2(Q^2)}{1 + \tau} + 2\tau G_M^2(Q^2) \tan^2 \frac{\theta}{2} \right]$$



Global dipole-like behavior

$$G_E^p(Q^2) = \frac{G_M^p(Q^2)}{2.79} = \frac{G_M^n(Q^2)}{-1.91} = G^{\text{dipole}}(Q^2)$$

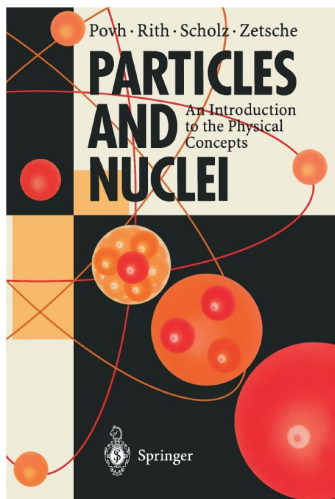
$$G^{\text{dipole}}(Q^2) = \left(1 + \frac{Q^2}{0.71 (\text{GeV}/c)^2} \right)^{-2}$$

Form factor and spatial distribution

$$\left(\frac{d\sigma}{d\Omega}\right)_{\text{exp}} = \left(\frac{d\sigma}{d\Omega}\right)_{\text{Mott}} \cdot |F(\mathbf{q}^2)|^2$$

$$F(\mathbf{q}^2) = \int d^3\mathbf{r} \rho(\mathbf{r}) \cdot e^{i\mathbf{q}\cdot\mathbf{r}}$$

Form factors and spatial distributions
(charge, magnetization)
are Fourier pairs

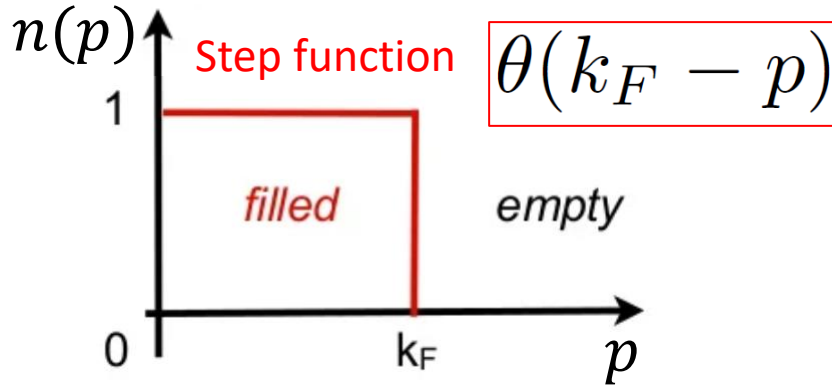


Charge distribution $\rho(r)$	Form factor $F(\mathbf{q}^2)$	Example
pointlike	constant	Electron
exponential	dipole	Proton
gauss	gauss	${}^6\text{Li}$
homogeneous sphere	oscillating	—
sphere with a diffuse surface	smeared oscillations	${}^{40}\text{Ca}$

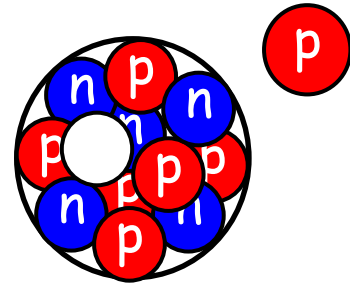
$r \longrightarrow$ $|\mathbf{q}| \longrightarrow$

An example of hadronic tensor for the nucleus excitations: Quasielastic (1p-1h) excitation in the Relativistic Fermi Gas (RFG)

- Relativistic Fermi Gas: Nucleus as ensemble of non interacting fermions (nucleons)
- In the RFG ground state all the momenta \mathbf{p} with $|\mathbf{p}| < k_F$ (Fermi momentum) are filled



EW current approximated by 1-body operator, which can produce only 1particle--1hole (1p1h) excitations



RFG 1p-1h (QE) hadronic tensor

J.E. Amaro et al. J.Phys.G 47 (2020) 12, 124001

$$W^{\mu\nu}(q, \omega) = \sum_{\mathbf{p}} \sum_{s, s'} \delta(E' - E - \omega) \frac{m_N^2}{EE'} J_{s's}^{\mu*}(\mathbf{p}', \mathbf{p}) J_{s's}^{\nu}(\mathbf{p}', \mathbf{p}) \theta(k_F - p) \theta(p' - k_F)$$

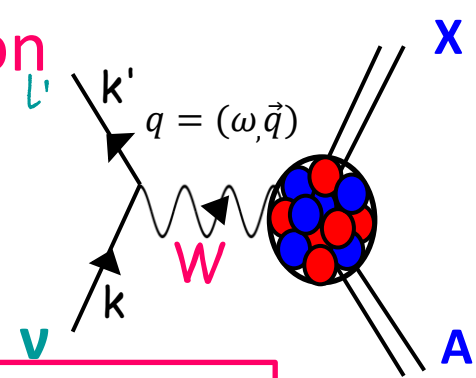
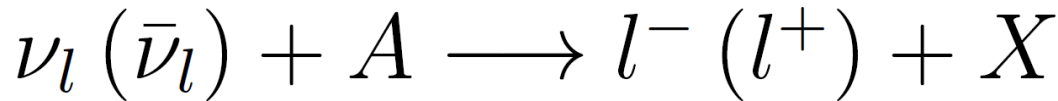
$$W^{\mu\nu}(q, \omega) = \frac{V}{(2\pi)^3} \int d^3p \delta(E' - E - \omega) \frac{m_N^2}{EE'} 2w_{s.n.}^{\mu\nu}(\mathbf{p}', \mathbf{p}) \theta(k_F - p) \theta(p' - k_F)$$

Single-nucleon
hadronic tensor

$$w_{s.n.}^{\mu\nu}(\mathbf{p}', \mathbf{p}) = \frac{1}{2} \sum_{ss'} J_{s's}^{\mu*}(\mathbf{p}', \mathbf{p}) J_{s's}^{\nu}(\mathbf{p}', \mathbf{p})$$

see slide 38 for the expressions of J^{μ}

Charged current neutrino-nucleus cross section



Lab frame

$$\frac{d^2\sigma}{d\Omega_{\mathbf{k}'} d\omega} = \frac{G_F^2 \cos^2 \theta_C}{4\pi^2} \frac{|\mathbf{k}'|}{|\mathbf{k}|} L_{\mu\nu} W^{\mu\nu}(\mathbf{q}, \omega)$$

$d\Omega_{\mathbf{k}'}$ differential solid angle in the direction specified by the charged-lepton momentum \mathbf{k}'

$$k \equiv (E_\nu, \mathbf{k}) \quad k' \equiv (E_l', \mathbf{k}') \quad q = k - k' \equiv (\omega, \mathbf{q}) \quad \omega = E_\nu - E_l'$$

initial and final lepton 4-momenta

four-momentum transfer

energy transfer

The charged current cross section is a linear combination of five contributions

$$\frac{d^2\sigma}{d\Omega_{\mathbf{k}'} d\omega} = \sigma_0 \left[L_{00} W^{00} + L_{33} W^{33} + (L_{03} + L_{30}) W^{03} + (L_{11} + L_{22}) W^{11} \pm (L_{12} - L_{21}) W^{12} \right]$$

- The notation {00; 03; 33; 11; 12} is often replaced by {00; 0z; zz; xx; xy} or {CC;CL; LL;T; T'} where the letters C, L and T stand for Coulomb, Longitudinal and Transverse respectively
- The explicit expression of the lepton coefficients L (which depend only on lepton kinematics) and of the components of the hadronic tensor W can be found in many books and articles. For example:
Walecka, J. D. (1995), "Theoretical nuclear and subnuclear physics", Oxford Stud. Nucl. Phys., 16
O'Connell et al. PRC 6 719-733 (1972); Nieves et al. PRC 70 055503 (2004); Amaro et al. PRC C 71 065501 (2005);
Martini et al. PRC 80 065501 (2009); Shen et al. PRC 86 035503 (2012)

A simplified expressions particularly useful for illustration

- Final lepton mass contributions ignored ($m_l=0$)
- Obtained by keeping only the leading terms for the hadronic tensor in the development of the hadronic current in p/M_N

$$\frac{d^2\sigma}{d\cos\theta d\omega} = \frac{G_F^2 \cos^2\theta_c}{\pi} |k'| E_l' \cos^2\frac{\theta}{2} \left[\frac{(\mathbf{q}^2 - \omega^2)^2}{\mathbf{q}^4} G_E^2 R_T(\mathbf{q}, \omega) + \frac{\omega^2}{\mathbf{q}^2} G_A^2 R_{\sigma\tau(L)}(\mathbf{q}, \omega) \right] \\ + 2 \left(\tan^2\frac{\theta}{2} + \frac{\mathbf{q}^2 - \omega^2}{2\mathbf{q}^2} \right) \left(G_M^2 \frac{\mathbf{q}^2}{4M_N^2} + G_A^2 \right) R_{\sigma\tau(T)}(\mathbf{q}, \omega) \pm 2 \frac{E_\nu + E_l'}{M_N} \tan^2\frac{\theta}{2} G_A G_M R_{\sigma\tau(T)}(\mathbf{q}, \omega)$$

Explicitly appear:

1. The different **kinematic variables** (related to the leptonic tensor)
2. The nucleon Electric, Magnetic, and Axial **form factors** (\leftrightarrow nucleon properties)
3. The **nuclear response functions** (\leftrightarrow nuclear dynamics)

Nuclear response functions $R(\mathbf{q}, \omega)$:

$$R_\alpha^{PP'}(\mathbf{q}, \omega) = \sum_n \langle n | \sum_{j=1}^A O_\alpha^P(j) e^{i\mathbf{q}\cdot\mathbf{x}_j} | 0 \rangle \langle n | \sum_{k=1}^A O_\alpha^{P'}(k) e^{i\mathbf{q}\cdot\mathbf{x}_k} | 0 \rangle^* \delta(\omega - E_n + E_0),$$

Isovector R_τ

$$O_\alpha^N(j) = \tau_j^\pm$$

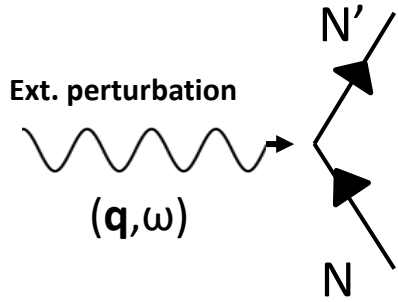
Isospin Spin-Longitudinal $R_{\sigma\tau(L)}$

$$(\boldsymbol{\sigma}_j \cdot \hat{\mathbf{q}}) \tau_j^\pm$$

Isospin Spin-Transverse $R_{\sigma\tau(T)}$

$$(\boldsymbol{\sigma}_j \times \hat{\mathbf{q}})^i \tau_j^\pm$$

Free (or bare) nuclear response function



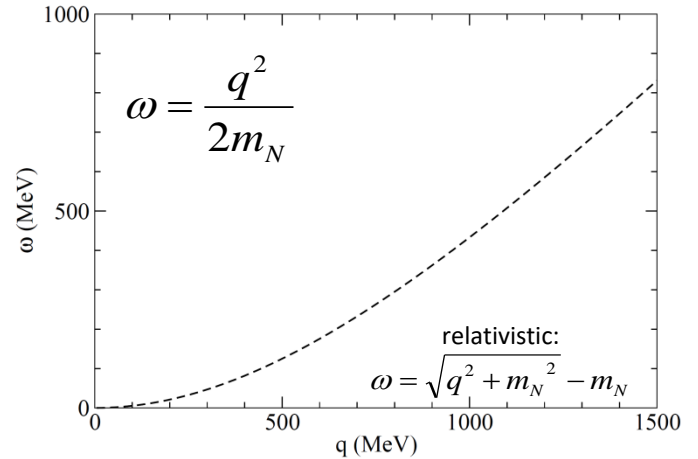
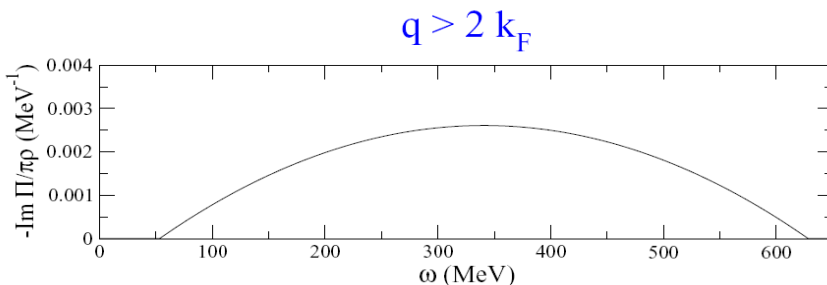
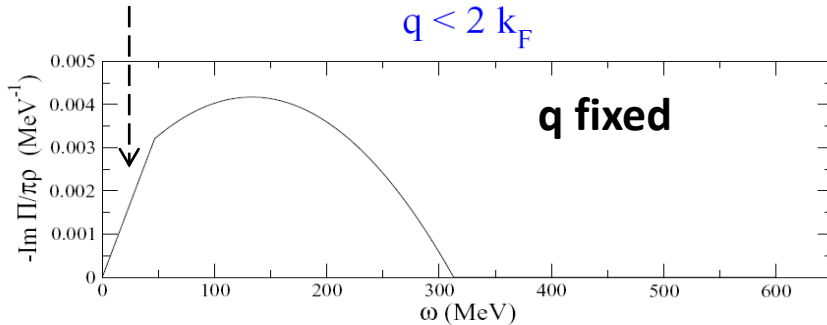
- Free nucleon at rest:
Response functions $\propto \delta(\omega - q^2/2m_N)$

- Nucleon inside the nucleus:

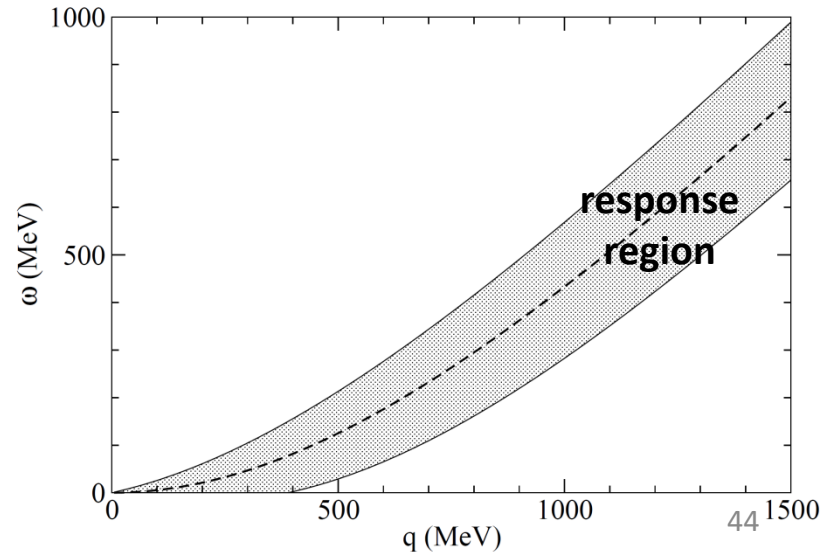
Nucleon-Nucleon interaction switched off \leftrightarrow Nucleons respond individually

Fermi Gas Quasielastic Response

- Fermi motion spreads δ distribution
- Pauli blocking cuts part of the low q and ω response



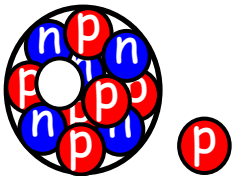
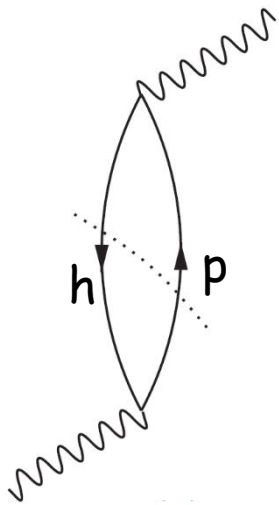
$$\frac{q^2}{2m_N} - \frac{qk_F}{m_N} \leq \omega \leq \frac{q^2}{2m_N} + \frac{qk_F}{m_N}$$



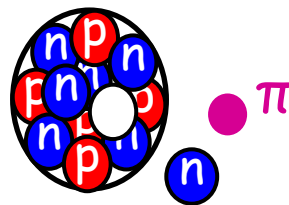
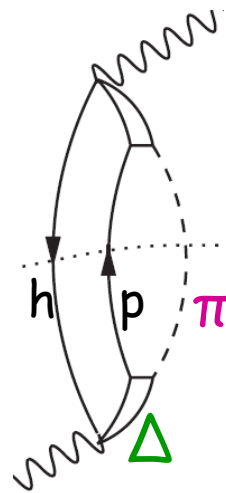
Nuclear Responses for different excitations

$$R_\alpha = \sum_{n \neq 0} |\langle n | \hat{O}_{(\alpha)} | 0 \rangle|^2 \delta[\omega - (E_n - E_0)]$$

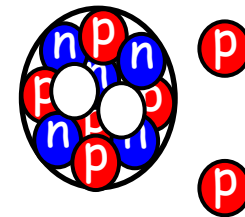
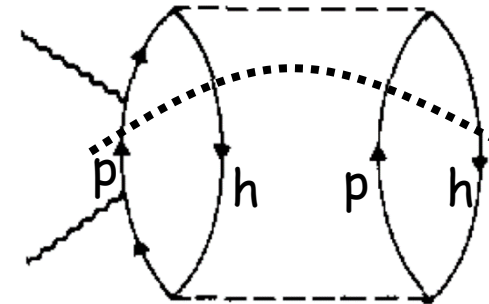
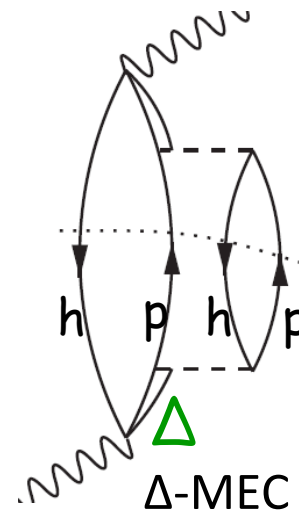
1p-1h
Quasielastic



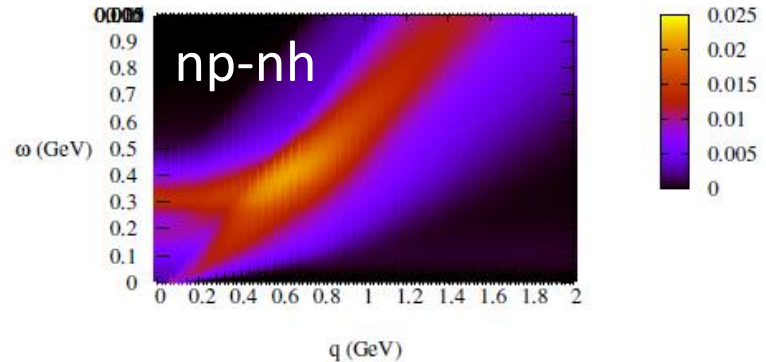
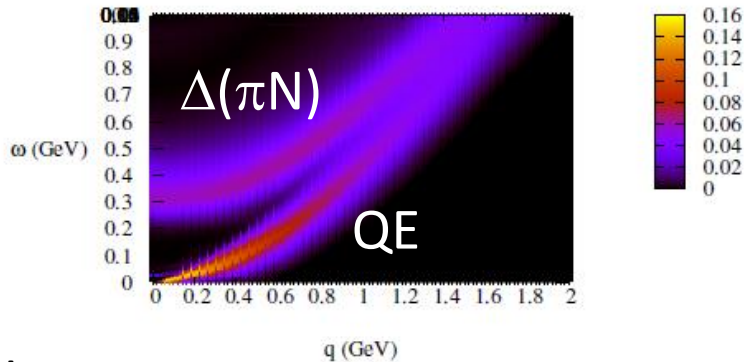
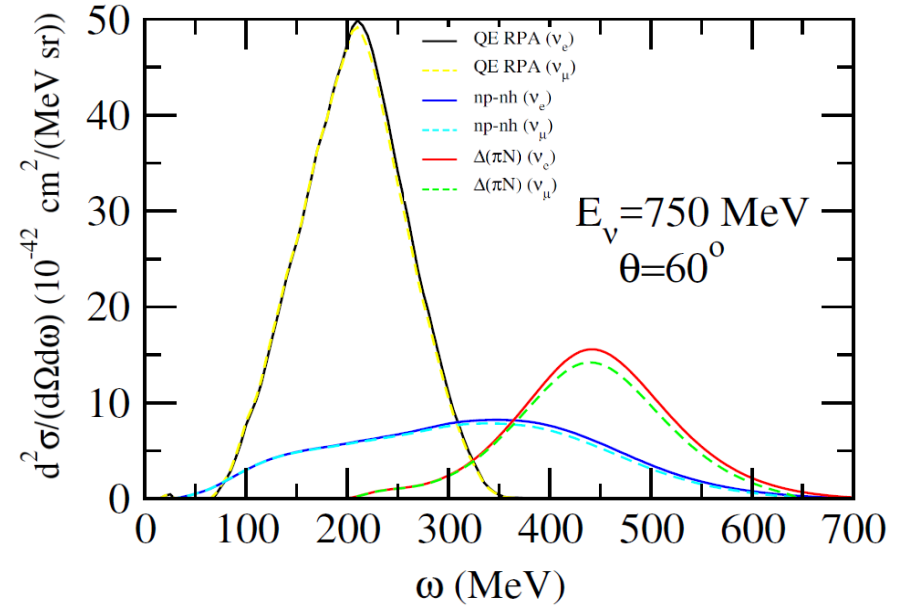
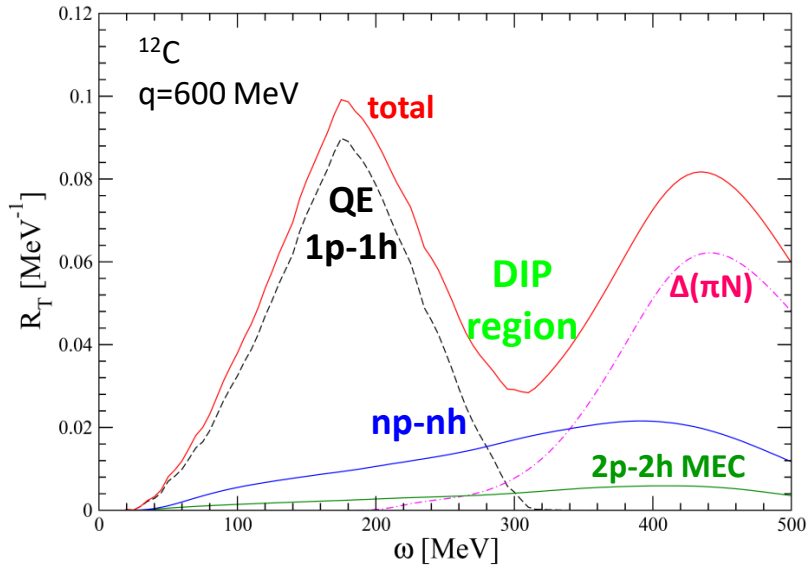
1p-1h
($\Delta \rightarrow \pi N$) 1π production



2p-2h:
two examples



Nuclear responses and neutrino cross sections at fixed kinematics



QE peak:

$$\omega = \sqrt{\mathbf{q}^2 + M_N^2} - M_N = \frac{Q^2}{2M_N} = \frac{\mathbf{q}^2 - \omega^2}{2M_N}$$

Δ peak:

$$\omega = \sqrt{\mathbf{q}^2 + M_\Delta^2} - M_N = \frac{Q^2}{2M_N} + \frac{M_\Delta^2 - M_N^2}{2M_N}$$

np-nh excitations fill the DIP region

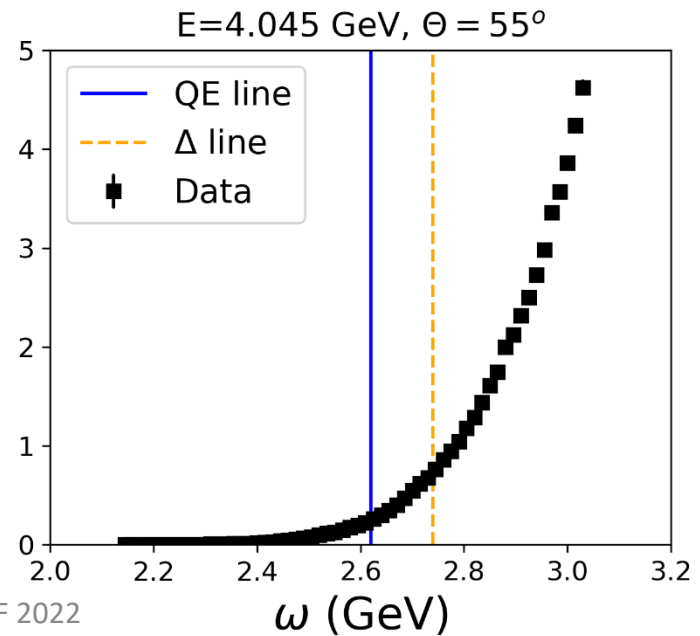
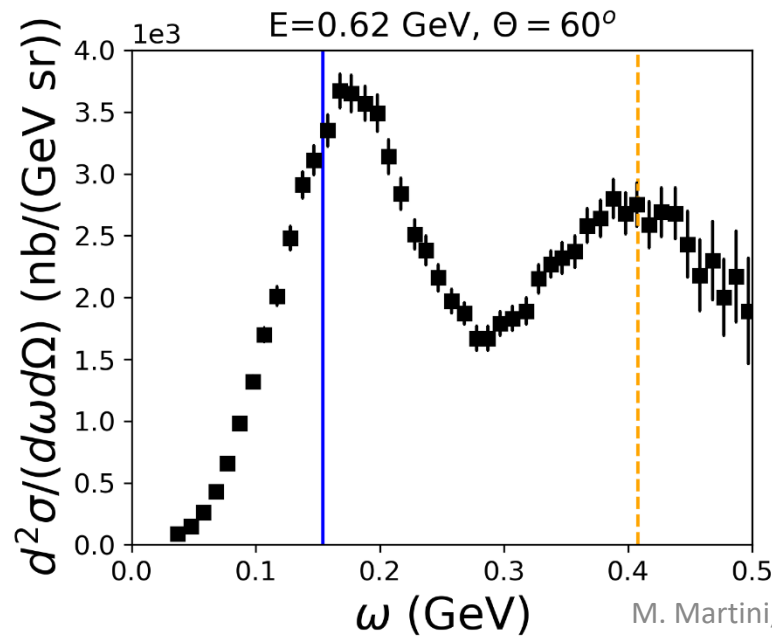
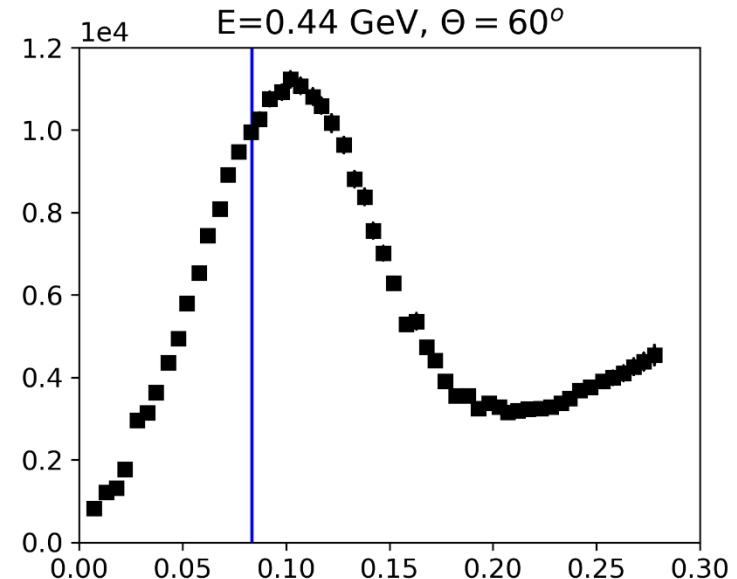
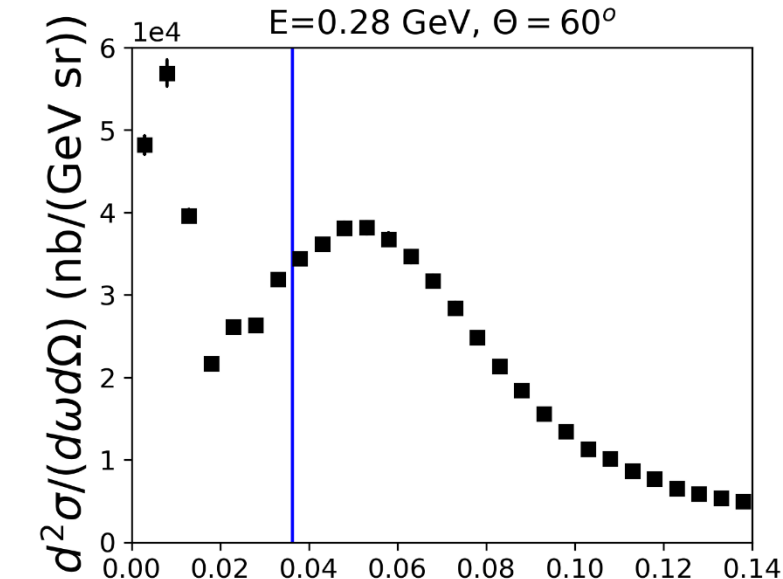
np-nh enlarges the region of response to the whole (ω, q) plane

Examples of electron scattering cross section on ^{12}C

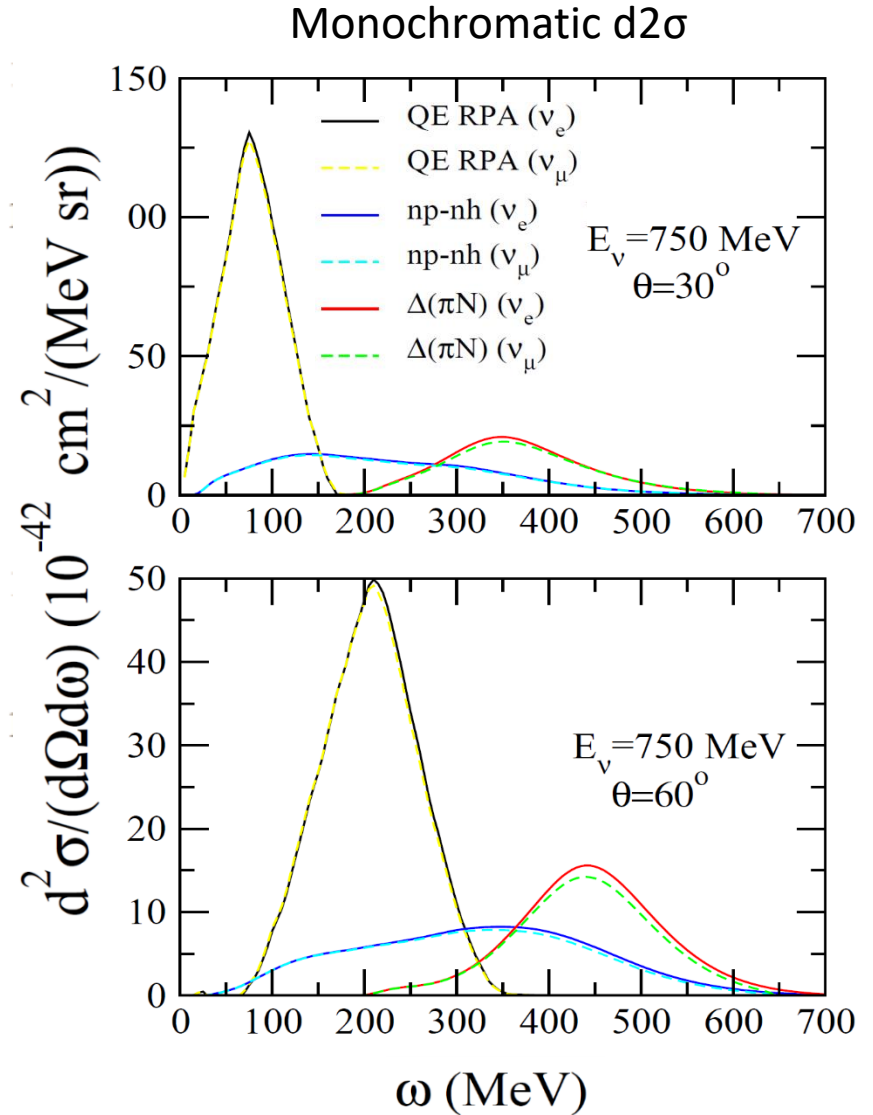
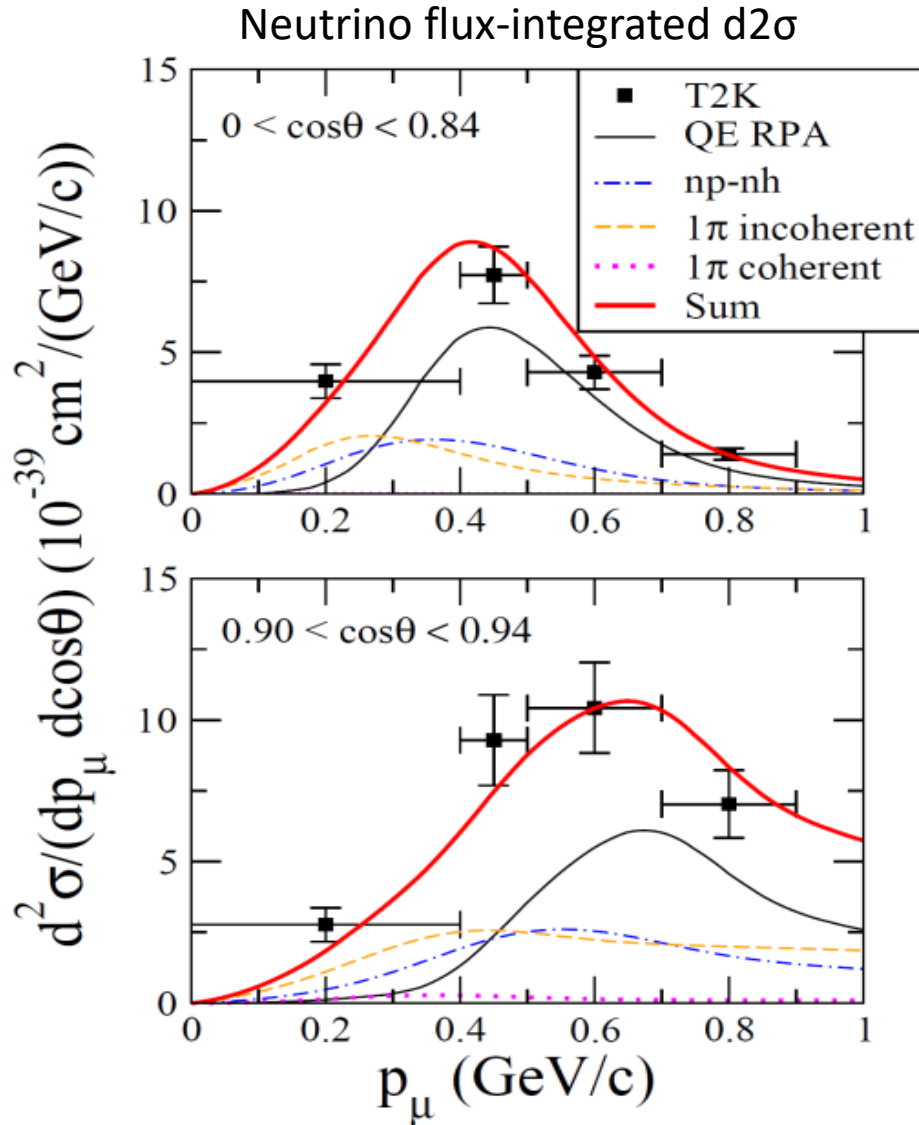
Remind: monochromatic beam

$$\omega_{QE} = \frac{E^2(1 - \cos\theta)}{M_N + E(1 - \cos\theta)}$$

$$\omega_{\Delta} = \frac{M_N\Delta M + E^2(1 - \cos\theta)}{M_N + E(1 - \cos\theta)},$$



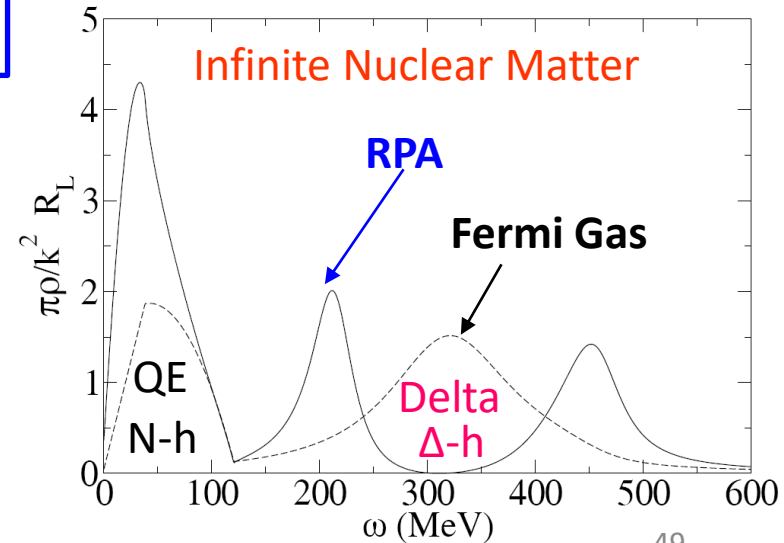
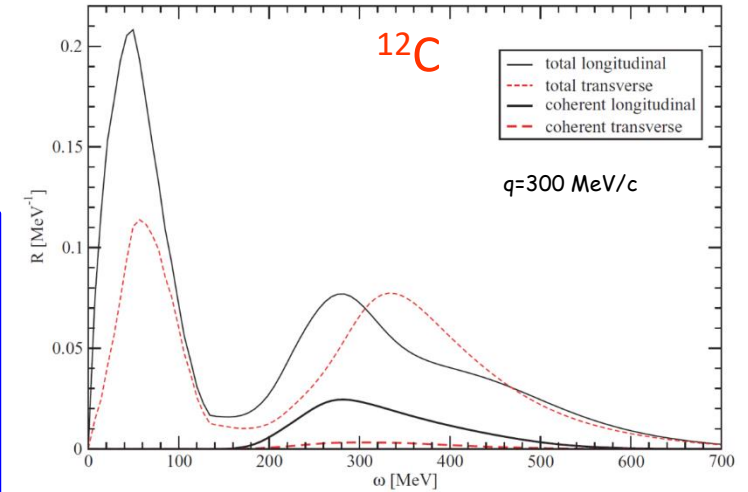
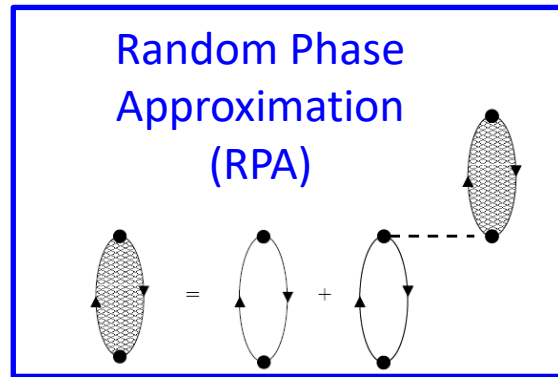
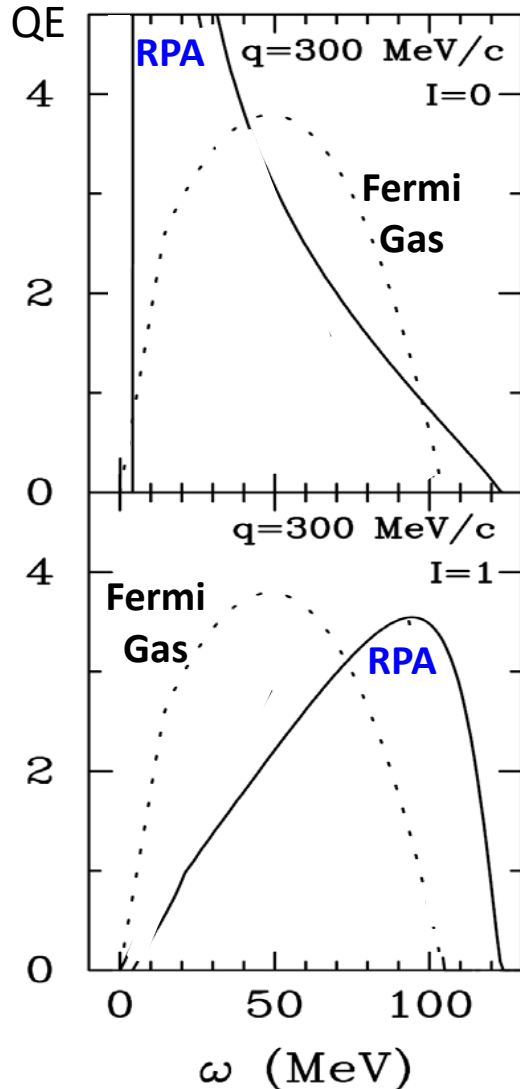
Remark: flux-integrated .vs. monochromatic beam cross sections



In the flux-integrated cross sections the different channels are entangled

Switching on the nucleon- nucleon interaction

- External force acting on one nucleon is transmitted to the neighbors by the interaction – **Long Range Correlations**
- The nuclear response becomes collective
- Shift of the peak with respect to Fermi Gas, decrease, increase depending on the channels of excitation



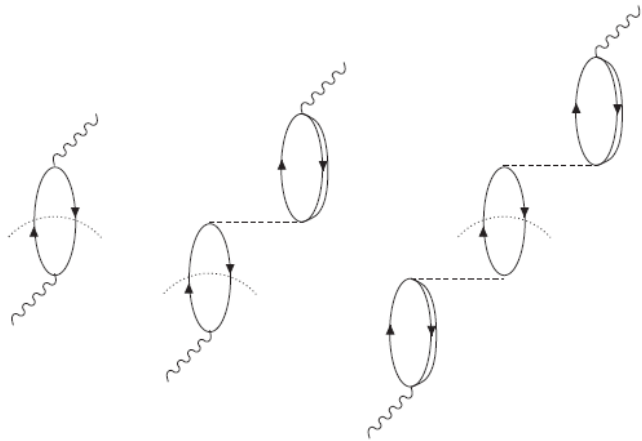
Neutrino scattering - Effects of the RPA in the genuine quasielastic channel

QE totally dominated by isospin spin-transverse response $R_{\sigma\tau(T)}$

RPA reduction

- expected from the repulsive character of p-h interaction in T channel
- also due to interference term $R^{N\Delta} < 0$
(Lorentz-Lorenz or Ericson-Ericson effect [*M. Ericson, T. Ericson, Ann. Phys. 36, 323 (1966)*])

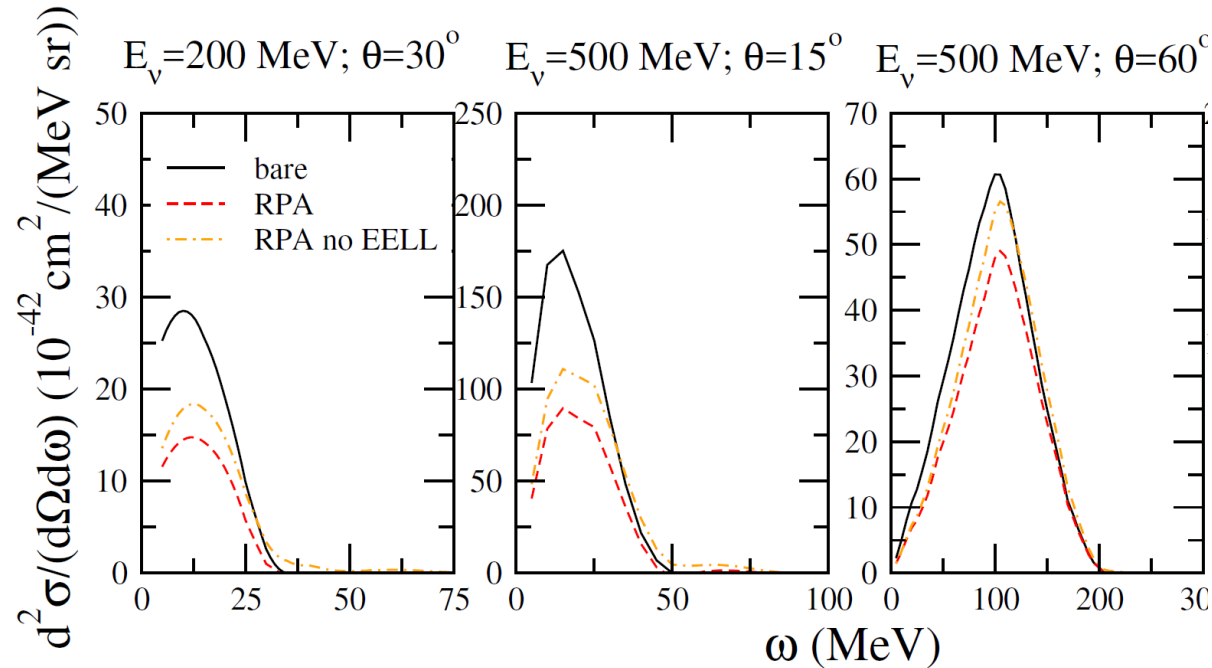
Lowest order contribution to QE:



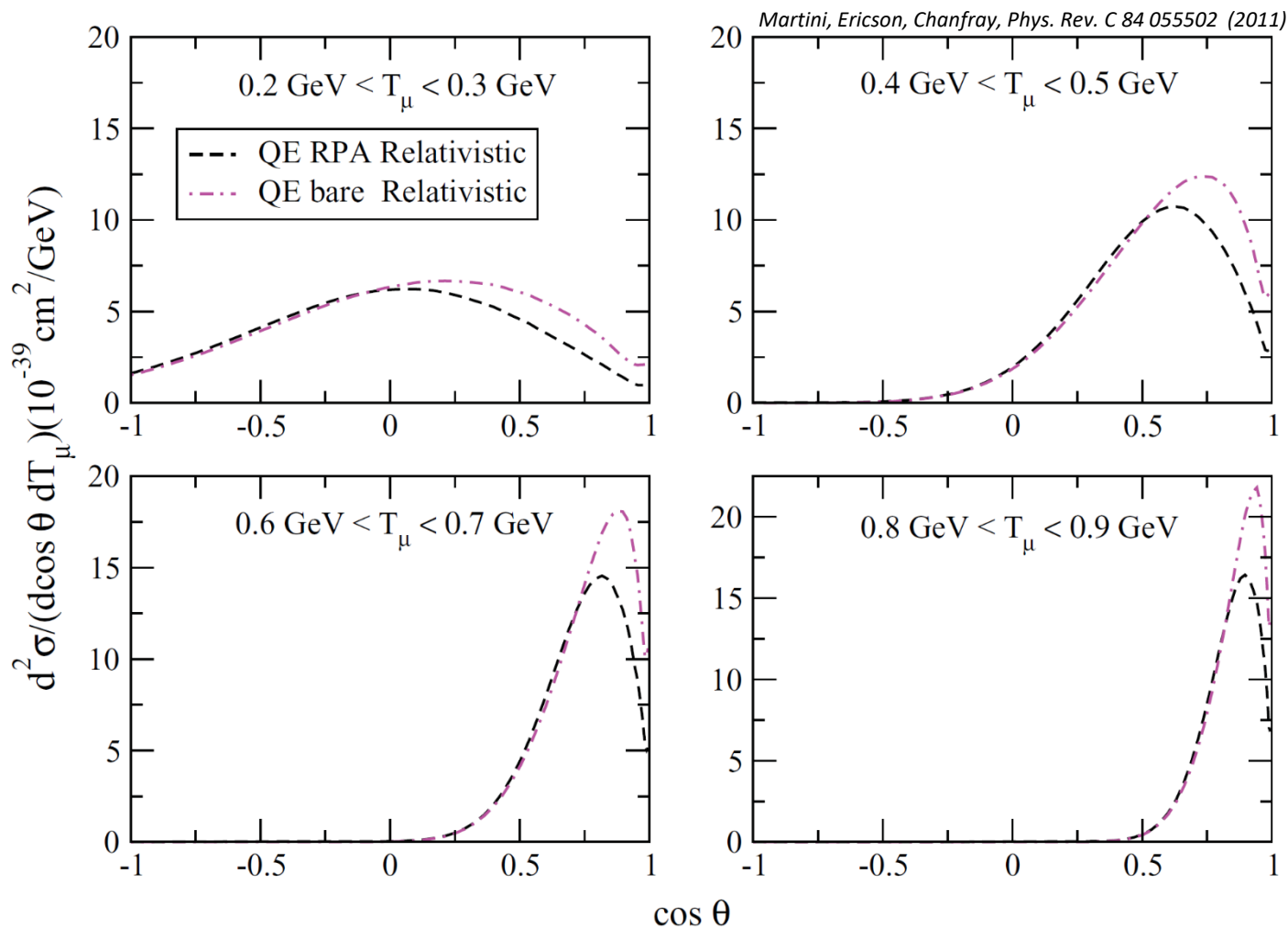
R_{QE}^{NN}

$R_{QE}^{N\Delta}$

$R_{QE}^{\Delta\Delta}$



Bare vs RPA for MiniBooNE flux integrated $d^2\sigma$ (genuine QE)



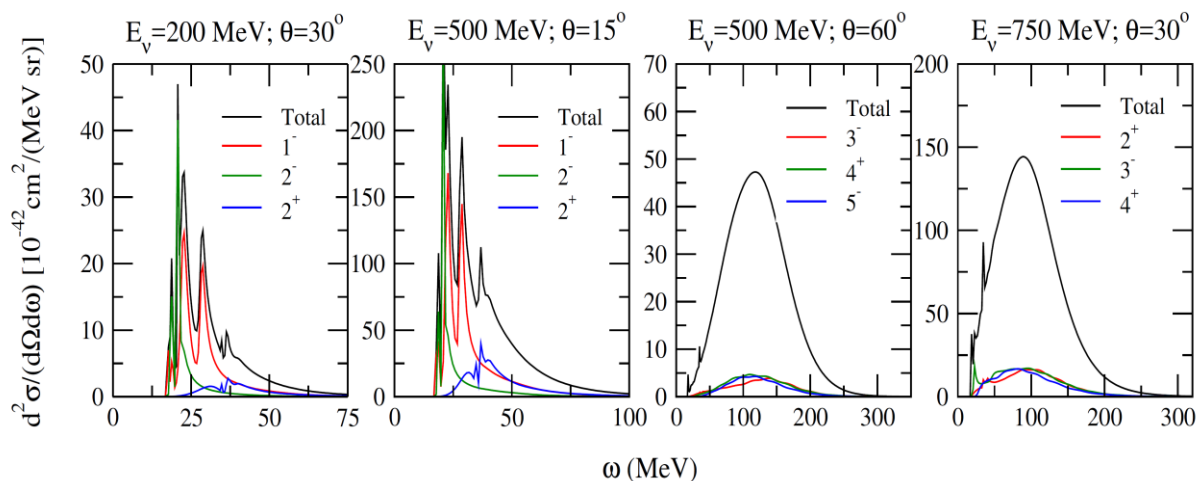
RPA produces a quenching and some shift towards larger angles

The Hartree Fock + Continuum RPA for giant resonances and QE

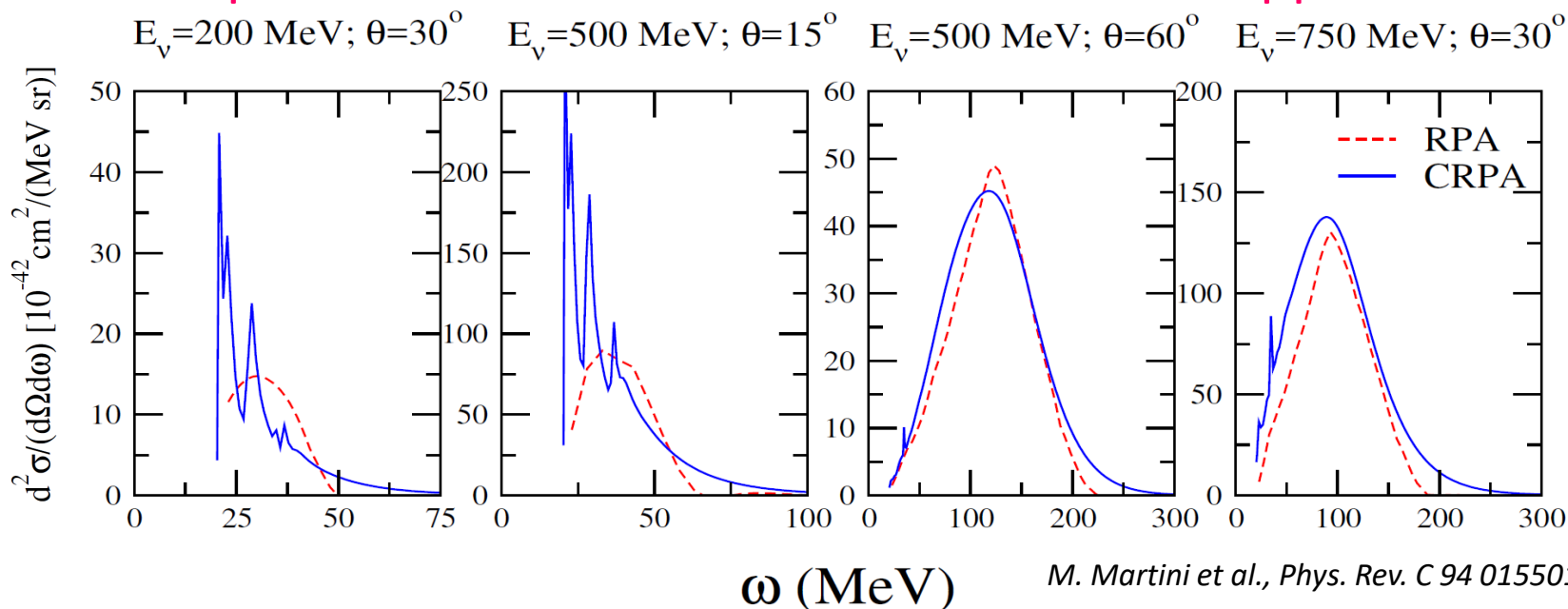
HF+CRPA (Ghent)

Pandey et al. Phys.Rev. C94 054609 (2016)

- Shell effects and giant resonances
- Different multipolar excitations



Comparison between LFG+RPA and HF+CRPA approaches



M. Martini et al., Phys. Rev. C 94 015501 (2016)

- The two approaches are essentially in agreement
- In the low energy part the LFG+RPA results represent the average of the HF+CRPA ones

Several models to calculate the responses and the ν cross sections

- Local Fermi Gas + Random Phase Approximation

Lyon M. Martini, M. Ericson, G. Chanfray, J. Marteau, *Phys. Rev. C* 80 065501 (2009)

Valencia J. Nieves, I. Ruiz Simo, M.J. Vicente Vacas, *Phys. Rev. C* 83 045501 (2011)

- Hartree-Fock + (Continuum) Random Phase Approximation

Ghent V. Pandey, N. Jachowicz, T. Van Cuyck, J. Ryckebusch, M. Martini, *Phys. Rev. C* 92 024606 (2015)

Other groups focused on giant resonances and below Kolbe et al. ; Volpe et al.; Co' et al.; ...

- SuSAv2 superscaling/relativistic mean field

Granada, Madrid, MIT, Sevilla, Torino

G.D. Megias, J.E. Amaro, M.B. Barbaro, J.A. Caballero, T.W. Donnelly, I. Ruiz Simo, *PRD* 94 093004 (2016)

- Spectral function approach

Roma N. Rocco, C. Barbieri, O. Benhar, A. De Pace, A. Lovato, *Phys. Rev. C* 99 025502 (2019)

- Relativistic Green's function

Pavia A. Meucci, C. Giusti, F. D. Pacati, *Nucl.Phys.A* 739 277-290 (2004)

- Green's function Monte Carlo ("ab initio")

Argonne, Los Alamos A. Lovato, J. Carlson, S. Gandolfi, N. Rocco, R. Schiavilla, *PRX* 10 031068 (2020)

- GiBUU transport theory

Giessen O. Buss, T. Gaitanos, K. Gallmeister, H. van Hees, M. Kaskulov, O. Lalakulich, A.B. Larionov, T. Leitner, J. Weil, U. Mosel, *Phys.Rept.* 512 1-124 (2012)

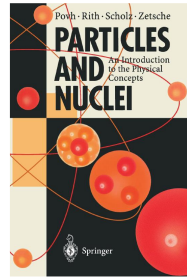
p.s. only one representative reference for each approach (not necessarily the founding paper)

For discussions and comparisons of different models see for example:

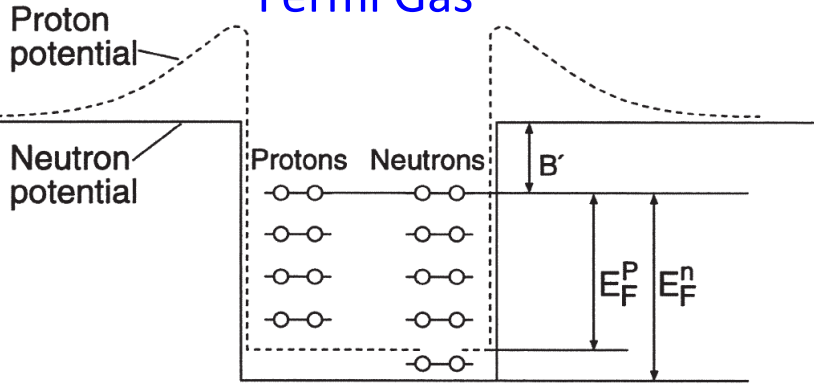
- G.T. Garvey, D.A. Harris, H.A. Tanaka, R. Tayloe, G.P. Zeller, *Phys.Rept.* 580 (2015) 1-45
- T. Katori, M. Martini, *J.Phys.G* 45 (2018) 1, 013001
- M. Sajjad Athar, A. Fatima, S. K. Singh *arxiv.* 2206.13792

Simple nuclear models in introductory books

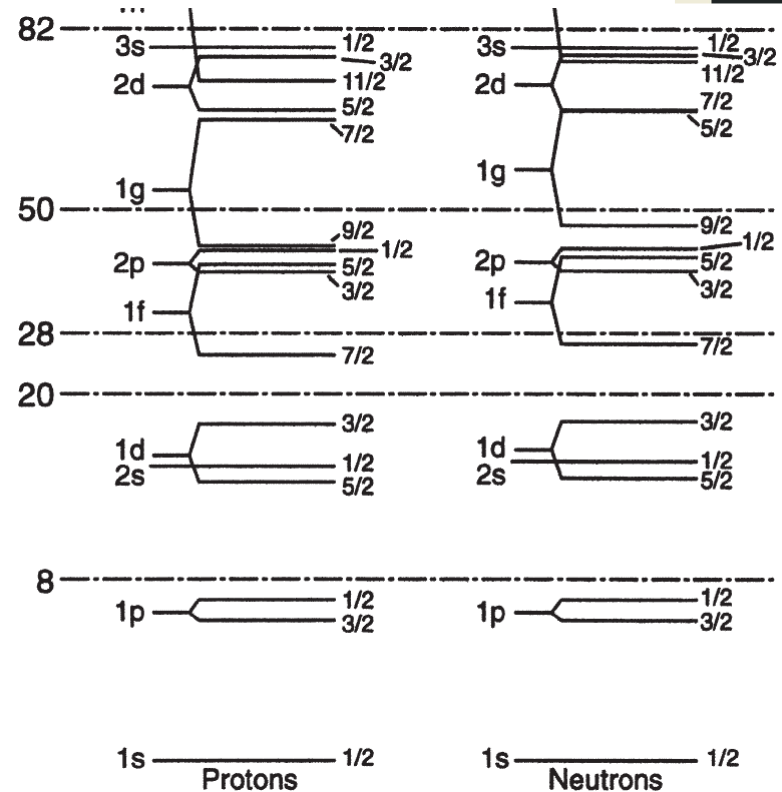
Independent particles models



Fermi Gas



Shell Model



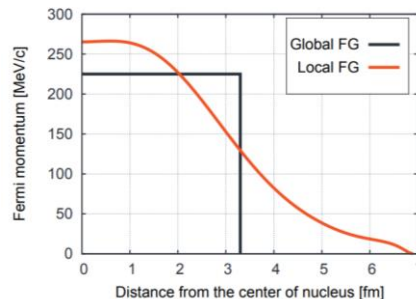
- Protons and neutrons move freely within the nuclear volume V
- Retained only statistical correlations (Pauli principle)
- In the nuclear ground state, the lowest states are all occupied up to a maximal momentum called Fermi momentum k_F

$$\frac{Z}{V} = \rho_p = \frac{(k_F^p)^3}{3\pi^2} \quad \frac{N}{V} = \rho_n = \frac{(k_F^n)^3}{3\pi^2} \quad \frac{A}{V} = \rho = \frac{2k_F^3}{3\pi^2}$$

Local Fermi Gas

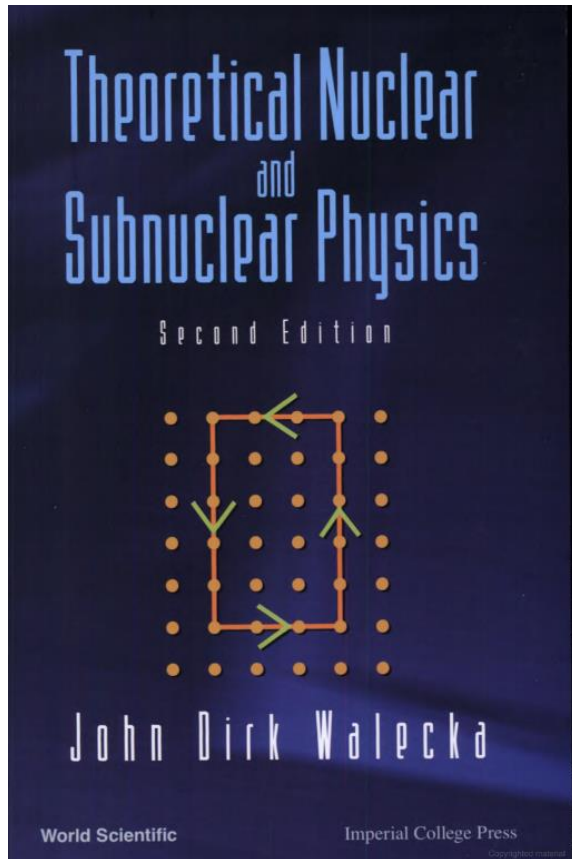
Local Density approximation

$$k_F(r) = [3/2 \pi^2 \rho(r)]^{1/3}$$

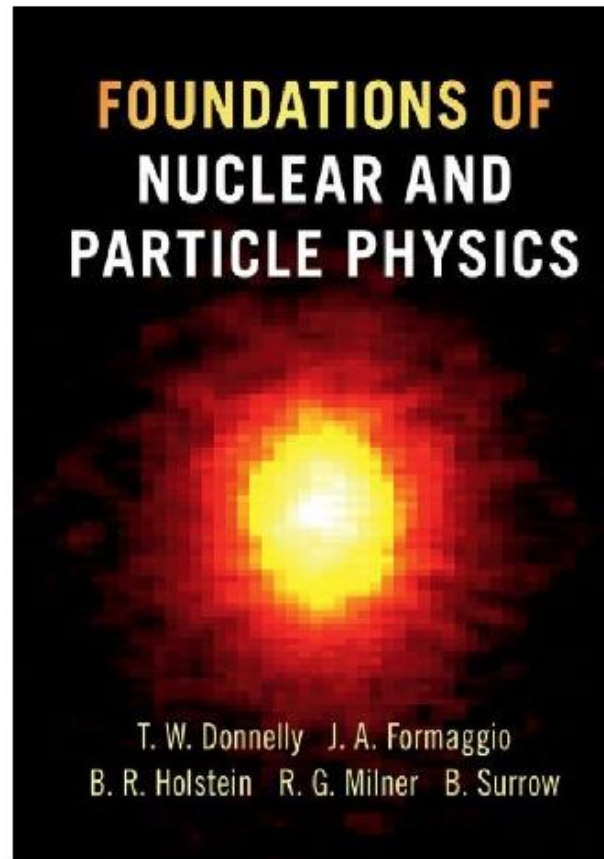


- The nucleons move inside a mean field potential produced by the other nucleons
- Discrete energy levels arise which are filled up according to the Pauli principle

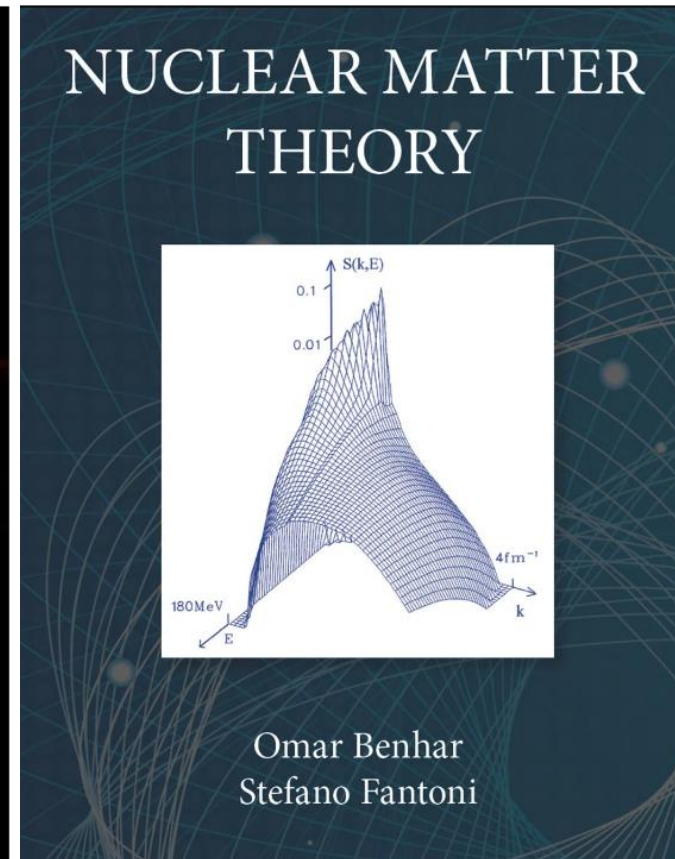
More sophisticated models in advanced books



- Hartree-Fock
- RPA
- Relativistic Mean Field
- Quantum Hadrodynamics



- Hartree-Fock
- Scaling
- Spectral function



- Spectral function
- Green's function methods
- Monte Carlo methods
- Variational methods (CBF, FHNC)
- Relativistic Mean Field

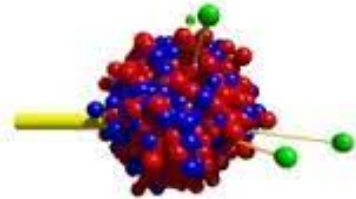
Monte Carlo Event Generators

Monte Carlo event generators connects theoretical models to experimental measurements

Main Event Generators for neutrino interactions:



GiBUU



NEUT



L. Alvarez-Ruso et al.,
EPJ Spec. Top. 230, 4449 (2021)

O. Buss et al.,
Phys.Rept. 512 1-124 (2012)

Y. Hayato and L. Pickering,
EPJ Spec. Top. 230, 4469 (2021)

T. Golan et al.,
NPB 229–232, 499 (2012)

PHYSICAL REVIEW D **105**, 092004 (2022)

Comparisons and challenges of modern neutrino-scattering experiments

M. Buizza Avanzini¹, M. Betancourt², D. Cherdack³, M. Del Tutto^{2,4}, S. Dytman⁵, A. P. Furmanski^{6,7},
S. Gardiner², Y. Hayato⁸, L. Koch⁹, K. Mahn¹⁰, A. Mastbaum¹¹, B. Messerly^{5,7}, C. Riccio^{12,13},
D. Ruterbories¹⁴, J. Sobczyk¹⁵, C. Wilkinson¹⁶ and C. Wret¹⁴

Main models implemented for the quasielastic (and 2p-2h):

- Relativistic global and local Fermi Gas
- RPA
- Spectral Function
- SuperScaling (SuSAv2)

We have already rapidly illustrated the Fermi Gas and the RPA.

In the following the SuperScaling and the spectral function will be briefly sketched
2p-2h will be discussed in the second lecture

SuperScaling

- The basic idea of the approach [J.E. Amaro et al., PRC71 (2005) 015501] is to exploit electron scattering in order to predict the neutrino scattering cross section based on the “superscaling” properties of inclusive electron scattering data, extensively analysed in the 90s [Day et al., Ann.Rev.Nucl.Part.Sci.40 (1990); Donnelly and Sick, PRL82; PRC60 (1999)]

- Extract a **SuperScaling function** from electron scattering inclusive data

$$f(q, \omega; k_F) = k_F \times \frac{[d^2\sigma/d\omega d\Omega]_{exp}^{(e,e')}}{\bar{\sigma}_{eN}}$$

- Plot it as function of a **Scaling variable** which is a combination of q and ω

$$\psi \equiv \psi(q, \omega; k_F)$$

- SuperScaling** is realized if:

$$\psi(q, \omega; k_F) \longrightarrow f(\psi)$$

- I) f is independent of the kinematics (q) for a given nucleus (scaling of first kind)
- II) f is independent of the nucleus (k_F) for given kinematics (scaling of second kind)

The SuperScaling function f is a universal function encoding the nuclear dynamics.

It can be extracted from electron scattering experiment or calculated within a model.

- Final step: Use the SuperScaling function to predict the **neutrino cross sections**

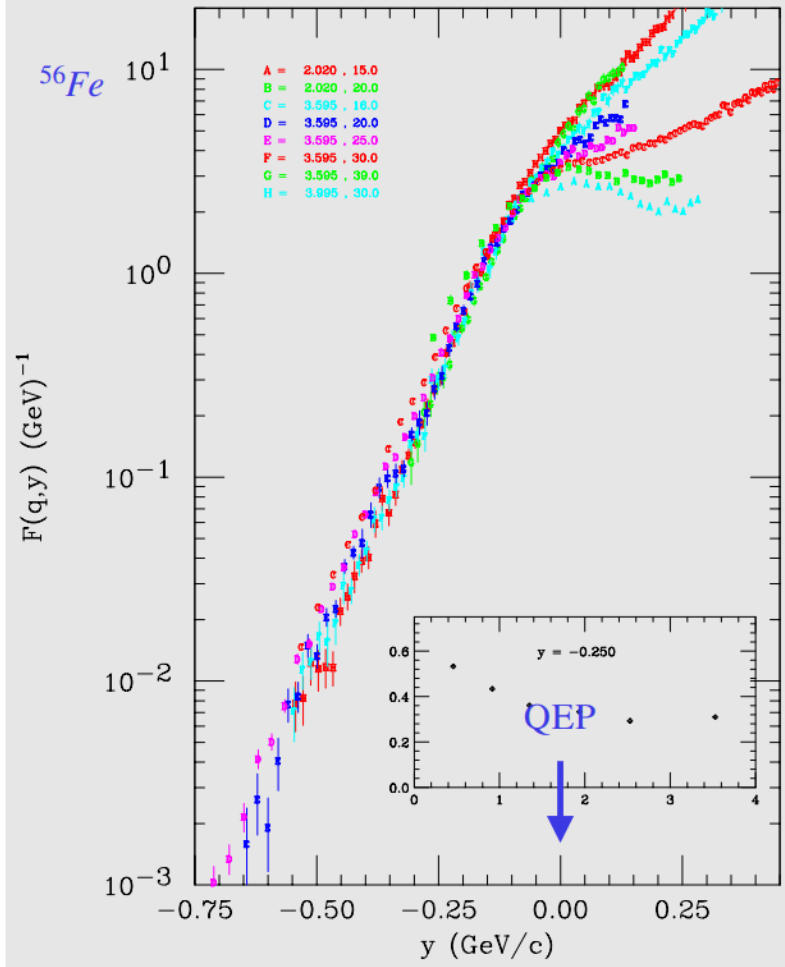
$$[d^2\sigma/d\omega d\Omega]^{(\nu,l)} = \frac{1}{k_F} \bar{\sigma}_{\nu N} f(\psi)$$

SuperScaling of inclusive electron scattering data

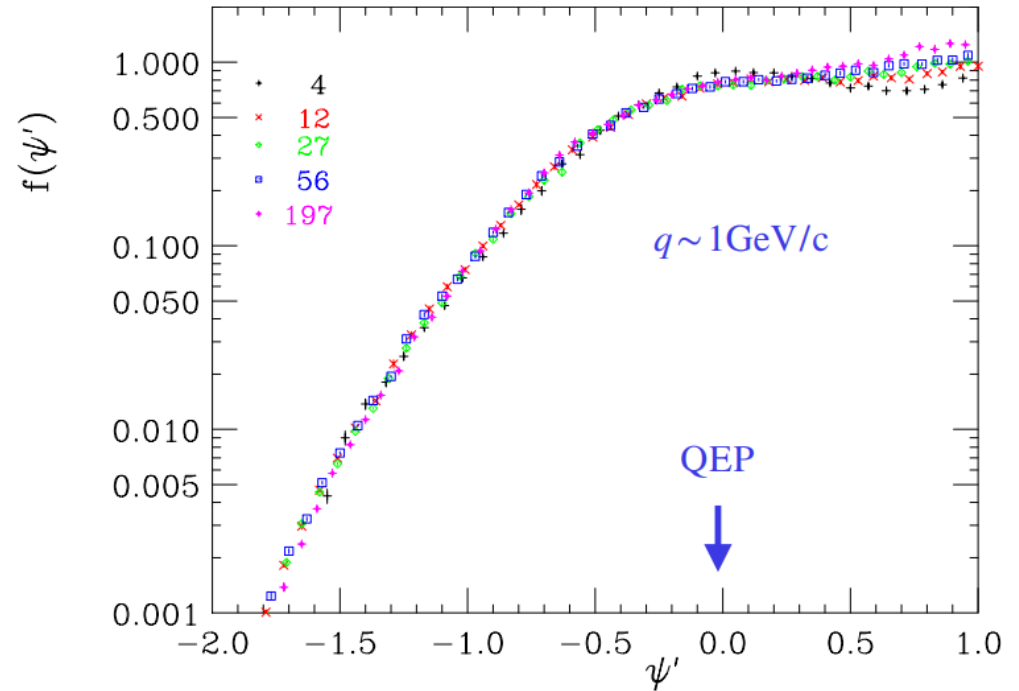
- How well and at which kinematics does SuperScaling work?

Day et al., *Ann.Rev.Nucl.Part.Sci.*40 (1990); Donnelly and Sick, *PRL*82; *PRC*60 (1999)

I kind: fixed target, varying kinematics



II kind: fixed kinematics, varying target



- SuperScaling is well realized below the Quasi Elastic Peak
- Scaling violations occur beyond the Quasi Elastic Peak

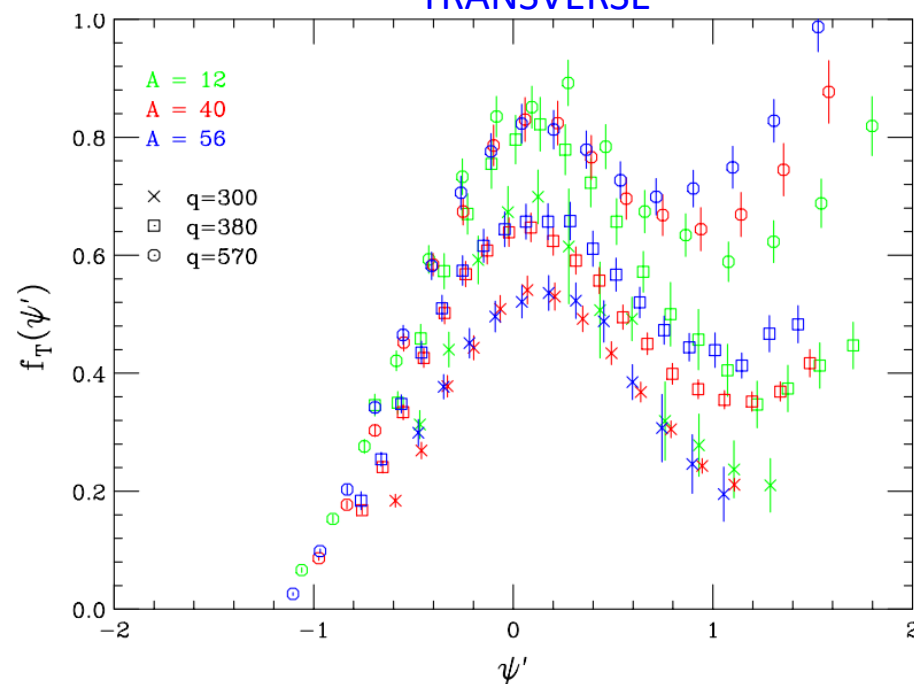
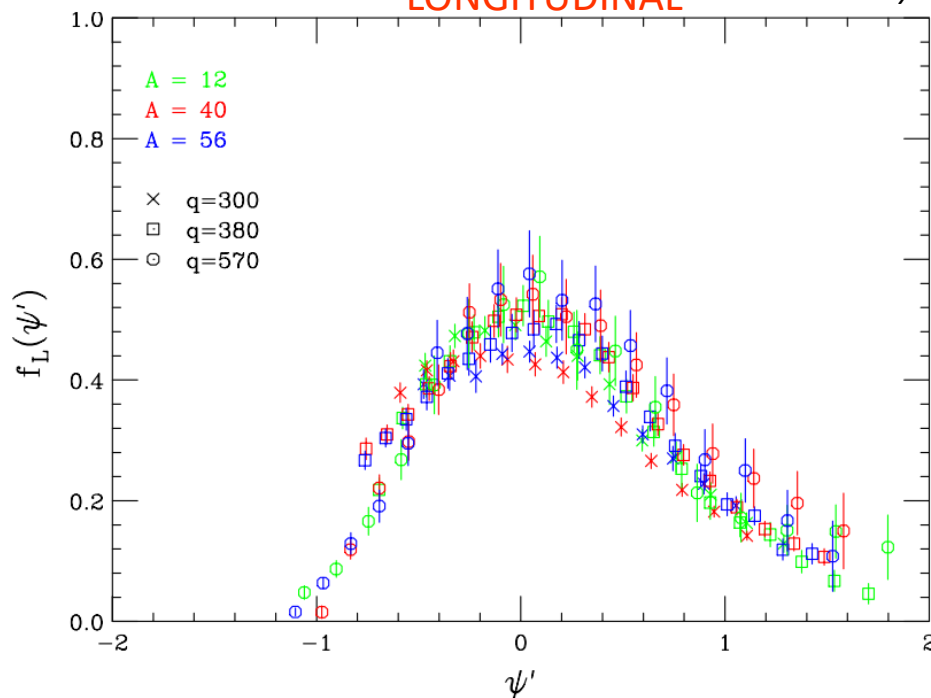
Scaling violations: longitudinal and transverse Superscaling

$$\frac{d^2\sigma}{d\theta d\omega} = \sigma_M \left\{ \frac{(\omega^2 - q^2)^2}{q^4} R_L(\omega, q) + \left[\tan^2\left(\frac{\theta}{2}\right) - \frac{\omega^2 - q^2}{2q^2} \right] R_T(\omega, q) \right\}$$

LONGITUDINAL

Donnelly et al. PRC 60 '99

TRANSVERSE



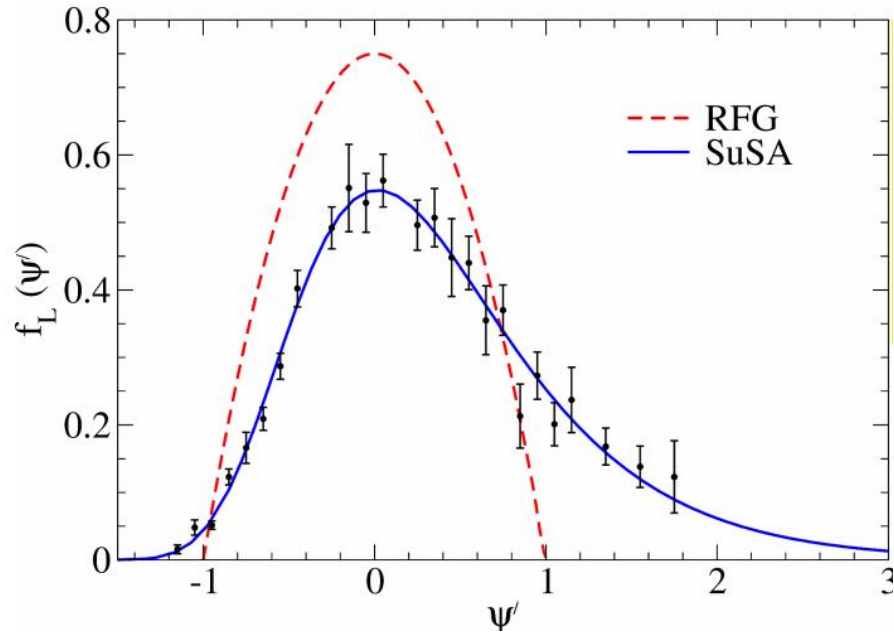
$$f_L(\psi) = k_F \frac{R_L(q, \omega)}{G_L^{e, e'}(q, \omega)}$$

$$f_T(\psi) = k_F \frac{R_T(q, \omega)}{G_T^{e, e'}(q, \omega)}$$

- The **longitudinal** response **scales**
- **Scaling violations** are mainly **transverse** (2p-2h, Δ resonance and other inelastic processes)

The SuSA and SuSAv2 models in the quasielastic region

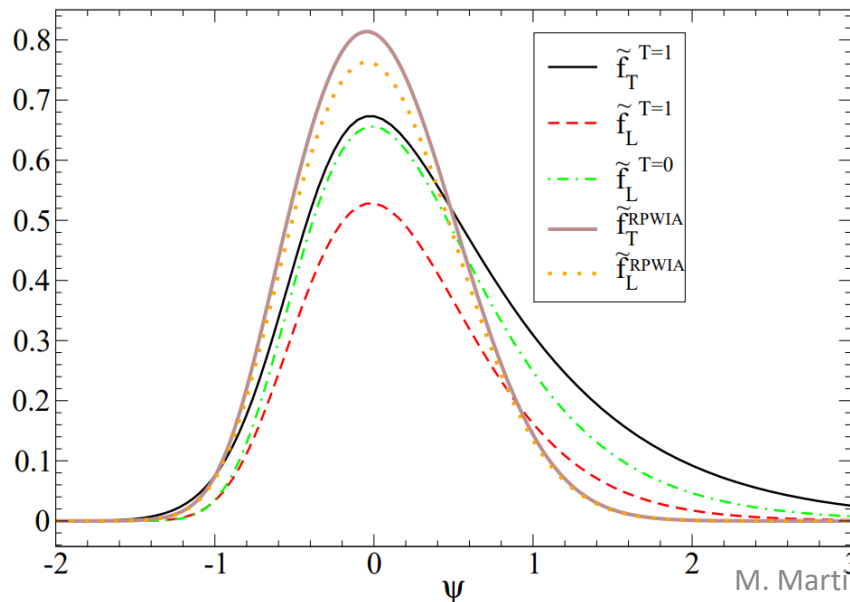
The scaling function(s) are used to describe simultaneously electron and neutrino scattering



SuSA model - phenomenological

J.E. Amaro et al., PRC71 (2005) 015501

- One scaling function extracted from longitudinal inclusive (e,e') data



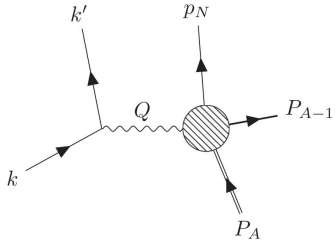
SuSAv2 model - microscopic

R. Gonzalez-Jimenez et al., PRC90 (2014) 035501

- Based on Relativistic Mean Field calculation
- A set of scaling functions in L,T and isospin channels

The Spectral Function

- The spectral function $S(E_m, \mathbf{p}_m)$ represents the joint probability of removing a nucleon of given momentum \mathbf{p}_m from the nuclear ground state A leaving the residual nucleus $A-1$ in a state characterized by missing energy E_m



Missing Energy

$$E_m = \omega - T_N - T_{A-1}$$

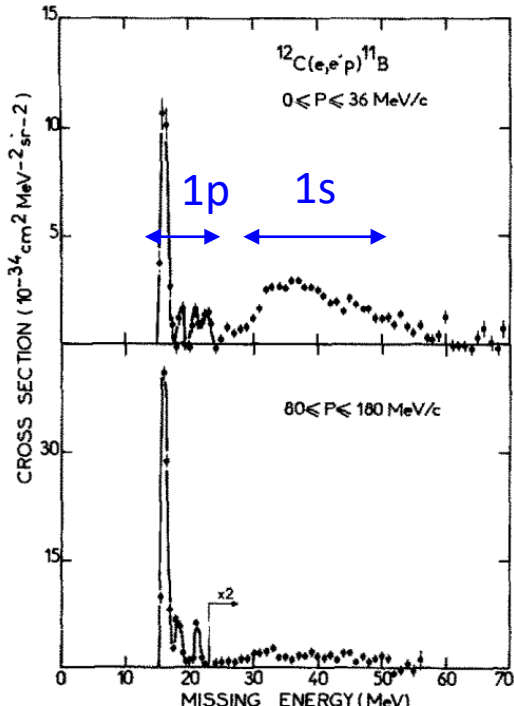
Missing momentum

$$\mathbf{p}_m = \mathbf{q} - \mathbf{p}_N = \mathbf{p}_{A-1} \quad \text{recoil momentum}$$

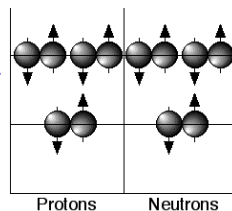
p.s. Often in literature the sign is opposite: $\mathbf{p}_m = \mathbf{p}_N - \mathbf{q} = -\mathbf{p}_{A-1}$

$$\frac{d\sigma}{d\epsilon' d\Omega_e dT' d\Omega_p} = K \left(\frac{d\sigma}{d\Omega_e} \right)_{ep} S(E, \mathbf{P})$$

J. Mougey et al, Nucl. Phys. A 262 (1976)



$1p_{3/2}$
 $1s_{1/2}$



Protons Neutrons

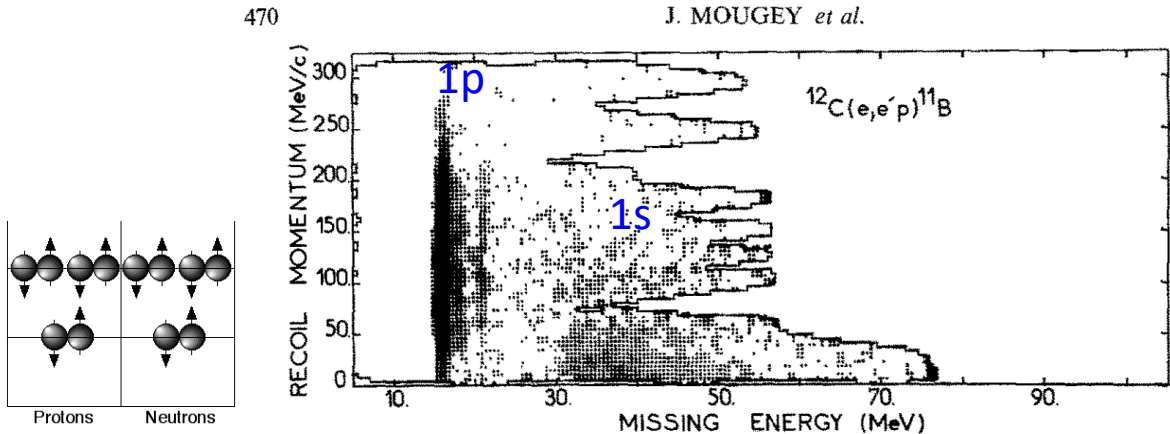
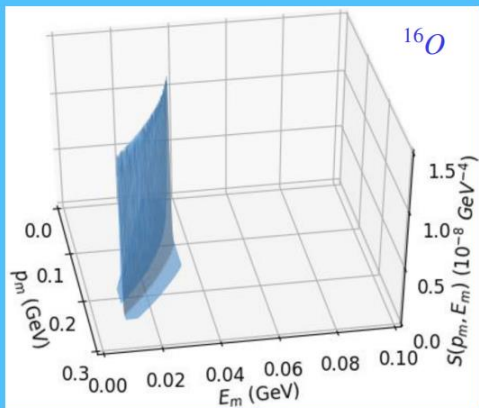


Fig. 8. Cross section $\sigma(E, P)$ for ^{12}C , showing the $1p$ shell at 17 MeV and the $1s$ shell around 38 MeV.

Different ^{16}O Theoretical Spectral Functions

RFG

$$S_{RFG}(p_m, E_m) = \theta(p_F - p_m) \delta(E_m - \sqrt{p_m^2 + m_N^2})$$



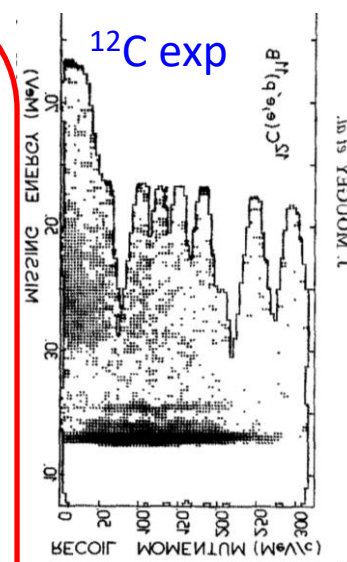
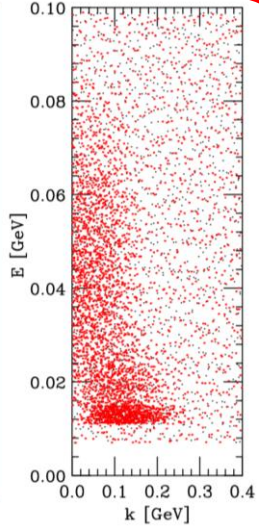
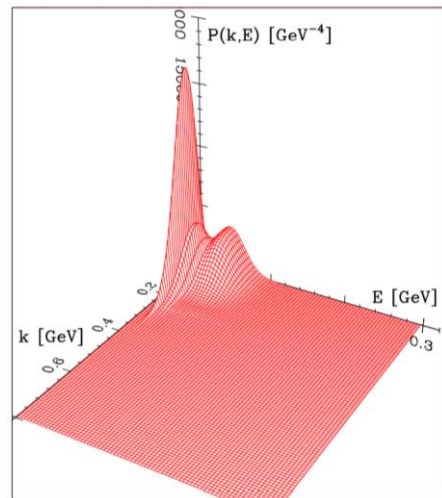
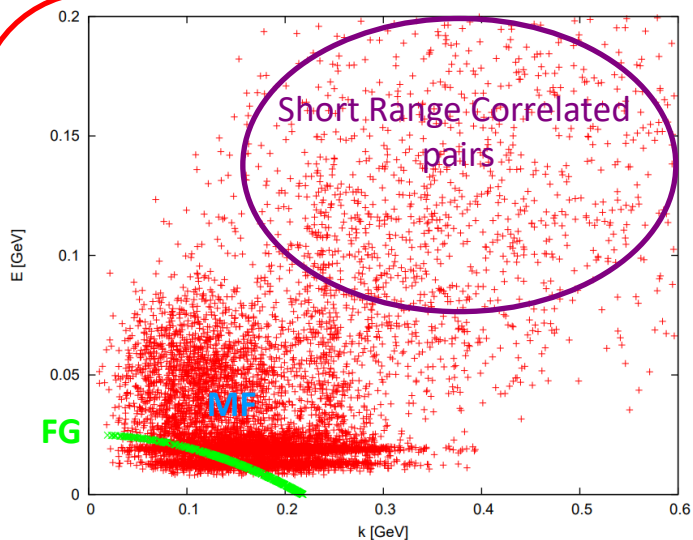
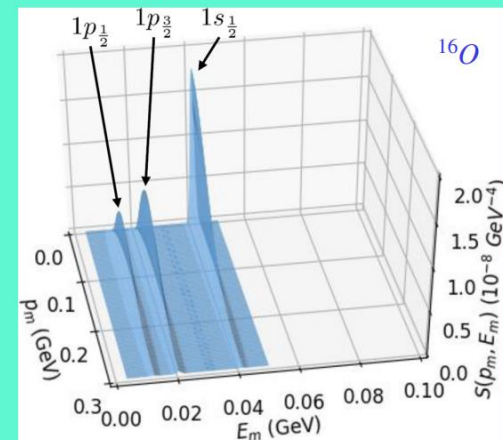
Independent-particle models

J. M. Franco Patino et al, PRC 102 064626 (2020)

Figures from M. B. Barbaro talk @NUFACT 2021

IPSM/RMF

$$S_{IPSM}(p_m, E_m) = \sum_{nlj} (2j+1) n_{nlj}(p_m) \delta(E_m - E_{nlj})$$



Correlated Basis Functions $S_{CBF}(p_m, E_m) = S_{MF}(p_m, E_m) + S_{corr}(p_m, E_m)$

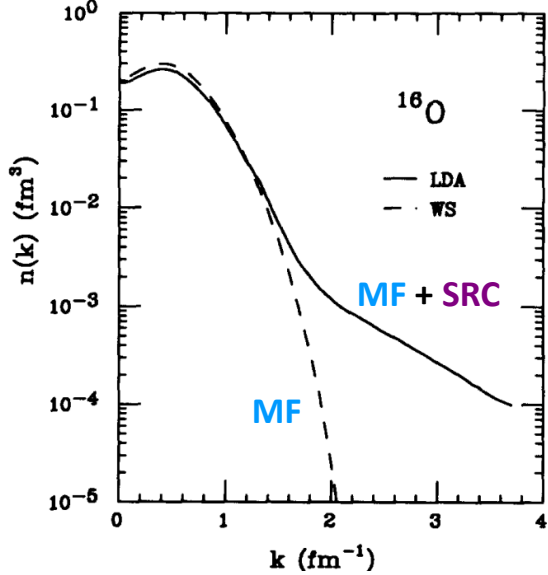
O. Benhar, A. Fabrocini, and S. Fantoni, Nucl. Phys. A505, 267 (1989)

Figures from N. Rocco talk @ESNT-CEA workshop 2016

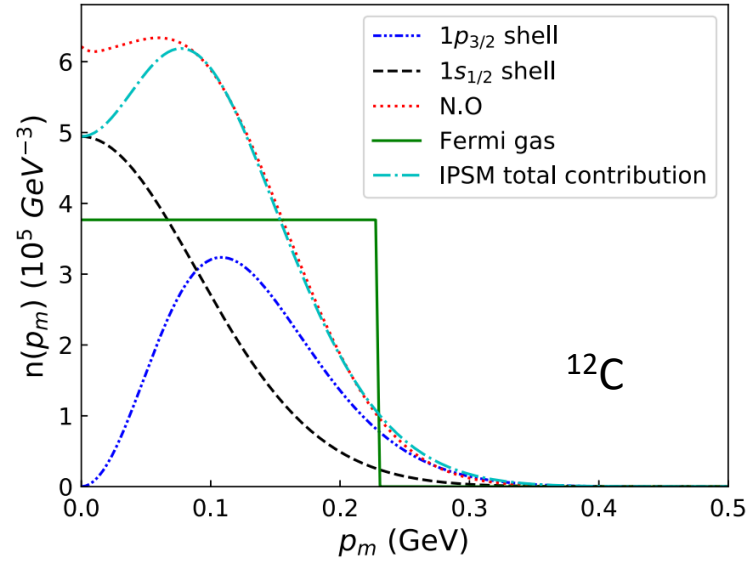
Nucleon momentum distribution

$$n(p_m) = \int_0^\infty dE_m S(p_m, E_m)$$

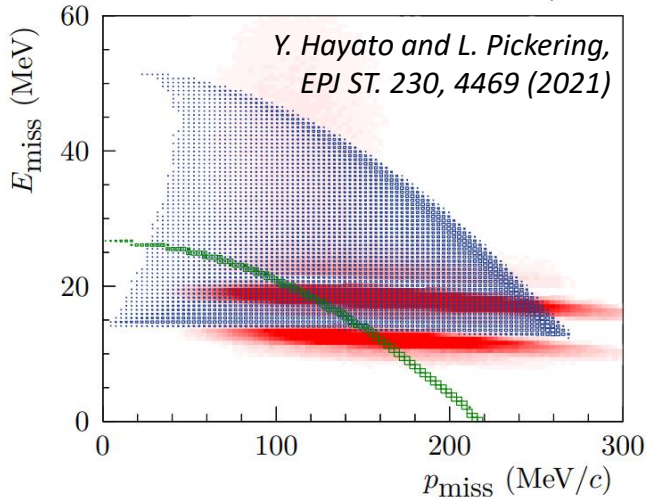
O. Benhar et al. Nucl.Phys. A 579 (1994)



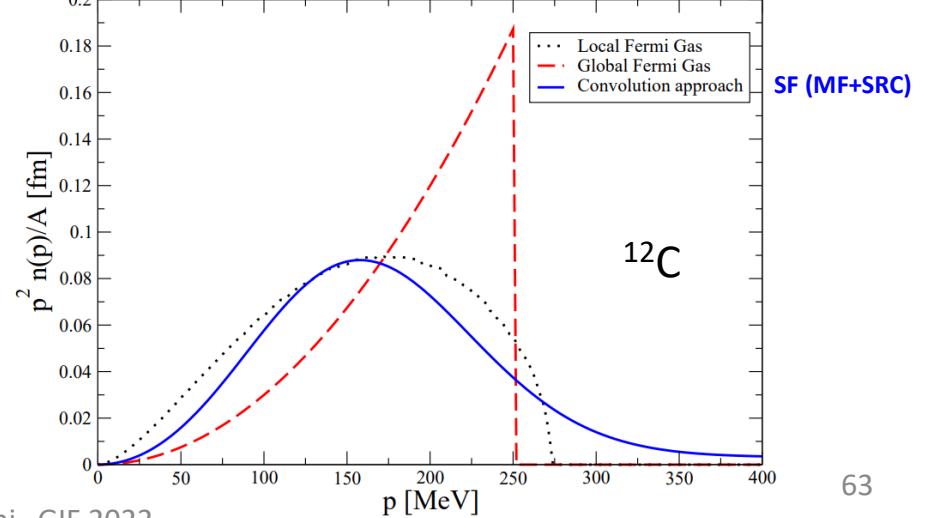
J. M. Franco Patino et al, PRC 102 064626 (2020)



■ Benhar SF — Local FG
 — Global FG NEUT 5.5.0, ν_μ ^{16}O

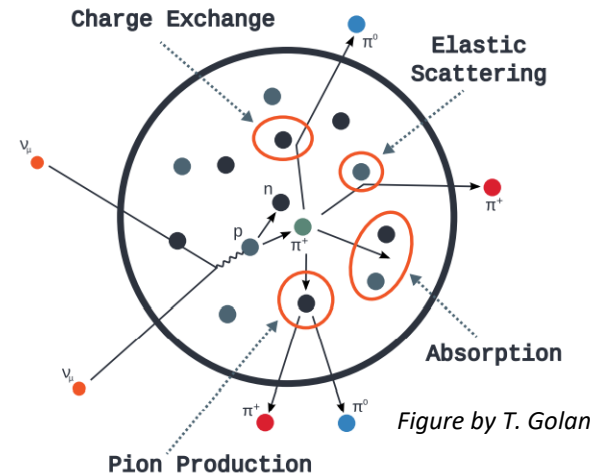
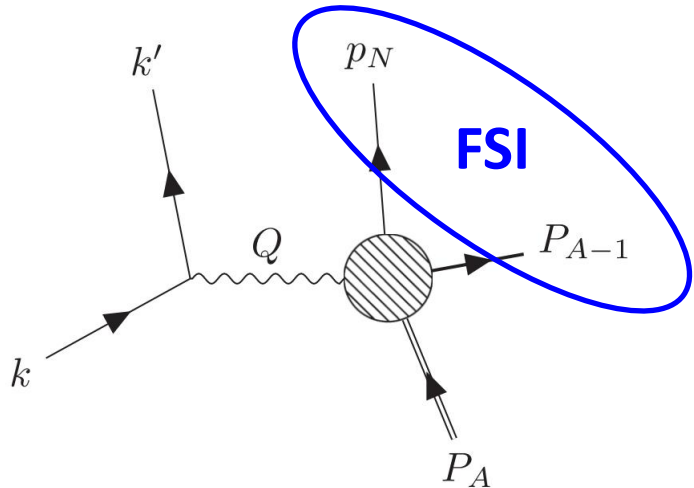


L. Alvarez-Ruso et al. New J.Phys. 16075015 (2014)



Final State Interactions

FSI between the knocked-out particle(s) and the residual nucleus



- FSI describe the propagation of the particles produced at the interaction vertex through the nucleus
- FSI include both elastic and inelastic reactions: elastic scattering with energy change, charge exchange, production of new particles, absorption
- Different interaction vertices can lead to the same final state due to FSI
- The inclusion of FSI effects is extremely important for the description of semi-inclusive data
- Monte Carlo event generators includes different models of intra-nuclear cascades: particles are assumed to be classical and move along a straight line
- FSI between the knocked-out nucleon and the residual nucleus can be theoretically treated using different approaches: Optical Potential, RMF, Energy-Dependent RMF
- Some recent references: *R. Gonzalez-Jimenez et al., PRC 101, 015503 (2020)* ;
J. Isaacson et al., PRC 103 015502 (2021); *A. Nikolakopoulos et al. PRC 105, 054603 (2022)*;
A. Ershova et al., PRD 106 032009 (2022)

Neutrino-nucleus cross sections

Second Lecture

Results and Perspectives

Charged current neutrino-nucleus cross section (remind)

Lab frame

$$\frac{d^2\sigma}{d\Omega_{\mathbf{k}'} d\omega} = \frac{G_F^2 \cos^2 \theta_C}{4\pi^2} \frac{|\mathbf{k}'|}{|\mathbf{k}|} L_{\mu\nu} W^{\mu\nu}(\mathbf{q}, \omega)$$

The charged current inclusive cross section is a linear combination of five contributions

$$\frac{d^2\sigma}{d\Omega_{\mathbf{k}'} d\omega} = \sigma_0 \left[L_{00}W^{00} + L_{33}W^{33} + (L_{03} + L_{30})W^{03} + (L_{11} + L_{22})W^{11} \pm (L_{12} - L_{21})W^{12} \right]$$

A simplified expressions particularly useful for illustration

$$\begin{aligned} \frac{d^2\sigma}{d\cos\theta d\omega} = & \frac{G_F^2 \cos^2 \theta_c}{\pi} |\mathbf{k}'| E_l' \cos^2 \frac{\theta}{2} \left[\frac{(\mathbf{q}^2 - \omega^2)^2}{\mathbf{q}^4} G_E^2 R_T(\mathbf{q}, \omega) + \frac{\omega^2}{\mathbf{q}^2} G_A^2 R_{\sigma\tau(L)}(\mathbf{q}, \omega) \right] \\ & + 2 \left(\tan^2 \frac{\theta}{2} + \frac{\mathbf{q}^2 - \omega^2}{2\mathbf{q}^2} \right) \left(G_M^2 \frac{\mathbf{q}^2}{4M_N^2} + G_A^2 \right) R_{\sigma\tau(T)}(\mathbf{q}, \omega) \pm 2 \frac{E_\nu + E_l'}{M_N} \tan^2 \frac{\theta}{2} G_A G_M R_{\sigma\tau(T)}(\mathbf{q}, \omega) \end{aligned}$$

Explicitly appear:

1. The different **kinematic variables** (related to the leptonic tensor)
2. The nucleon Electric, Magnetic, and Axial **form factors** (\leftrightarrow nucleon properties)
3. The **nuclear response functions** (\leftrightarrow nuclear dynamics)

The Form Factors

Standard dipole parameterization

Vector (see slide 39)

$$\underline{G_E(Q^2)} = \underline{G_M(Q^2)} / (\mu_p - \mu_n) = (1 + Q^2 / M_V^2)^{-2}$$

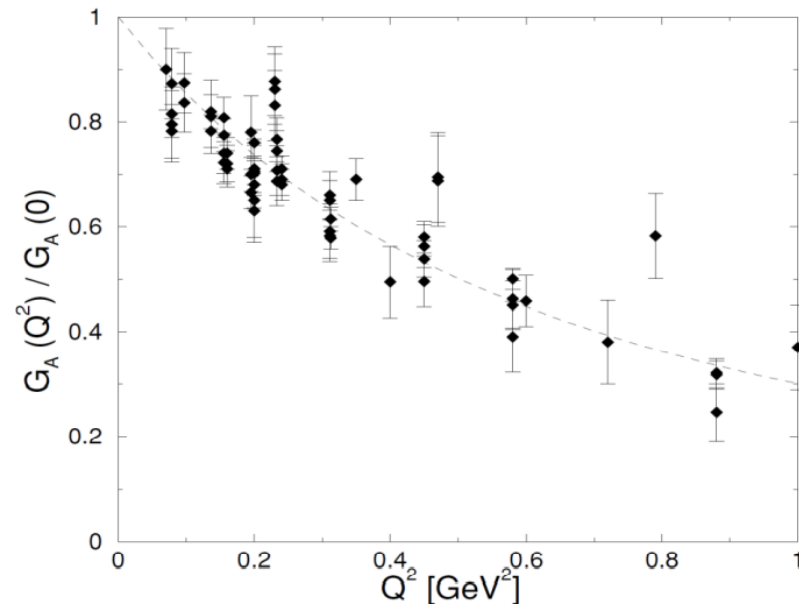
$$Q^2 = q^2 - \omega^2$$

Axial

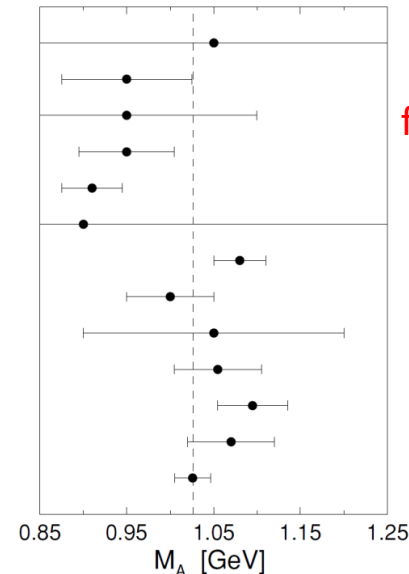
$$\underline{G_A(Q^2)} = g_A (1 + Q^2 / M_A^2)^{-2}$$

$g_A = 1.26$ from neutron β decay

$$M_A = (1.026 \pm 0.021) \text{ GeV} / c^2$$



- Argonne (1969)
- Argonne (1973)
- CERN (1977)
- Argonne (1977)
- CERN (1979)
- BNL (1980)
- BNL (1981)
- Argonne (1982)
- Fermilab (1983)
- BNL (1986)
- BNL (1987)
- BNL (1990)
- Average



from ν -deuterium CCQE
and
from π electroproduction

V. . Bernard, *J.Phys. G28 (2002) R1-R35*

CCQE, CCQE-like and CC0 π

MiniBooNE CC Quasielastic cross section on Carbon and the M_A puzzle

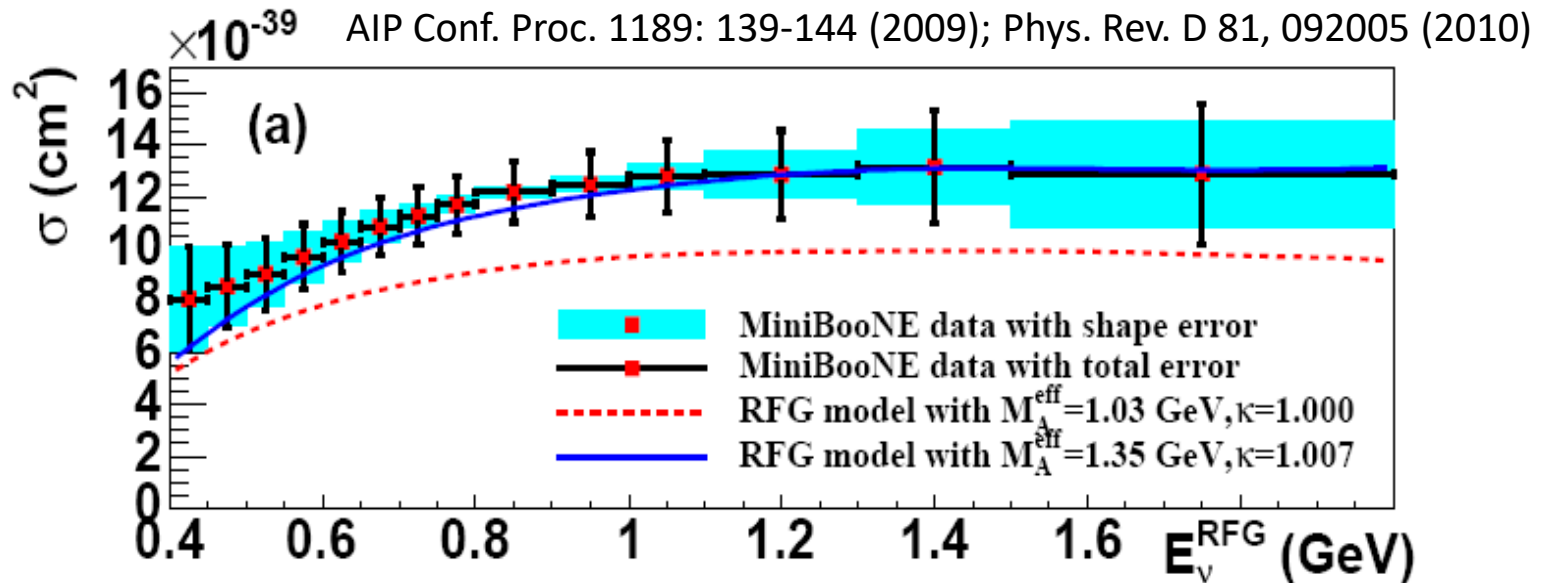
First Measurement of Muon Neutrino Charged Current Quasielastic (CCQE) Double Differential Cross Section

Cite as: AIP Conference Proceedings 1189, 139 (2009); <https://doi.org/10.1063/1.3274144>
Published Online: 02 December 2009

Tepepei Katori and MiniBooNE collaboration

PHYSICAL REVIEW D 81, 092005 (2010)

First measurement of the muon neutrino charged current quasielastic double differential cross section

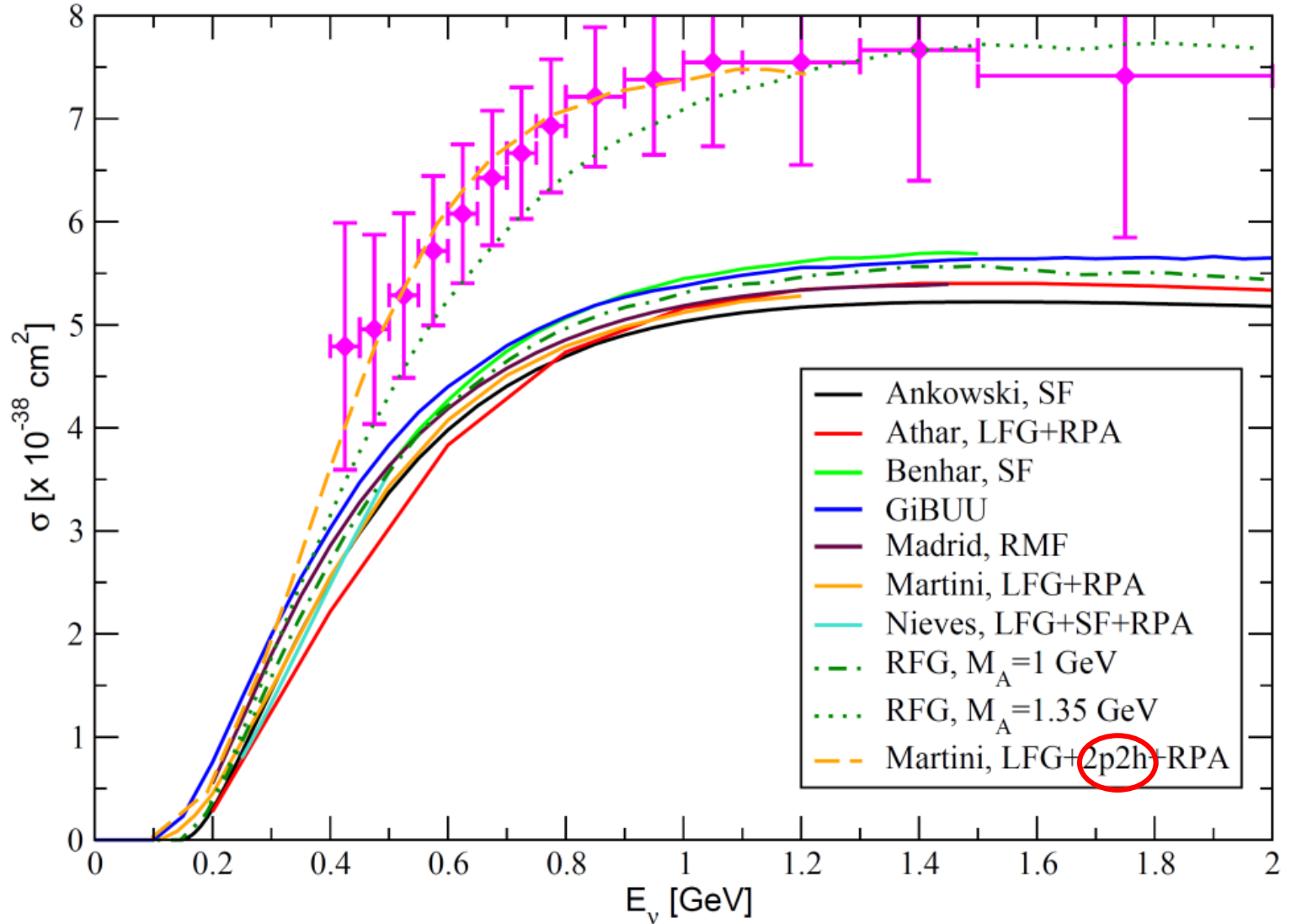


Comparison with a prediction based on RFG using $M_A=1.03$ GeV (standard value) reveals a discrepancy

In the Relativistic Fermi Gas (RFG) model an axial mass of **1.35 GeV** is needed to account for data **puzzle??**

Comparison of different theoretical models for Quasielastic

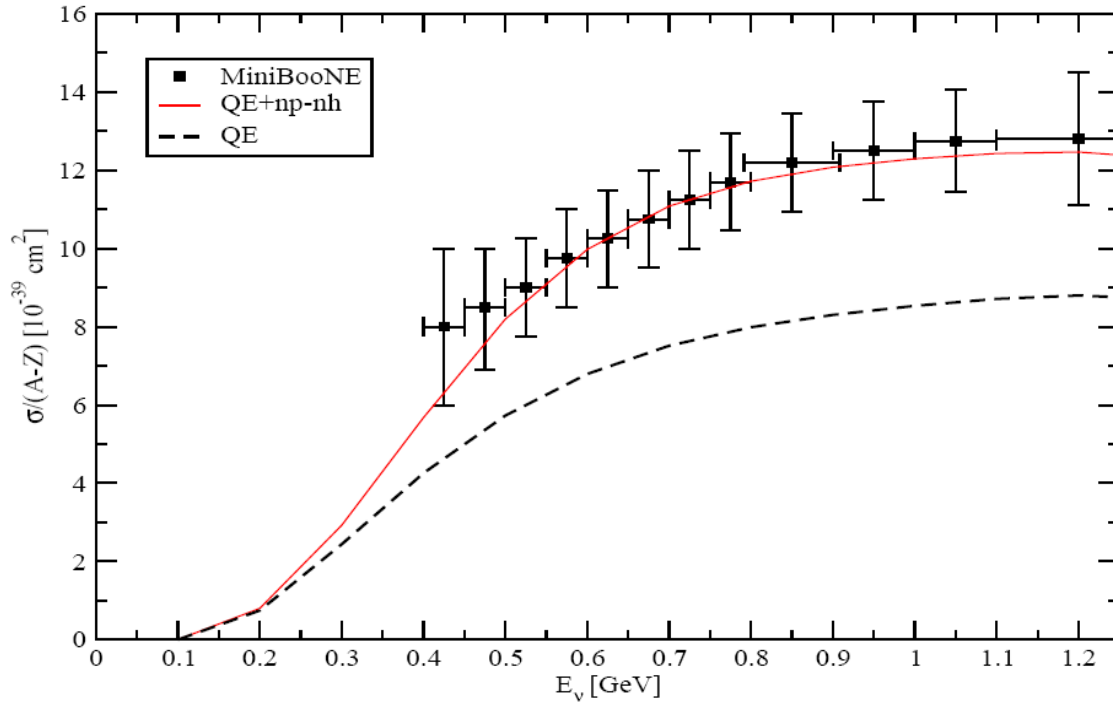
L. Alvarez-Ruso , arXiv:1012.3871 (Neutrino 2010)



puzzle??

An explanation of this puzzle

Inclusion of the multinucleon emission channel
($np-nh = 2p-2h + 3p-3h$)

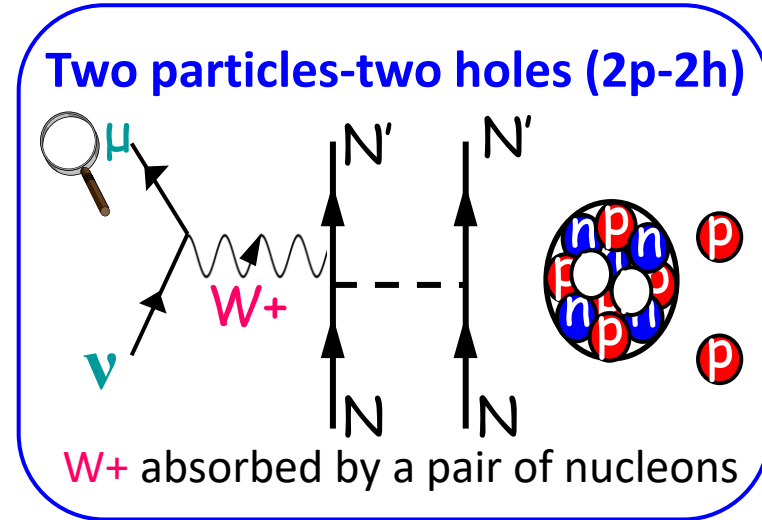
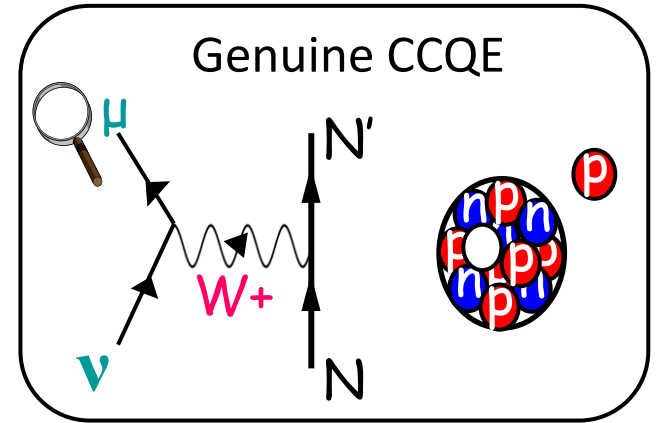


CCQE-like = Genuine CCQE + $np-nh$

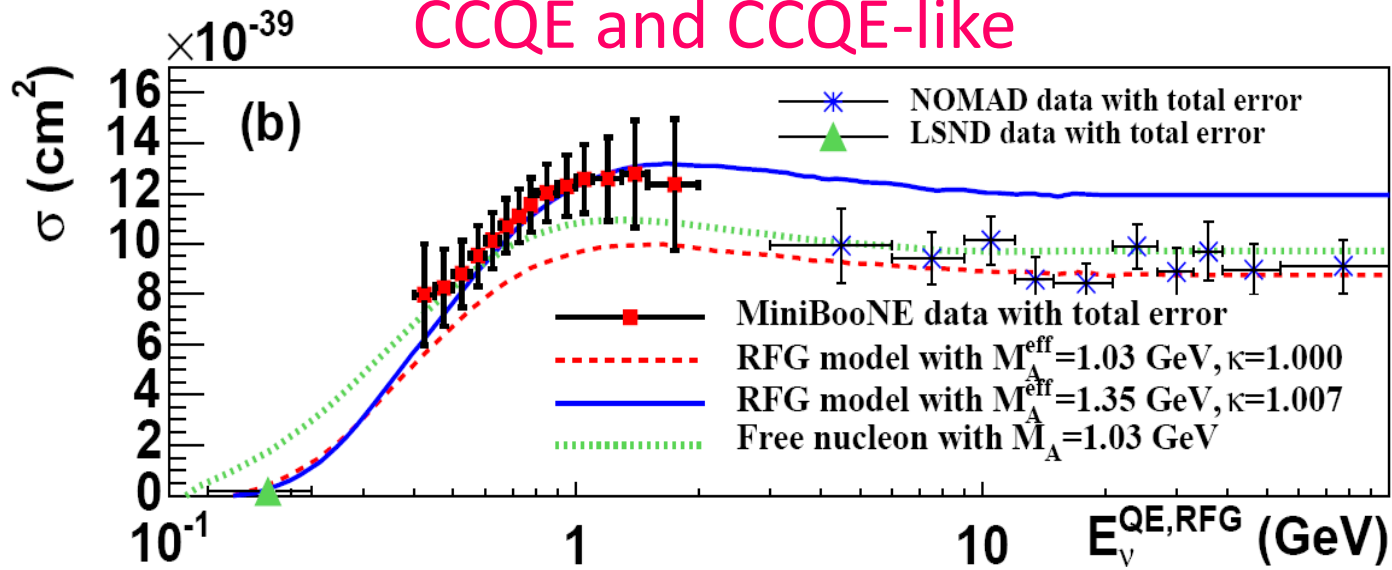
M. Martini, M. Ericson, G. Chanfray, J. Marteau, Phys. Rev. C 80 065501 (2009)

Agreement with MiniBooNE without increasing M_A

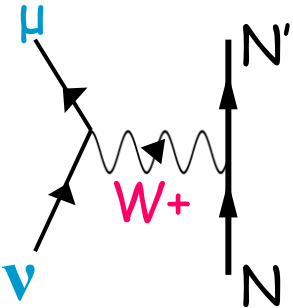
➡ MiniBooNE measured CCQE-like, not genuine CCQE



CCQE and CCQE-like

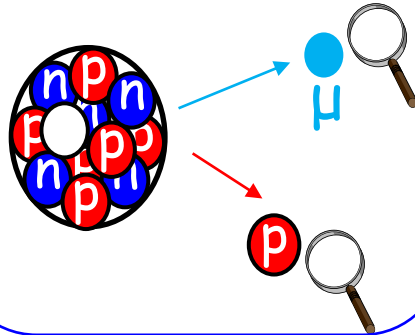


CCQE interaction vertex



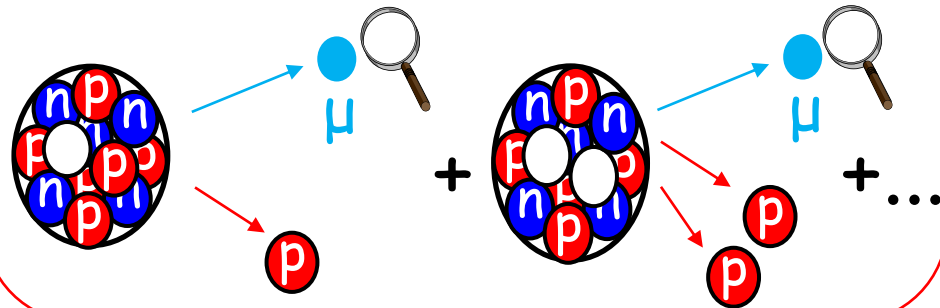
Tracking detectors

e.g. NOMAD, MINERvA, T2KND280, MicroBooNE



Cherenkov detectors

e.g. MiniBooNE, SuperKamiokande



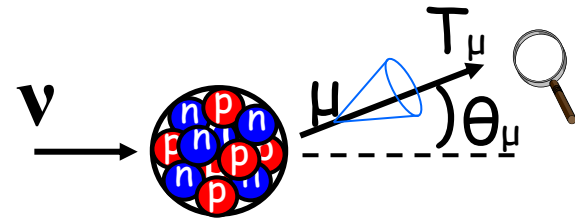
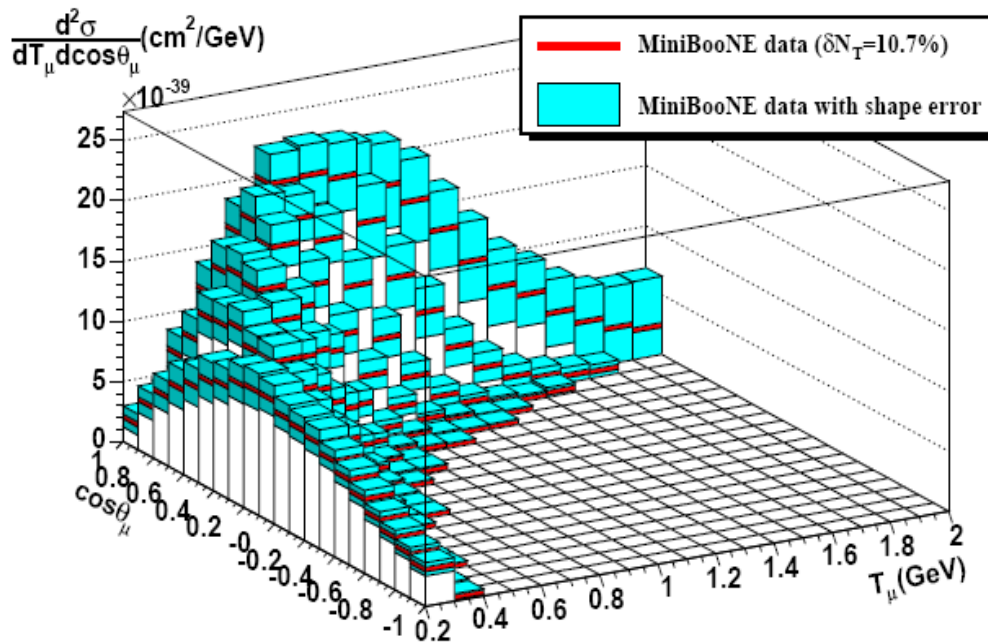
- Cherenkov detectors measure “CCQE-like” which includes np-nh contributions
- After MiniBooNE: CCQE-like = CCQE + np-nh
- Very recently [e.g. MicroBooNE PRL 125, 201803, 2020] “CCQE-like” has been used with another meaning
- After MiniBooNE it has become more popular to present the data in terms of final state particles

Flux-integrated double differential cross section

$$\left(\frac{d^2\sigma}{dT_l \cos\theta} \right)_i = \frac{\sum_j U_{ij}(d_j - b_j)}{\Phi \cdot T \cdot \epsilon_i \cdot (\Delta T_l, \Delta \cos\theta)_i} \quad (\text{see slide 19})$$

PHYSICAL REVIEW D **81**, 092005 (2010)

First measurement of the muon neutrino charged current quasielastic **double differential cross section**

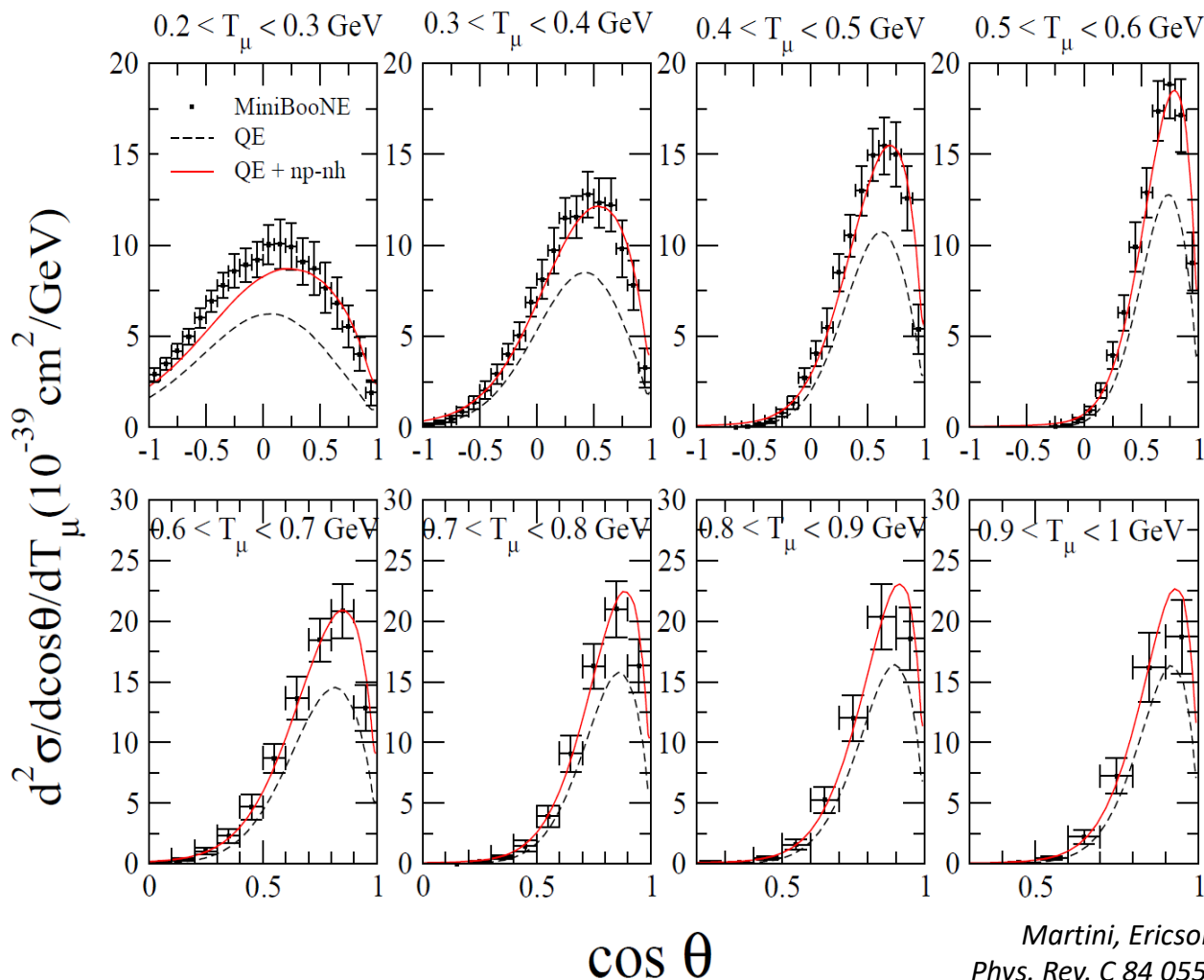


- Function of two measured variables
- Less model dependent than $\sigma(E_\nu)$: free from the neutrino energy reconstruction problem (see later)
- Flux dependent

Flux-integrated differential cross section is where theorists and experimentalists meet for ν interaction

MiniBooNE CCQE-like flux-integrated double differential cross section

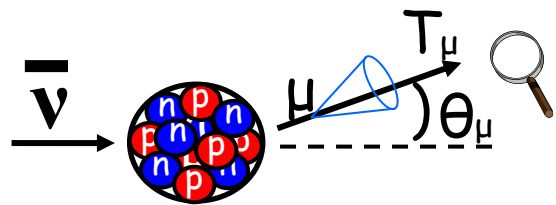
$$\frac{d^2\sigma}{dT_l d\cos\theta} = \frac{1}{\int \Phi(E_\nu) dE_\nu} \int dE_\nu \left[\frac{d^2\sigma}{d\omega d\cos\theta} \right]_{\omega=E_\nu-E_l} \Phi(E_\nu)$$



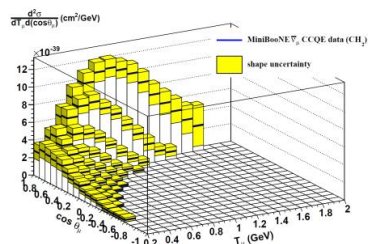
Martini, Ericson, Chanfray,
Phys. Rev. C 84 055502 (2011)

- Good agreement with data once multinucleon contributions are included
- Similar conclusions obtained by different theoretical calculations (see later)

MiniBooNE CCQE-like flux-integrated double differential cross section

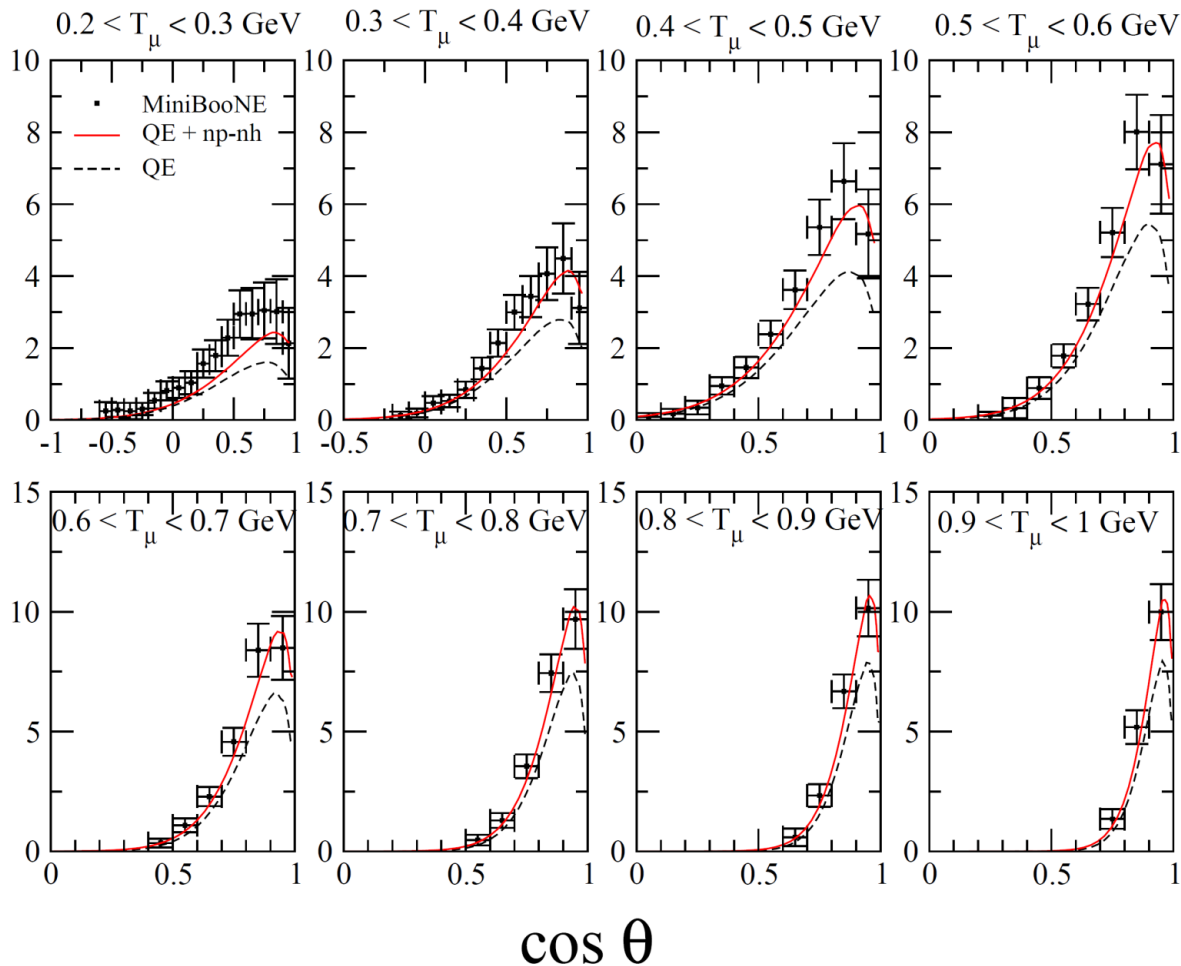


$\bar{\nu}$



MiniBooNE, *Phys. Rev. D* 88 032001 (2013)

$\frac{d^2 \sigma}{d \cos \theta / d T_\mu} (10^{-39} \text{ cm}^2 / \text{GeV})$



Martini, Ericson, *Phys. Rev. C* 87 065501 (2013)

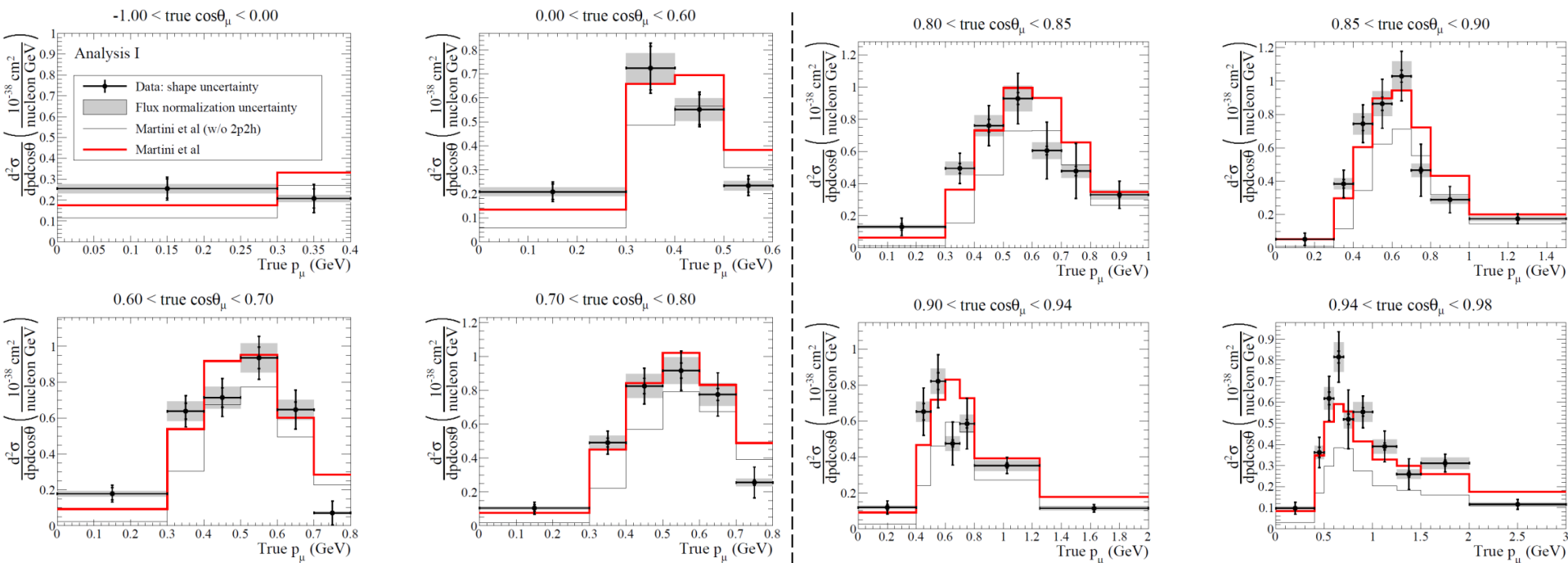
Similar conclusion also for the MiniBooNE CCQE-like antineutrino cross sections

The $CC0\pi$ measurement

After MiniBooNE, it has become more popular to present the data in terms of final state particles
 $CC0\pi = CCQE$ -like without subtraction of π absorption background ($CC0\pi \geq CCQE$ -like)

PHYSICAL REVIEW D **93**, 112012 (2016)

Measurement of double-differential muon neutrino charged-current interactions on C_8H_8 without pions in the final state using the T2K off-axis beam



— Including np - nh
 — Without np - nh

Better agreement including np - nh

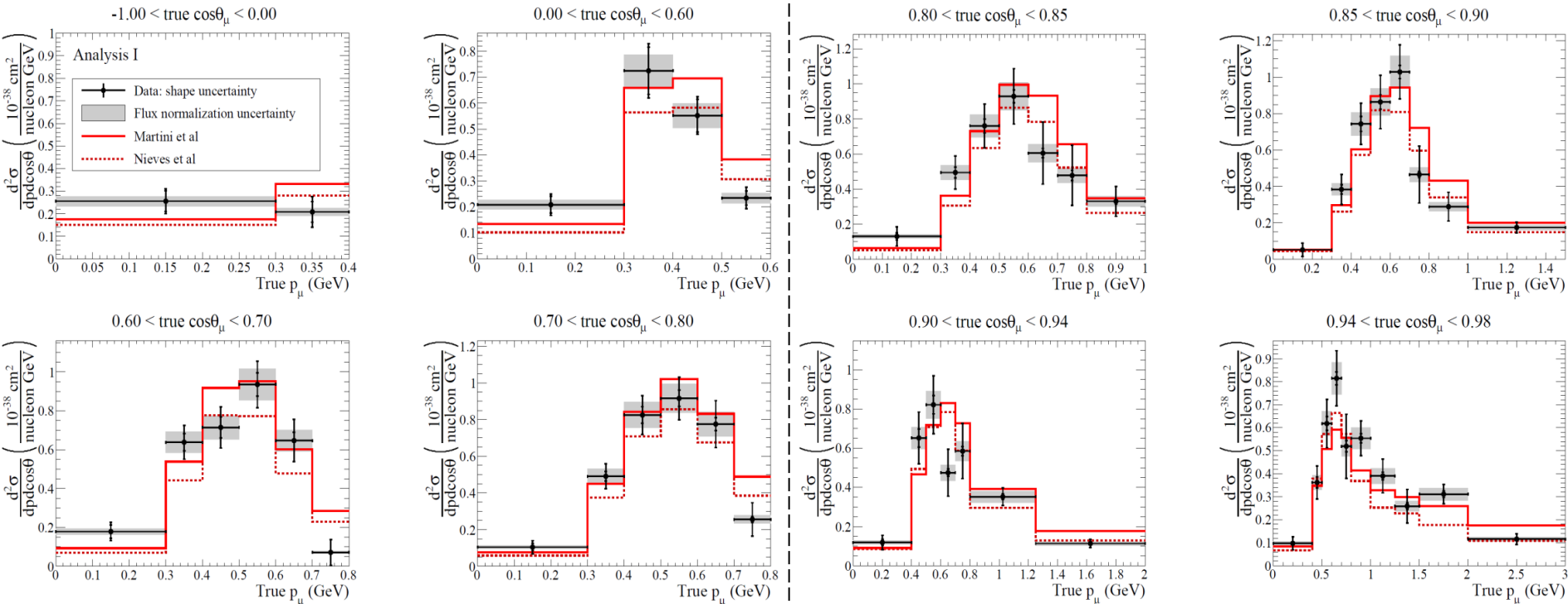
The $CC0\pi$ measurement

After MiniBooNE, it has become more popular to present the data in terms of final state particles

$CC0\pi = CCQE$ -like without subtraction of π absorption background

PHYSICAL REVIEW D **93**, 112012 (2016)

Measurement of double-differential muon neutrino charged-current interactions on C_8H_8 without pions in the final state using the T2K off-axis beam



— Martini et al.
 Nieves et al.

- Two theoretical models including np-nh are compatible with data
- Differences between models' predictions

The T2K $\text{CC}0\pi$ data and the Monte Carlo predictions

M. BUIZZA AVANZINI *et al.*

PHYS. REV. D **105**, 092004 (2022)

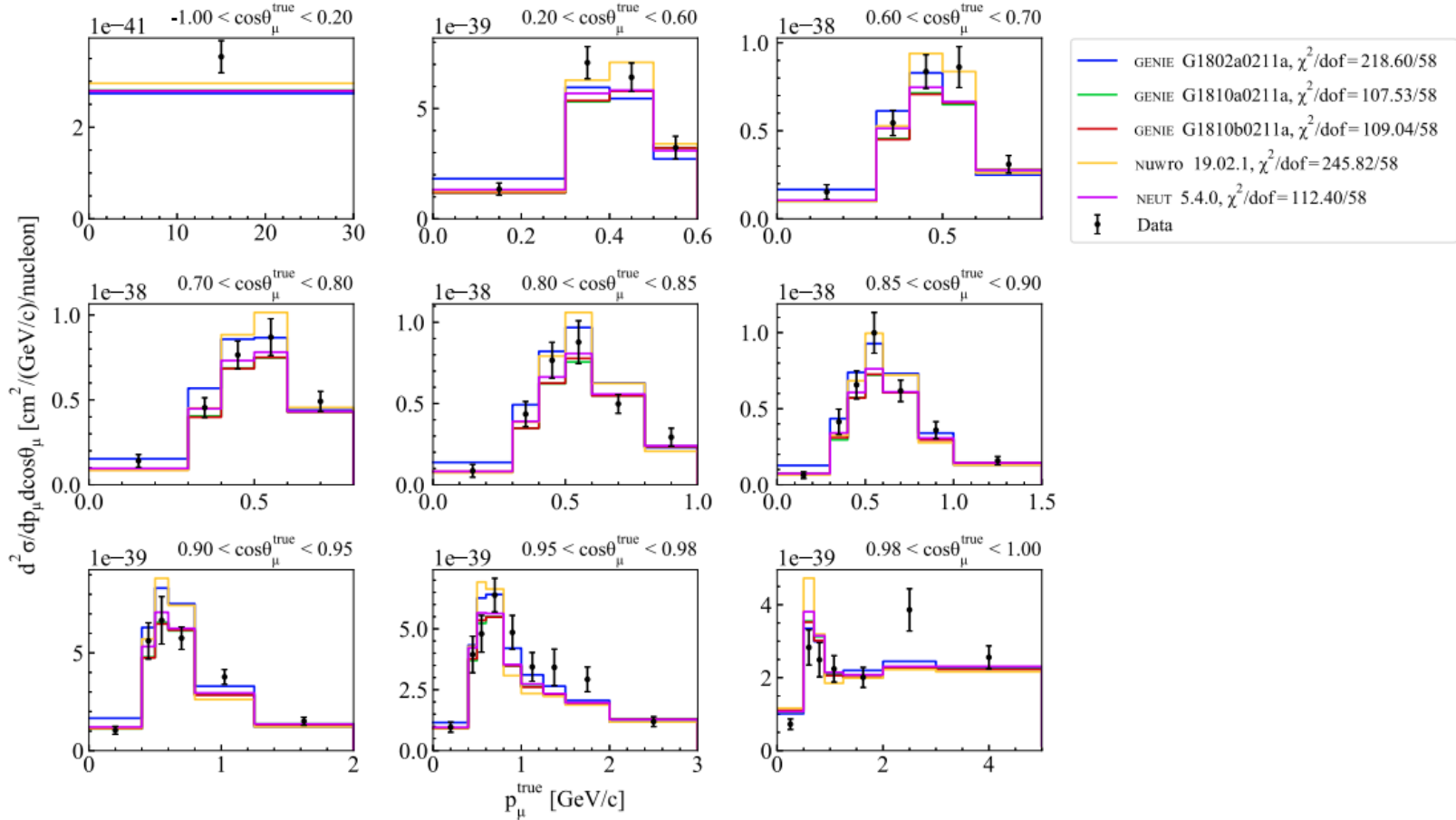
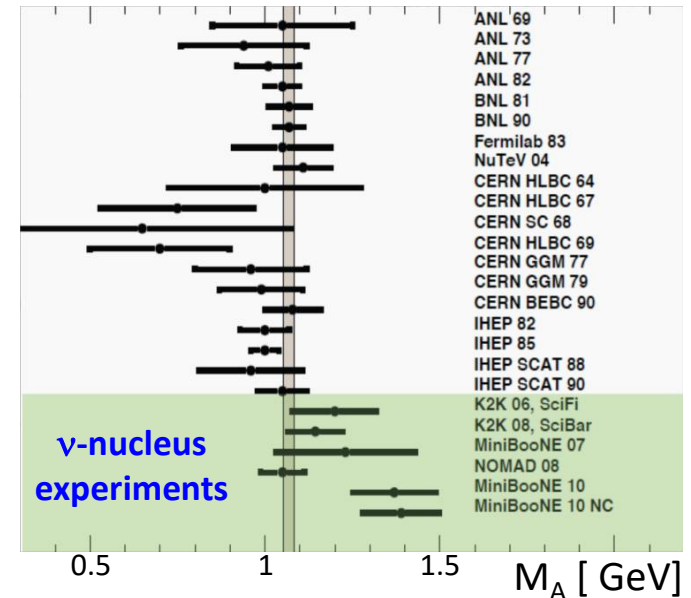


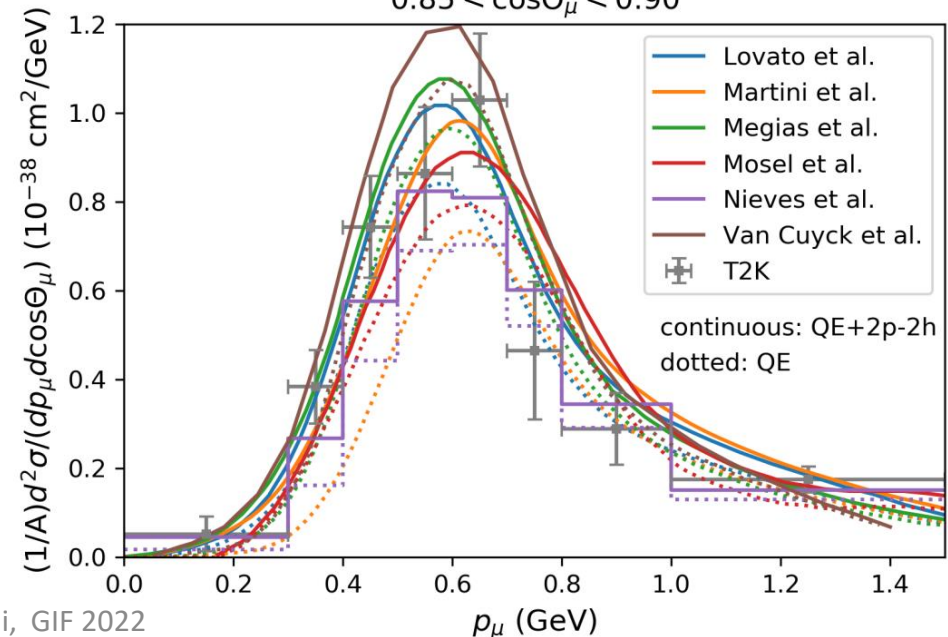
FIG. 10. Measured T2K ν_μ CC- 0π double-differential cross sections on hydrocarbon in bins of true muon kinematics. The results are compared to GENIE v3 G18_02a (blue), G18_10a (green), and G18_10b (red), NuWro 19.02.1 (orange), and NEUT 5.4.0 (violet). The last bin in momentum is not displayed for readability.

The multinucleon emission channel (or np-nh, or 2p-2h)

- A lot of interest in these last 13 years (starting from the explanation of MiniBooNE CCQE-like)
- Explanation of the axial mass puzzle
- Before MiniBooNE it was not included in the generators used for the analyses of ν cross sections and oscillations experiments
- The effort to include this np-nh channel in several Monte Carlo is still in progress
- Several theoretical calculations agree on its crucial role but there are differences on the results obtained for this channel
- One of the most important source of the cross section uncertainties (systematic errors in oscillation experiments)



A. Branca et al. Symmetry 13 (2021) 9, 1625
 $0.85 < \cos\Theta_\mu < 0.90$

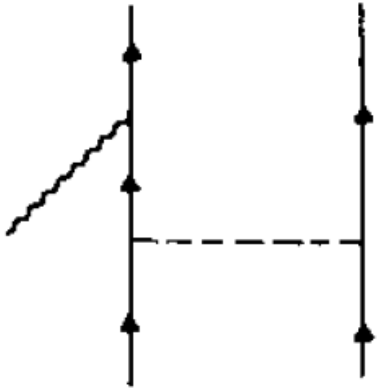


Some theoretical details on 2p-2h

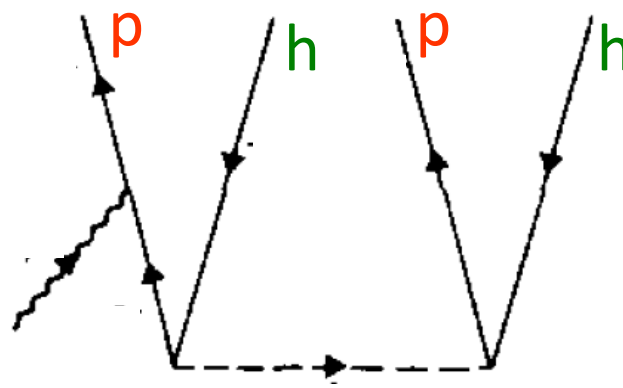
Two particle-two hole sector (2p-2h)

Three equivalent representations of the same process

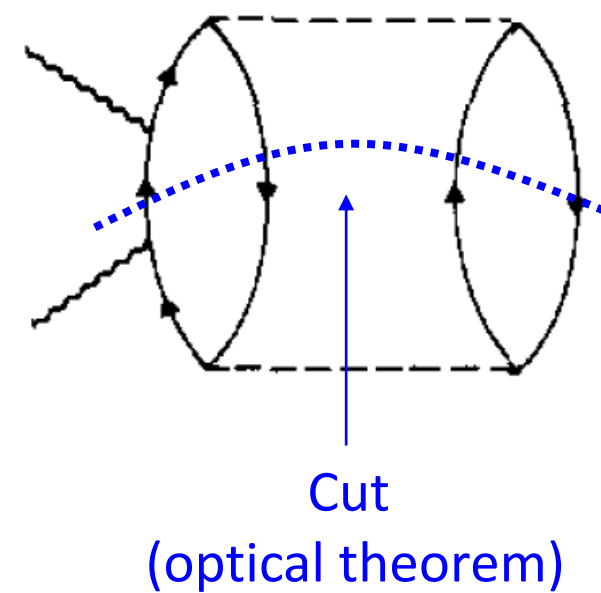
2 body current



2p-2h matrix element



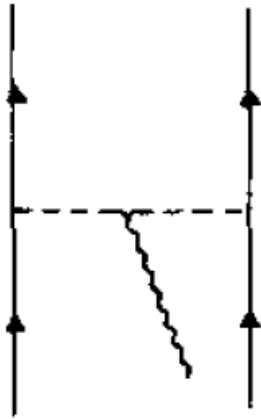
2p-2h response



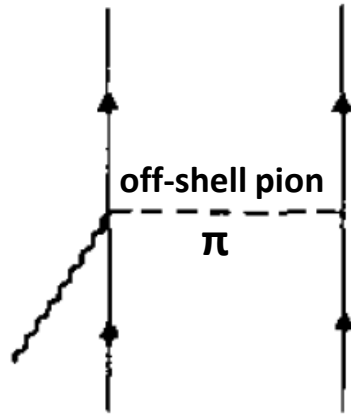
Final state: two particles-two holes

Diagrams for 2 body currents

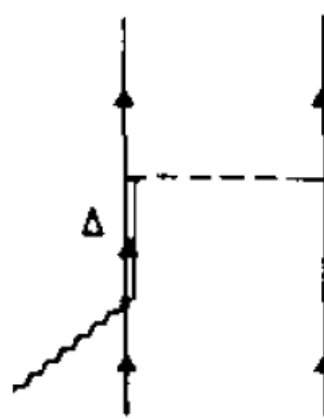
Meson Exchange Currents (MEC) J^{MEC}



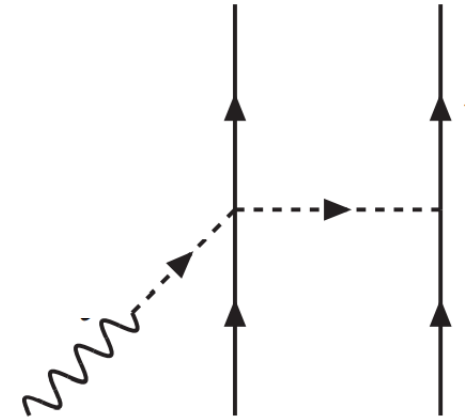
Pion in flight



Seagull or
Contact

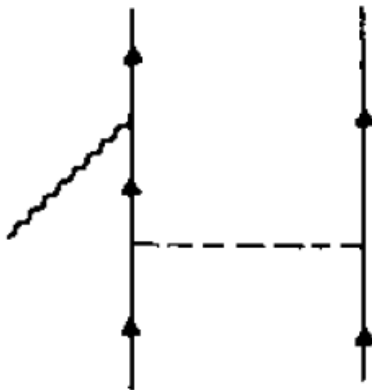


Delta



Pion pole
(purely axial)

Nucleon-Nucleon Correlations (SRC) J^{corr}



- An additional two-body current to be included in the framework of independent particle models such as LFG or Hartree-Fock.
- Absent in the approaches which start from the description of the nucleus in terms of correlated wave functions (such as CBF spectral function or GFMC) since the matrix elements of the one body current already includes this contribution.
- There is a risk of a double counting of SRC in the Monte Carlo if different contributions to the neutrino cross sections are taken from different models.

Some two-body currents

Electromagnetic

- Seagull or contact:

$$j_s^\mu(\mathbf{p}'_1, \mathbf{p}'_2, \mathbf{p}_1, \mathbf{p}_2) = \frac{f^2}{m_\pi^2} i\epsilon_{3ab} \bar{u}(\mathbf{p}'_1) \tau_a \gamma_5 \not{K}_1 u(\mathbf{p}_1) \frac{F_1^V}{K_1^2 - m_\pi^2} \bar{u}(\mathbf{p}'_2) \tau_b \gamma_5 \gamma^\mu u(\mathbf{p}_2) + (1 \leftrightarrow 2) .$$

- Pion-in-flight:

$$j_p^\mu(\mathbf{p}'_1, \mathbf{p}'_2, \mathbf{p}_1, \mathbf{p}_2) = \frac{f^2}{m_\pi^2} i\epsilon_{3ab} \frac{F_\pi (K_1 - K_2)^\mu}{(K_1^2 - m_\pi^2)(K_2^2 - m_\pi^2)} \bar{u}(\mathbf{p}'_1) \tau_a \gamma_5 \not{K}_1 u(\mathbf{p}_1) \bar{u}(\mathbf{p}'_2) \tau_b \gamma_5 \not{K}_2 u(\mathbf{p}_2) .$$

- Correlation:

$$j_{\text{cor}}^\mu(\mathbf{p}'_1, \mathbf{p}'_2, \mathbf{p}_1, \mathbf{p}_2) = \frac{f^2}{m_\pi^2} \bar{u}(\mathbf{p}'_1) \tau_a \gamma_5 \not{K}_1 u(\mathbf{p}_1) \frac{1}{K_1^2 - m_\pi^2} \bar{u}(\mathbf{p}'_2) [\tau_a \gamma_5 \not{K}_1 S_F(P_2 + Q) \Gamma^\mu(Q) + \Gamma^\mu(Q) S_F(P'_2 - Q) \tau_a \gamma_5 \not{K}_1] u(\mathbf{p}_2) + (1 \leftrightarrow 2) .$$

Amaro et al. Phys.Rev.C 82 044601 (2010)

Weak

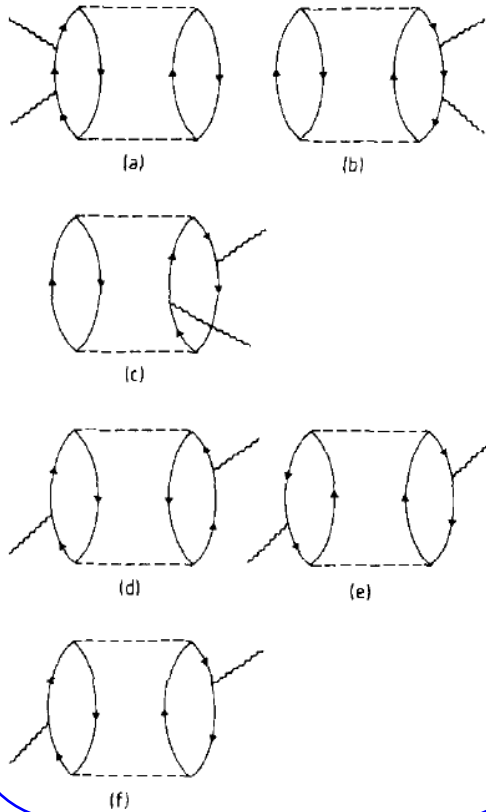
- CC Seagull

$$j_s^\mu(\mathbf{p}'_1, \mathbf{p}'_2, \mathbf{h}_1, \mathbf{h}_2) = (\tau_0 \otimes \tau_{+1} - \tau_{+1} \otimes \tau_0) \frac{f}{m_\pi} \frac{1}{\sqrt{2} f_\pi} \bar{u}(\mathbf{p}'_1) \gamma_5 \not{K}_1 u(\mathbf{h}_1) \frac{\bar{u}(\mathbf{p}'_2) [g_A F_1^V(Q^2) \gamma_5 \gamma^\mu + F_\rho(K_2^2) \gamma^\mu] u(\mathbf{h}_2)}{K_1^2 - m_\pi^2} - (1 \leftrightarrow 2)$$

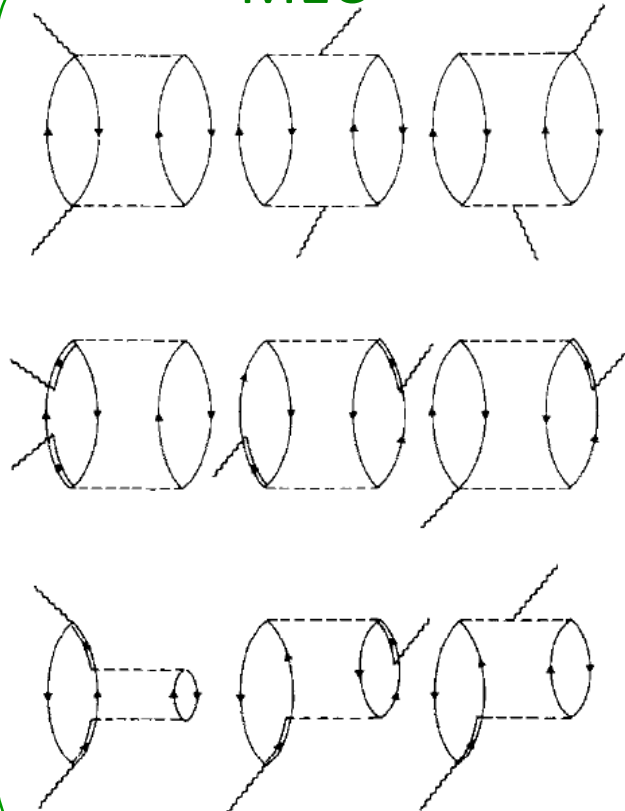
Ruiz-Simo et al. Phys.Rev.D 90 033012 (2014); J.Phys.G 44 065105 (2017)

Some diagrams for 2p-2h responses

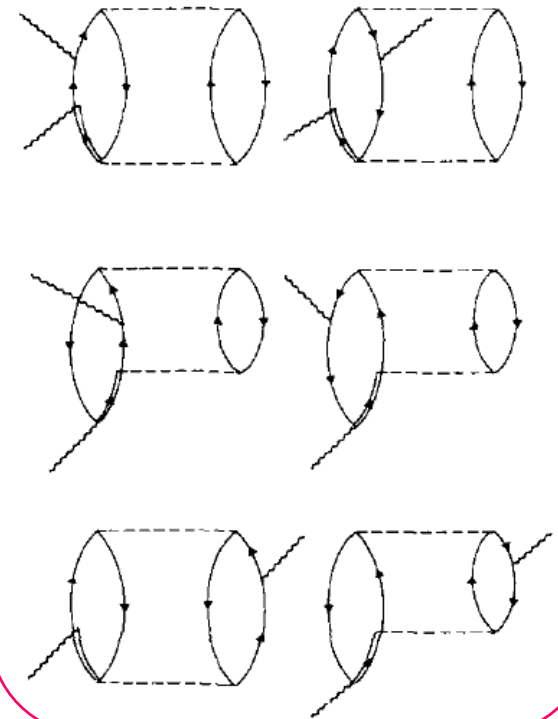
NN correlations



MEC

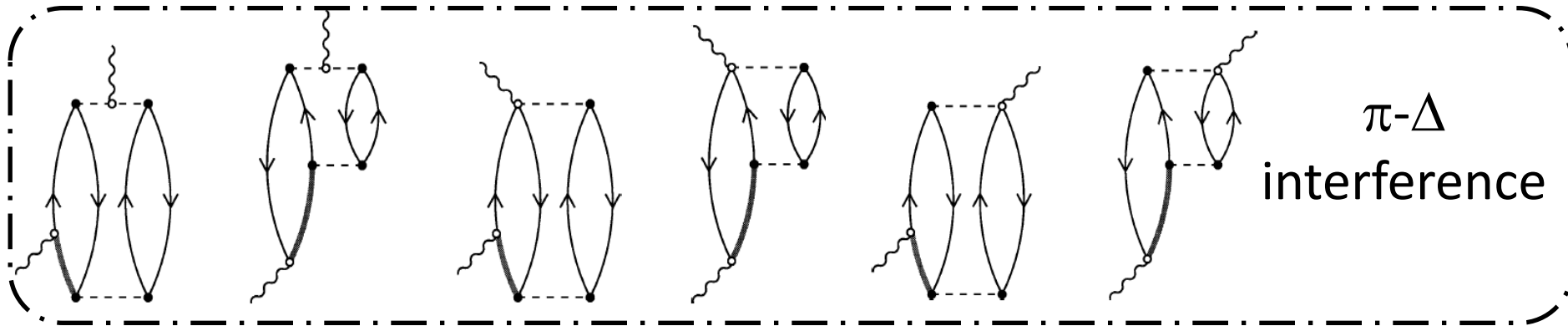
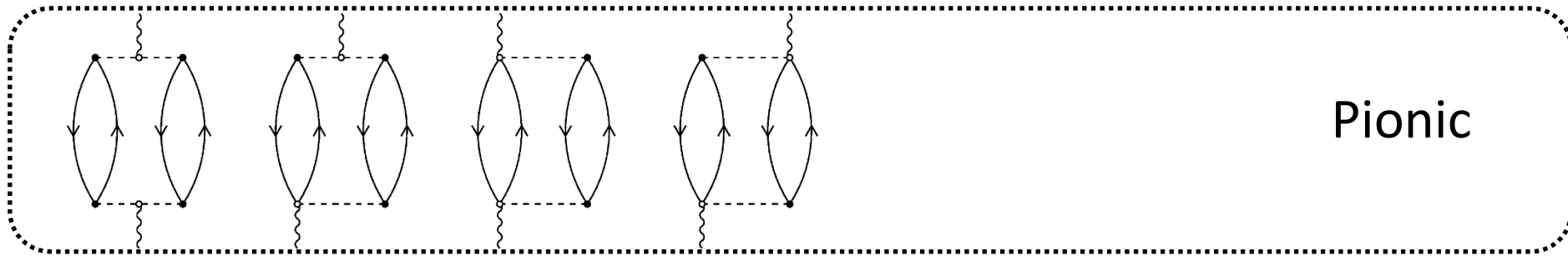
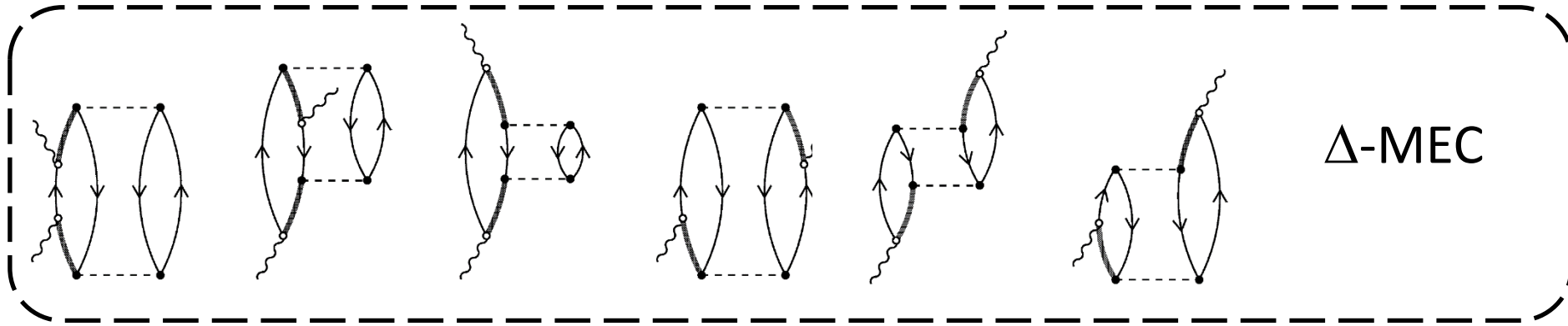


NN correlation-MEC interference



Alberico, Ericson, Molinari, Ann. Phys. 154, 356 (1984)

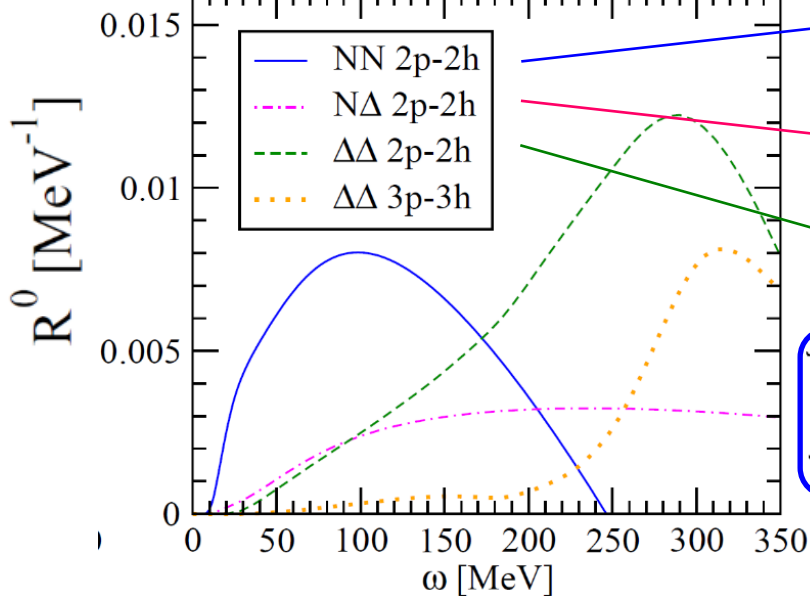
MEC contributions



De Pace, Nardi, Alberico, Donnelly, Molinari, NPA741 (2004)

Separation of np-nh contributions in the nuclear responses

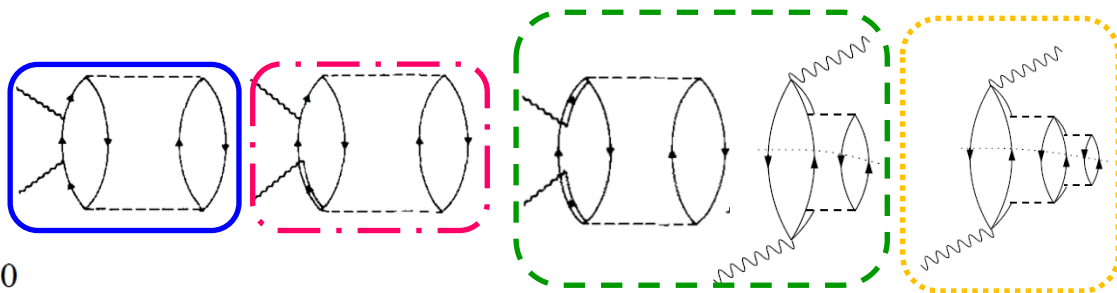
M. Martini, M. Ericson, G. Chanfray, J. Marteau, PRC 80 065501 (2009)



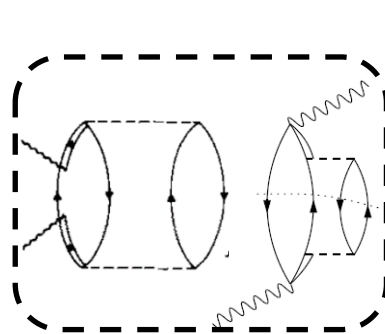
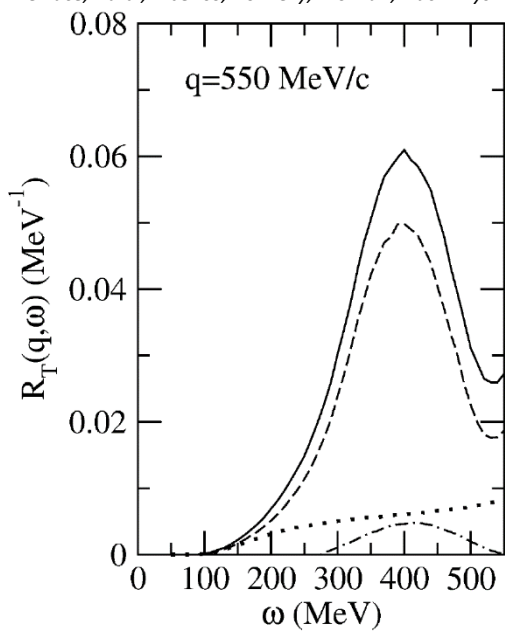
also called NN SRC; part of 1-body current contribution in correlated nuclear wave functions approaches, like SF or GFMC

$N\Delta$ interference, also called NN correlation- Δ MEC interference or 1-body—2-body interference

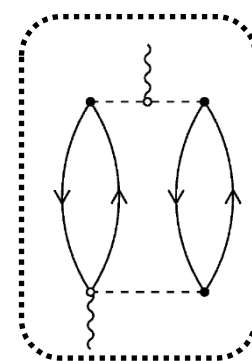
Δ mediated MEC



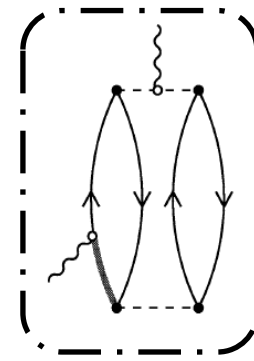
De Pace, Nardi, Alberico, Donnelly, Molinari, Nucl. Phys. A741, 249 (2004)



Δ



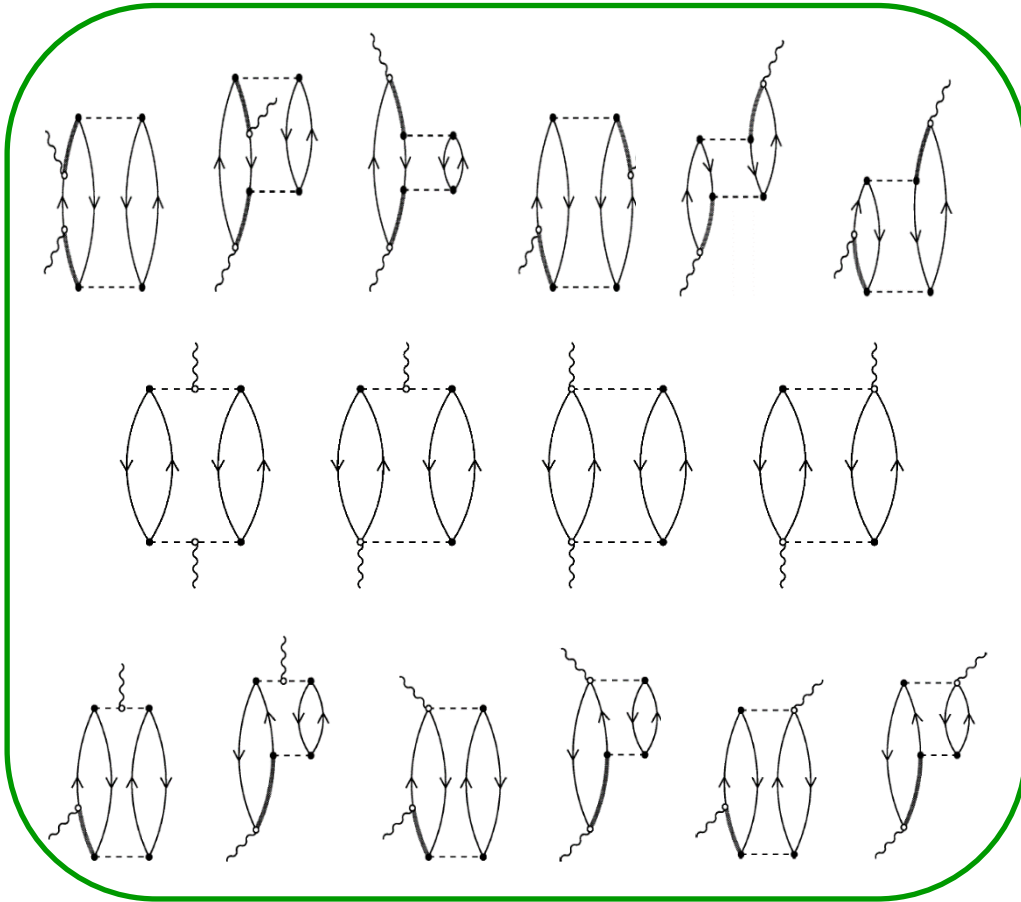
π



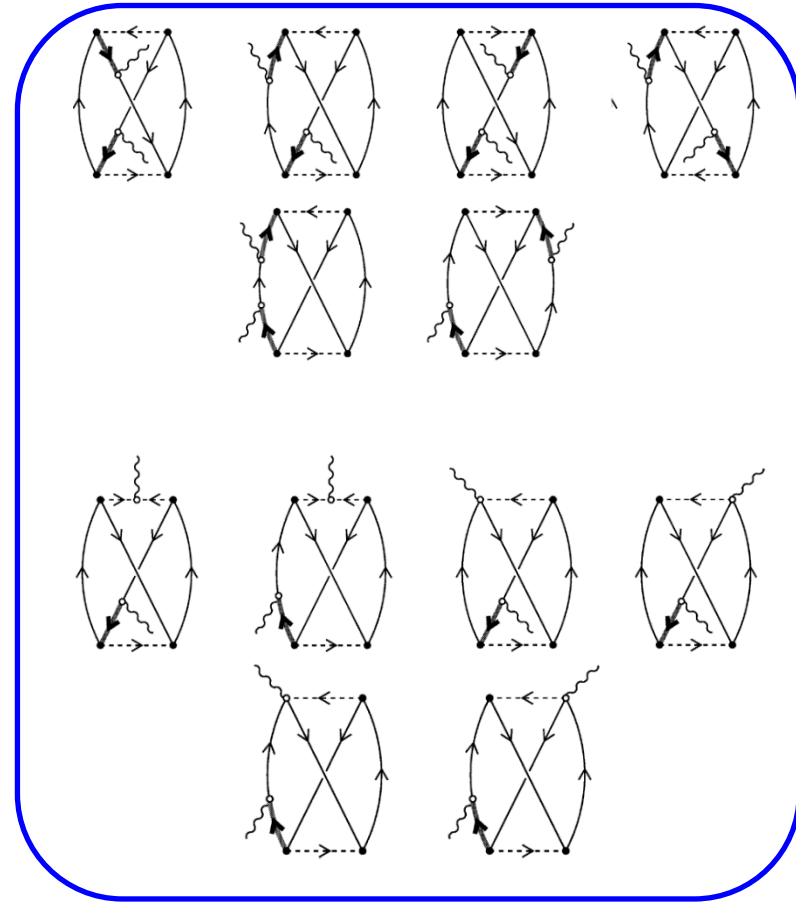
π - Δ intf.

Direct and exchange MEC contributions

Direct



Exchange



Fully relativistic calculation of *De Pace, Nardi, Alberico, Donnelly, Molinari, NPA741 (2004)*:

3000 direct terms

More than **100 000** exchange terms

Main difficulties in the np-nh sector

$$W^{\mu\nu}(\mathbf{q}, \omega) = W_{1p1h}^{\mu\nu}(\mathbf{q}, \omega) + W_{2p2h}^{\mu\nu}(\mathbf{q}, \omega) + \dots$$

$$W_{2p-2h}^{\mu\nu}(\mathbf{q}, \omega) = \frac{V}{(2\pi)^9} \int d^3p'_1 d^3p'_2 d^3h_1 d^3h_2 \frac{m_N^4}{E_1 E_2 E'_1 E'_2} \theta(p'_2 - k_F) \theta(p'_1 - k_F) \theta(k_F - h_1) \theta(k_F - h_2) \\ \underbrace{\langle 0 | J^\mu | \mathbf{h}_1 \mathbf{h}_2 \mathbf{p}'_1 \mathbf{p}'_2 \rangle \langle \mathbf{h}_1 \mathbf{h}_2 \mathbf{p}'_1 \mathbf{p}'_2 | J^\nu | 0 \rangle}_{\text{matrix elements}} \delta(E'_1 + E'_2 - E_1 - E_2 - \omega) \delta(\mathbf{p}'_1 + \mathbf{p}'_2 - \mathbf{h}_1 - \mathbf{h}_2 - \mathbf{q})$$

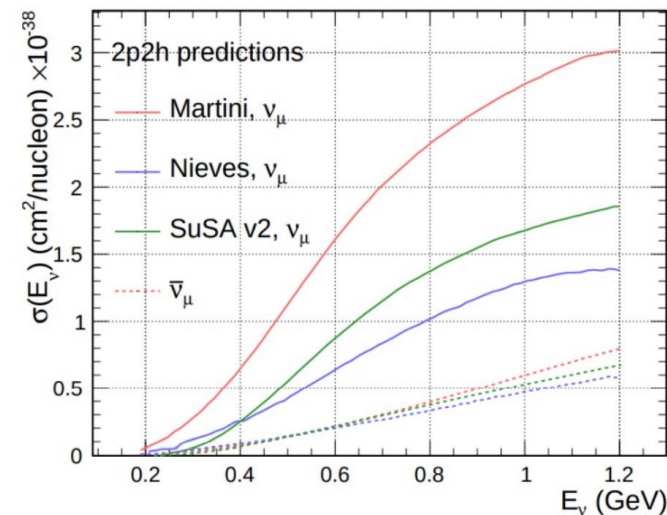
- 7-dimensional integrals $\int d^3h_1 d^3h_2 d\theta'_1$ of thousands of terms
- Huge number of diagrams and terms
- Divergences (angular distribution; NN correlations contributions)
- Calculations for all the kinematics compatible with the experimental neutrino flux

Computing very demanding

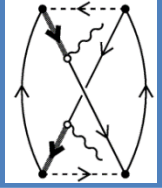
Hence different approximations by different groups:

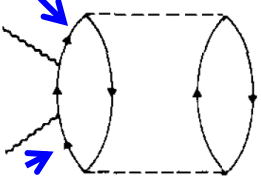
- choice of subset of diagrams and terms;
- different prescriptions to regularize the divergences;
- reduce the dimension of the integrals
(7D --> 2D if non relativistic; 7D --> 1D if $h_1 = h_2 = 0$)

⇒ Different final results by different groups



Different approximations for the 2p-2h calculations

Approach	Vector	Axial	NN correlations	MEC	NN-MEC interference	Relativistic	
RPA Lyon Martini et al.	Yes	Yes	$ \pi, g' $	Yes (Only Δ MEC)	Yes	Some ingredients	No
RPA Valencia Nieves et al.	Yes	Yes	$ \pi, \rho, g' $	Yes	Yes	Approximations in the WNN π vertex	No
SuSAv2	Yes	Yes	Already in Superscaling function (1p-1h part)	Yes	No	Fully Relativistic	Yes



$$(p_0 - E_{\mathbf{p}} + i\epsilon)^{-2}$$

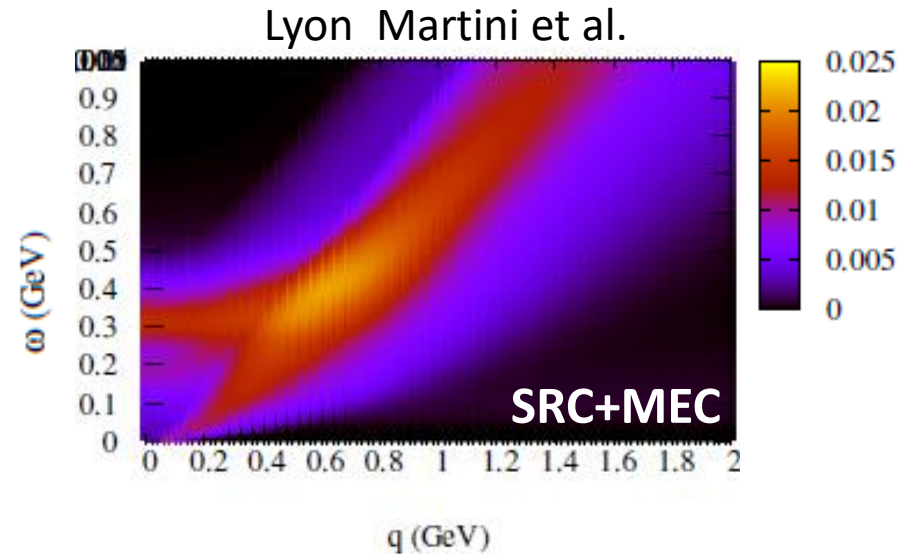
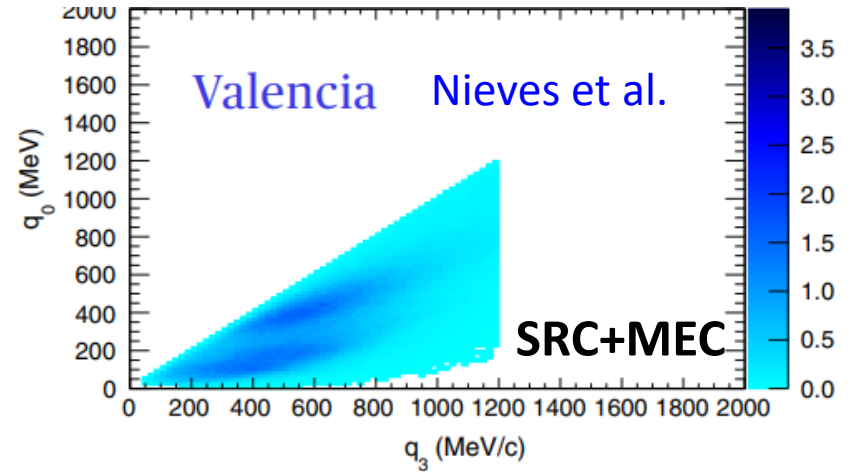
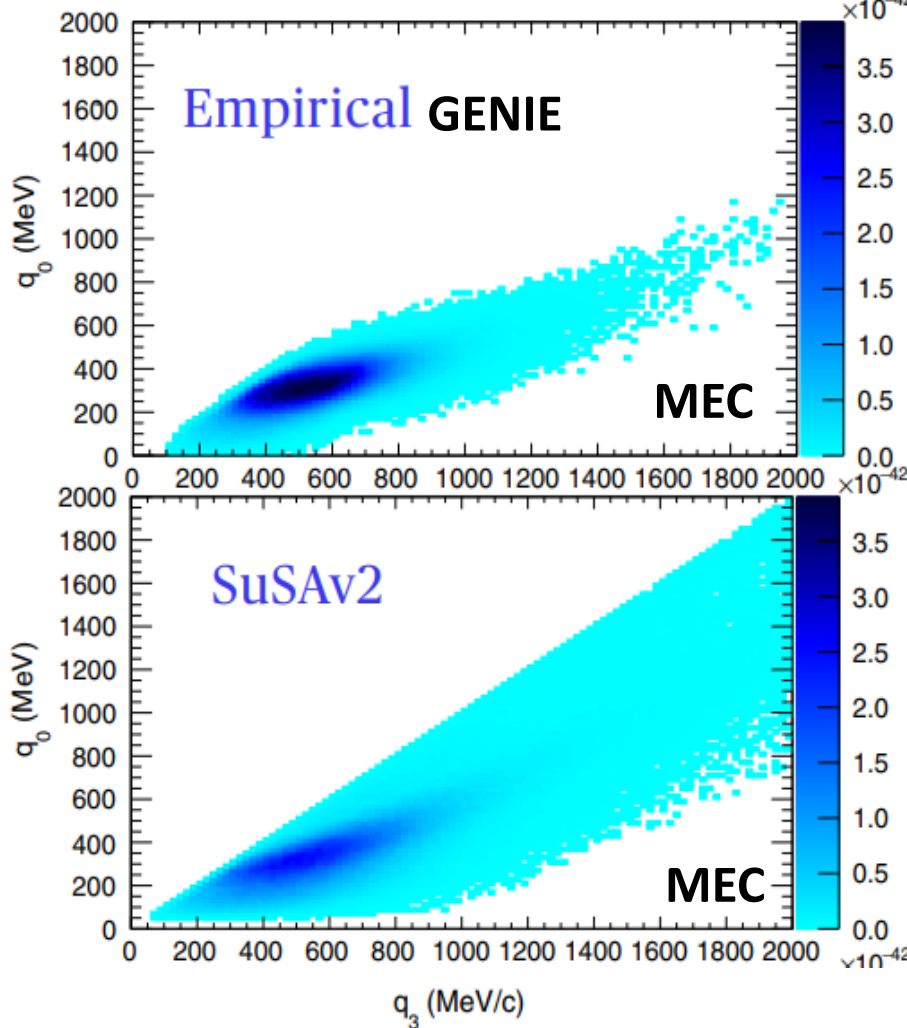
• Divergences in NN correlations, prescriptions:

- nucleon propagator only off the mass shell (*Alberico et al. Ann. Phys. 1984*)
- kinematical constraints + nucleon self energy in the medium (*Nieves et al PRC 83*)
- regularization parameter taking into account the finite size of the nucleus to be fitted to data (*Amaro et al. PRC 82 044601 2010*)

T. Katori, M. Martini, J.Phys.G 45 (2018) 1, 013001

Example of different results for 2p-2h in the (q, ω) or (q_0, q_3) plane

S. Dolan, G.D. Megias, S. Bolognesi, Phys.Rev.D 101 033003 (2020)

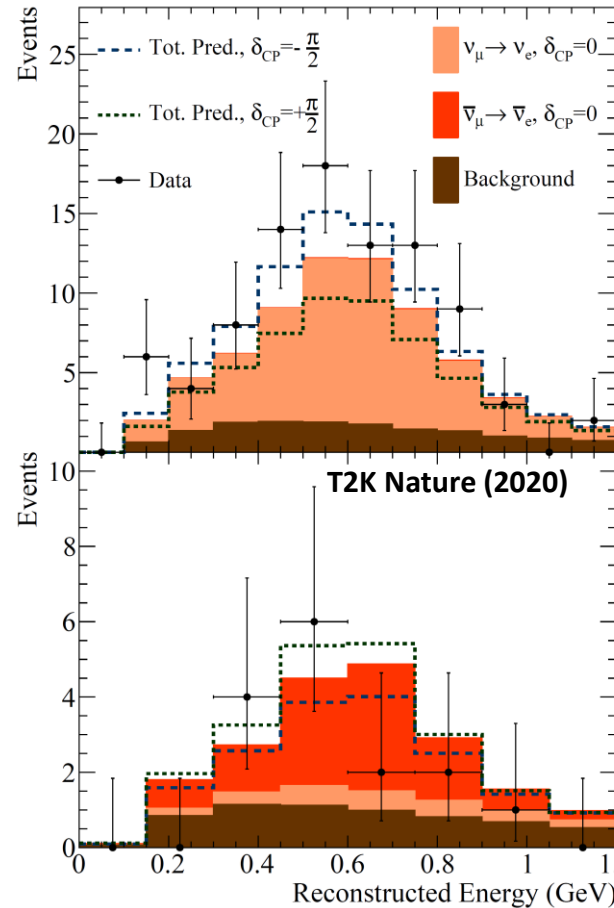
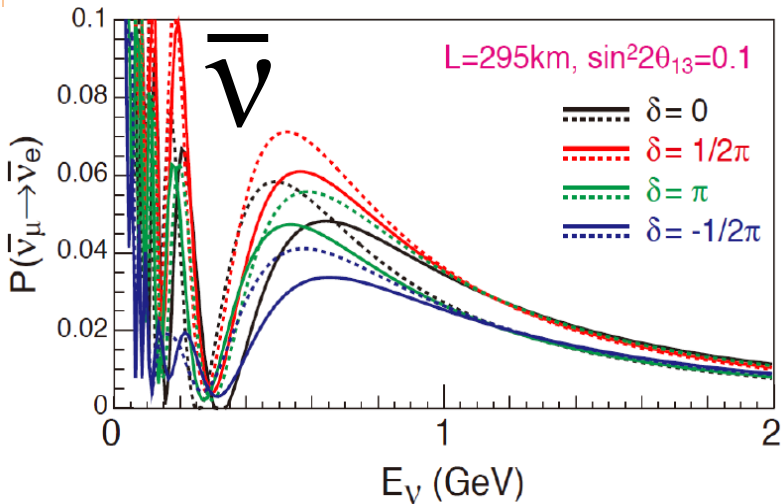
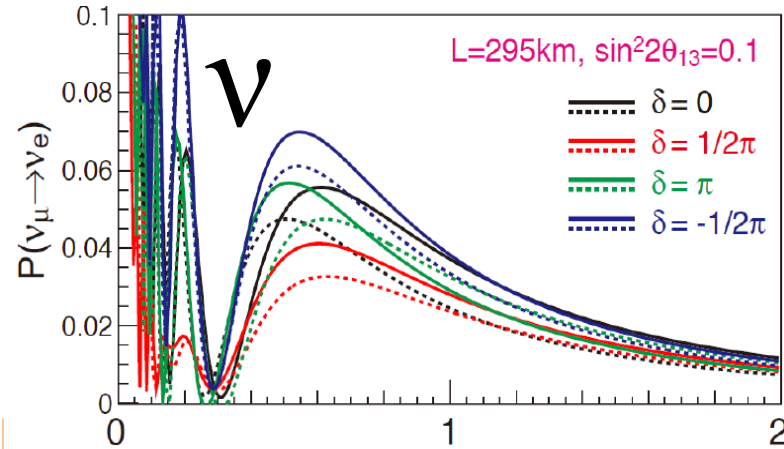


T. Katori, M. Martini, J.Phys.G 45 (2018) 1, 013001

ν .vs. $\bar{\nu}$ and ν_{μ} .vs. ν_e

What about ν vs $\bar{\nu}$ interaction? And ν_μ vs ν_e ?

$$P(\nu_\mu \rightarrow \nu_e) \stackrel{?}{\neq} P(\bar{\nu}_\mu \rightarrow \bar{\nu}_e)$$



$\nu_\mu \rightarrow \nu_e$

$\bar{\nu}_\mu \rightarrow \bar{\nu}_e$

A precise and simultaneous knowledge of the four cross sections is important in connection to the oscillation experiments aiming at the search for CP violation in the lepton sector.

Neutrino vs Antineutrino interactions

The ν and anti ν cross sections differ by the sign of the V-A interference term

$$\frac{d^2\sigma}{d\cos\theta d\omega} = \frac{G_F^2 \cos^2\theta_c |\mathbf{k}'| E_l' \cos^2\frac{\theta}{2}}{\pi} \left[\frac{(\mathbf{q}^2 - \omega^2)^2}{\mathbf{q}^4} G_E^2 R_\tau(\mathbf{q}, \omega) + \frac{\omega^2}{\mathbf{q}^2} G_A^2 R_{\sigma\tau(L)}(\mathbf{q}, \omega) \right. \\ \left. + 2 \left(\tan^2\frac{\theta}{2} + \frac{\mathbf{q}^2 - \omega^2}{2\mathbf{q}^2} \right) \left(G_M^2 \frac{\mathbf{q}^2}{4M_N^2} + G_A^2 \right) R_{\sigma\tau(T)}(\mathbf{q}, \omega) \pm 2 \frac{E_\nu + E_l'}{M_N} \tan^2\frac{\theta}{2} G_A G_M R_{\sigma\tau(T)}(\mathbf{q}, \omega) \right]$$

Vector-Axial interference

$$\begin{cases} + & (\nu) \\ - & (\bar{\nu}) \end{cases}$$

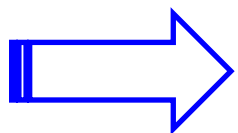
Vector-Axial interference:

basic asymmetry from weak interaction theory

different sign in the Leptonic tensor

$$L_{\mu\nu} = k_\mu k'_\nu + k_\nu k'_\mu - g_{\mu\nu} k \cdot k' \mp i\varepsilon_{\mu\nu\alpha\beta} k^\alpha k'^\beta$$

ν
 $\bar{\nu}$

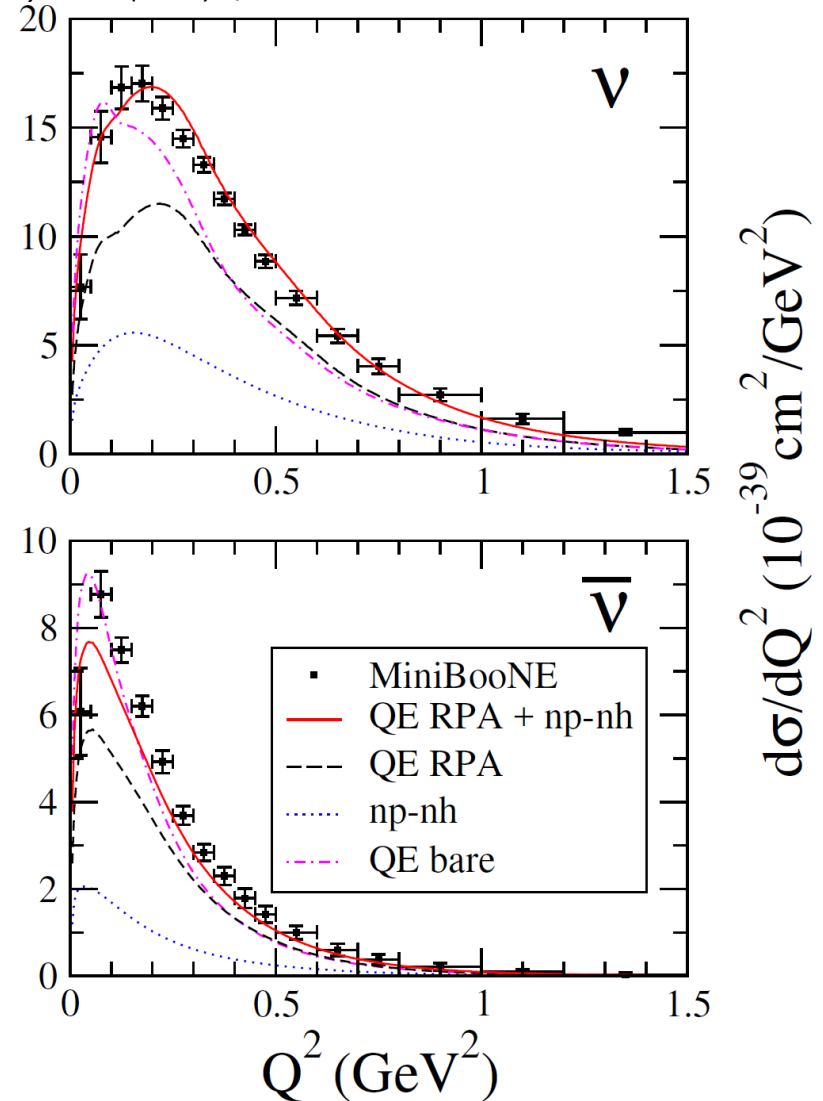
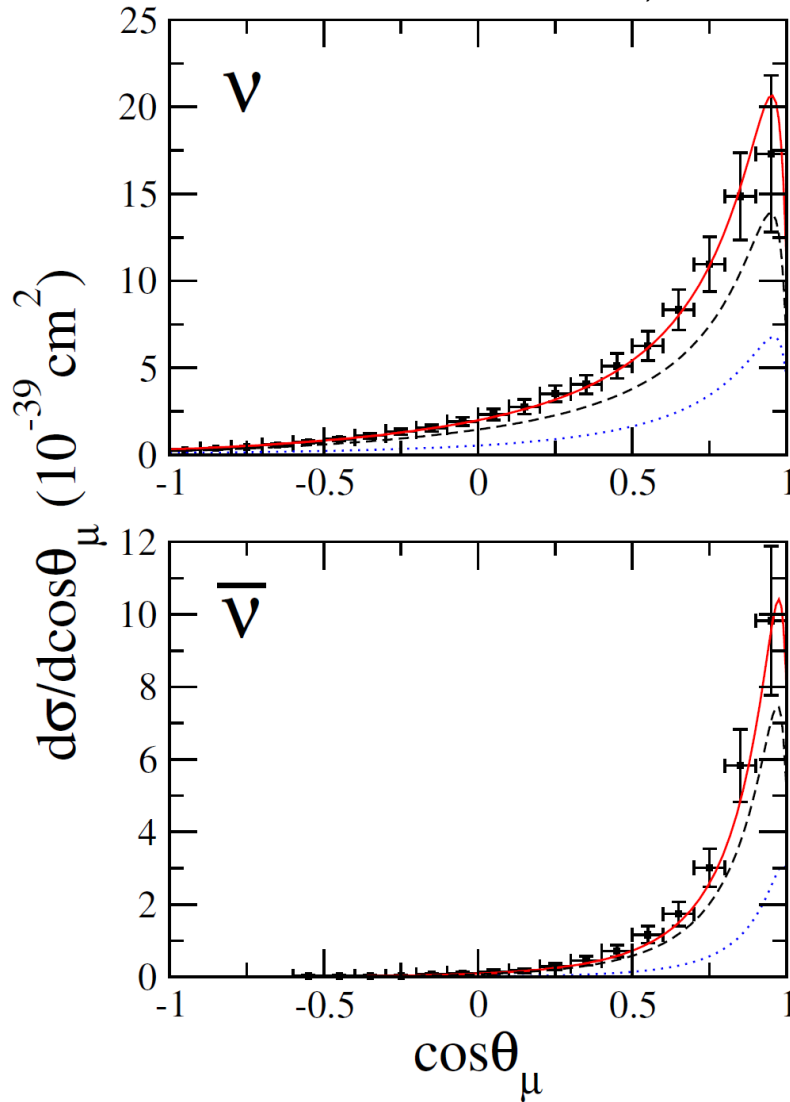


Even neglecting nuclear effects, the absolute value and the kinematic behavior of neutrino and antineutrino cross sections are different

$d\sigma/d\cos\theta$

Q^2 distribution

T. Katori, M. Martini, *J.Phys.G* 45 (2018) 1, 013001



- Antineutrino cross section falls more rapidly than the neutrino one
- Antineutrino Q^2 distribution peaks at smaller Q^2 values than the neutrino one

Neutrino vs Antineutrino interactions and nuclear effects

$$\frac{d^2\sigma}{d\cos\theta d\omega} = \frac{G_F^2 \cos^2\theta_c}{\pi} |\mathbf{k}'| E_l' \cos^2\frac{\theta}{2} \left[\frac{(\mathbf{q}^2 - \omega^2)^2}{\mathbf{q}^4} G_E^2 R_\tau(\mathbf{q}, \omega) + \frac{\omega^2}{\mathbf{q}^2} G_A^2 R_{\sigma\tau(L)}(\mathbf{q}, \omega) \right]$$

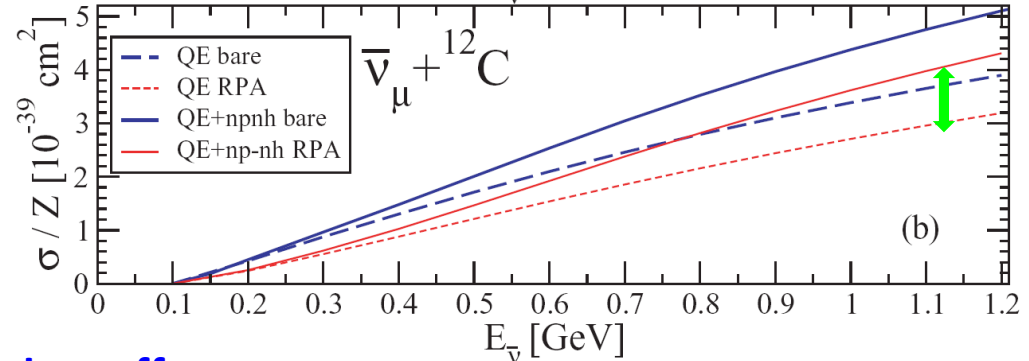
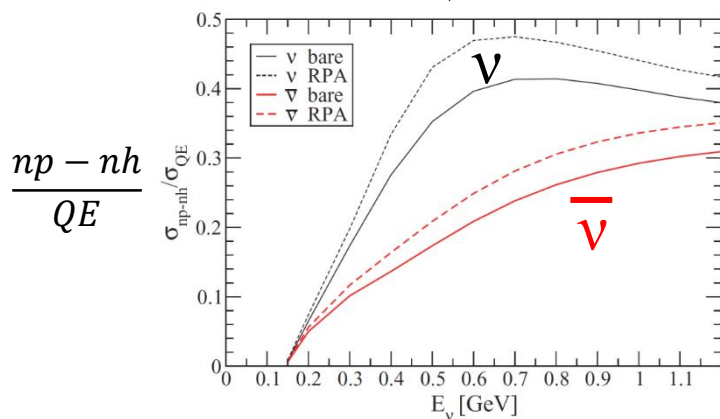
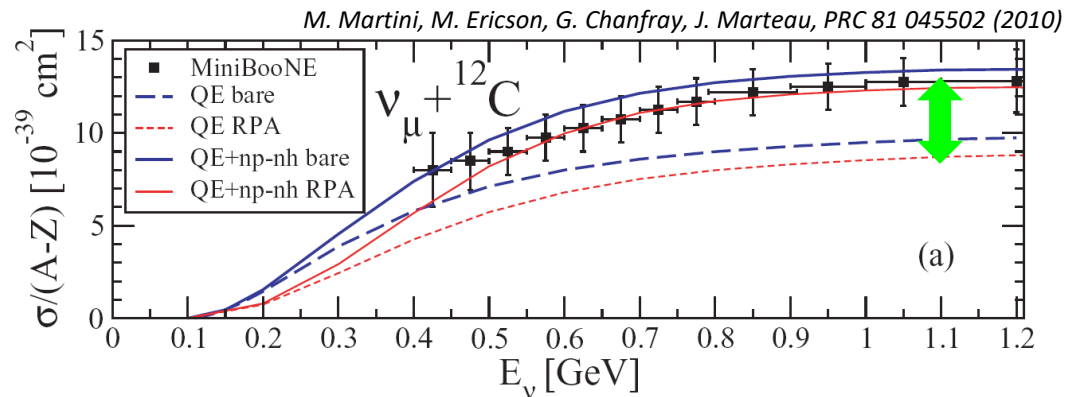
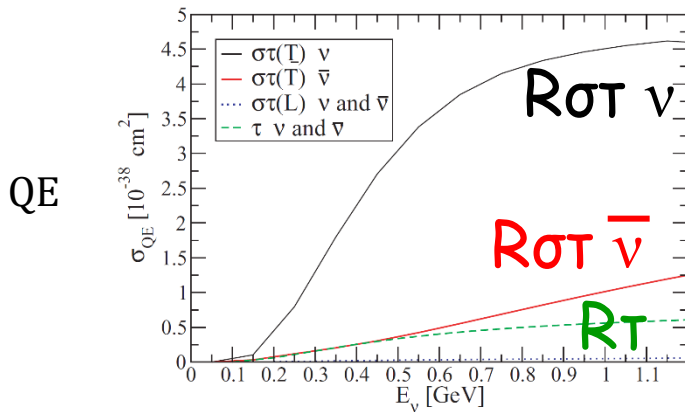
$$+ 2 \left(\tan^2\frac{\theta}{2} + \frac{\mathbf{q}^2 - \omega^2}{2\mathbf{q}^2} \right) \left(G_M^2 \frac{\mathbf{q}^2}{4M_N^2} + G_A^2 \right) R_{\sigma\tau(T)}(\mathbf{q}, \omega) \pm 2 \frac{E_\nu + E_l'}{M_N} \tan^2\frac{\theta}{2} G_A G_M R_{\sigma\tau(T)}(\mathbf{q}, \omega)$$

Vector-Axial interference

The ν and anti ν interactions differ by the sign of the V-A interference term

→ the relative weight of the different nuclear responses is different for neutrinos and antineutrinos

→ the relative role of np-nh contributions is different for neutrinos and antineutrinos



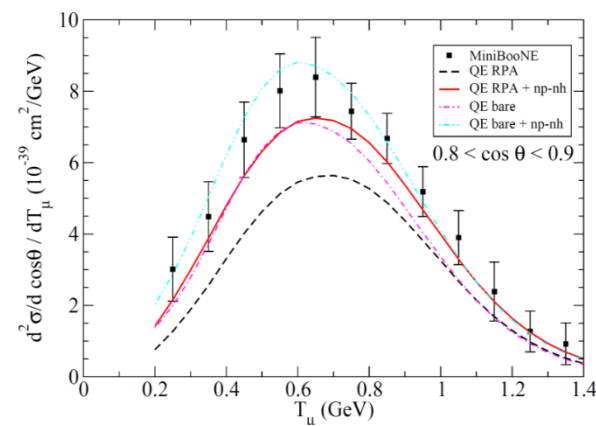
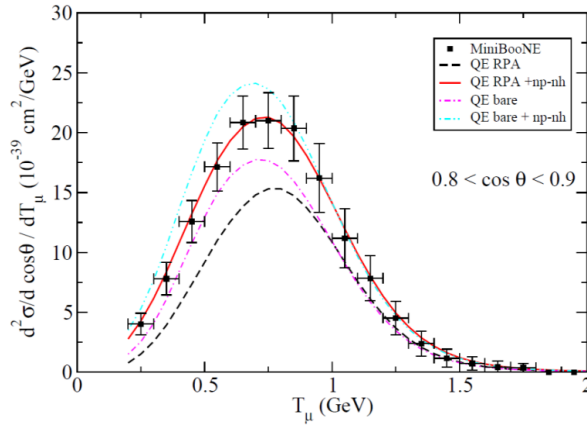
**Nuclear effects generate an asymmetry
unrelated to CP violation**

The relative role of np-nh for neutrinos and antineutrinos is different in different approaches



Lyon RPA
Martini et al.

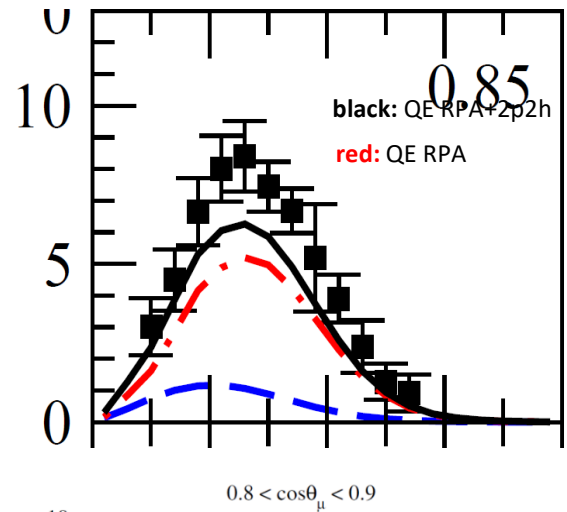
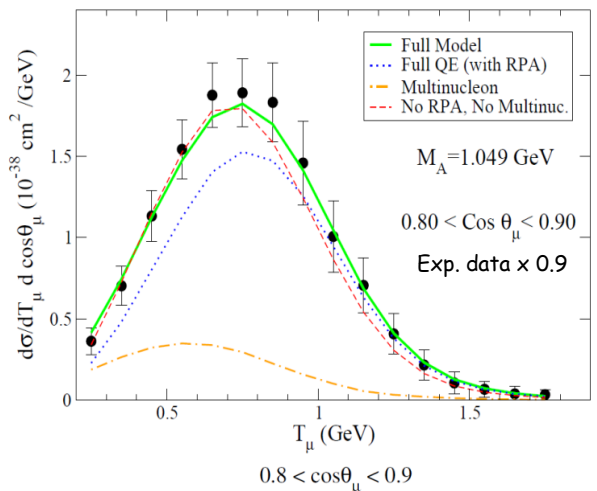
PRC 84 (2011)



PRC 87 (2013)

Valencia RPA
Nieves et al.

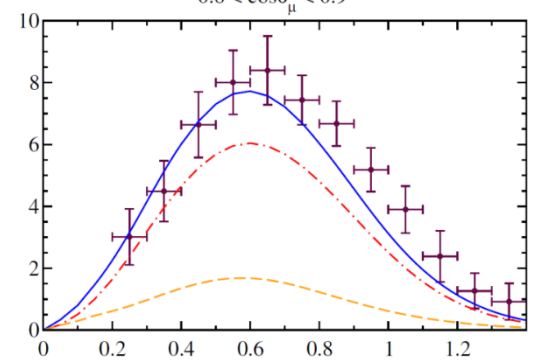
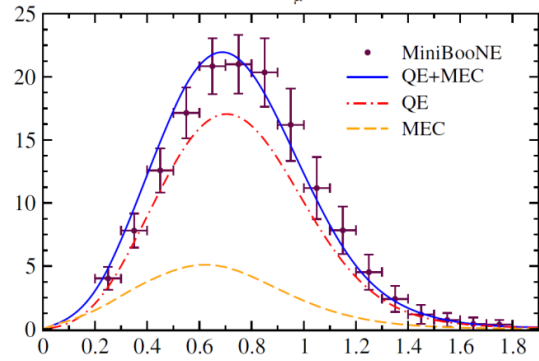
PLB 707 (2012)



PLB 721 (2013)

SuSAv2

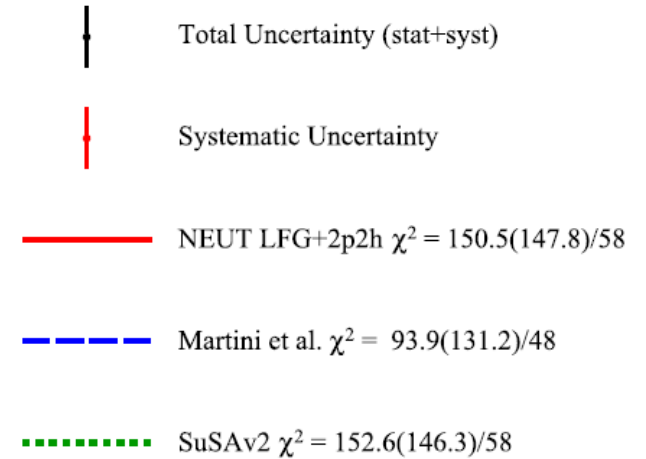
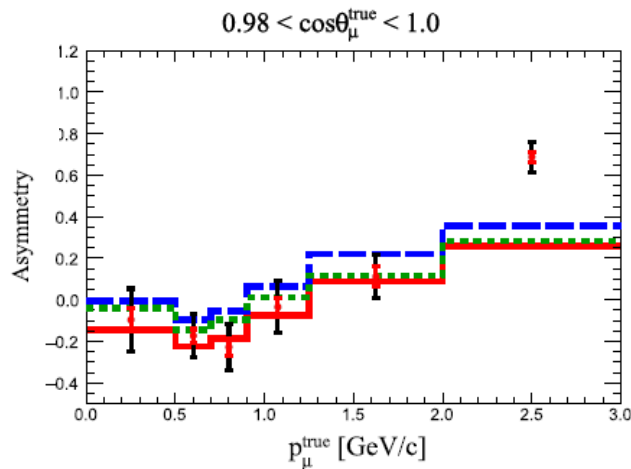
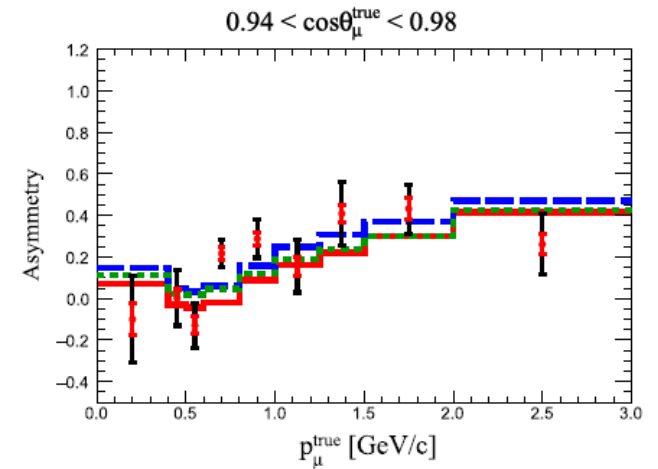
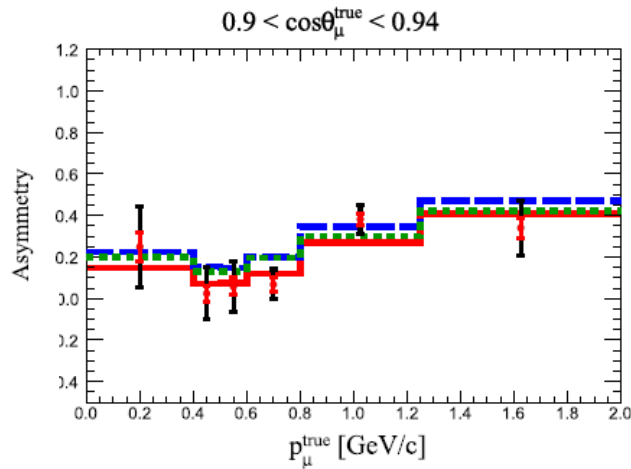
PRD 94 (2016)



PRD 94 (2016)

First combined measurement of the muon neutrino and antineutrino charged-current cross section without pions in the final state at T2K

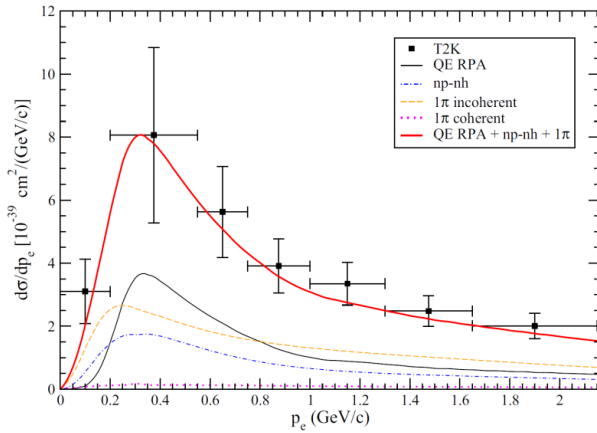
$$\frac{\nu - \bar{\nu}}{\nu + \bar{\nu}}$$



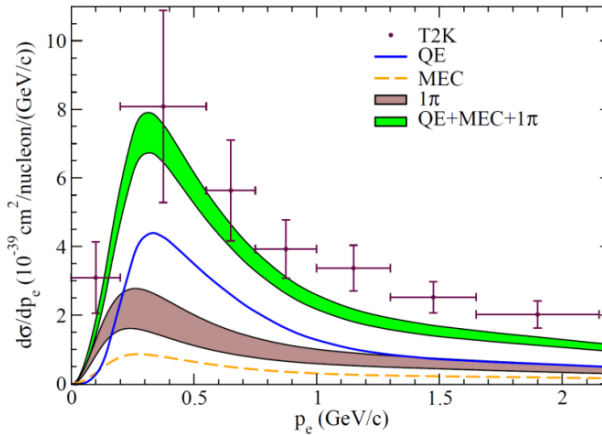
ν_e cross sections

- There are few published results on ν_e cross sections. This is essentially due the relatively small component of ν_e fluxes with respect to the ν_μ ones hence to small statistics.
- The ν_e experimental published results essentially concern inclusive cross sections
T2K flux-integrated ν_e CC inclusive differential cross sections on carbon

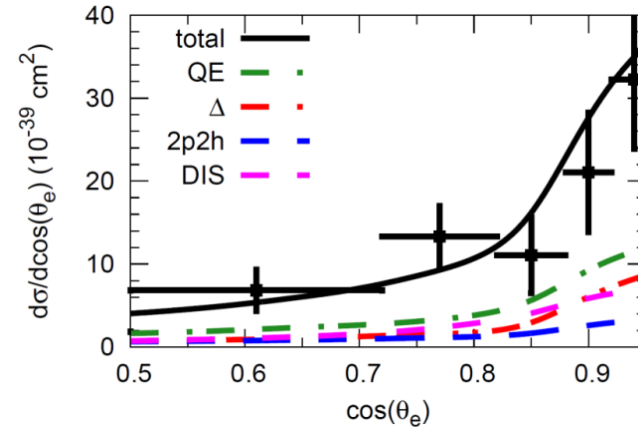
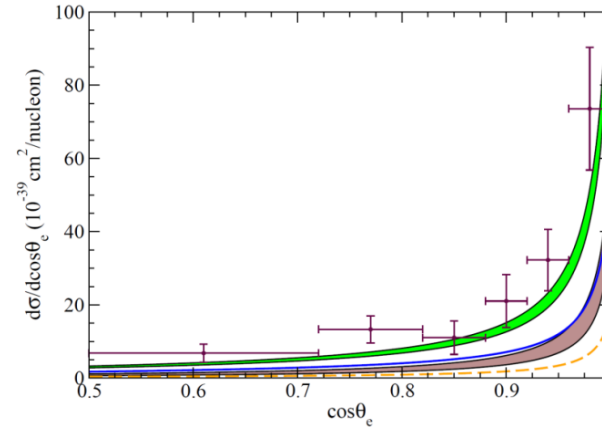
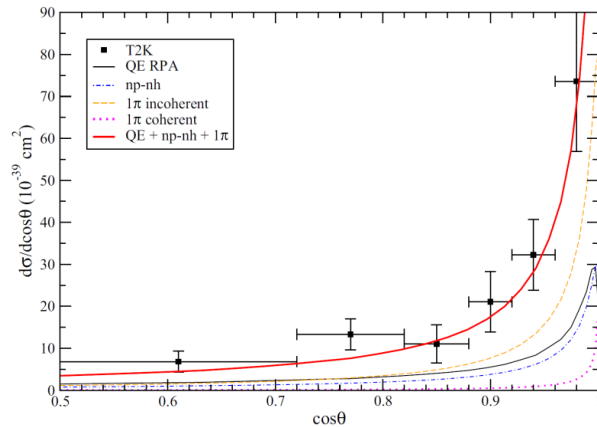
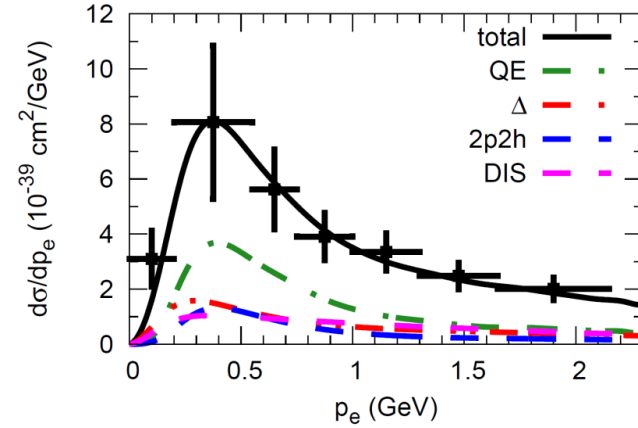
Martini et al., PRC 94 (2016)



Megias et al., PRD 94 (2016)

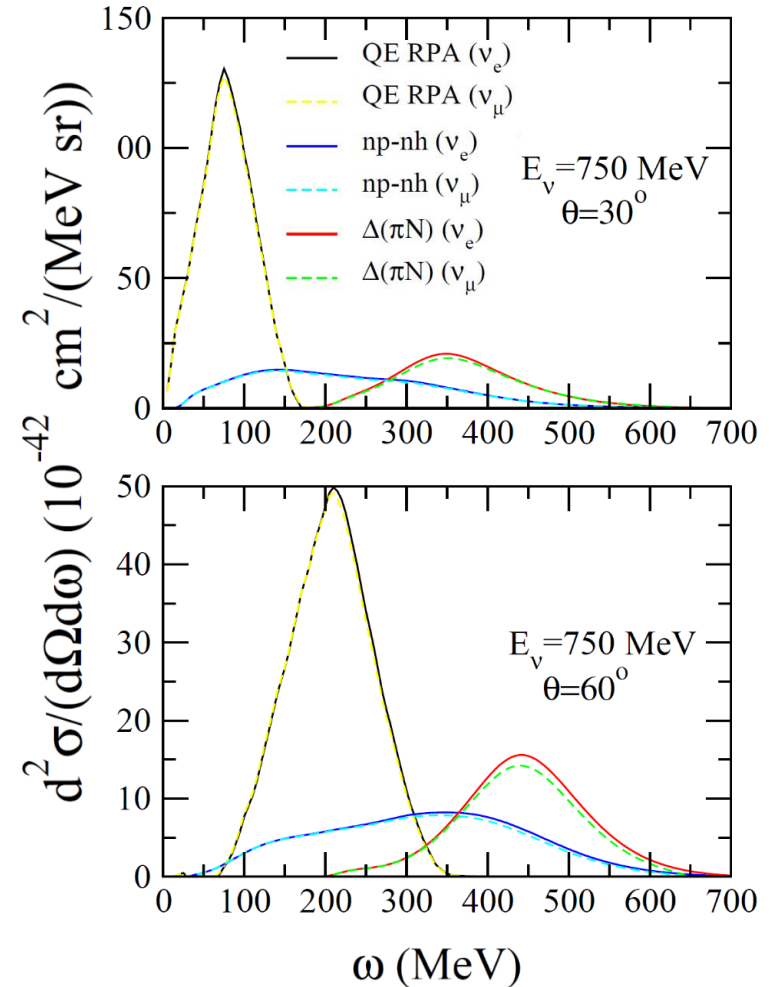
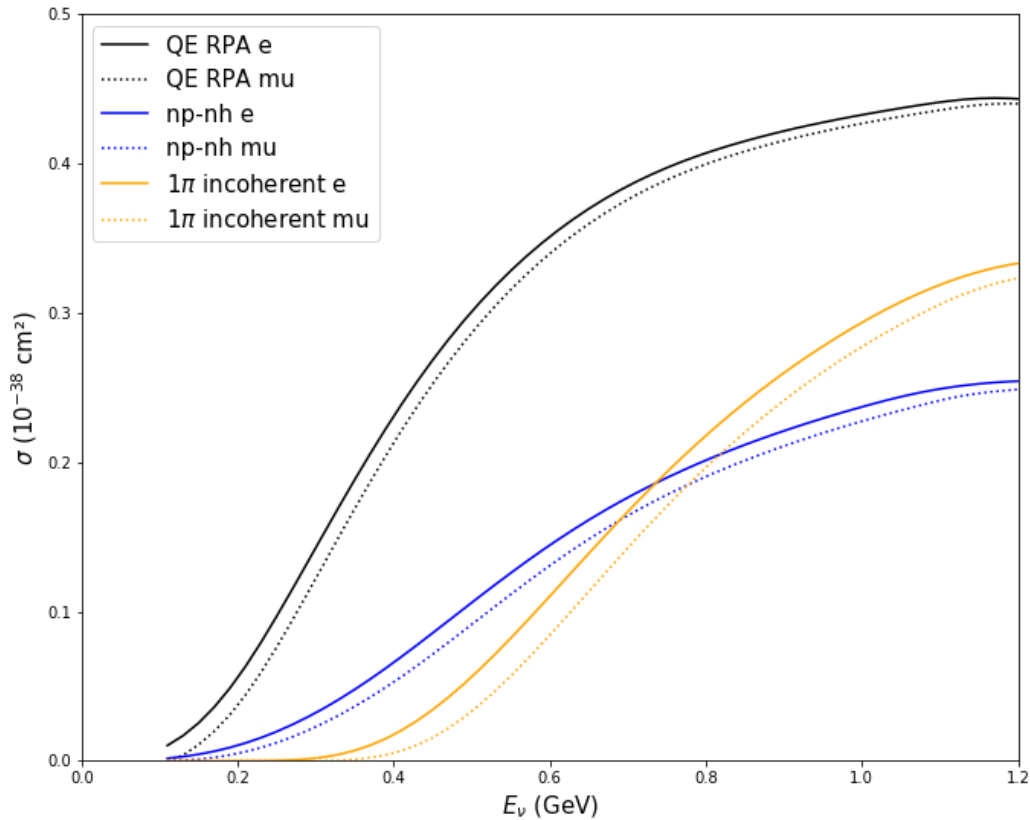


Gallmeister et al. PRC 94(2016)



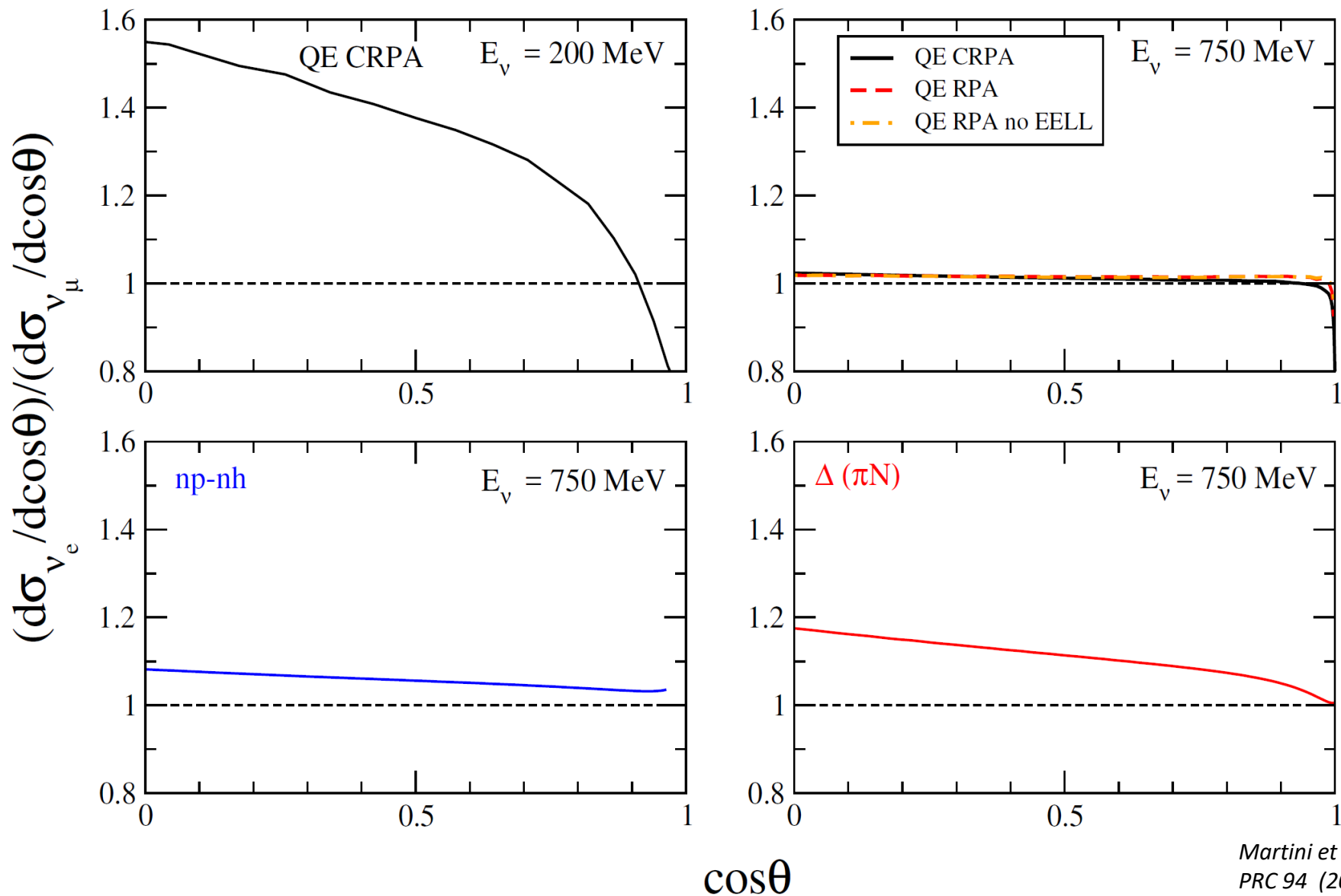
- Theoretical results agree with data
- Similarity of the theoretical results for the inclusive $d\sigma$

ν_e and ν_μ total and double differential cross sections



Due to the different kinematic limits, the ν_e cross sections are expected to be larger than the ν_μ ones

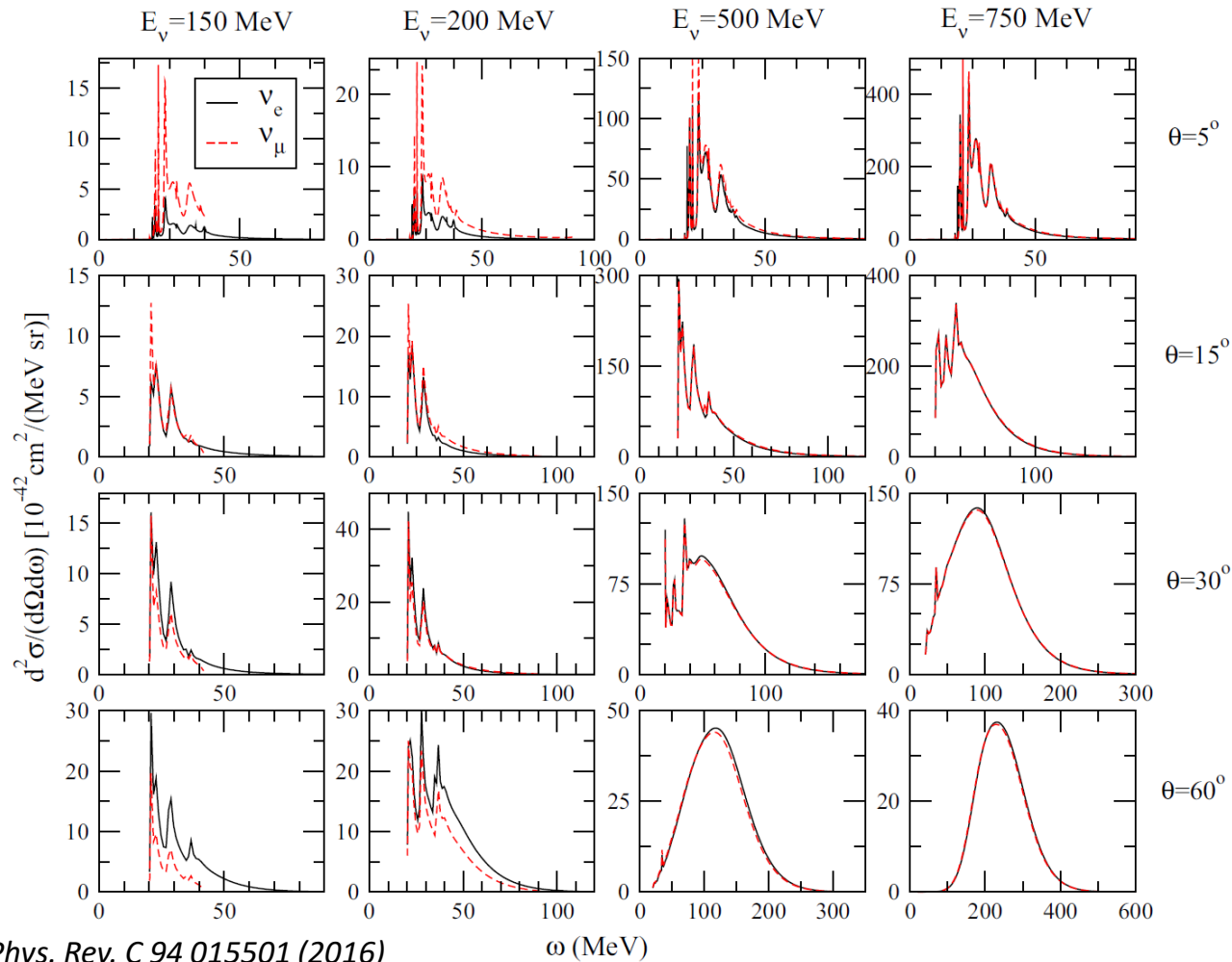
Ratio v_e/v_μ for $d\sigma/d\cos\theta$ in different channels



Martini et al.,
PRC 94 (2016)

Due to the different kinematic limits, the ν_e cross sections are expected to be larger than the ν_μ ones. However for forward scattering angles this hierarchy is opposite in the QE channel.

A theoretical study (HF+CRPA Ghent) of the ν_μ and ν_e $d^2\sigma$



M. Martini et al., Phys. Rev. C 94 015501 (2016)

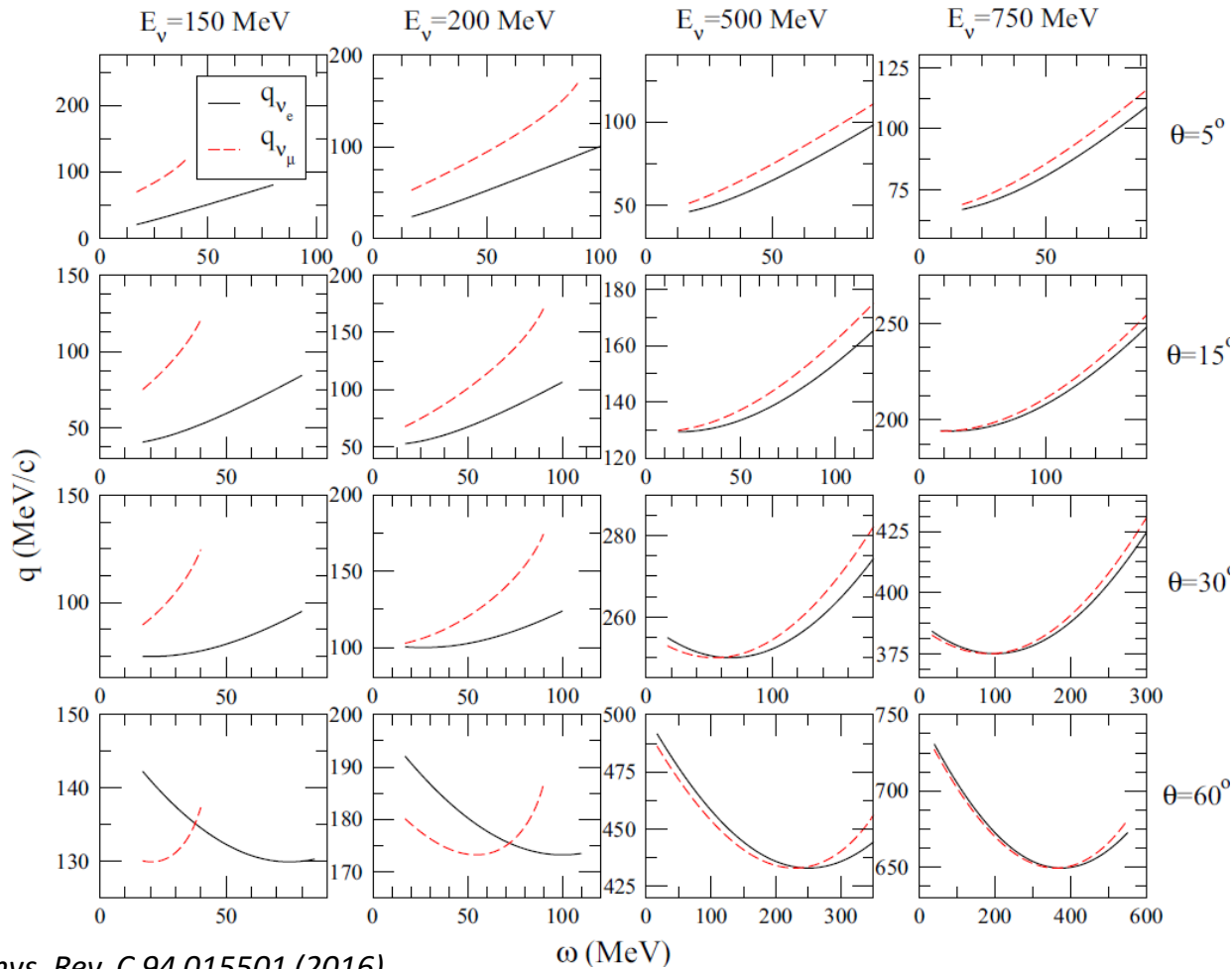
Due to the different kinematic limits, the ν_e cross sections are expected to be larger than the ν_μ ones. However for forward scattering angles this hierarchy is opposite.

The only difference between ν_μ and ν_e cross sections is the mass of the outgoing lepton.

But the mass affects the three momentum transfer which enters into the kinematics as well as the dynamics of the nuclear model

Momentum transfer q versus transferred energy ω for ν_μ and ν_e $d^2\sigma$

Kinematical conditions of the previous slide



M. Martini et al., Phys. Rev. C 94 015501 (2016)

$$q^2 = E_\nu^2 + p_l^2 - 2E_\nu p_l \cos \theta$$

$$p_l^2 = E_l^2 - m_l^2 = (E_\nu - \omega)^2 - m_l^2$$

The only difference between ν_μ and ν_e cross sections is the mass of the outgoing lepton. But the mass affects the three-momentum transfer which enters into the kinematics as well as the dynamics of the nuclear model

Neutrino energy reconstruction

Energy reconstruction in neutrino oscillation experiments

$$N_{\nu\beta}(\overline{E_\nu}) \sim \int \Phi_{\nu\alpha}(E_\nu) P_{\nu\alpha \rightarrow \nu\beta}(E_\nu, L, \{\Theta\}) \sigma_{\nu\beta}(E_\nu) \epsilon_{\text{det.}} d(E_\nu, \overline{E_\nu}) dE_\nu$$

Reconstructed ν energy
True ν energy
Number of detected events

ν flux	ν oscillation probability	ν cross section	Detector efficiency	Migration matrix
------------	-------------------------------	---------------------	---------------------	-------------------------

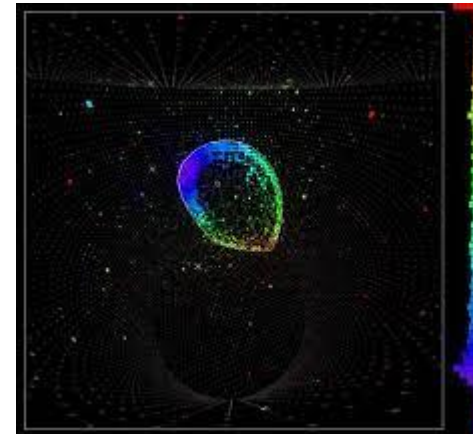
Two methods for ν energy reconstruction

Tracking detectors

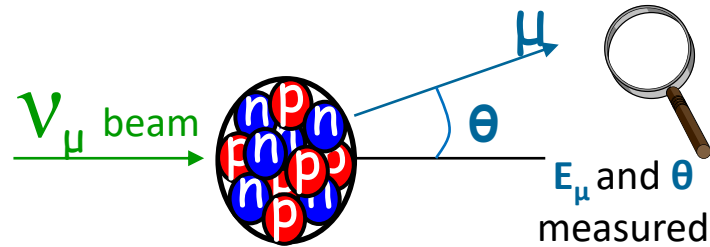
- Use all the detected particles
- Calorimetric method

Cherenkov detectors

- Use only lepton
- Quasielastic-based method



Quasielastic-based neutrino energy reconstruction



Reconstructed neutrino energy

$$\overline{E_{\nu}} = \frac{m_p^2 - (m_n - E_b)^2 - m_{\mu}^2 + 2(m_n - E_b)E_{\mu}}{2(m_n - E_b - E_{\mu} + p_{\mu} \cos \theta_{\mu})}$$

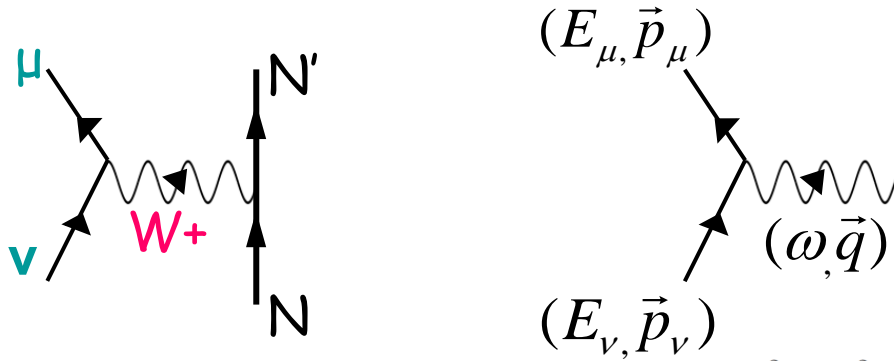
via two-body kinematics

$$\overline{E_{\nu}} = E_{\nu}$$

is exact only for CCQE with free nucleon

reconstructed neutrino energy $\overline{E_{\nu}}$ \longleftrightarrow E_{ν} true neutrino energy

QE Scattering with free nucleon at rest: two-body kinematics



$$\omega = E_\nu - E_\mu$$

$$q^2 = E_\nu^2 + p_\mu^2 - 2E_\nu p_\mu \cos \theta$$

$$q^2 - \omega^2 = 4(E_\mu + \omega)E_\mu \sin^2 \frac{\theta}{2} - m_\mu^2 + 2(E_\mu + \omega)(E_\mu - p_\mu) \cos \theta$$

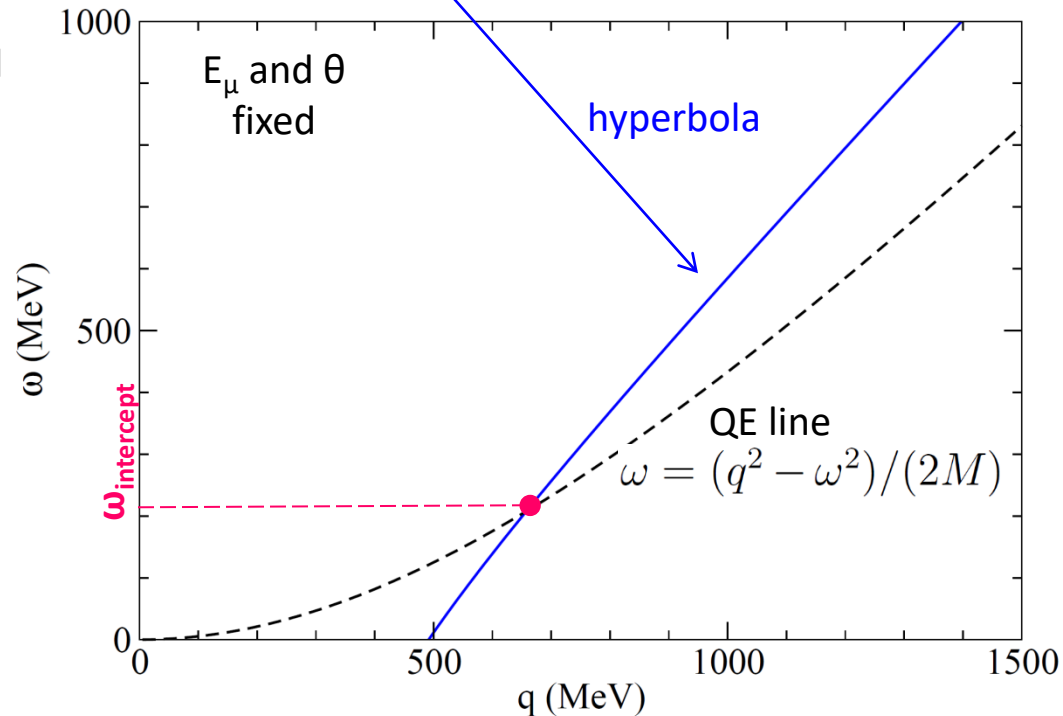
The nuclear response function is proportional to the delta distribution

$$\delta \left[\omega - \left(\sqrt{q^2 + M^2} - M \right) \right]$$

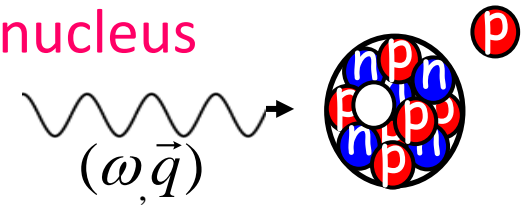
The intercept of the **hyperbola** with the **QE line** fixes the possible ω and q values for given E_μ and θ .

Hence the neutrino energy is determined

$$E_\nu = E_\mu + \omega_{\text{intercept}}$$



QE Scattering with nucleon inside the nucleus



The intercept of the **hyperbola** with the **response region** gives several possible ω

Broadening of the neutrino energy

$$E_\nu = E_\mu + (\omega_{\min} \leq \omega \leq \omega_{\max})$$

Nuclear effects in genuine CCQE (1p-1h)

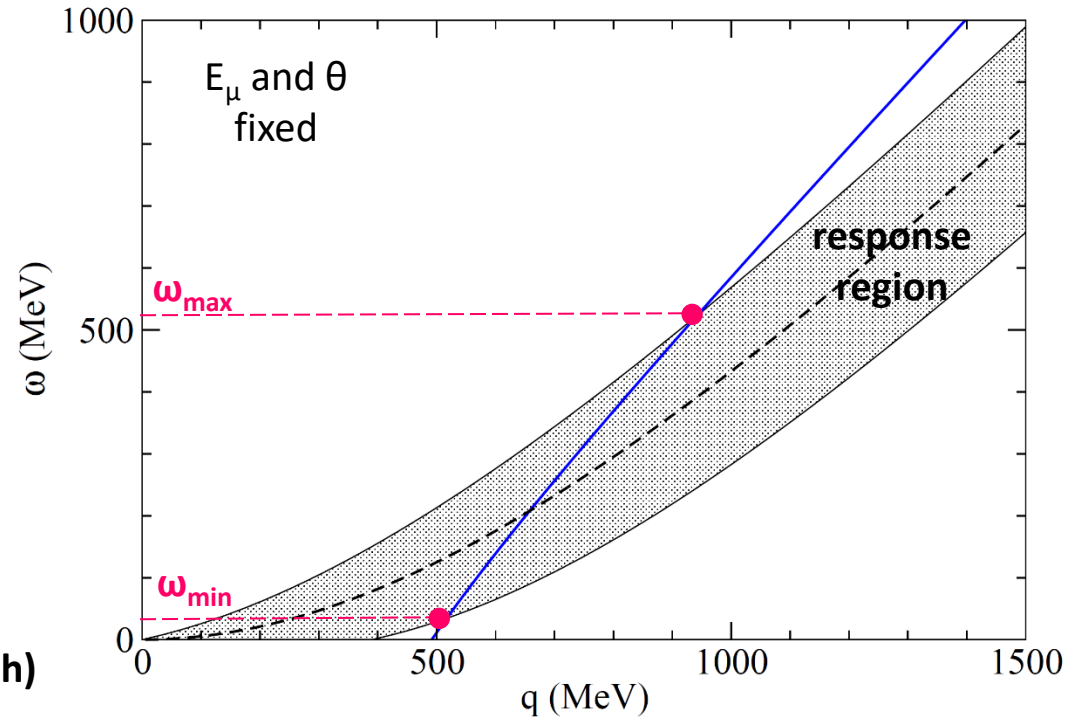
Fermi motion spreads δ distribution

Pauli blocking cuts part of the nuclear response

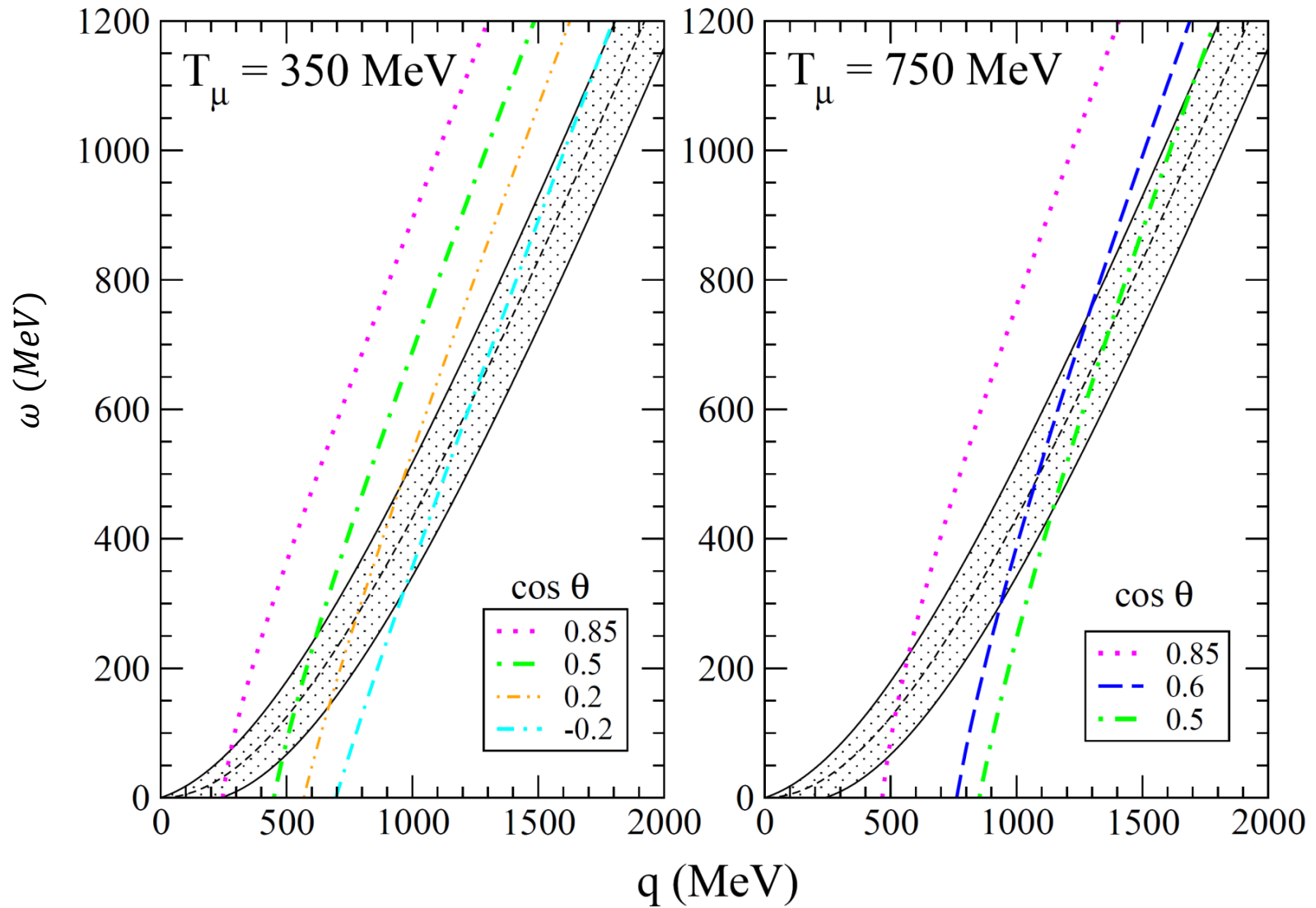
Binding energy E_B

Long Range Correlations (RPA collective effects)

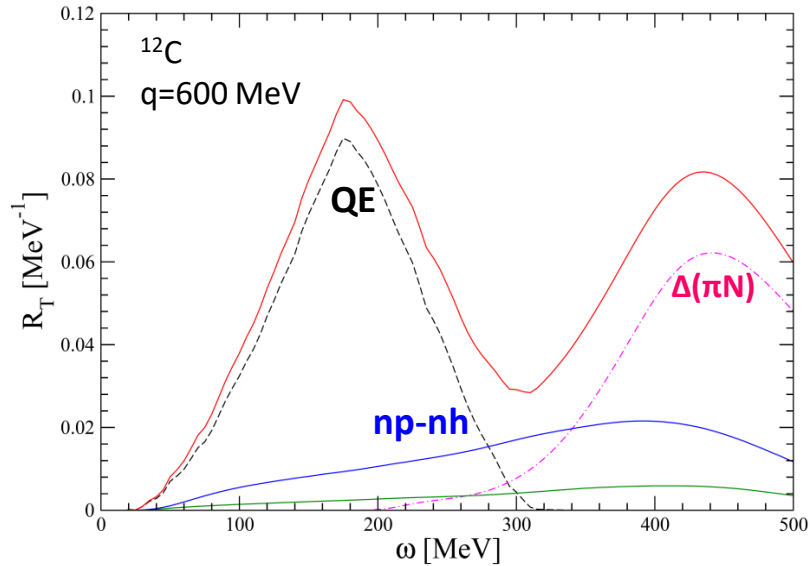
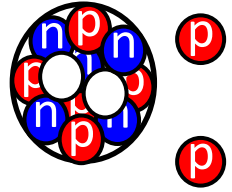
Final State interactions (FSI)



P.S. QE Response region and hyperbolas for several T_μ and θ

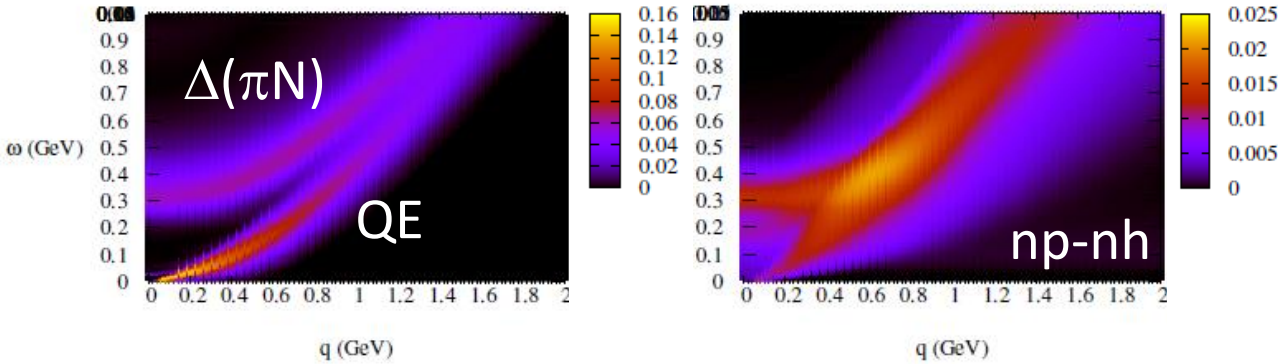


Multinucleon emission

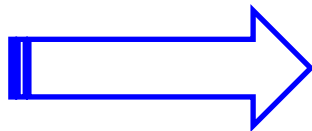


np-nh creates a high energy tail above the QE peak

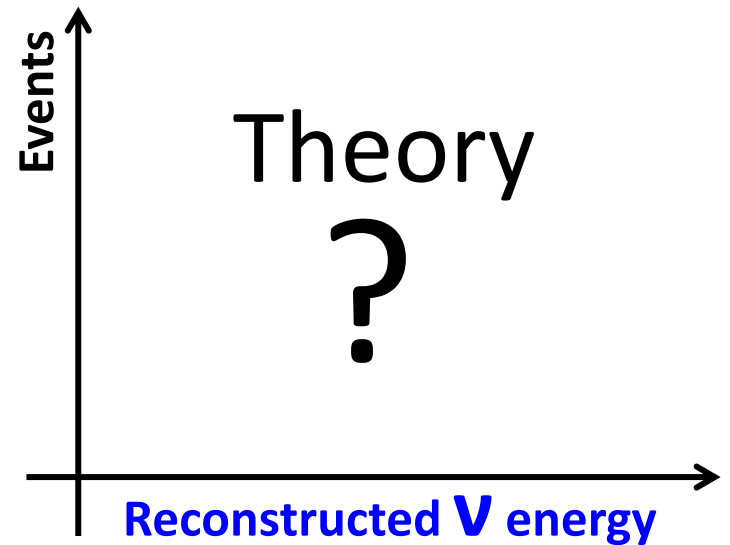
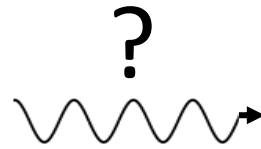
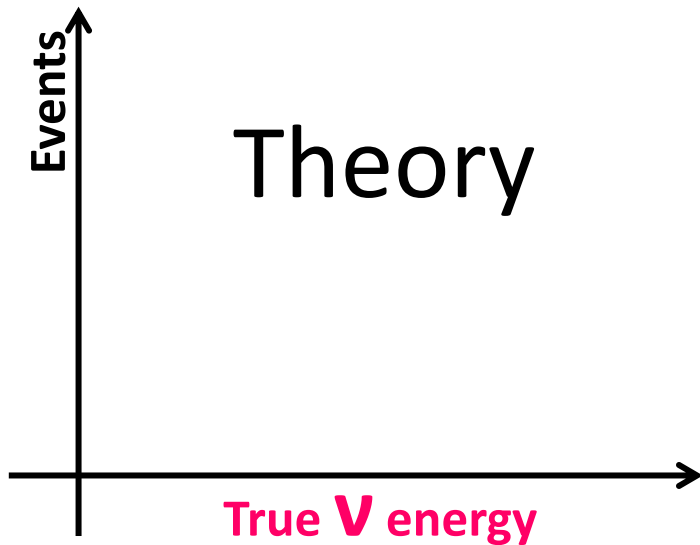
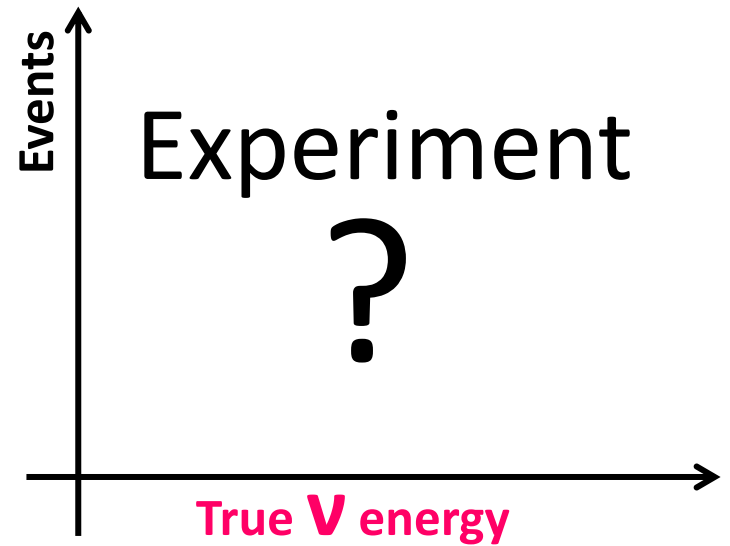
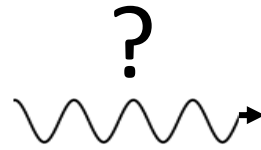
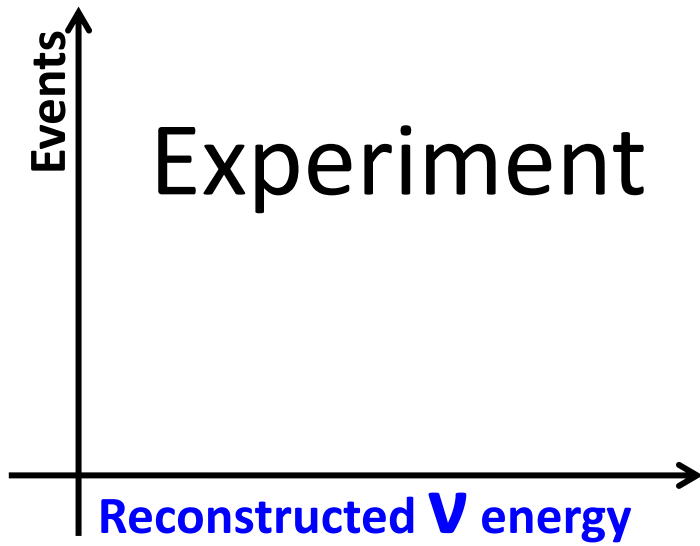
T. Katori, M. Martini, J. Phys. G 45 1, 013001 (2018)



np-nh enlarges the region of response to the whole (ω, q) plane



no reason to fulfill the QE relation for E_ν reconstruction



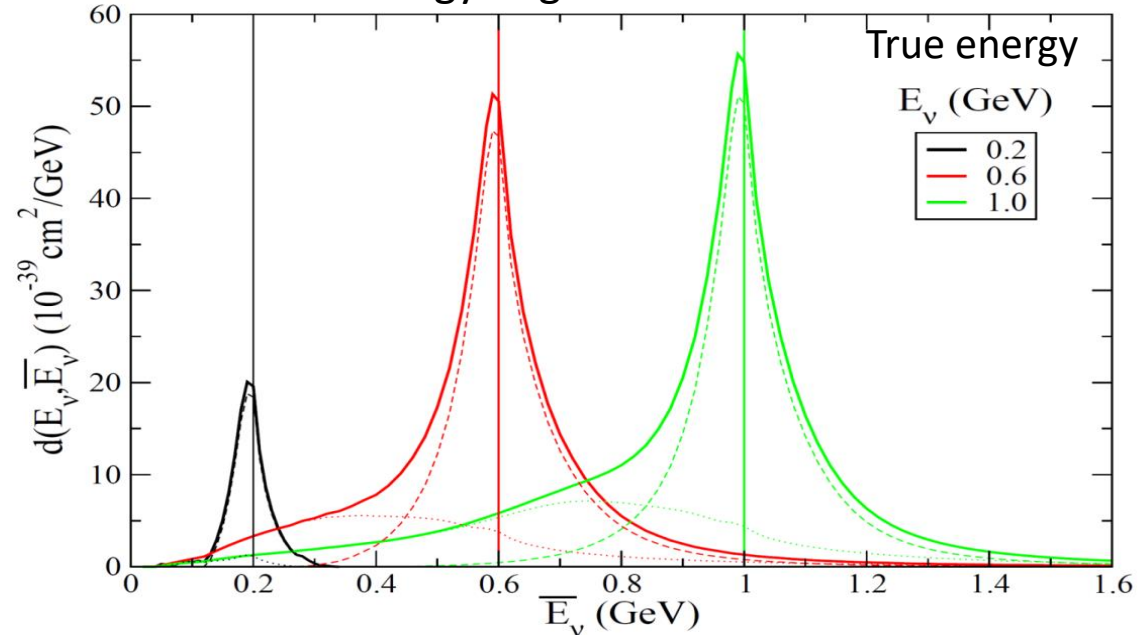
From true neutrino energy to reconstructed neutrino energy

$$D_{rec}(\bar{E}_\nu) = \int dE_\nu \Phi(E_\nu) \int_{E_l^{min}}^{E_l^{max}} dE_l \frac{ME_l - m_l^2/2}{\bar{E}_\nu^2 P_l} \left[\frac{d^2\sigma}{d\omega d\cos\theta} \right]_{\omega=E_\nu-E_l, \cos\theta=\cos\theta(E_l, \bar{E}_\nu)}$$

v energy migration matrix

The quantity $D_{rec}(\bar{E}_\nu)$ corresponds to the product $\sigma(E_\nu)\Phi(E_\nu)$ but in terms of reconstructed neutrino energy

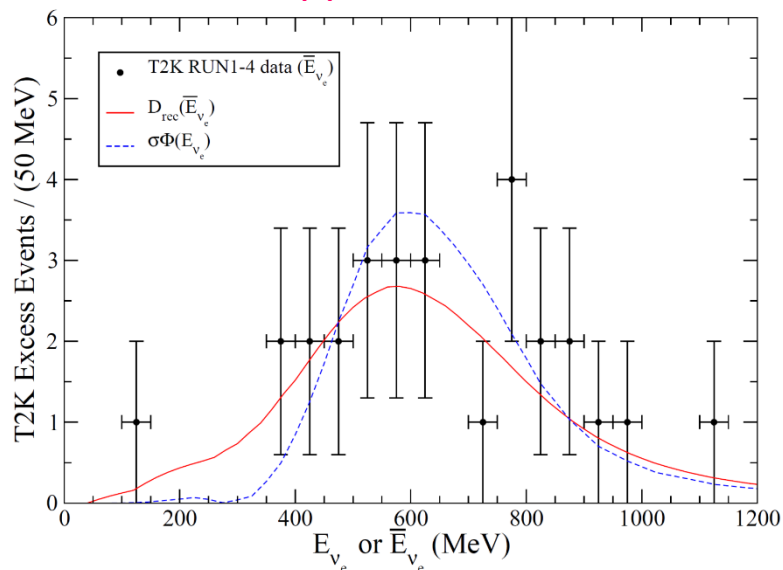
M. Martini, M. Ericson, G. Chanfray
 - *Phys. Rev. D* 85 093012 (2012)
 - *Phys. Rev. D* 87 013009 (2013)



- Distributions not symmetrical around E_ν
- Crucial role of np-nh: low energy tail

QE-based neutrino energy reconstruction and neutrino oscillations

$\bar{\nu}_e$ appearance T2K



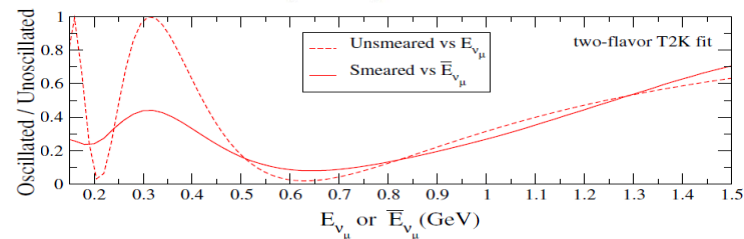
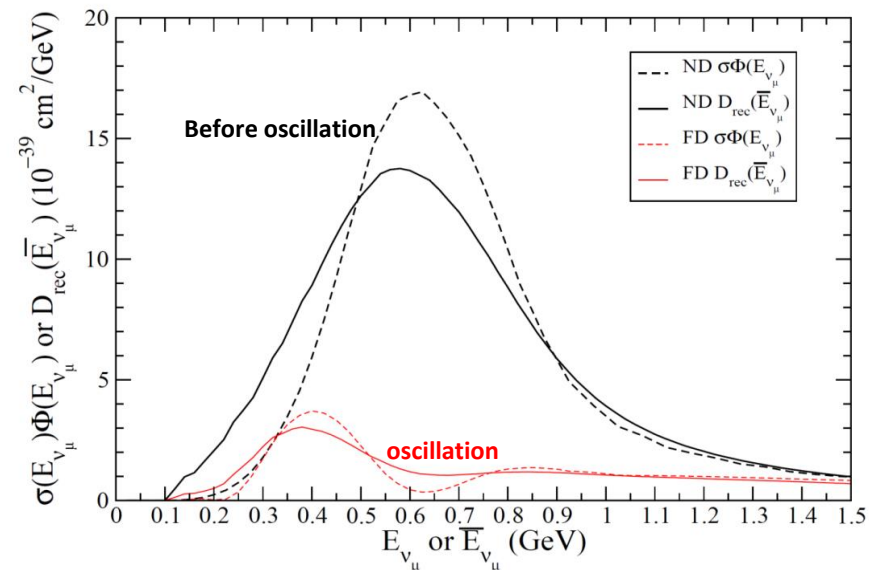
The reconstruction correction tends to make events leak outside the high flux region, especially towards the low energy side

M. Martini, M. Ericson, G. Chanfray
Phys. Rev. D 85 093012 (2012); *Phys. Rev. D* 87 013009 (2013)

Similar results in:

- Nieves, Sanchez, Simo, Vicente Vacas *PRD* 85 113008 (2012)
- Lalakulich, Mosel, Gallmeister, *PRC* 86 054606 (2012)

$\bar{\nu}_\mu$ disappearance T2K



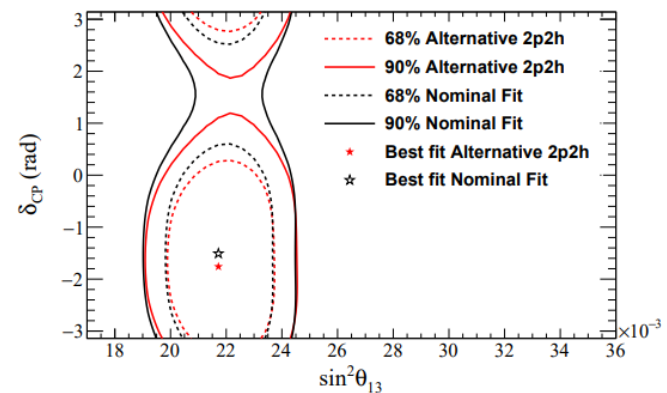
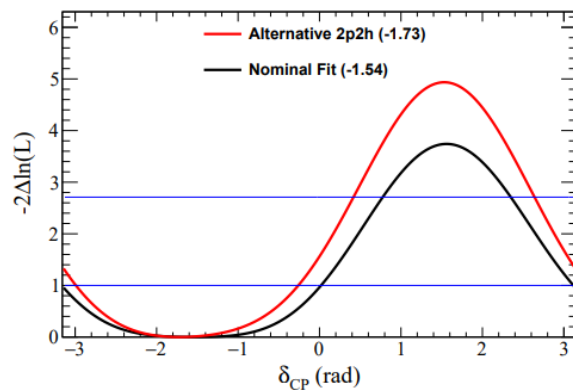
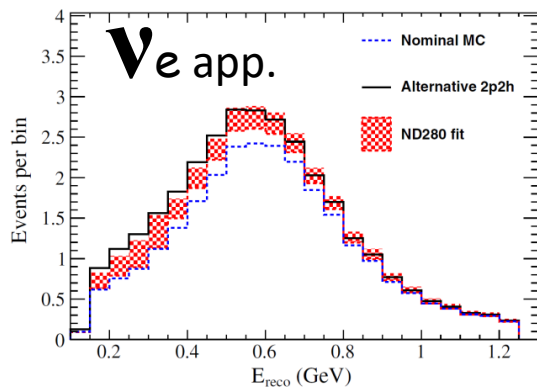
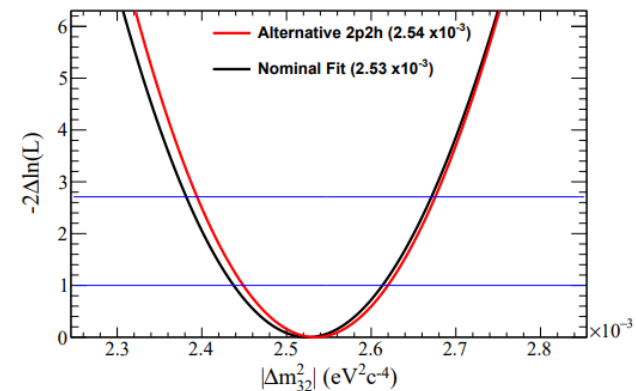
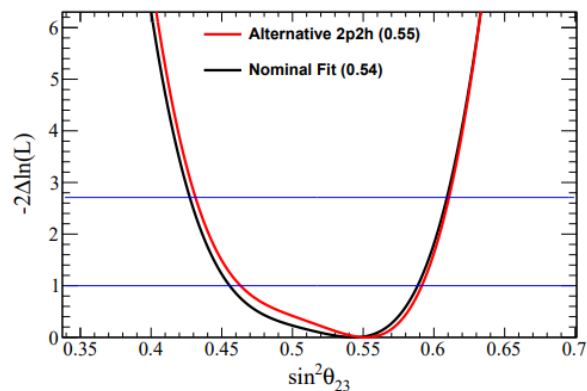
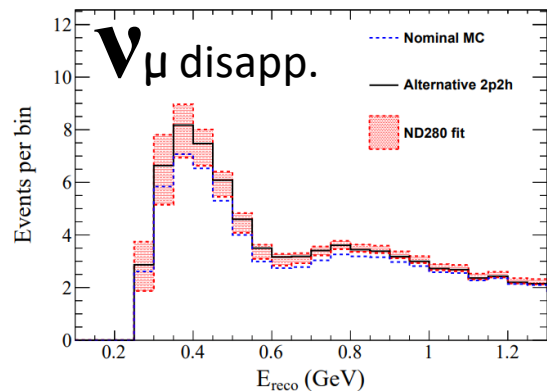
After reconstruction:

- Near Detector:
clear low energy enhancement
- Far Detector:
low energy tail and
the middle hole is largely filled

Neutrino energy reconstruction and neutrino oscillation analysis are affected by np-nh

Impact of 2p-2h modeling on T2K oscillation analysis

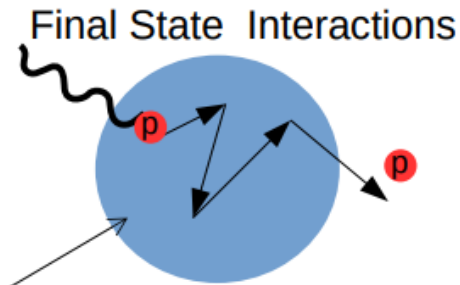
T2K Phys.Rev.D 96 (2017) 9, 092006



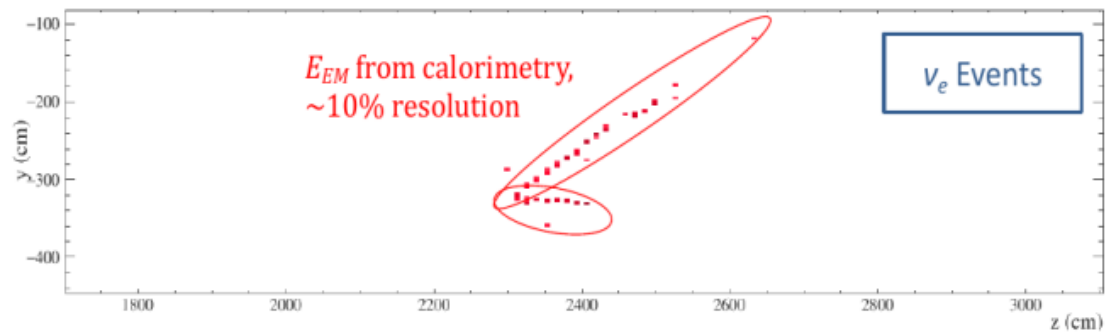
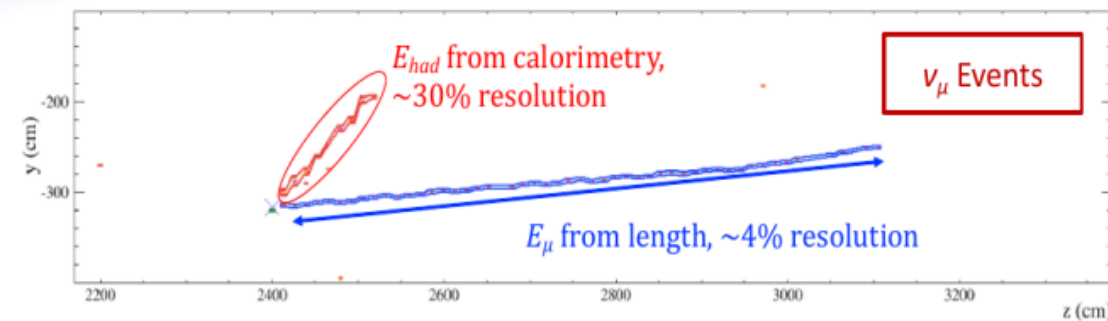
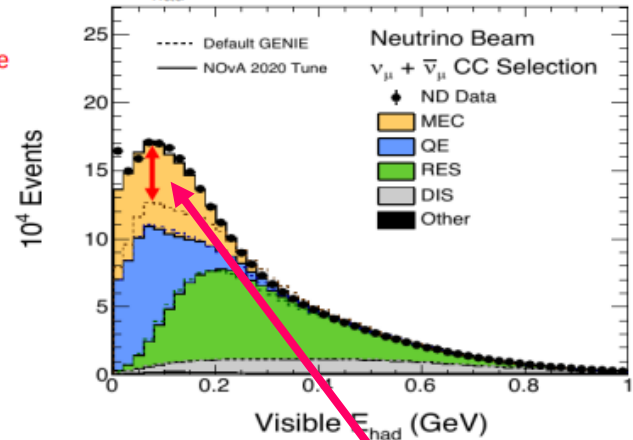
See S. Bolognesi and S. Lavignac lectures

E_ν reconstruction NOvA

- E_ν reconstructed with hadronic deposits:
 - important difference $\nu - \bar{\nu}$: proton vs neutron (~undetected)
 - proton/pion energy smeared by Final State Interactions
- Different reconstruction and energy resolution for ν_μ and ν_e



Important to tune model predictions for E_{had} **NOvA Preliminary**

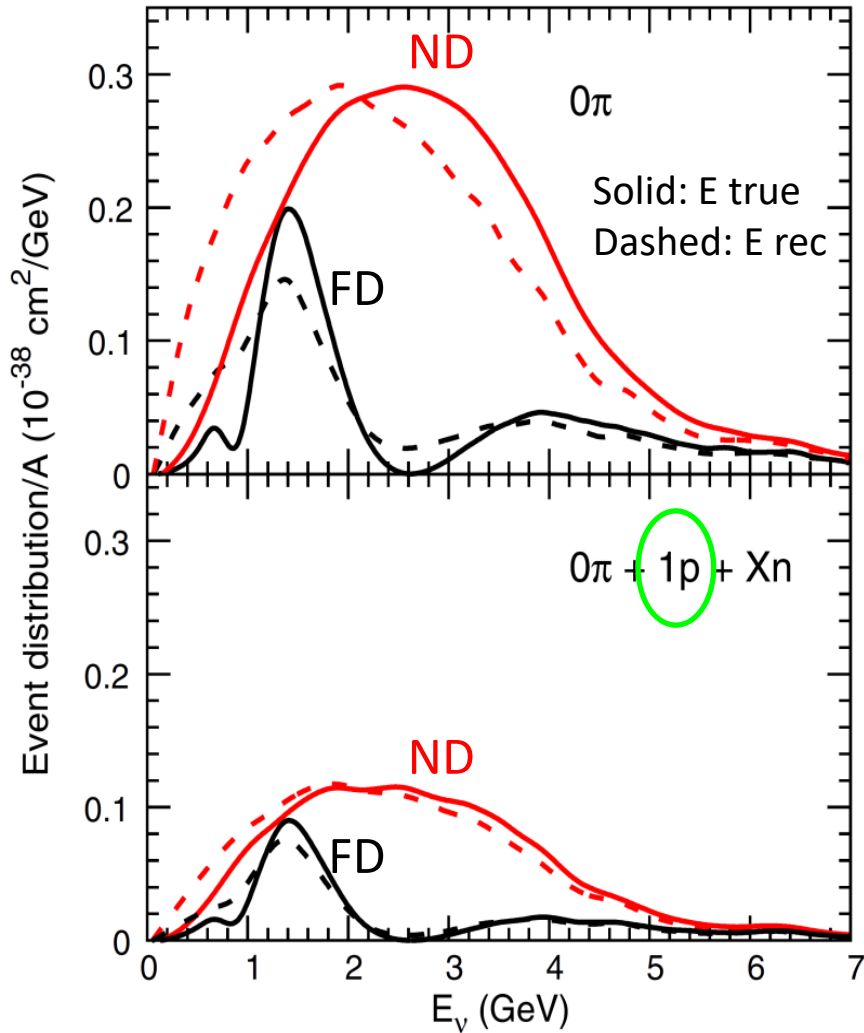


S. Bolognesi slide

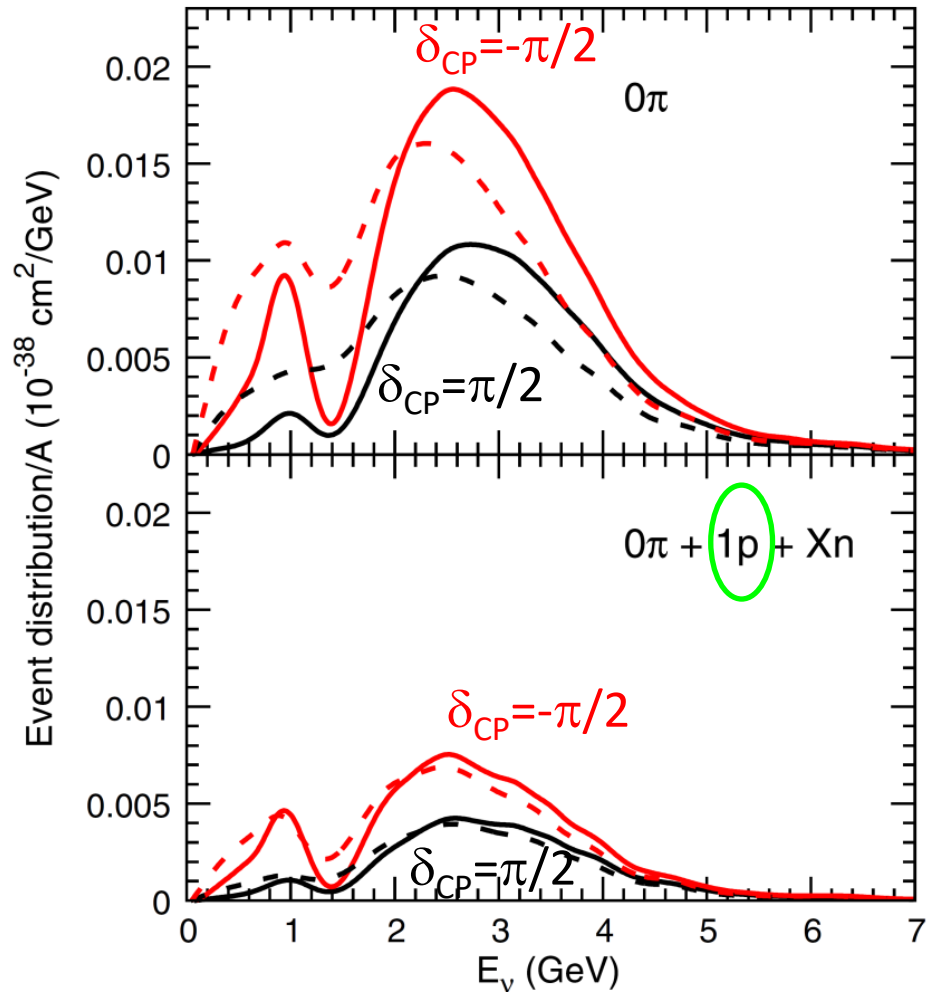
119

QE-based E_ν reconstruction using proton information

ν_μ disappearance in DUNE



ν_e appearance in DUNE



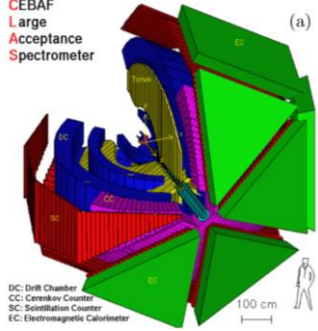
Major improvement in $0\pi + 1p + Xn$ sample, events down by only factor 3

Electron-beam energy reconstruction for ν oscillation measurements

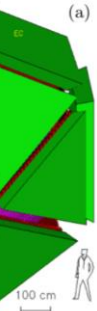
$e4\nu$



CEBAF
Large
Acceptance
Spectrometer

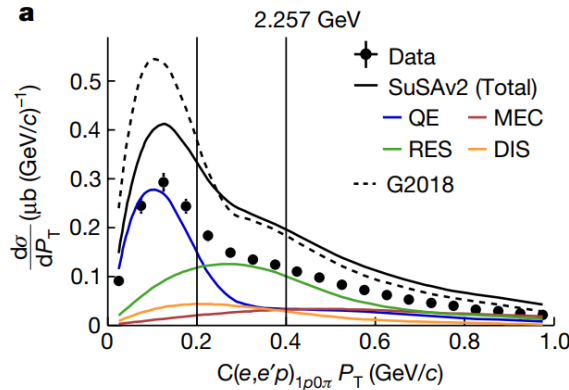


DC: Drift Chamber
CC: Cerenkov Counter
SC: Scintillation Counter
EC: Electromagnetic Calorimeter

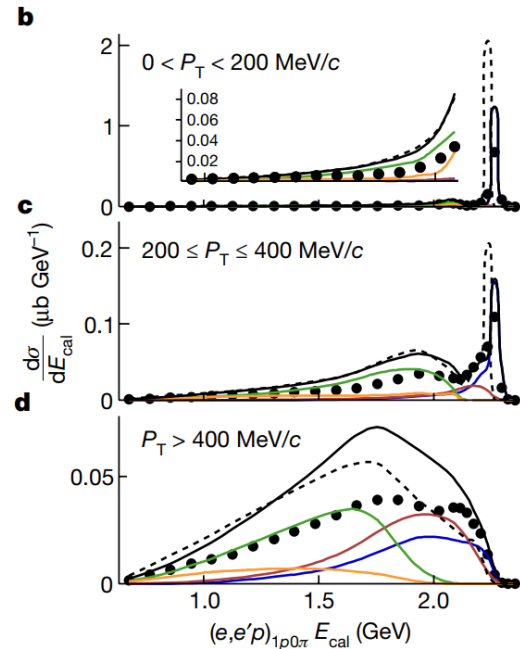


Nature 599 (2021) 7886, 565-570

QE-based
(e, e')



$$\mathbf{P}_T = \mathbf{P}_T^{e'} + \mathbf{P}_T^p$$

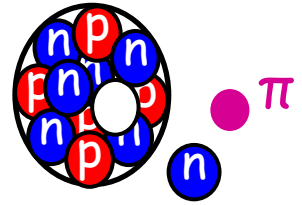


Calorimetric
-based
($e, e'p$)

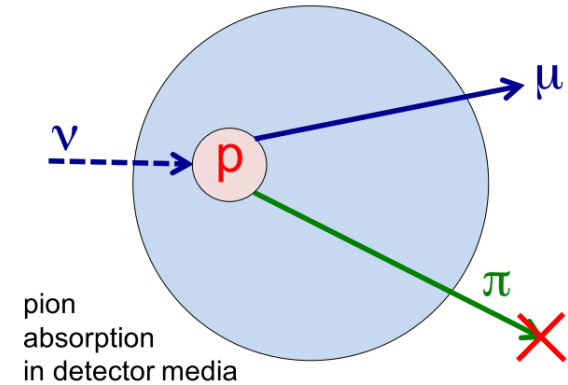
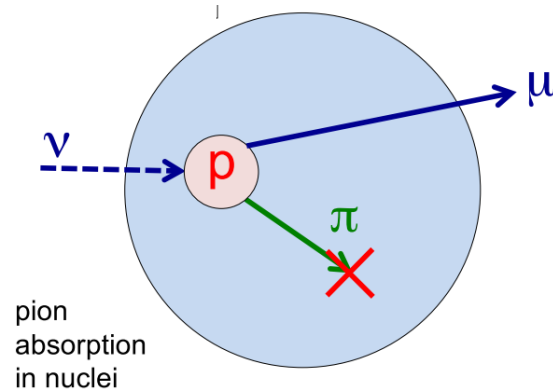
1π production

The one pion production channel

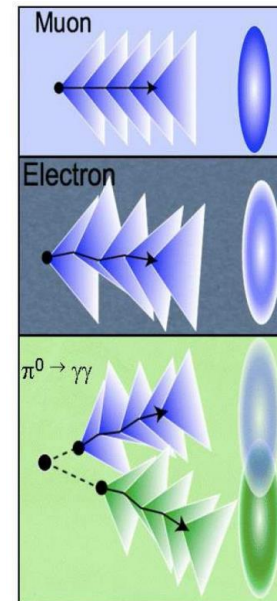
Important for two reasons:



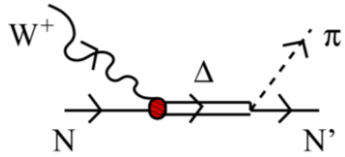
- CC1 π can mimic CCQE if the pion is not detected



- NC1 π^0 can mimic in Cherenkov detectors electron-like signal in $\nu_\mu \rightarrow \nu_e$ oscillation search



The 1π production via $\Delta(1232)$ resonance excitation and decay



At energies of our interest, it is the dominant mechanism of the reaction

$$W N \rightarrow N' \pi$$

E. Hernandez et al. Phys. Rev. D 76, 033005 (2007)

$$W^+ n \rightarrow \Delta^+ \quad \text{Hadron matrix element} \quad \langle \Delta^+; p_\Delta = p + q | j_{cc+}^\mu(0) | n; p \rangle = \bar{u}_\alpha(\vec{p}_\Delta) \Gamma^{\alpha\mu}(p, q) u(\vec{p}) \cos \theta_C$$

Electroweak vertex

$$\Gamma^{\alpha\mu}(p, q) = \left[\frac{C_3^V}{M} (g^{\alpha\mu} \not{q} - q^\alpha \gamma^\mu) + \frac{C_4^V}{M^2} (g^{\alpha\mu} q \cdot p_\Delta - q^\alpha p_\Delta^\mu) + \frac{C_5^V}{M^2} (g^{\alpha\mu} q \cdot p - q^\alpha p^\mu) + C_6^V g^{\mu\alpha} \right] \gamma_5$$

$$+ \left[\frac{C_3^A}{M} (g^{\alpha\mu} \not{q} - q^\alpha \gamma^\mu) + \frac{C_4^A}{M^2} (g^{\alpha\mu} q \cdot p_\Delta - q^\alpha p_\Delta^\mu) + C_5^A g^{\alpha\mu} + \frac{C_6^A}{M^2} q^\mu q^\alpha \right], \quad p_\Delta = p + q$$

Vector form factors $C_{3,4,5,6}^V$ can be extracted from single-pion electro-production data

Axial form factors $C_{3,4,5,6}^A$ $C_5^A(Q^2) = \frac{C_5^A(0)}{(1 + Q^2/M_{A\Delta}^2)^2}$ $C_6^A = M^2/(m_\pi^2 + Q^2) \cdot C_5^A$ PCAC $C_4^A = -1/4 \cdot C_5^A$ Adler C_3^A Small, usually neglected

Δ propagator

$$G^{\mu\nu}(p_\Delta) = \frac{P^{\mu\nu}(p_\Delta)}{p_\Delta^2 - M_\Delta^2 + iM_\Delta\Gamma_\Delta}$$

Spin 3/2 projection operator

$$P^{\mu\nu}(p_\Delta) = -(\not{p}_\Delta + M_\Delta) \left[g^{\mu\nu} - \frac{1}{3} \gamma^\mu \gamma^\nu - \frac{2}{3} \frac{p_\Delta^\mu p_\Delta^\nu}{M_\Delta^2} + \frac{1}{3} \frac{p_\Delta^\mu \gamma^\nu - p_\Delta^\nu \gamma^\mu}{M_\Delta} \right]$$

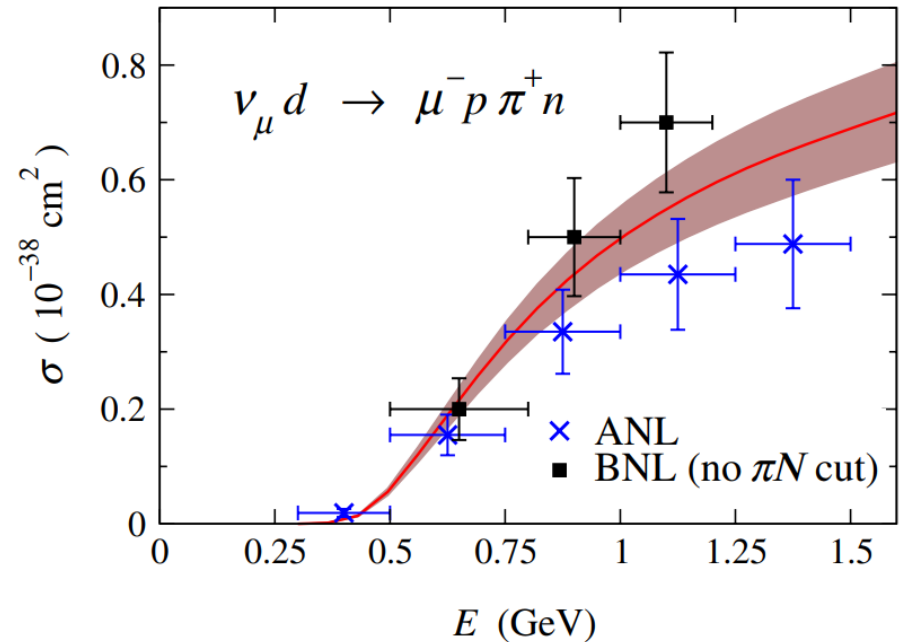
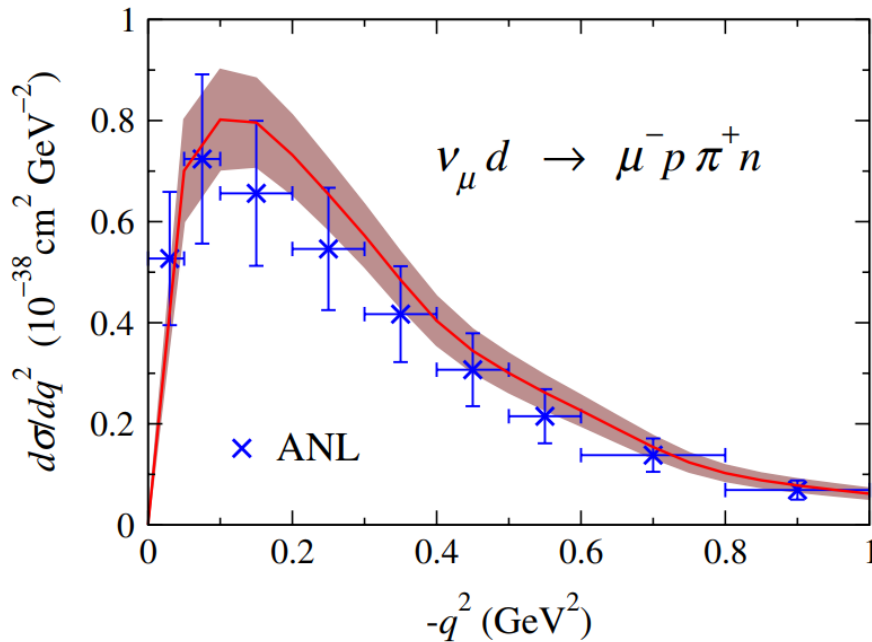
$N\Delta\pi$ coupling

$$\mathcal{L}_{\pi N \Delta} = \frac{f^*}{m_\pi} \bar{\Psi}_\mu \vec{T}^\dagger (\partial^\mu \vec{\phi}) \Psi + \text{h.c.}$$

1π production in neutrino deuteron scattering

- “Old” deuteron bubble-chamber experiments (Argonne ANL and Brookhaven BNL)
[Campbell J et al 1973 Phys. Rev. Lett. 30 335; Radecky G et al 1982 Phys. Rev. D 25 1161; Kitagaki T et al 1986 Phys. Rev. D 34 2554]
- Both ANL and BNL data suffer from a large flux-normalization error

E. Hernandez et al. Phys. Rev. D 87, 113009 (2013)



$$C_5^A(Q^2) = \frac{C_5^A(0)}{(1 + Q^2/M_{A\Delta}^2)^2}$$

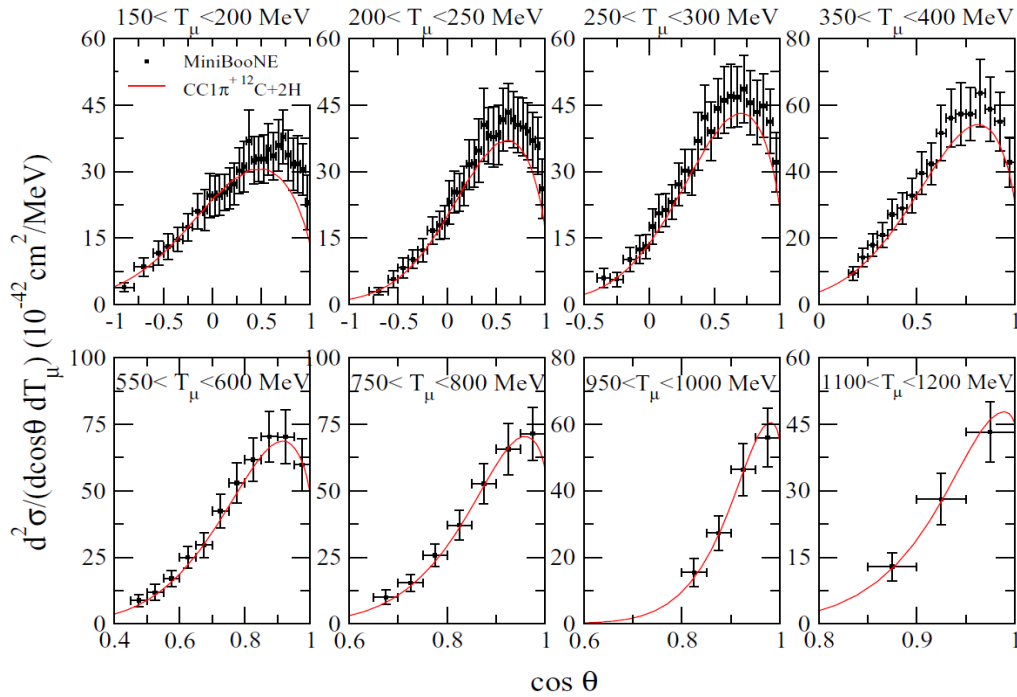
There is also a strong desire to repeat bubble-chamber experiments to better determine the C_5^A form factor

Nowadays due to the tighter safety regulations of modern experiments, hydrogen or deuteron bubble-chamber experiments are not easily approved, especially underground, where most of neutrino beams are located.

CC1 π^+ flux-integrated differential cross sections on carbon

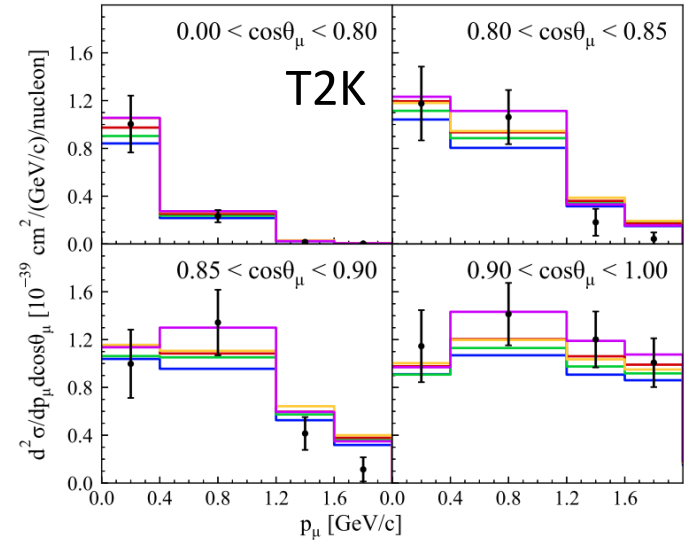
Results in terms of muon variables

MiniBooNE

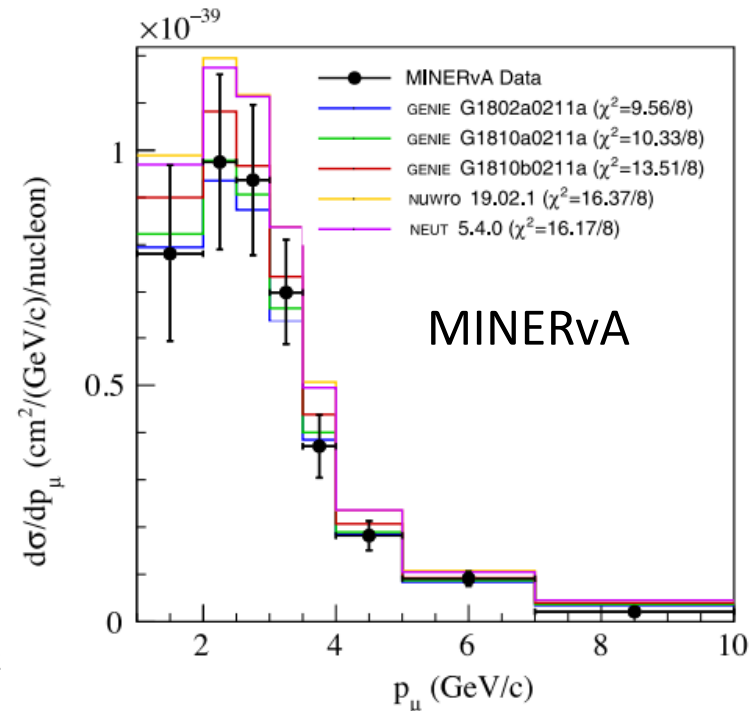


M. Martini, M. Ericson, *Phys. Rev. C* 90 025501 (2014)

Reasonable agreement between models and data



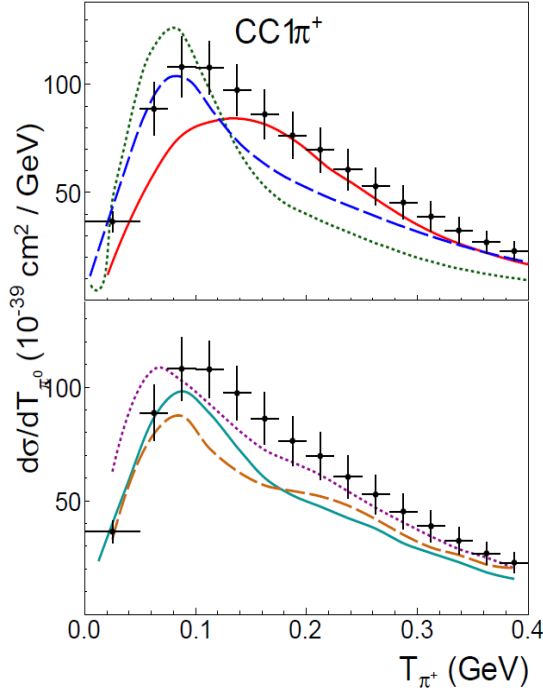
M. Buizza Avanzini et al. *PRD* 105, 092004 (2022)



CC1 π results in terms of pion variables

MiniBooNE

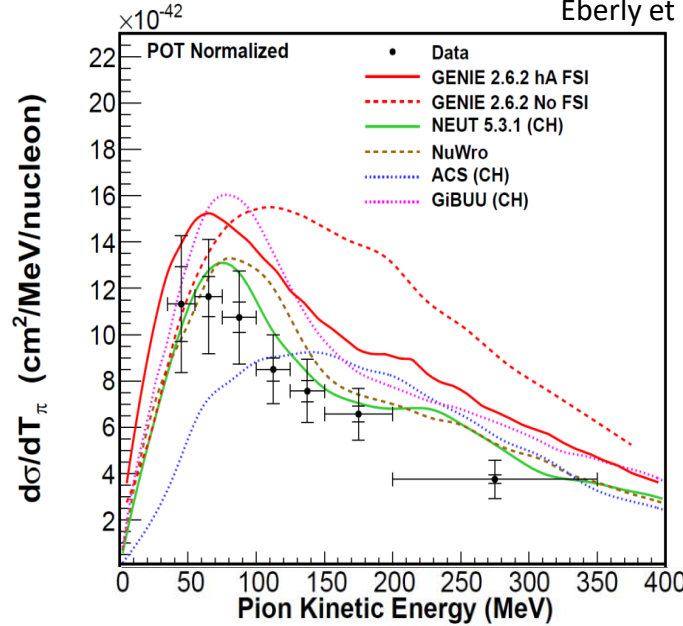
Rodrigues, AIP Conf. Proc. 1663 (2015)



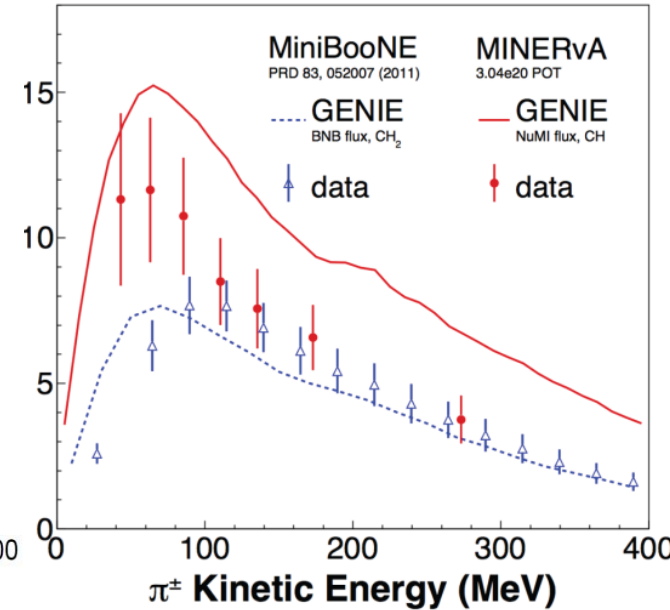
— Athar *et al.* - - - Nieves *et al.* - - - GiBUU — NuWro
 - - - GENIE — NEUT — + MB data

MINERvA

Eberly *et al.*, PRD 92 (2015)



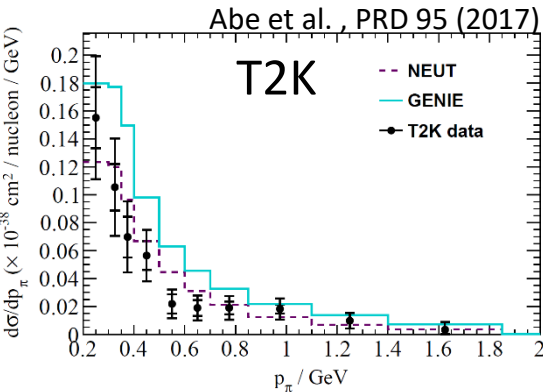
MiniBooNE - MINERvA



Historically many tensions

- models .vs. data ??
- models .vs. models??
- data .vs. data (through models)??

the 1 π puzzle



Pion puzzle – Tension 2016 Workshop

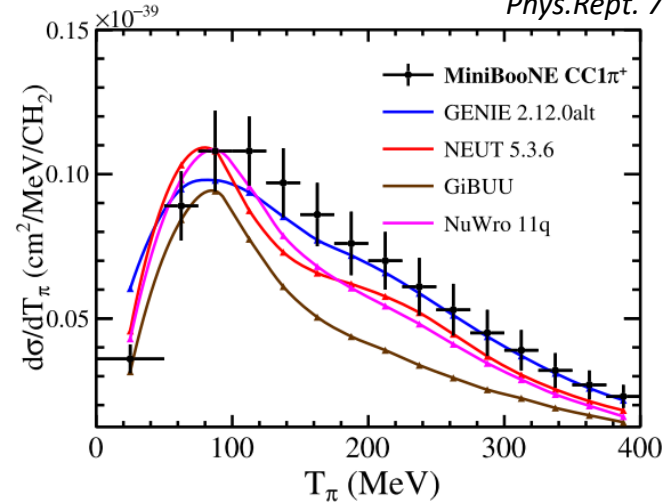
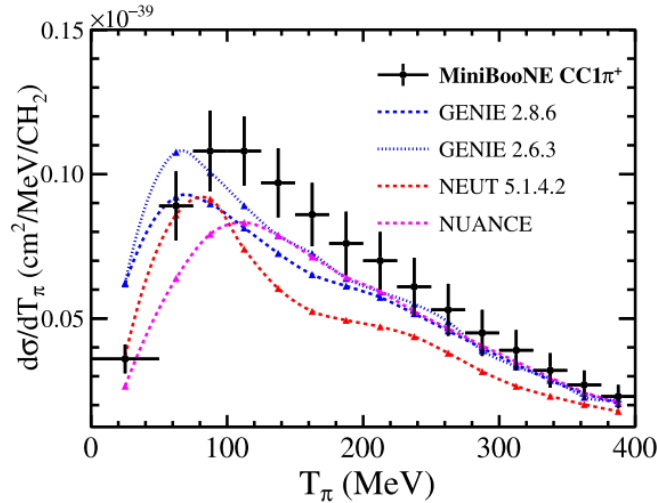
Old

New (after Tension)

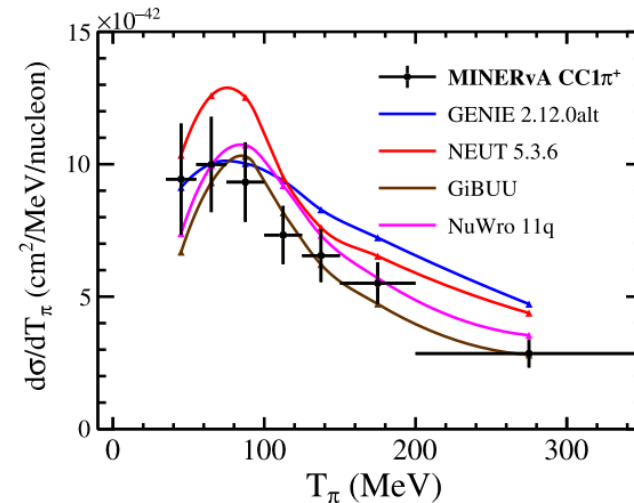
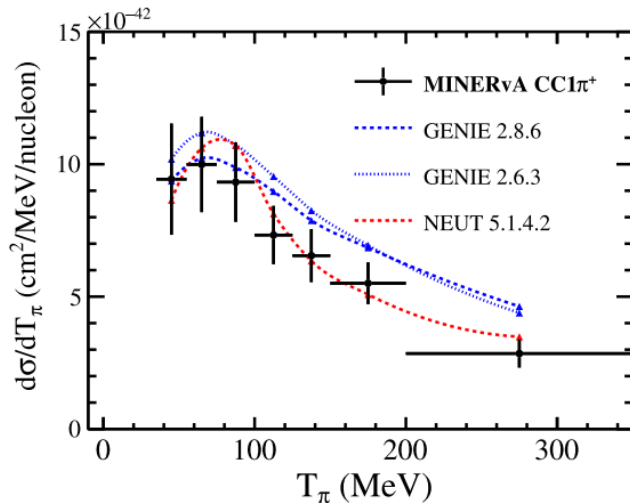
M. Betancourt et al.

Phys.Rept. 773-774 (2018) 1-28

MiniBooNE



MINERVA



- Same models, correct signal definition, proper flux averaging
- Updated flux prediction from MINERVA

Better normalization agreement but shape discrepancies remain

Pion puzzle – Tuning GENIE with MINERvA data (2019)

P. Stowell et al. PRD 100 (2019) 7, 072005

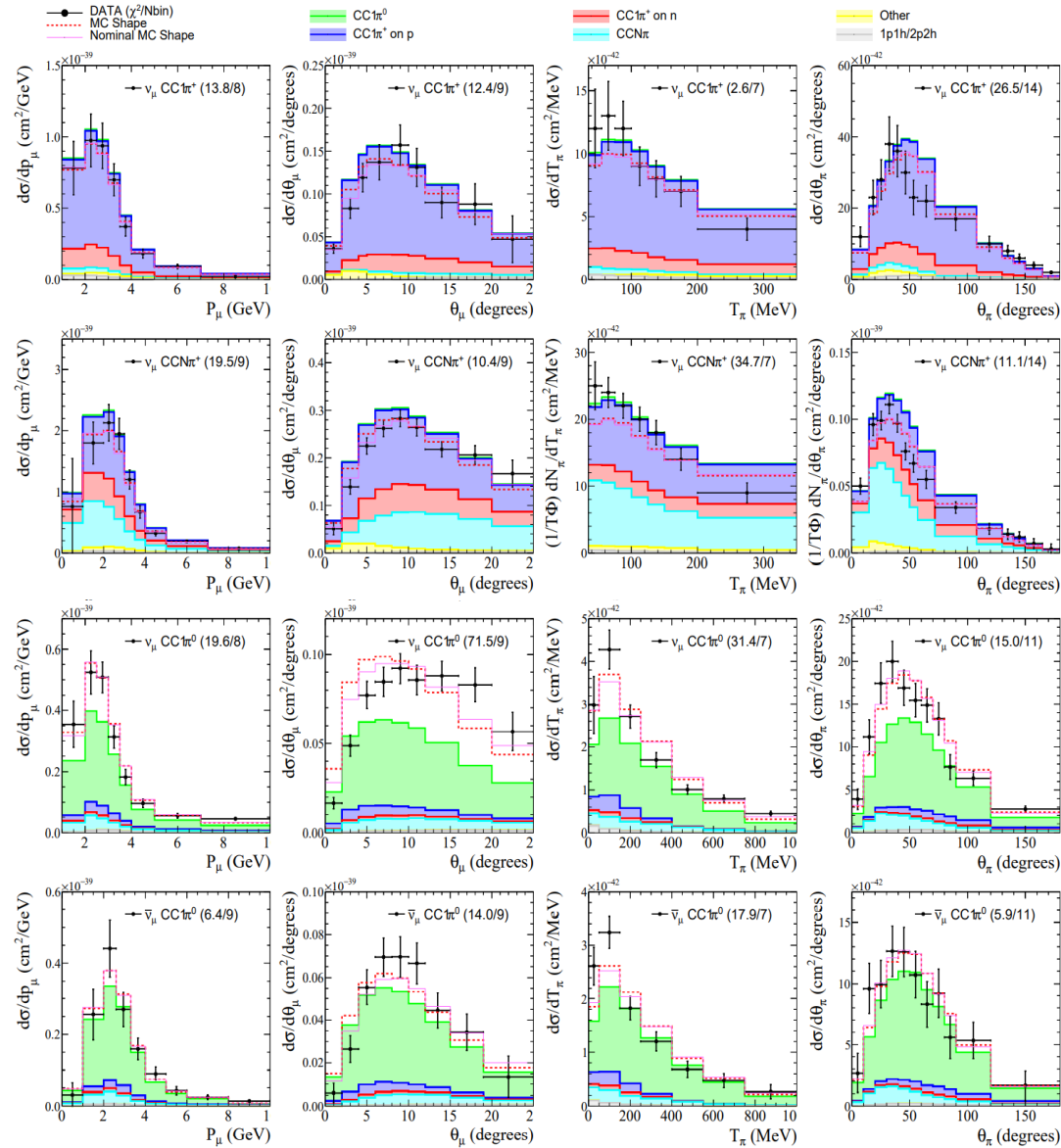
Tune Monte Carlo to simultaneously fit 4 datasets

$$\nu_{\mu} CC1\pi^{+}$$

$$\nu_{\mu} CCN\pi^{+}$$

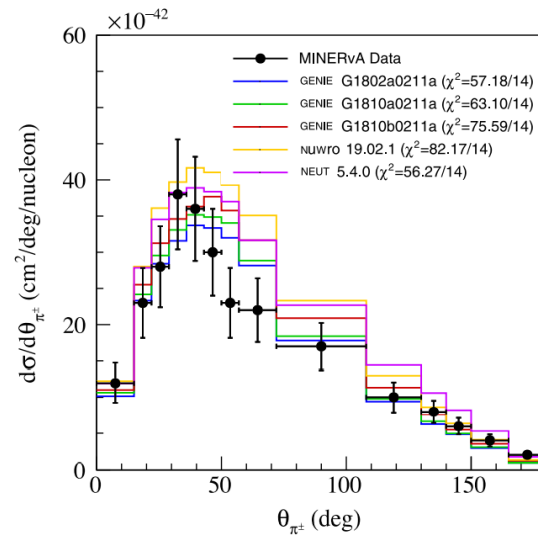
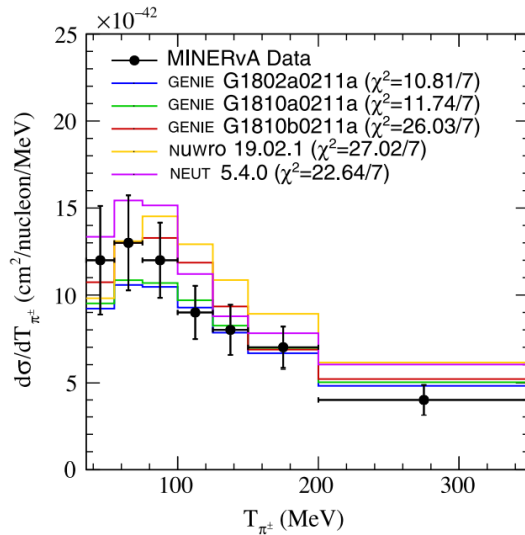
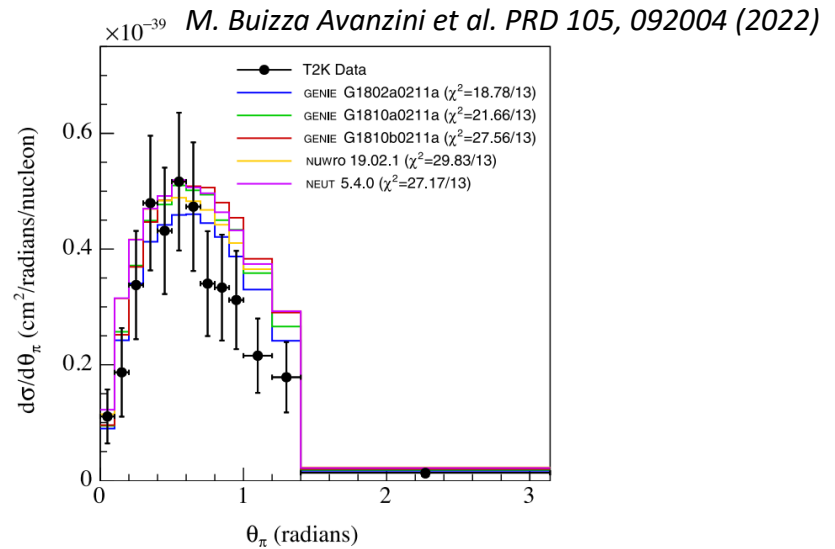
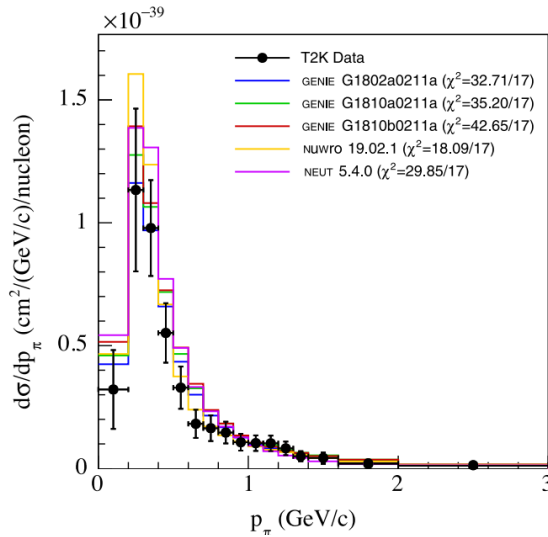
$$\nu_{\mu} CC1\pi^{0}$$

$$\bar{\nu}_{\mu} CC1\pi^{0}$$



The tuning improves the model, but tensions remain

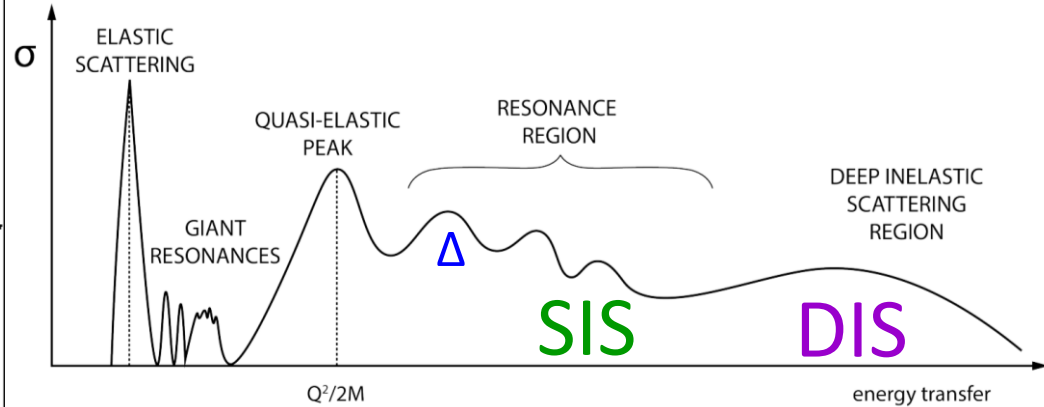
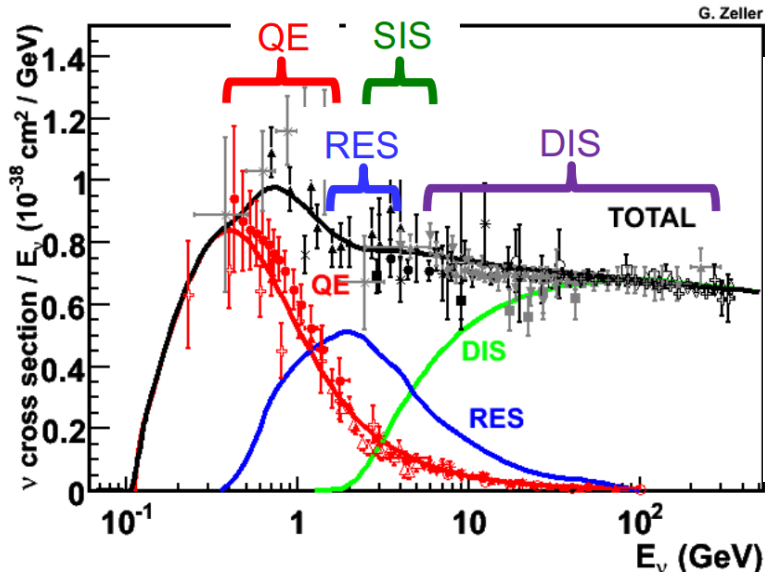
Pion puzzle – T2K and MINERvA data .vs. Monte Carlo (2022)



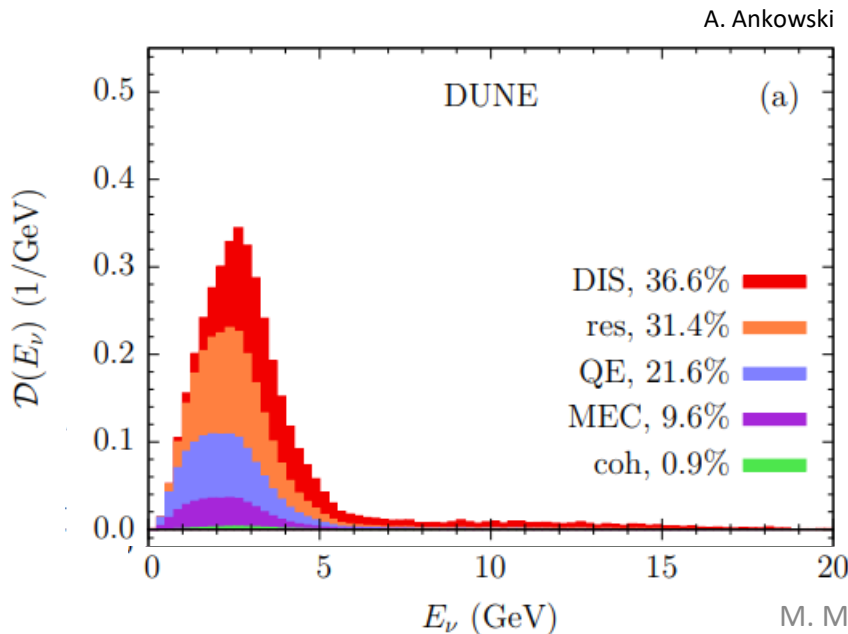
Tensions remain

- The generators used to extract the cross section is often the one with the best description of the data
- Experimental collaborations have more advanced analyses in progress
- These studies are Δ dominated interactions
- None of the common event generators include nuclear medium effects for the Δ

Beyond Δ resonance



- The complications of pion data analyses lay not only on the modeling of primary production and pion FSI but also on the fact that all hadronic processes related to shallow inelastic scattering (SIS) and DIS regions must be modeled correctly
- SIS and DIS have been minimally studied both experimentally and theoretically with neutrino scattering
- Another major challenge important in particular for DUNE

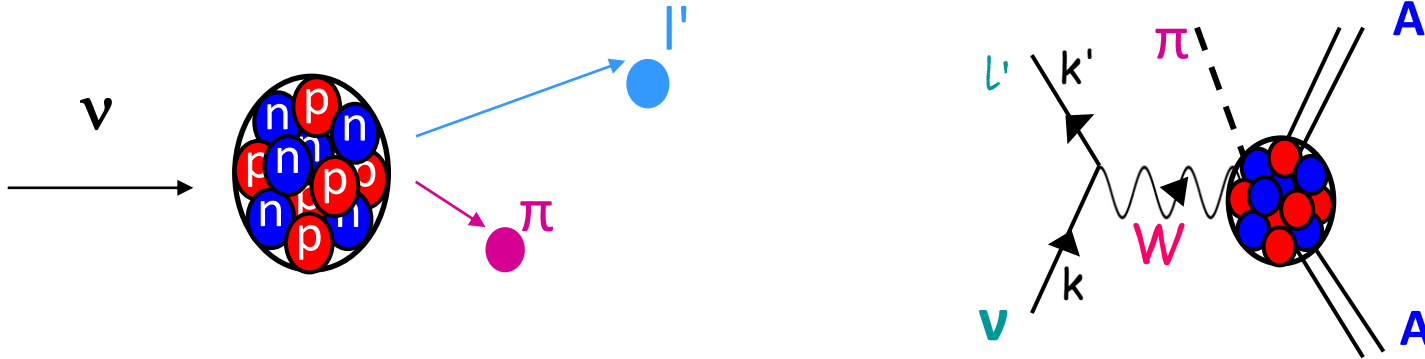


- T. Katori, M. Martini, J.Phys.G 45 1, 013001 (2018)*
L. Alvarez-Ruso et al. Prog. Part. Nucl. Phys. 100, 1–68 (2018)
M. Sajjad Athar, J. G. Morfín, J.Phys. G 48, 034001 (2021)

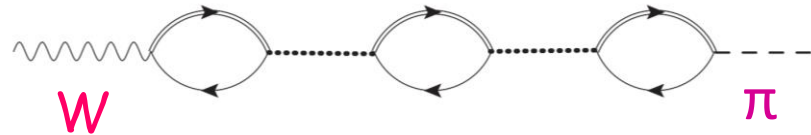
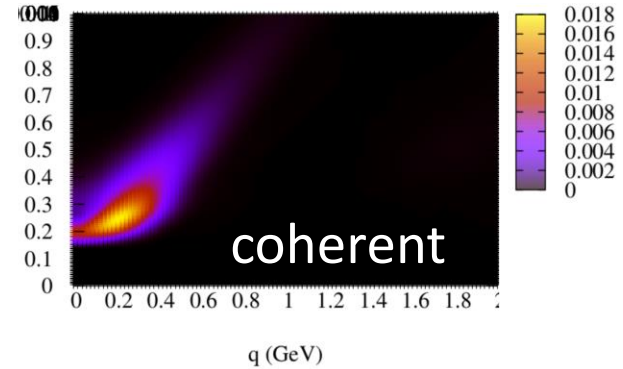
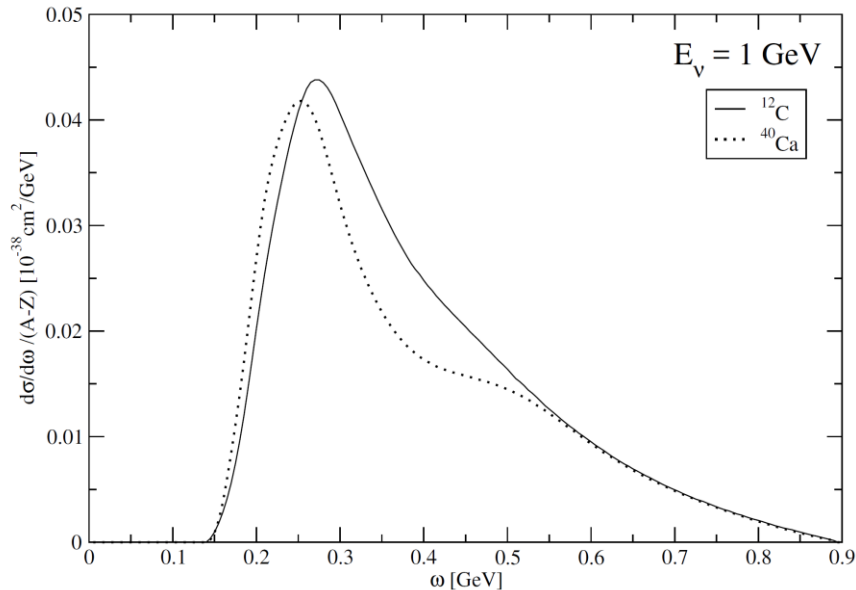
The coherent 1π production

Production of 1 pion with the nucleus remaining in its ground state

Relatively rare interaction channel, but can mimic oscillation signals



M. Martini, M. Ericson, G. Chanfray, J. Marteau, PRC 80 065501 (2009)



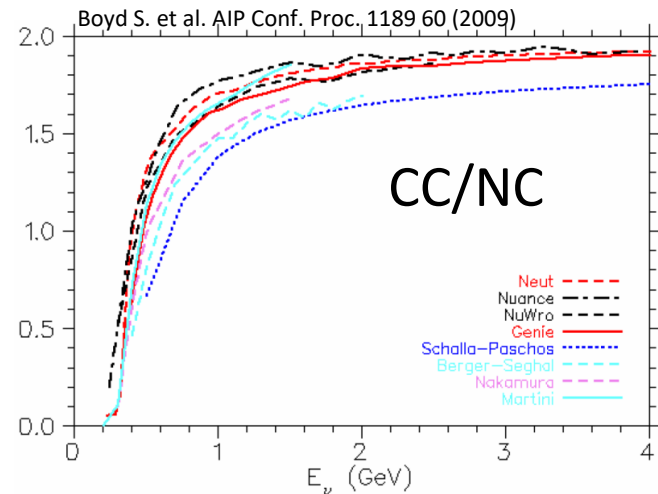
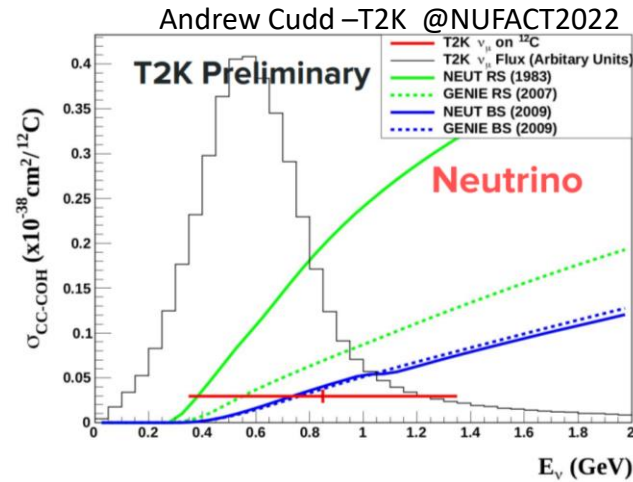
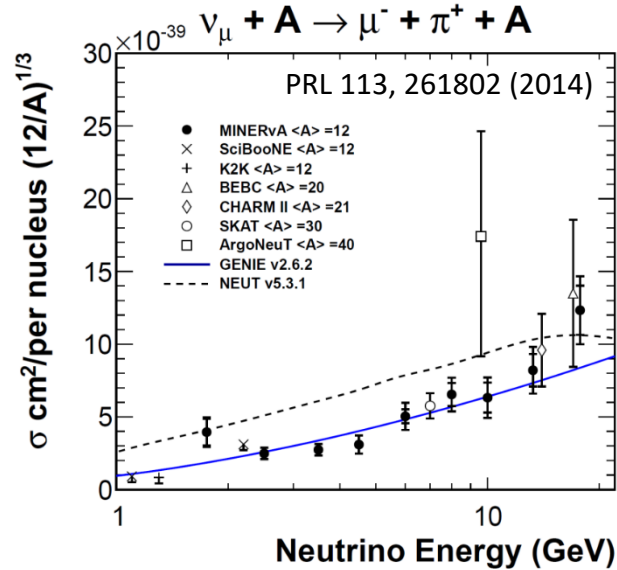
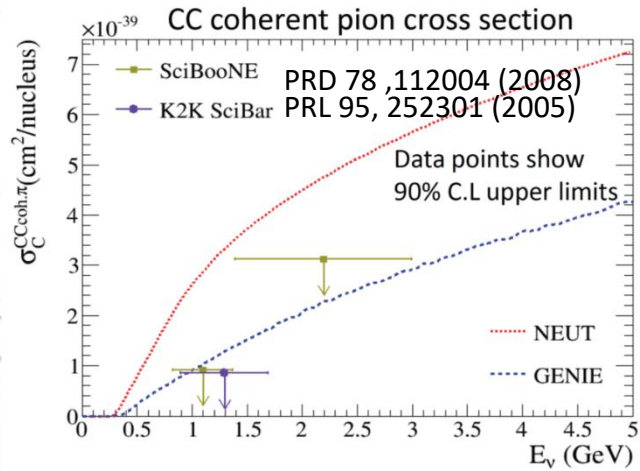
Cross sections reshaped by nuclear collective effects

Coherent 1π production experimental results

K2K and SciBooNE did not observe coherent π^+ production at neutrino energies $\sim 1\text{GeV}$

MINERvA and ArgoNeut see evidence for CC coherent pion production

Preliminary T2K cross section measurement: coherent π^+ production at neutrino energies $\sim 1\text{GeV}$



Coherent puzzle at $E_\nu \sim 1\text{ GeV}$

Theoretical models:

$$\frac{\pi^+ \text{ coh. CC}}{\pi^0 \text{ coh. NC}} = 1.5 \sim 2$$

SciBooNE:

$$\frac{\pi^+ \text{ coh. CC}}{\pi^0 \text{ coh. NC}} = 0.14^{+0.30}_{-0.28}$$

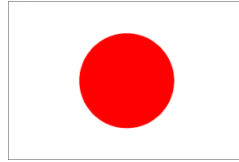
Kurimoto et al, PRD 81 (2010)

Recent hot topics and perspectives

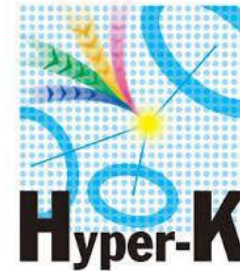
- Different nuclear targets, in particular Argon
- Semi-inclusive processes (proton detection)
- Single Transverse Kinematics Imbalance

Nuclear targets of present and future LBL oscillation experiments

Present



Future



Carbon: T2K(ND) and NOvA

Oxygen (water): T2K (SuperK) and Hyper-K

Argon: DUNE

In the last 15 years many cross sections measurements and theoretical studies have been performed for Carbon (^{12}C). Less for Oxygen (^{16}O) and Argon (^{40}Ar)

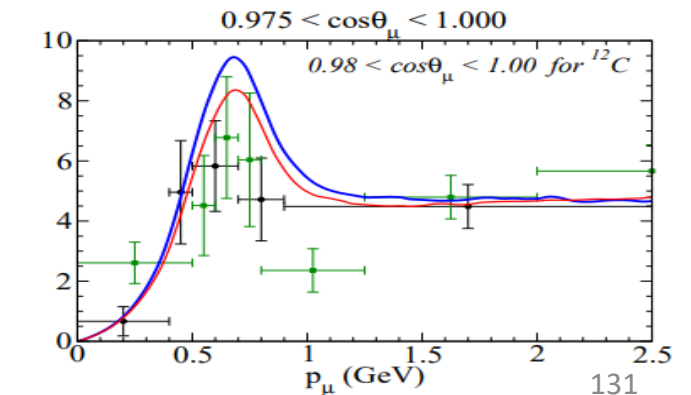
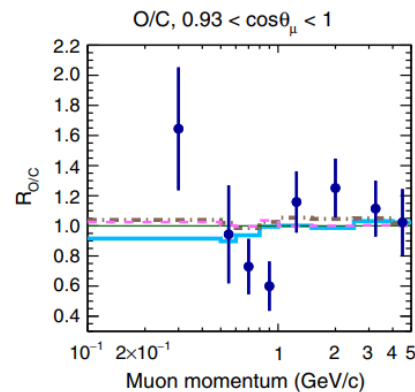
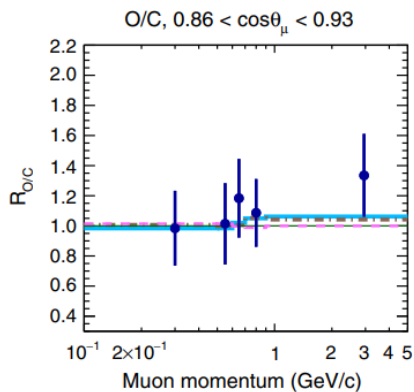
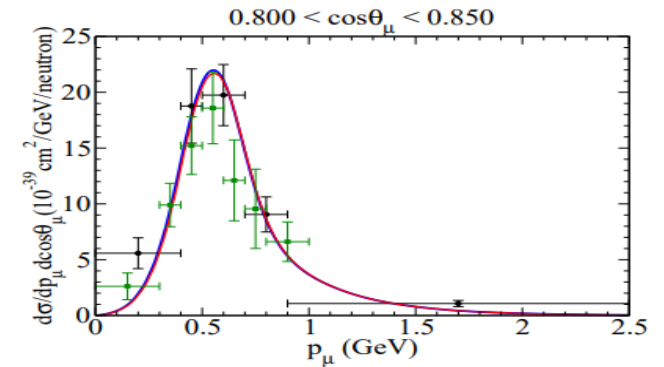
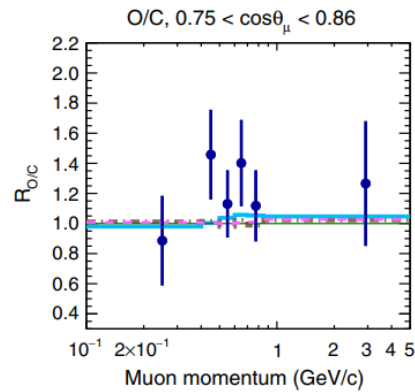
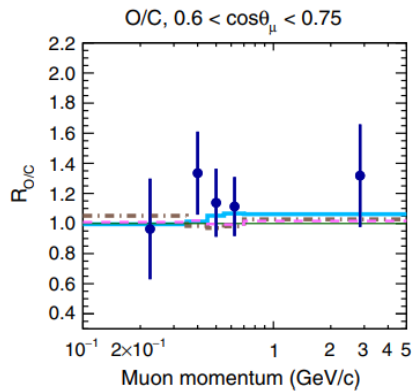
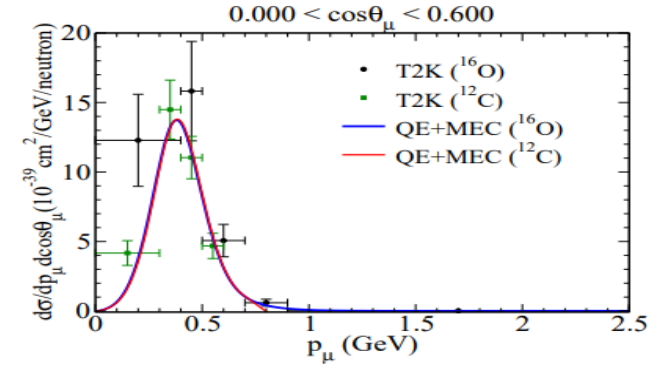
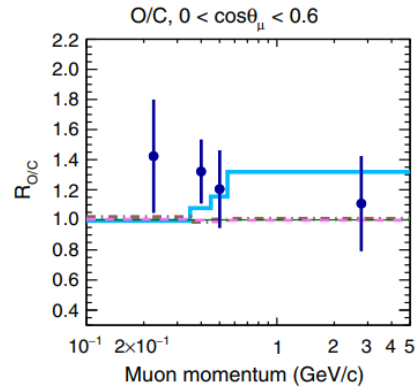
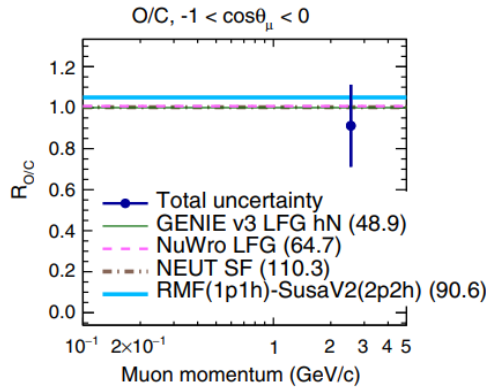
T2K CC0 π d² σ cross sections on oxygen and carbon

Ratio $^{16}\text{O}/^{12}\text{C}$ per nucleon

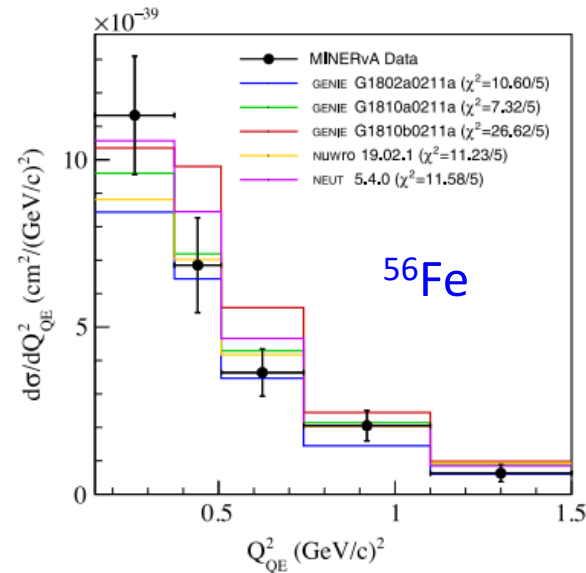
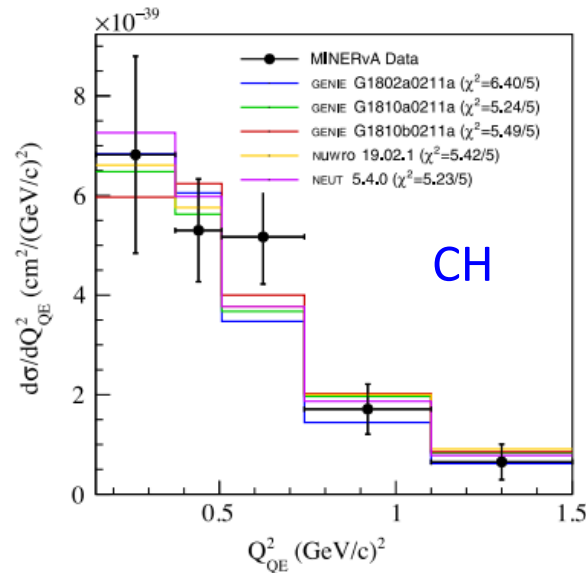
T2K PRD 101 (2020)

SuSAv2+MEC

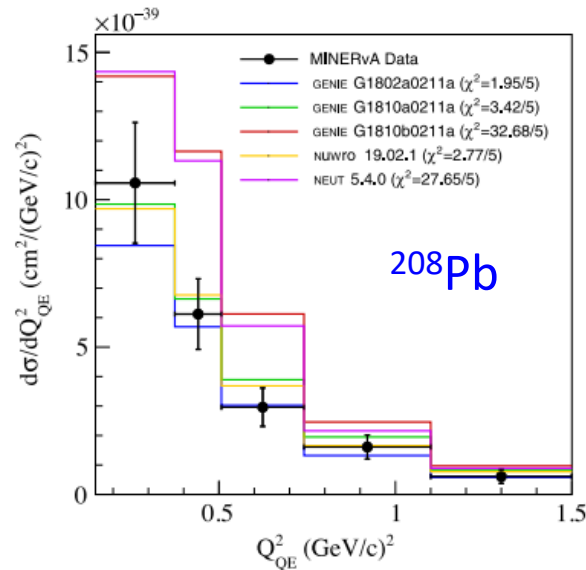
Megias et al., JPG46 (2019)



MINERvA CC0 π 1p(at least) Q²distributions for carbon, iron, lead



M. Buizza Avanzini et al. PRD 105, 092004 (2022)

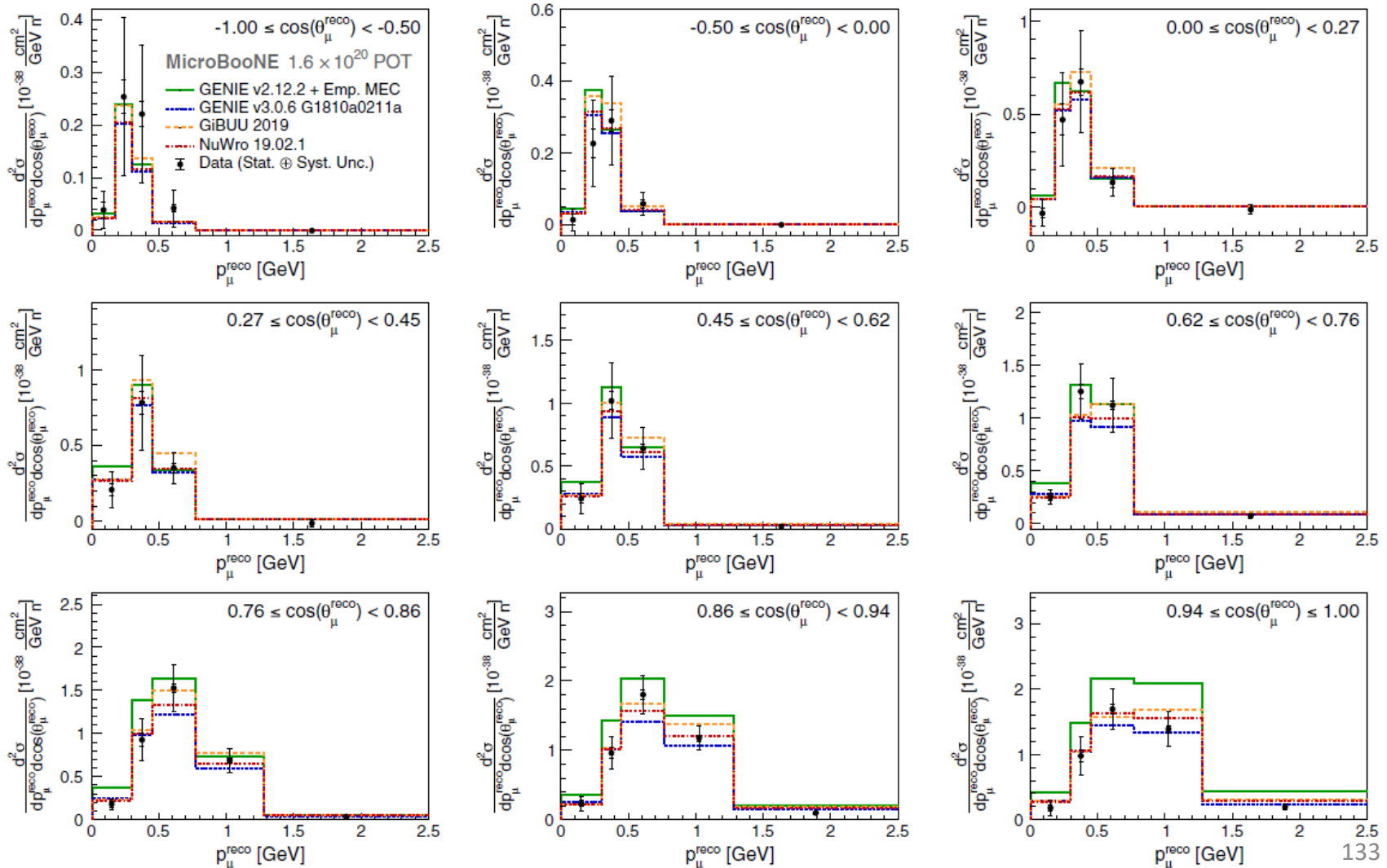


- The spread of distributions predicted by generators increases from carbon to lead
- Most significant deviations are at low Q² where nuclear effects are more important

First MicroBooNE measurement on Argon: inclusive $d^2\sigma/dp_\mu d\cos\theta_\mu$

- CC Inclusive: only the charged lepton is detected. All reaction mechanisms contribute
- Inclusive measurements are less affected by background subtraction with respect to exclusive ones
- Inclusive measurements accumulate more rapidly enough statistics of events

PHYSICAL REVIEW LETTERS **123**, 131801 (2019)

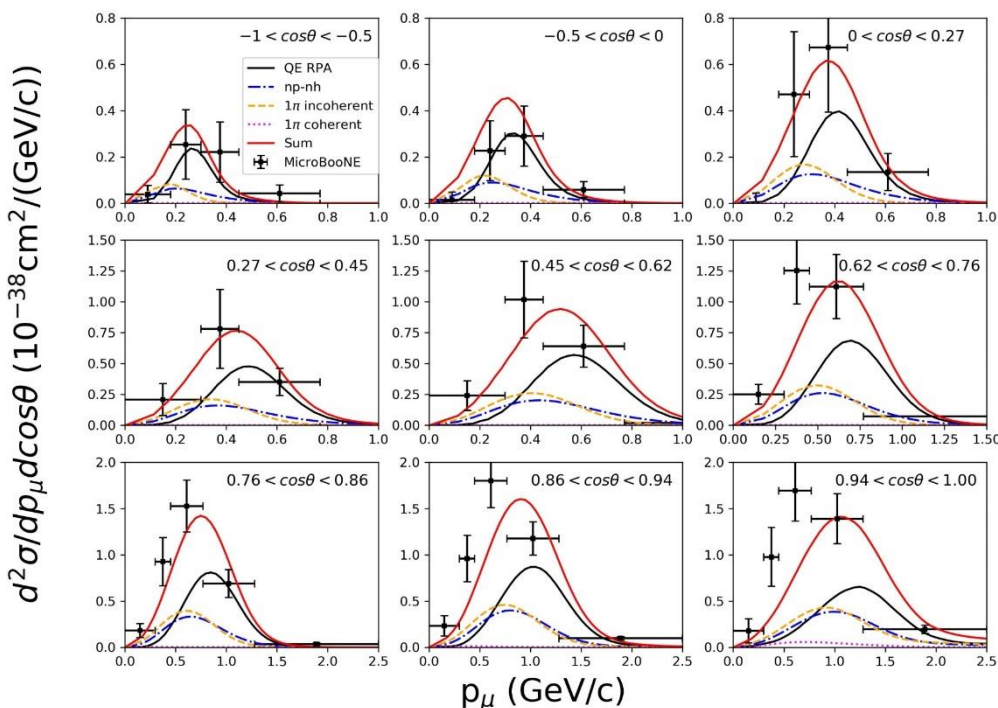


RPA and SuSAv2 calculations of MicroBooNE inclusive $d^2\sigma$ on argon

RPA

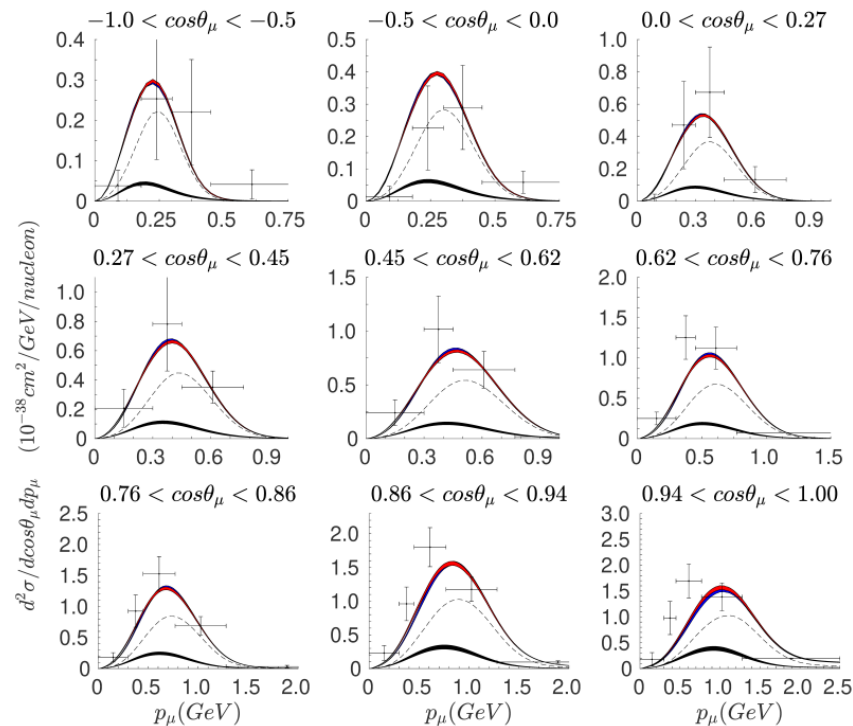
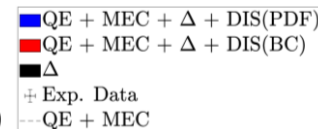
Total = QE + np-nh + 1π inc. + 1π coh.

M. Martini, M. Ericson, G. Chanfray, PRC 106 (2022)



SuSAv2

Gonzalez-Rosa et al. PRD 105 (2022)



Results also with SuSA

Barbaro et al. Universe 7 (2021)

- Reasonable overall agreement, though not as good as in the ^{12}C T2K inclusive case (see next slide)
- At backward angles the predictions of the different models are slightly shifted to lower values of p_μ , whereas the reverse occurs at forward angles

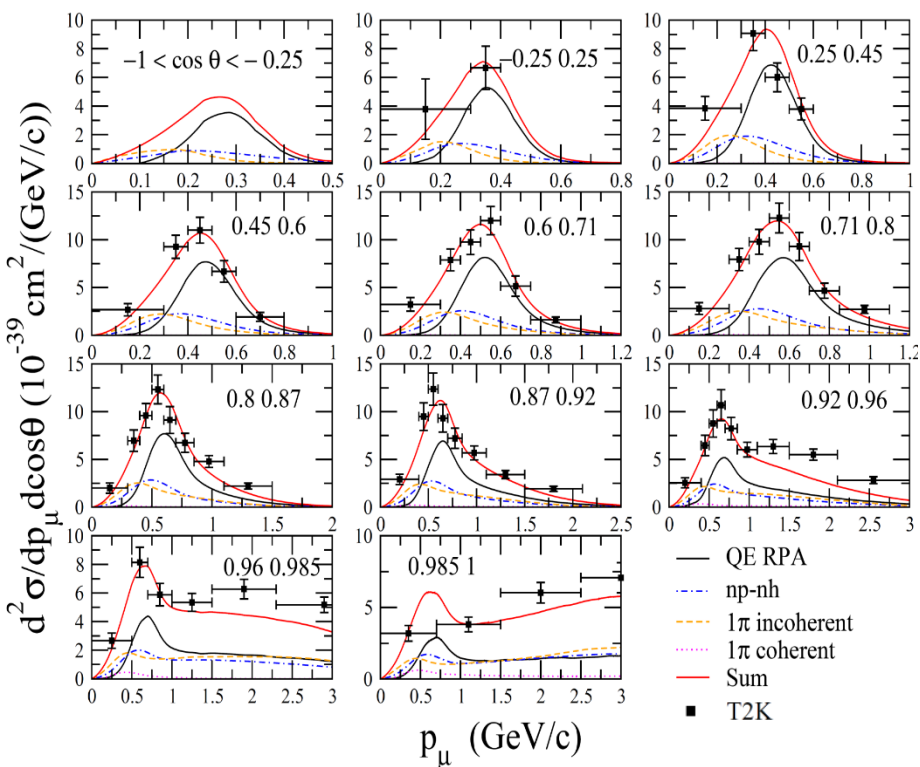
RPA and Monte Carlo calculations of T2K inclusive $d^2\sigma$ on carbon

PHYSICAL REVIEW D **98**, 012004 (2018)

Measurement of inclusive double-differential ν_μ charged-current cross section with improved acceptance in the T2K off-axis near detector

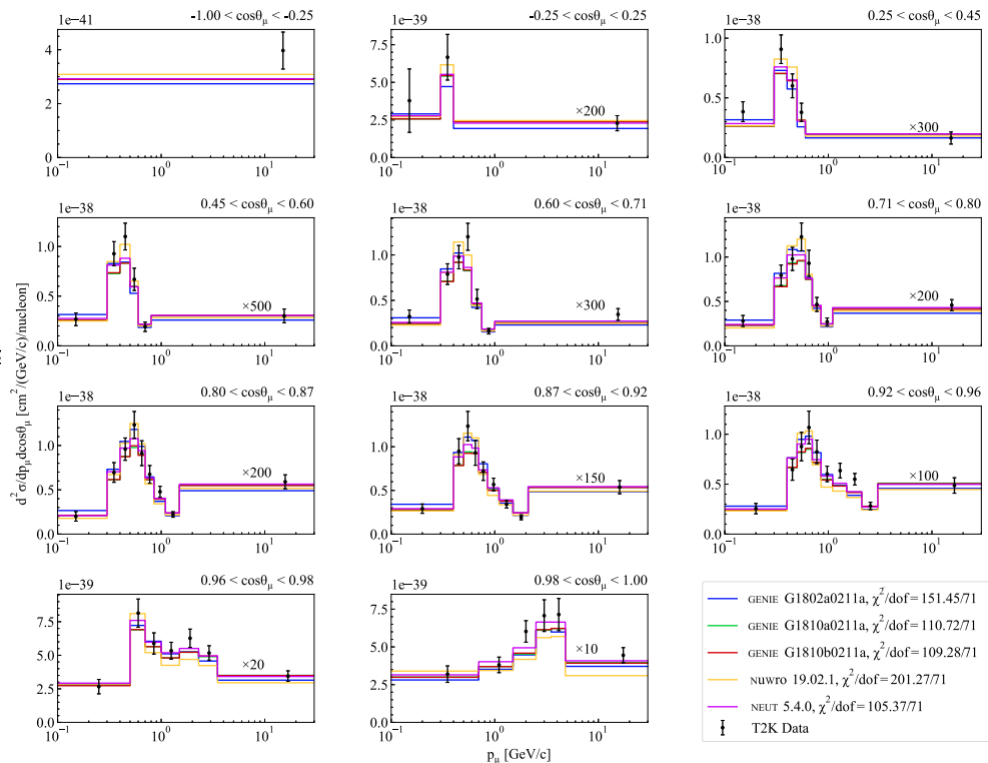
RPA

M. Martini, M. Ericson, G. Chanfray, PRC 106, 015503 (2022)



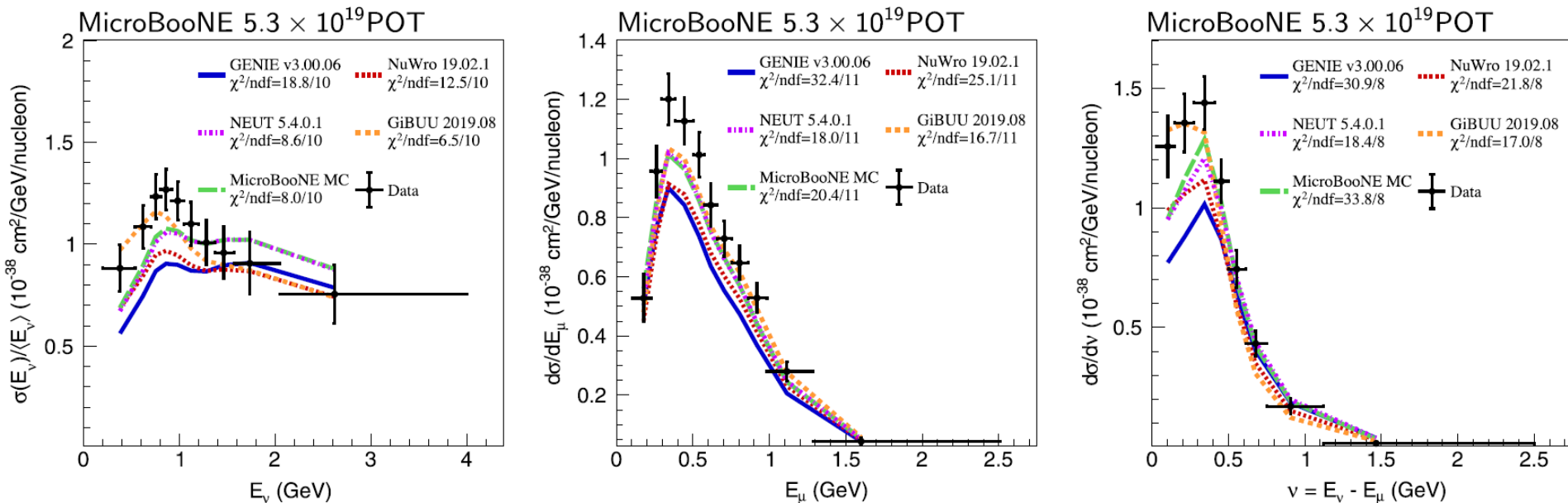
Monte Carlo

M. Buizza Avanzini et al. PRD 105, 092004 (2022)



Remarkable agreement

First Measurement of Energy-Dependent Inclusive Muon Neutrino Charged-Current Cross Sections on Argon with the MicroBooNE Detector

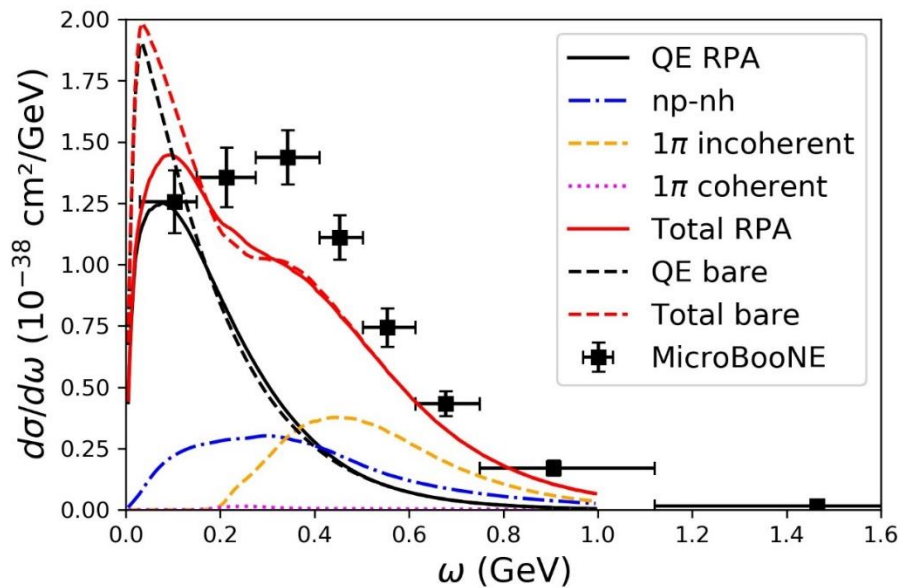
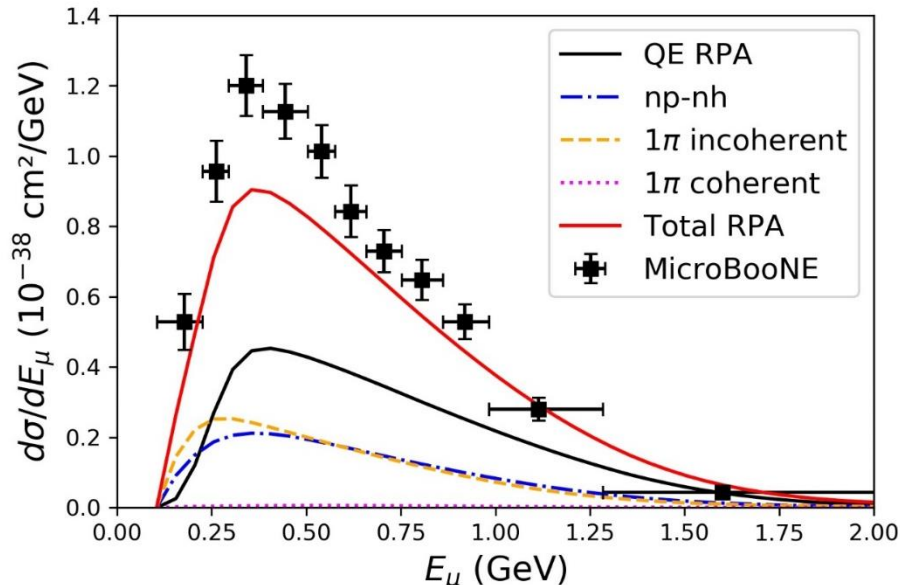


Experimental results presented for the first time as a function of true neutrino energy E_{ν} and transferred energy (ν or ω)

This has been made possible by a new procedure (based on the comparison between the data and the Monte Carlo predictions constrained on the lepton kinematics) allowing the mapping between the true E_{ν} and ω on one hand, and the reconstructed neutrino energy E_{ν}^{rec} and hadronic energy $E_{\text{had}}^{\text{rec}}$ on the other hand

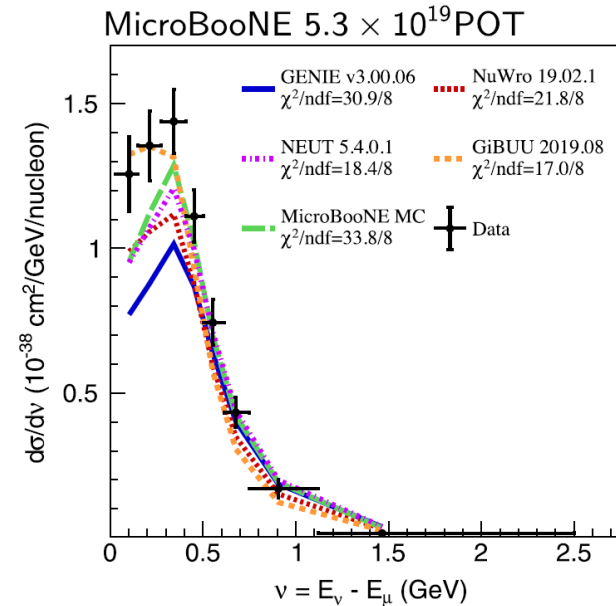
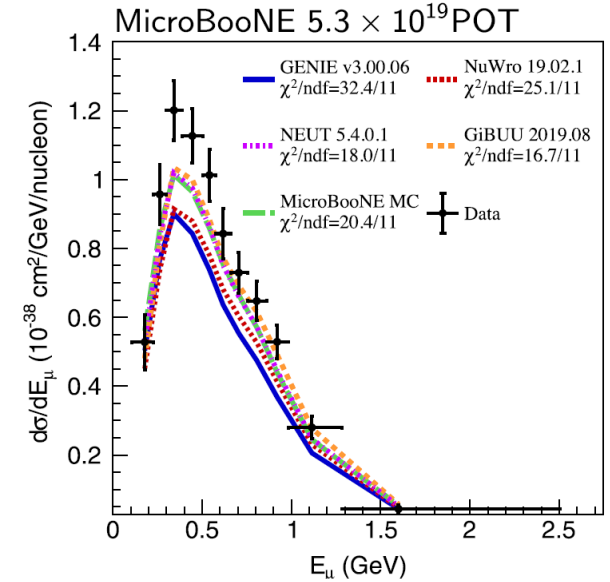
MicroBooNE flux-averaged inclusive $d\sigma/dE_\mu$ and $d\sigma/d\omega$ on argon

M. Martini, M. Ericson, G. Chanfray, Phys. Rev. C 106, 015503 (2022)



$d\sigma/d\omega$ allows a better separation of the different channels

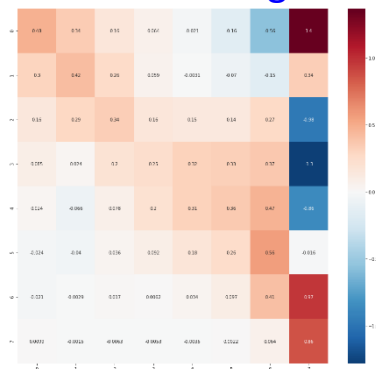
PRL 128, 151801 (2022)



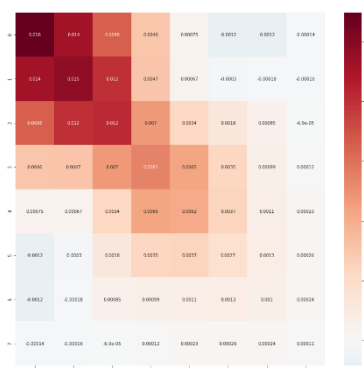
Quantitative analysis of MicroBooNE inclusive $d\sigma/d\omega$ on argon

MicroBooNE shared additional smearing and covariant matrices for quantitative analysis

Additional Smearing Matrix



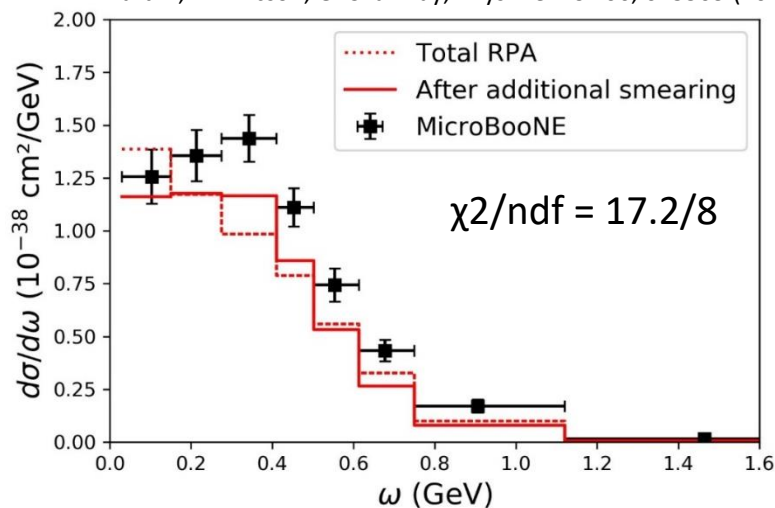
Covariant Matrix



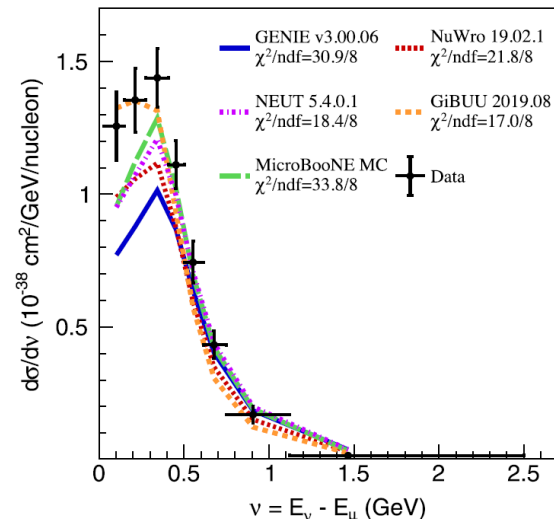
$$\sigma_{smeared} = M_{add_smr} \times \sigma_{model}$$

$$\chi^2 = (M - P)^T \times Cov_{full}^{-1}(M, P) \times (M - P)$$

M. Martini, M. Ericson, G. Chanfray, Phys. Rev. C 106, 015503 (2022)



PRL 128, 151801 (2022)
MicroBooNE 5.3×10^{19} POT



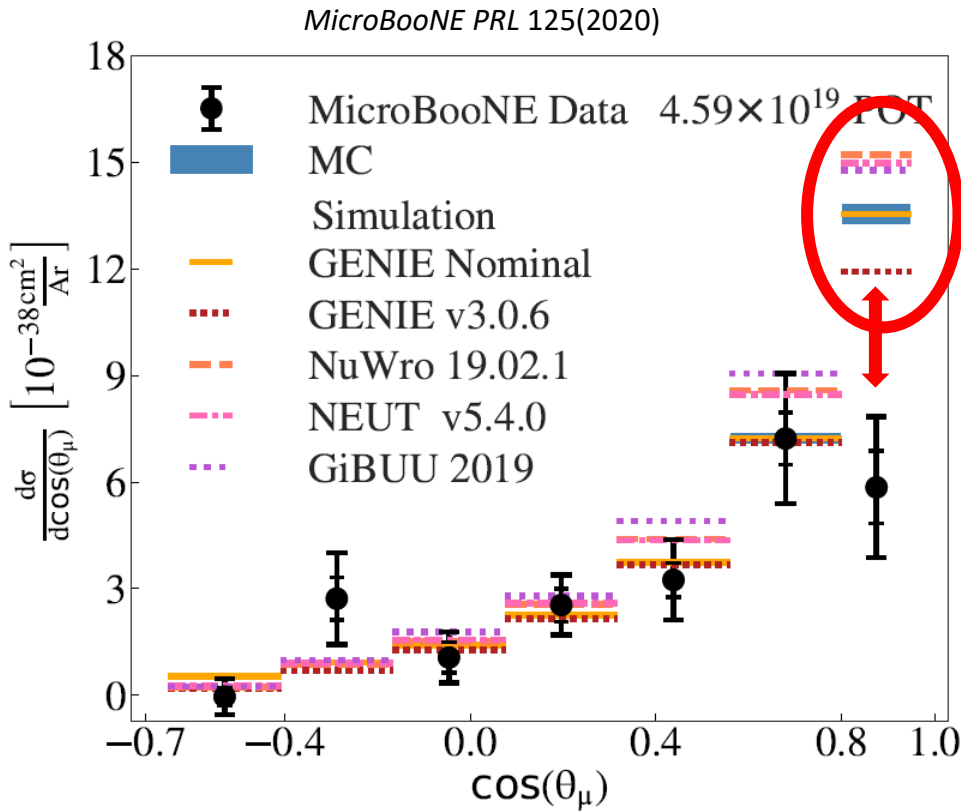
- RPA $\chi^2/ndf=17.2/8$. Comparable with the one of GiBUU and better than all the Monte Carlo predictions
- A possible reason is that GENIEv3, MicroBooNE MC, NEUT and NuWro implement np-nh contribution deduced by Nieves et al. model. This contribution is smaller than the one of other evaluations (GiBUU, Martini et al,...)

MicroBooNE semi-inclusive CC0 π 1p on argon

PHYSICAL REVIEW LETTERS **125**, 201803 (2020)

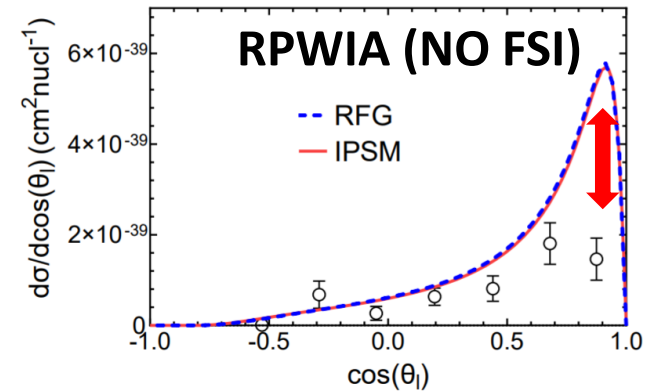
First Measurement of Differential Charged Current Quasielasticlike ν_μ -Argon Scattering Cross Sections with the MicroBooNE Detector

?! CCQE-like with another meaning than in the past

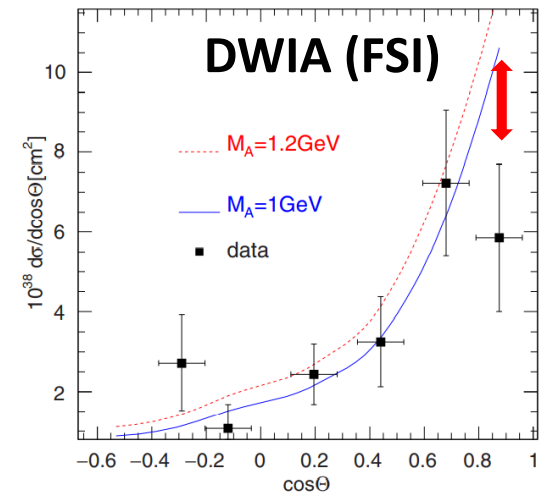


Overestimation in the muon forward direction

J. M. Franco-Patino et al. PRD 104 (2021) 7, 073008

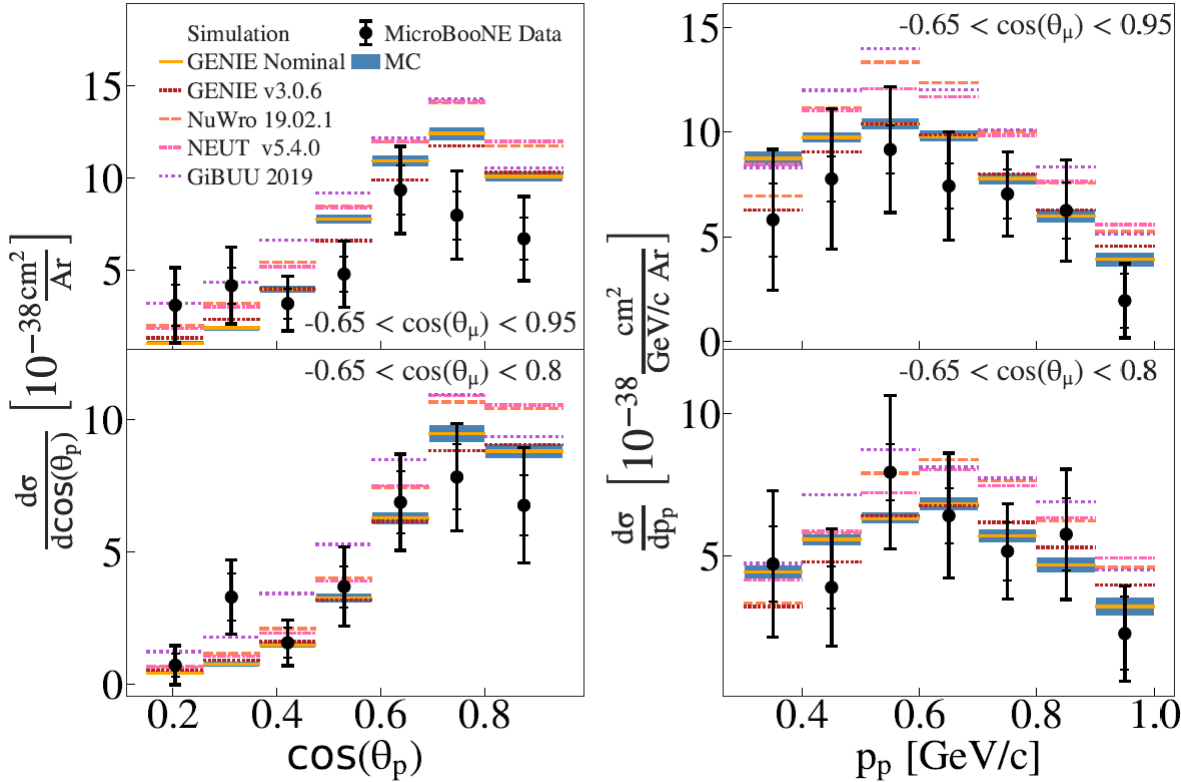


A.V. Butkevich PRC 105 (2022) 2, 025501



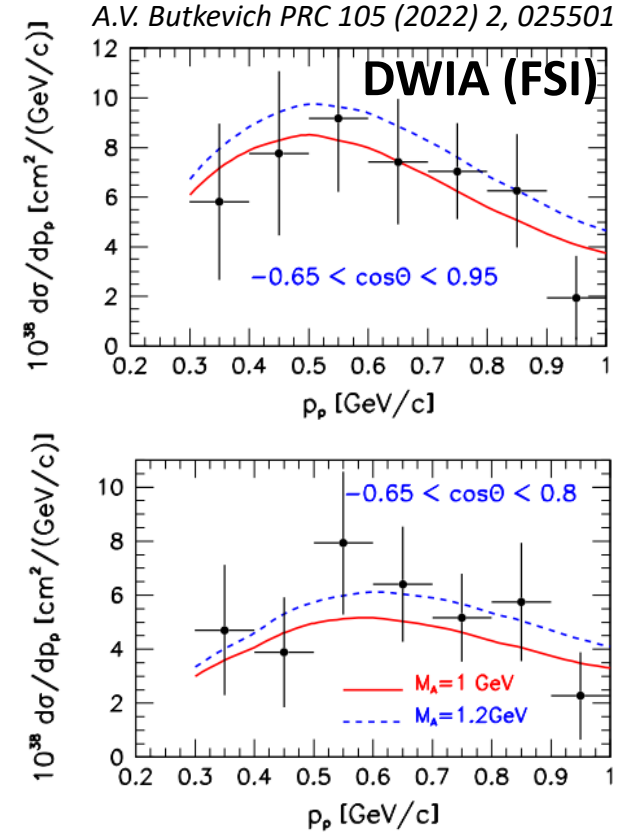
MicroBooNE semi-inclusive CC0 π 1p on argon versus proton variables

MicroBooNE PRL 125(2020)



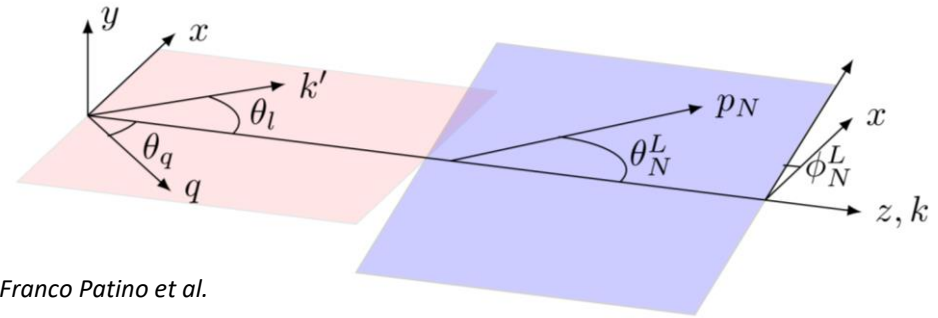
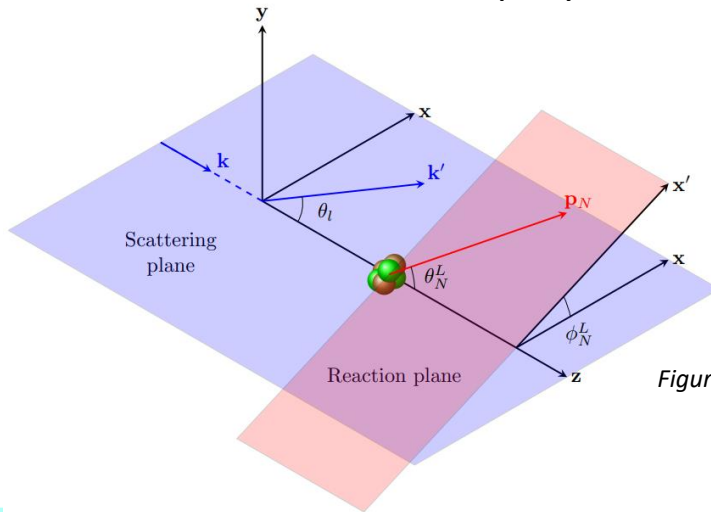
- Poor Monte Carlo – data agreement
- Spread of Monte Carlo predictions

How good are the approximations (use inclusive models, factorization) of the present MC?



The semi-inclusive neutrino cross section

There is a rapidly increasing interest on semi-inclusive cross sections



Figures by J. M. Franco Patino et al.

M. B. Barbaro talk @NUFACT 2021

$$\begin{aligned} \mathcal{F}_\chi^2 &= L_{\mu\nu} W^{\mu\nu} \\ &= V_{CC} R^{CC} + 2V_{CL} R^{CL} + V_{LL} R^{LL} + V_T R^T + V_{TT} R^{TT} + V_{TC} R^{TC} + V_{TL} R^{TL} + \chi (V_T R^{T'} + V_{TC'} R^{TC'} + V_{TL'} R^{TL'}) \end{aligned}$$

The $(\nu_\mu, \mu p)$ cross section is decomposed in **10 independent response functions** of **5 variables** $(\omega, q, \mathbf{p}_N)$.

More complex structure than in the **inclusive** (ν_μ, μ) case: **5 new responses**, which vanish after integration over the final nucleon variables

$$R^{TT,TC,TL,TC',TL'} \propto \cos(\phi), \cos(2\phi) \quad \phi \text{ outgoing nucleon azimuthal angle}$$

Semi-inclusive \rightarrow Inclusive (but not viceversa!)

Theoretical situation:

- few models and papers for genuine CCQE [J. M. Franco Patino et al, PRC 102 (2020); PRD 104 (2021), 2207.02086; A. V. Butkevich PRC 105 (2022)]
- one (incomplete due to the absence of Δ -MEC) model for 2p-2h [T. Van Cuyck et al. PRC 94 (2016); PRC 95 (2017)]

Semi-inclusive cross section: impact of different initial state modeling

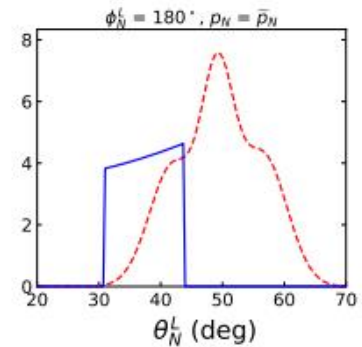
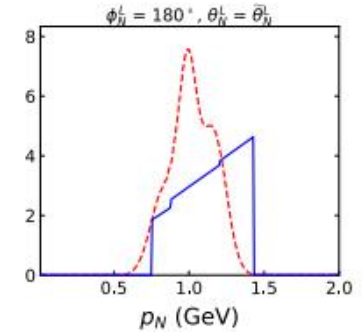
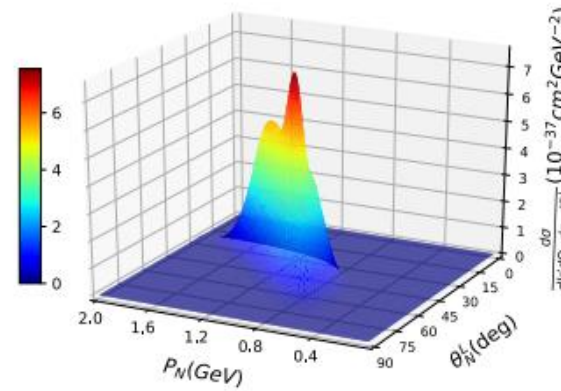
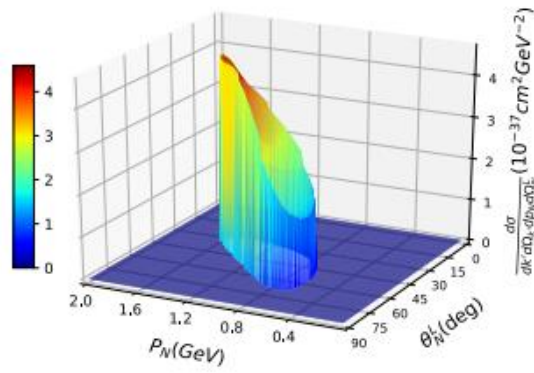
M. Barbaro
talk @IPSA
2022

6-differential semi-inclusive cross section ($\nu_\mu, \mu p$) nucleon knock-out

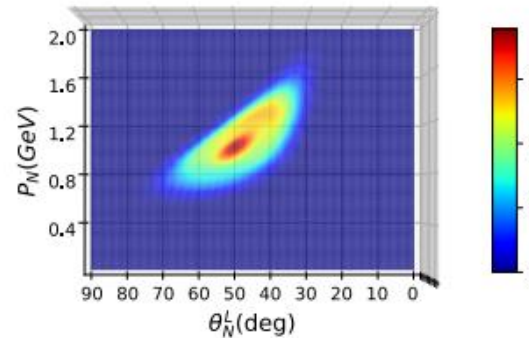
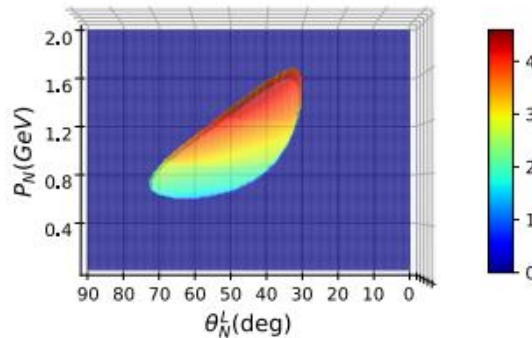
$${}^{40}\text{Ar}(\nu_\mu, \mu^- p){}^{39}\text{Cl} \quad \text{DUNE flux} \quad k' = 1.5 \text{ GeV}, \theta_\mu = 30^\circ, \phi_N^L = \pi$$

Relativistic Fermi Gas

Independent Particle Shell Model



--- IPSM
— RFG



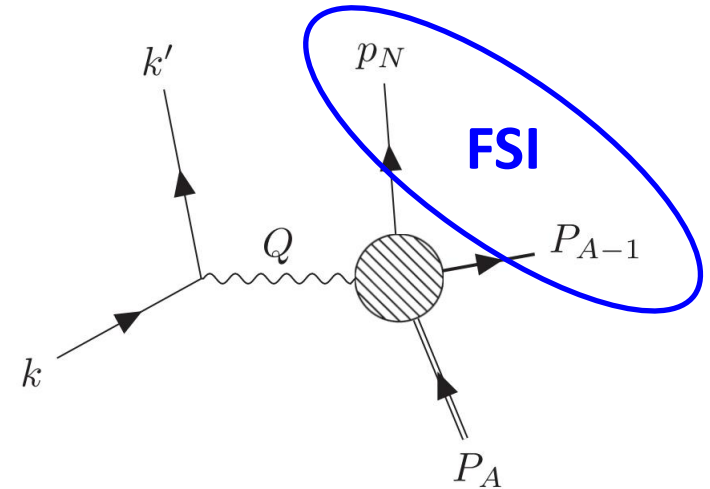
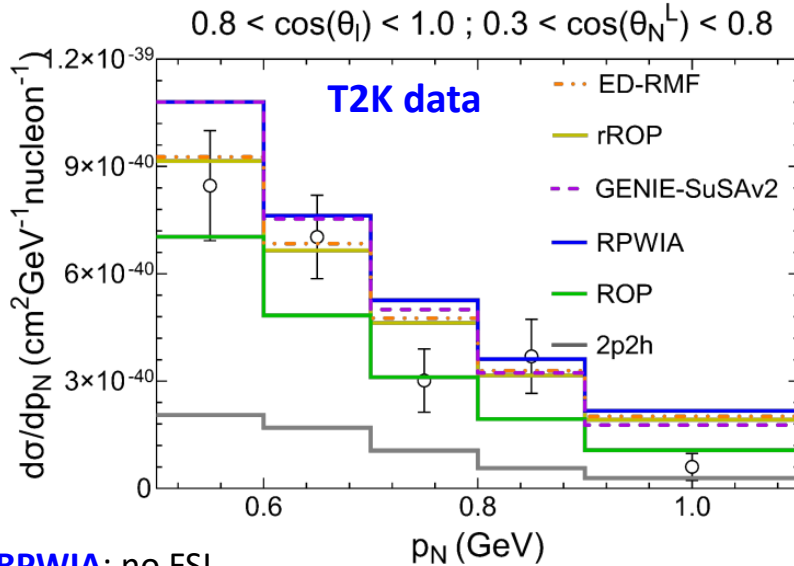
J.M. Franco-Patiño *et al.*, PRC 102, 064626 (2020)

Relativistic Plane Wave Impulse Approximation (no FSI included)

Striking differences in the cross section due to initial state physics described by different spectral functions.
The precise knowledge of the SF is crucial for a reliable modelling of semi-inclusive reactions.

Semi-inclusive CC0 π cross section on carbon: role of proton FSI

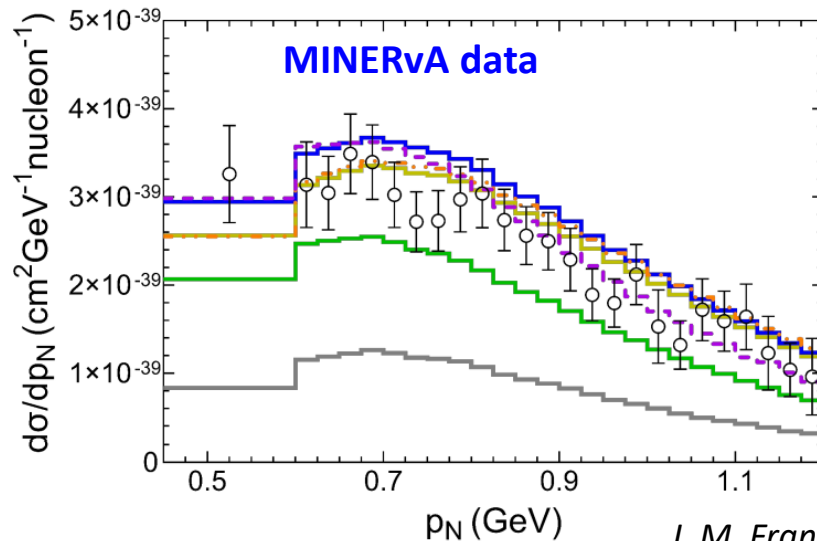
Adapted from M. Barbaro talk @IPSA 2022



RPWIA: no FSI

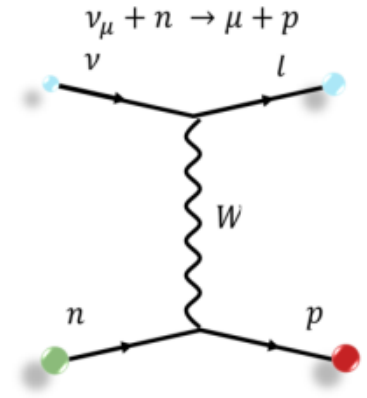
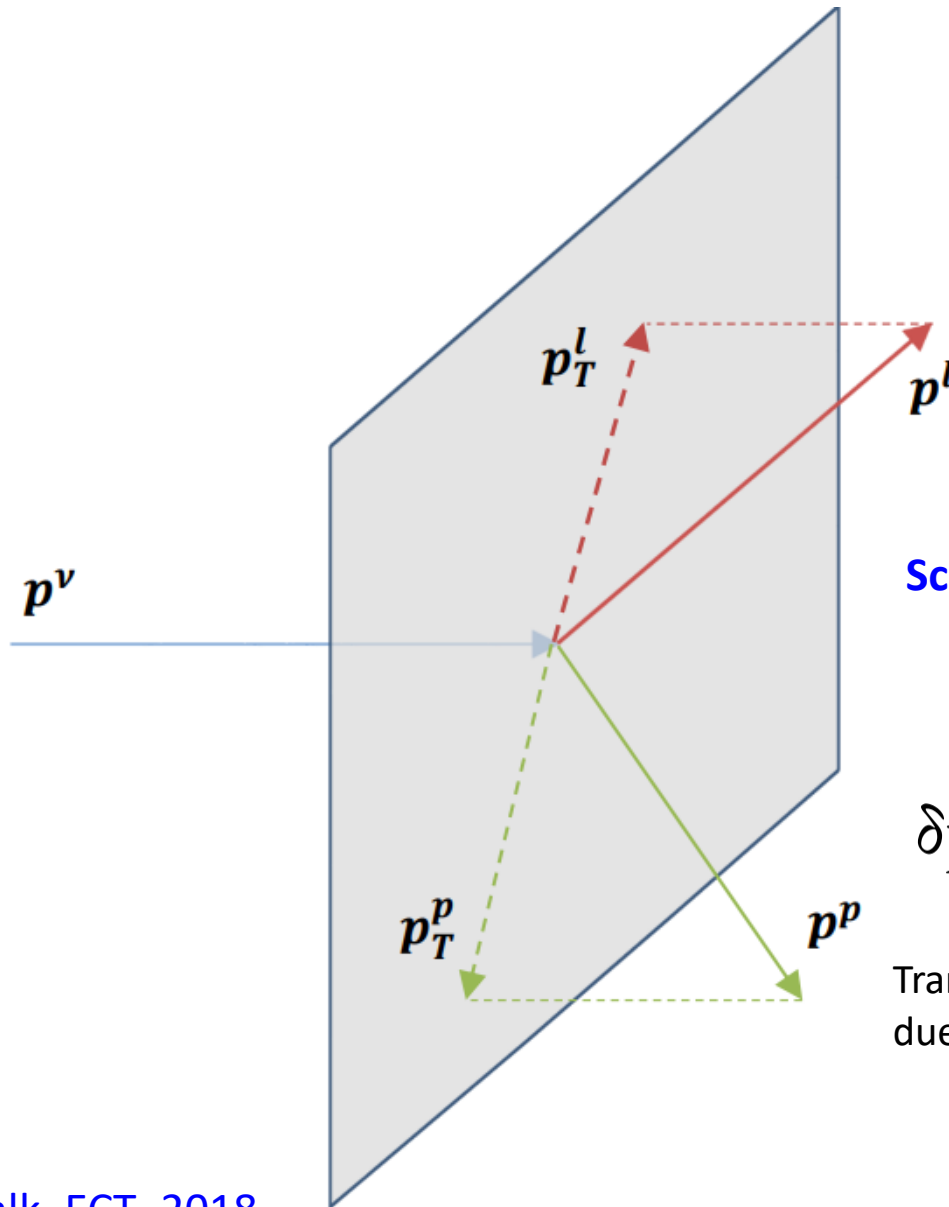
GENIE-SuSAv2: include FSI but from inclusive model (factorization)

ED-RMF, **rROP**, **ROP**: different theoretical approaches for FSI



- FSI improve the agreement with data respect to the RPWIA prediction
- Ambiguity in the way of implementing FSI, which the data error bars are not sufficient to resolve
- 2p2h give non-negligible contribution

Single Transverse Kinematic Variables



No nuclear Effects

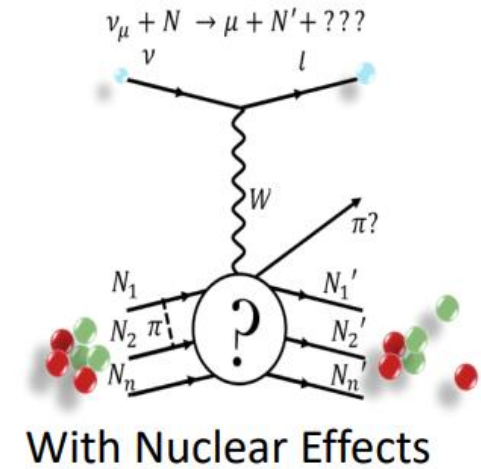
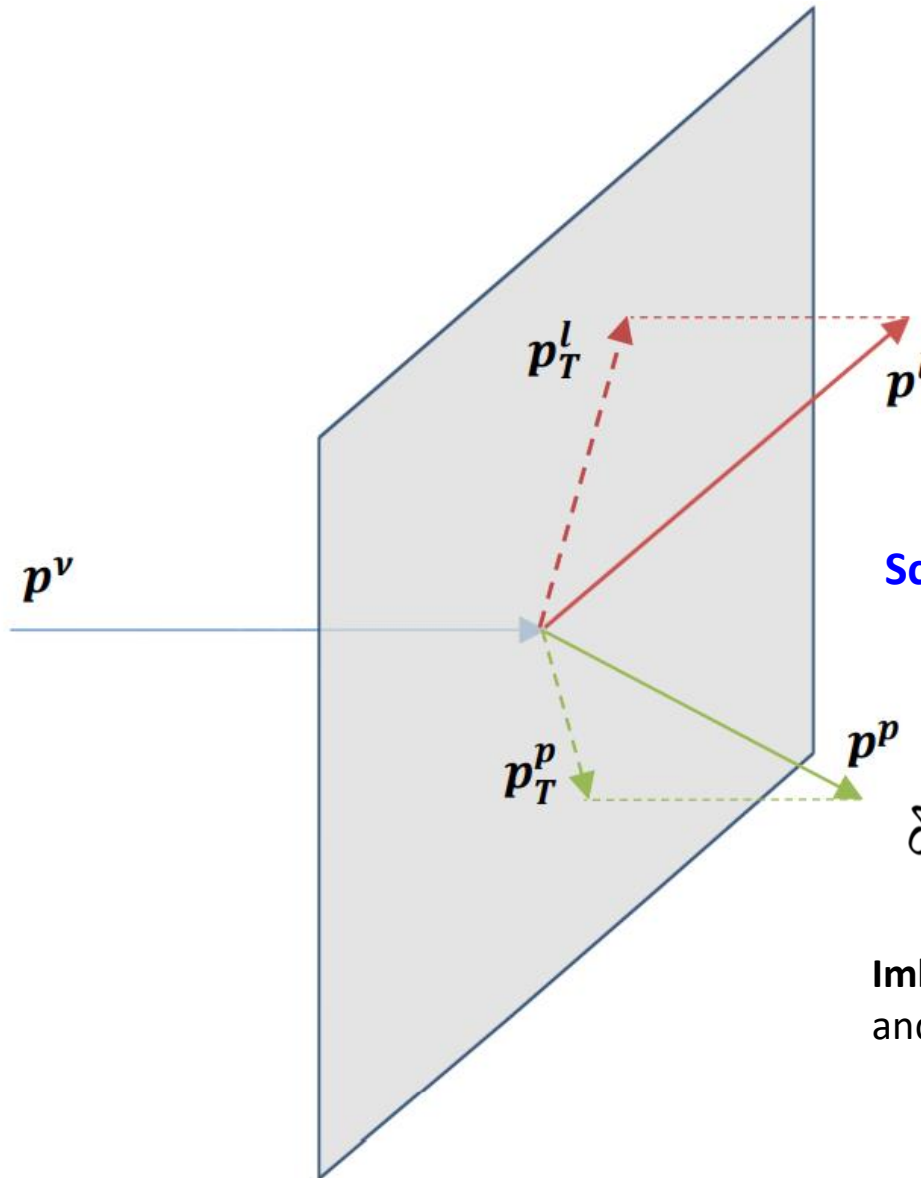
Scattering on a free nucleon at rest

$$\mathbf{p}_T^l = -\mathbf{p}_T^p$$

$$\delta p_T = |\mathbf{p}_T^\mu + \mathbf{p}_T^p| = 0$$

Transverse projections equal and opposite due to momentum conservation

Single Transverse Kinematic imbalance (STKI)



Scattering on nucleus

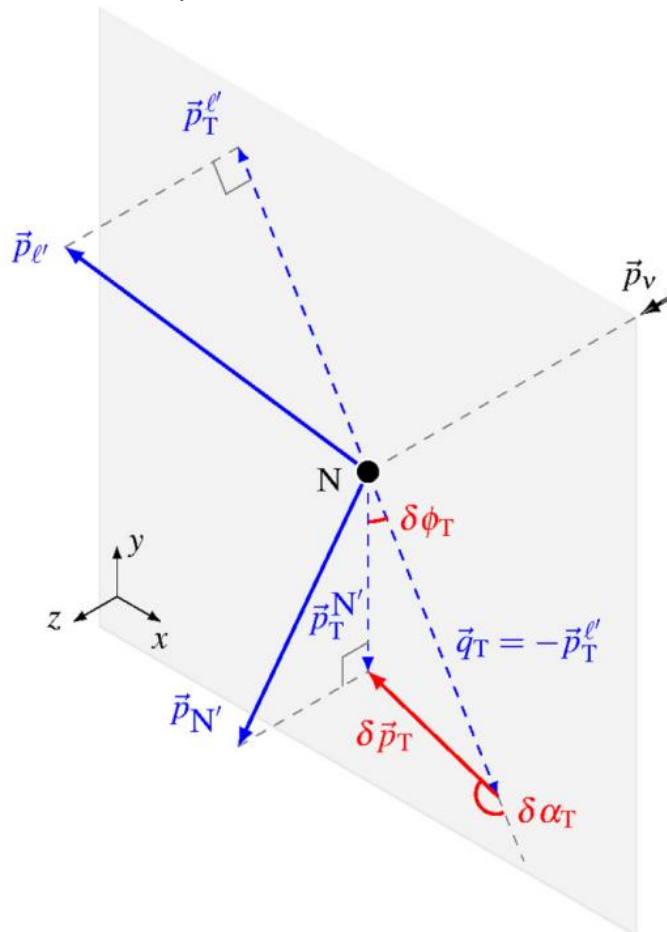
$$\mathbf{p}_T^l \neq -\mathbf{p}_T^p$$

$$\delta p_T = |\mathbf{p}_T^\mu + \mathbf{p}_T^p| > 0$$

Imbalance due to initial nucleon motion and other nuclear effects

Measurement of nuclear effects in neutrino interactions with minimal dependence on neutrino energy

X.-G. Lu,^{1,*} L. Pickering,² S. Dolan,¹ G. Barr,¹ D. Coplowe,¹ Y. Uchida,² D. Wark,^{1,3} M. O. Wascko,² A. Weber,^{1,3} and T. Yuan⁴



Single Transverse Variables (STV)

$$\delta \vec{p}_T \equiv \vec{p}_T^{\ell'} + \vec{p}_T^{N'}$$

$$\delta \alpha_T \equiv \arccos \frac{-\vec{p}_T^{\ell'} \cdot \delta \vec{p}_T}{p_T^{\ell'} \delta p_T}$$

$$\delta \phi_T \equiv \arccos \frac{-\vec{p}_T^{\ell'} \cdot \vec{p}_T^{N'}}{p_T^{\ell'} p_T^{N'}}$$

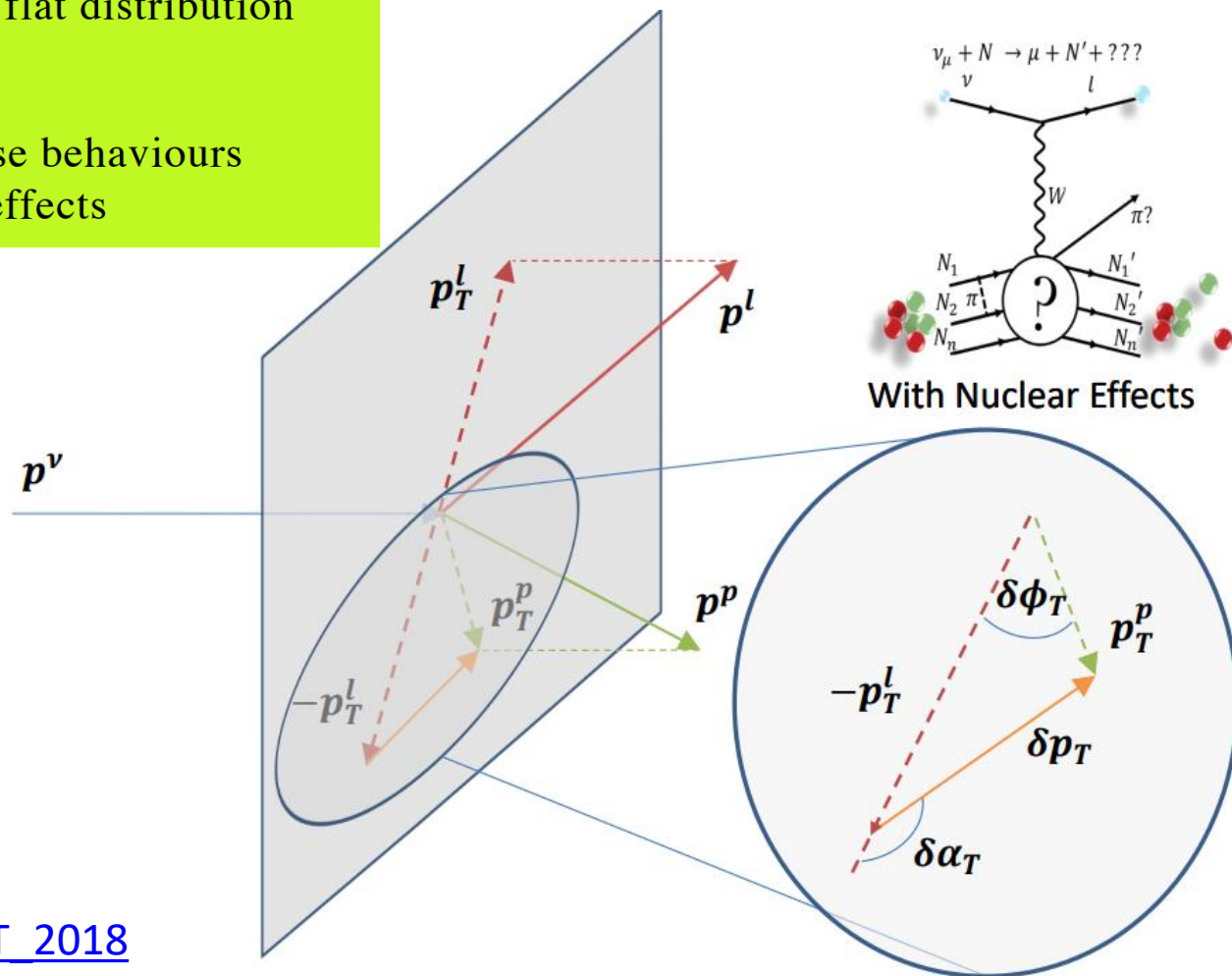
Single Transverse Kinematic imbalance (STKI) – 3 variables (STV)

On a free nucleon at rest $\vec{p}_T^{l'} = -\vec{p}_T^{N'}$:

$\delta p_T = \delta \phi_T = 0 \rightarrow$ peaked distribution

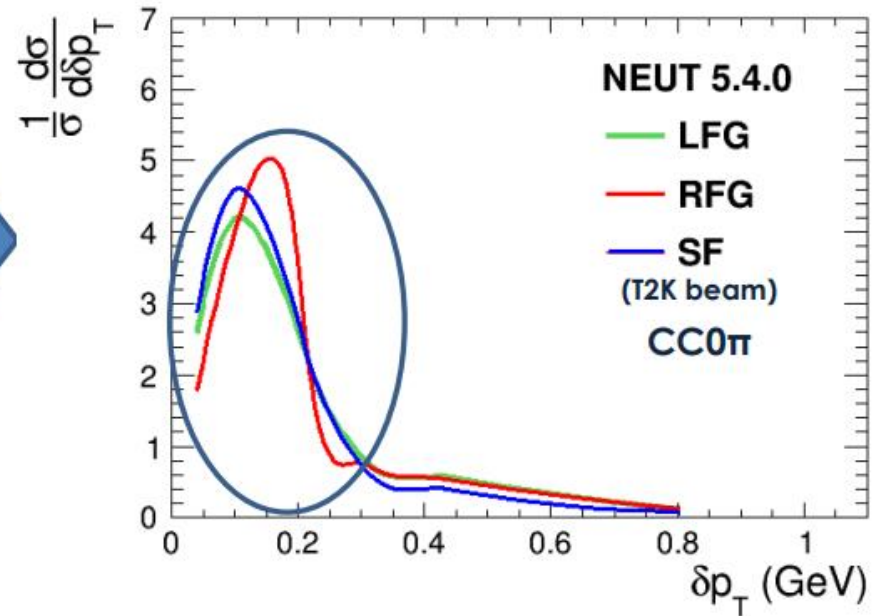
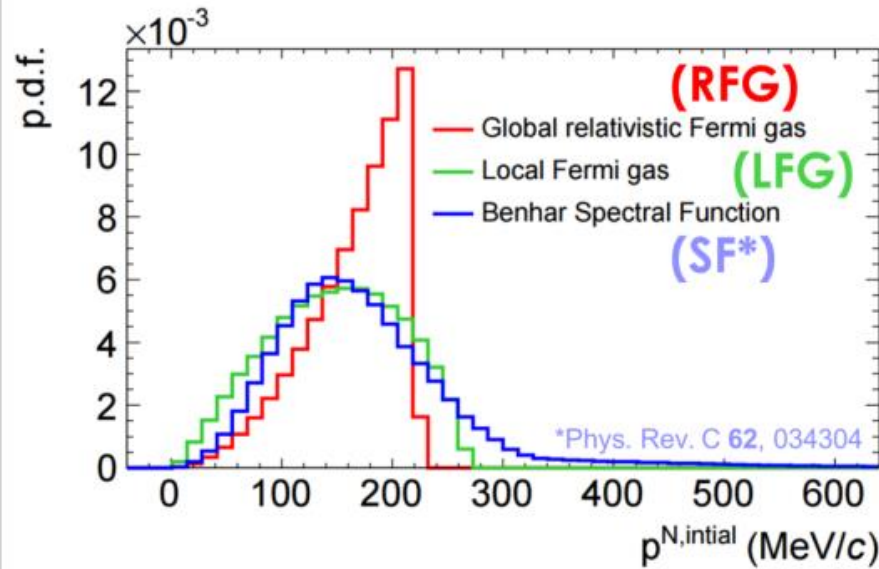
$\delta \alpha_T$ undefined \rightarrow flat distribution

Deviations from these behaviours
“measure” nuclear effects



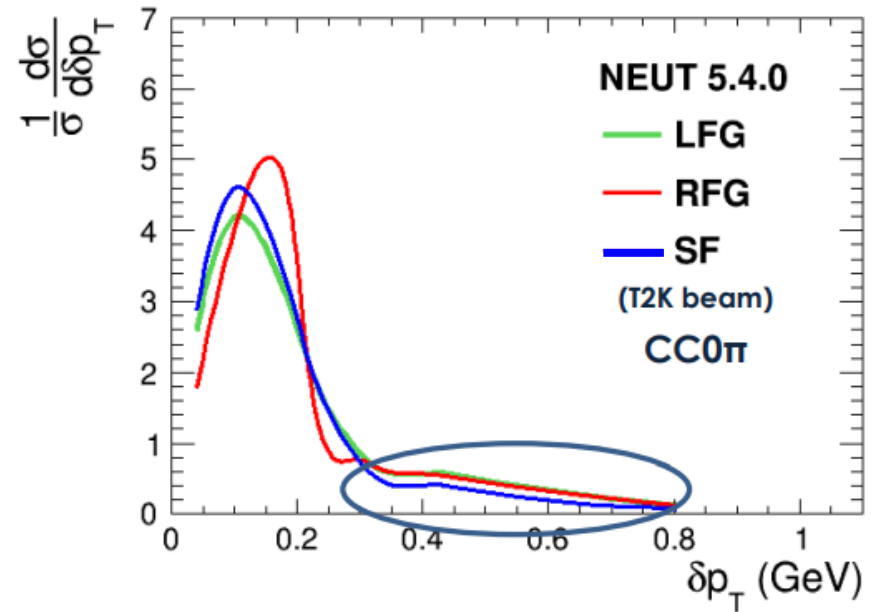
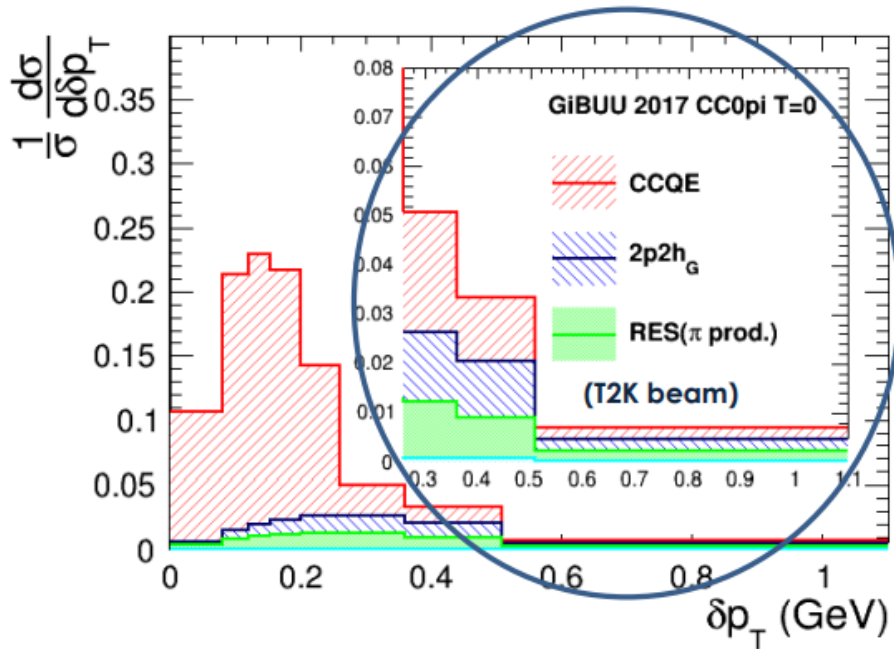
[S Dolan Talk ECT 2018](#)

STV model discrimination - δp_T



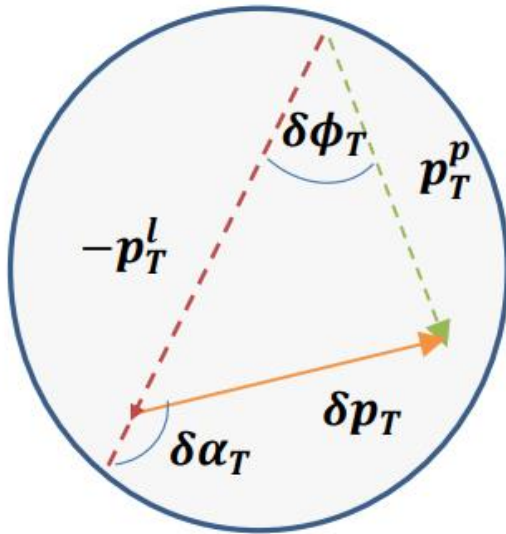
- In the absence of other nuclear effects, δp_T is the transverse projection of the Fermi motion.
- Since this motion is isotropic, $\delta p_T \rightarrow$ Fermi motion

STV model discrimination - δp_T

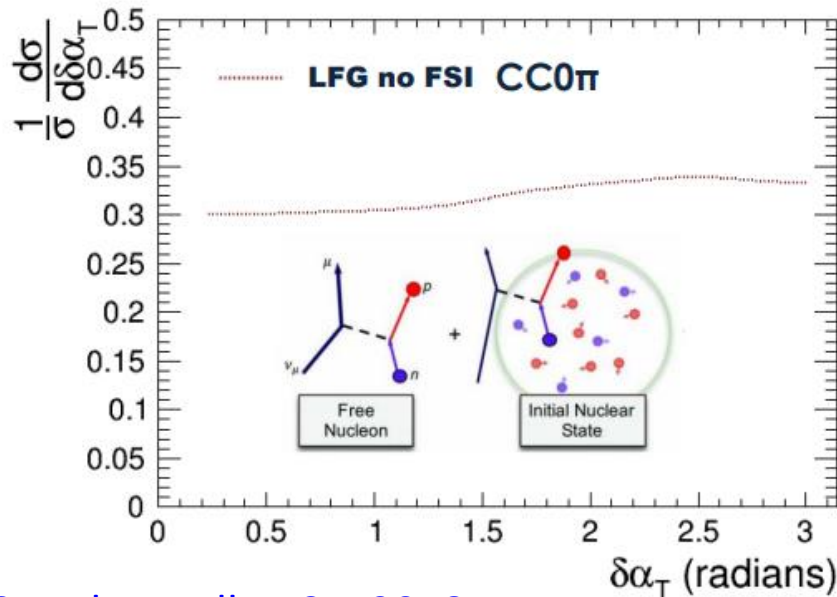


- In the absence of other nuclear effects, δp_T is the transverse projection of the Fermi motion.
- Since this motion is isotropic, $\delta p_T \rightarrow$ Fermi motion
- Cross section beyond the Fermi momentum must come from physics beyond RFG \rightarrow 2p2h, FSI, SRCs ...

STV model discrimination - $\delta\alpha_T$

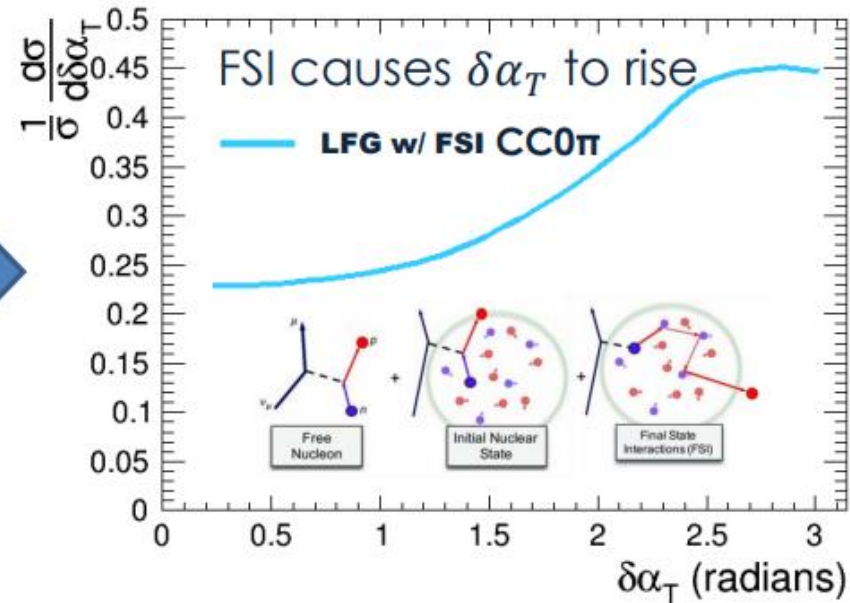
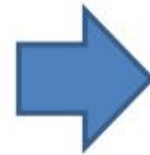
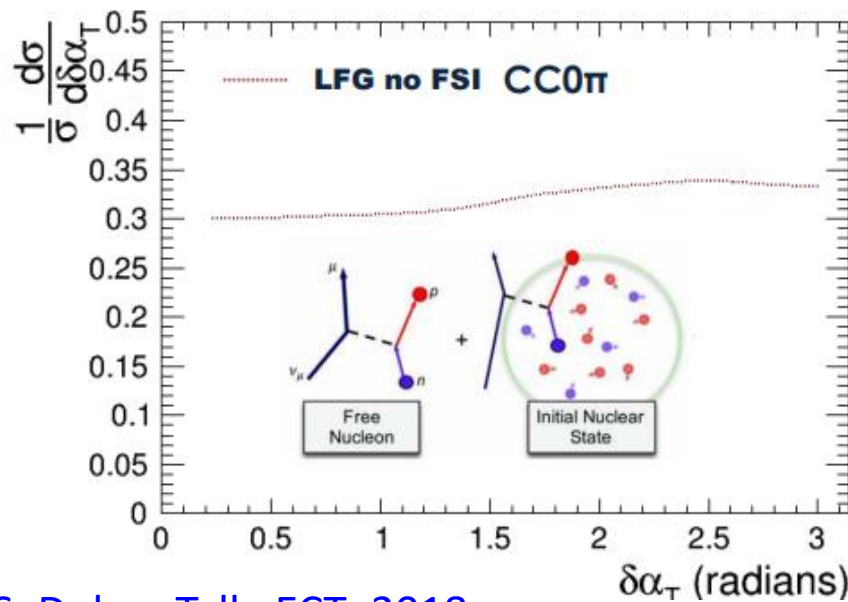
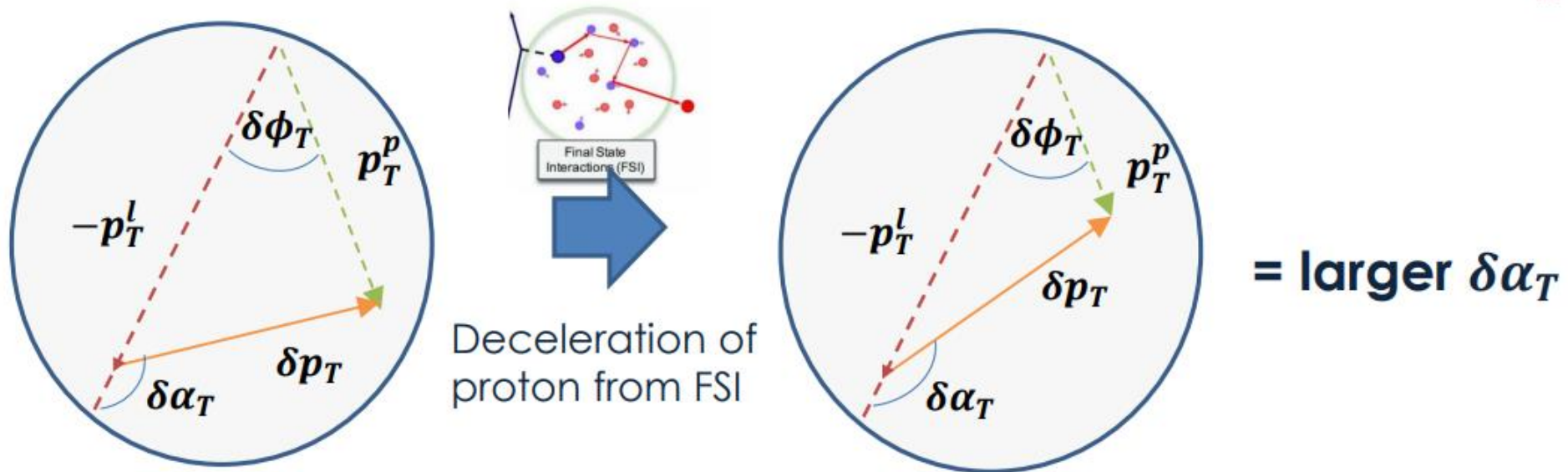


Consider imbalance from only Fermi motion

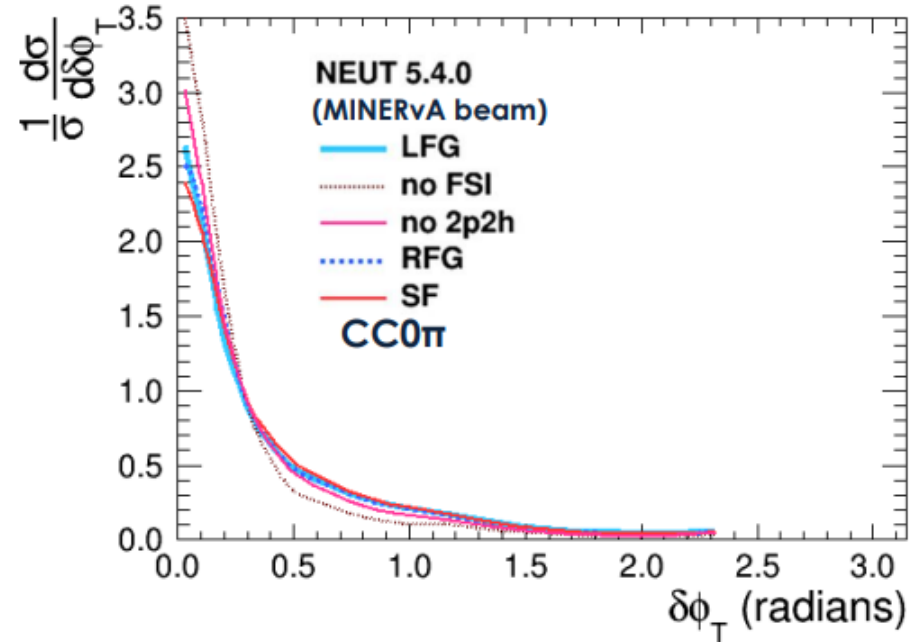
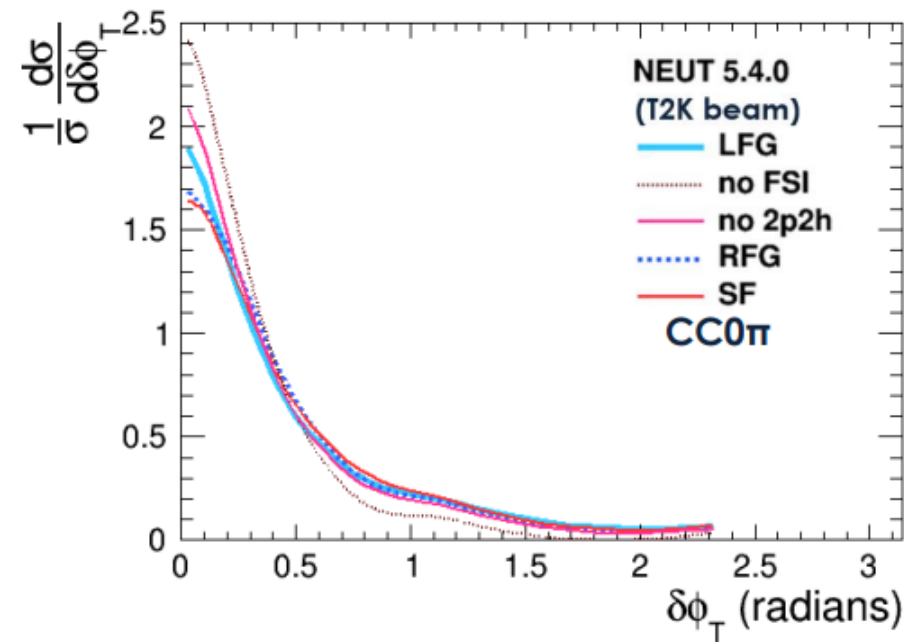


Fermi motion is isotropic so no preferred $\delta\alpha_T$ direction

STV model discrimination - $\delta\alpha_T$



STV model discrimination - $\delta\phi_T$



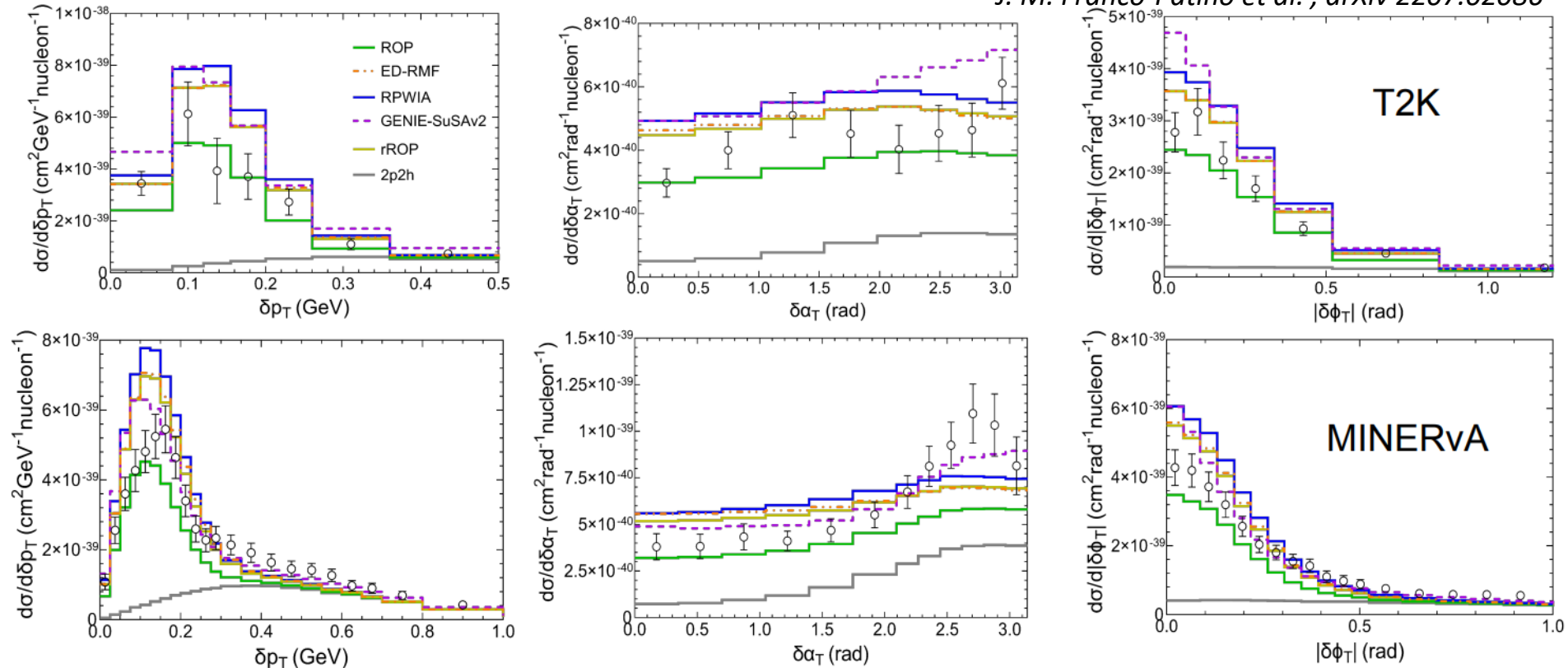
- A more general measure of transverse imbalance, more 2p2h and FSI give a larger contribution in the tail
- Not quite as powerful as δp_T and $\delta\alpha_T$
- But only requires outgoing particle angles and not their momentum → **much better detector resolution on $\delta\phi_T$**

Semi-inclusive $CC0\pi$ $d\sigma$ on carbon versus STKI Variables:

discrimination of FSI modeling

A very recent theoretical study

J. M. Franco-Patino et al., arXiv 2207.02086



RPWIA: no FSI

GENIE-SuSAv2: include FSI but from inclusive model (factorization)

ED-RMF, rROP, ROP: different theoretical approaches for FSI

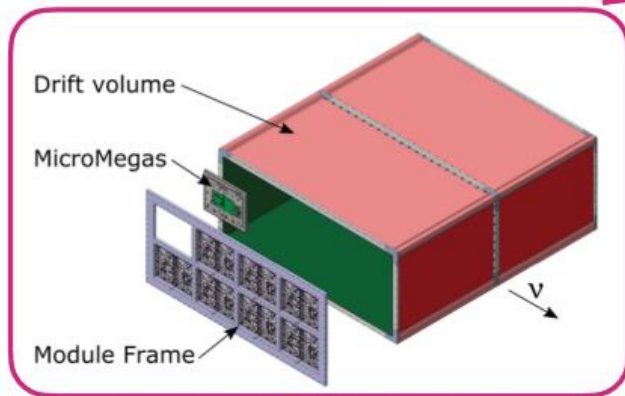
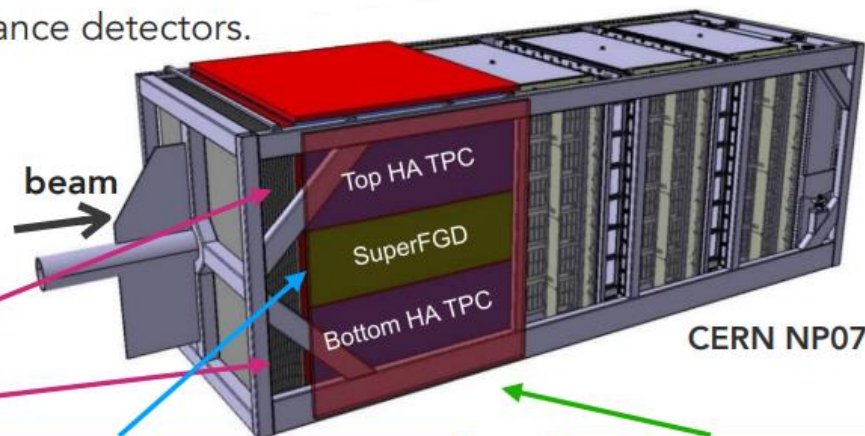
- FSI improve the agreement with data respect to the RPWIA prediction
- STKI Variables helps to discriminate between different FSI models: data (at least T2K) seem to prefer **ROP**
- 2p2h give non-negligible contribution

ND280 Upgrade

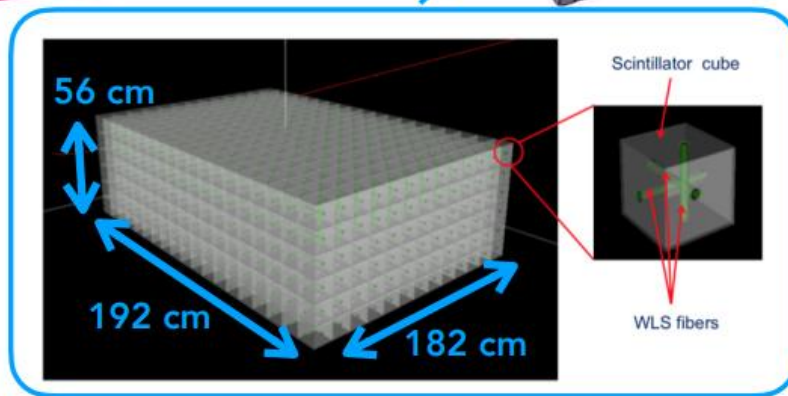
- Pi-0 detector will be replaced with new 4π acceptance detectors.

- **SuperFGD** : fully active plastic scintillator.
- **High-Angle TPC**: high resolution tracking of charged particles.
- **Time-of-Flight** : Provide time information.

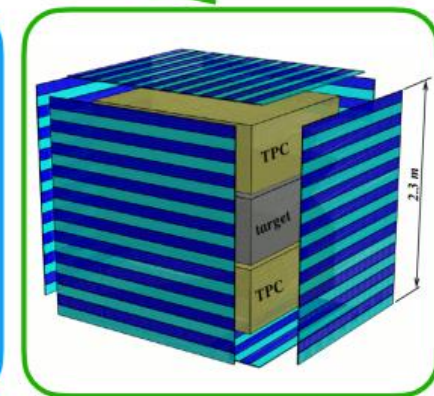
- Technical Design Report on [arXiv:1901.03750](https://arxiv.org/abs/1901.03750)



High-Angle TPC (HATPC)



Super Fine-Grained Detector (SuperFGD)



Time-of-Flight (TOF)

[A Eguchi T2KND280upgrade NuFACT2022 \(fnal.gov\)](https://arxiv.org/abs/1901.03750)

see also S. Bognesi lecture

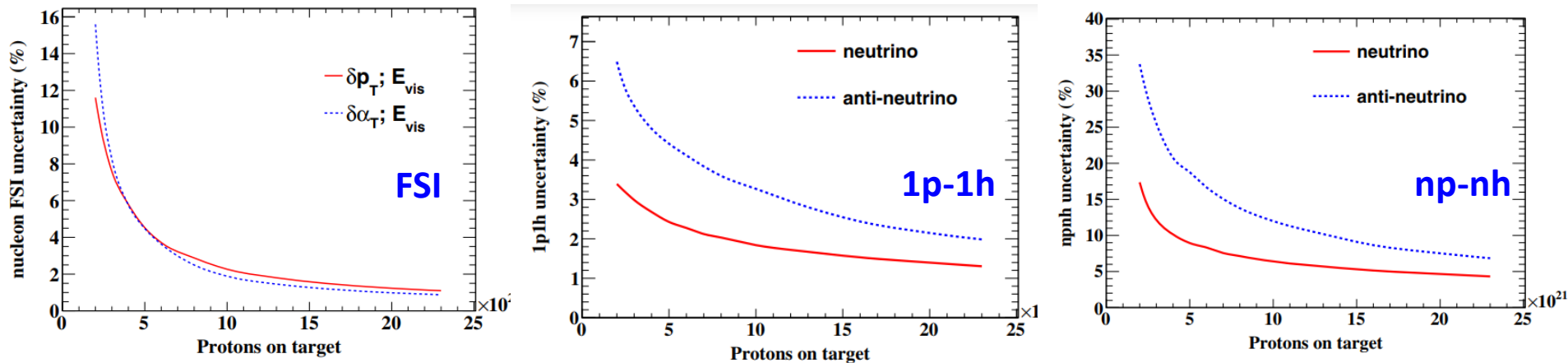
The T2K ND280 Upgrade – Physics sensitivity studies

- More mass, more data, better acceptance
- Improved reconstruction at high and backward lepton angles
- Better reconstruction of outgoing nucleons

The Upgrade opens the door to new multi-dimensional analyses (e.g. δp_T in bins of $\delta \alpha_T$)

PHYSICAL REVIEW D **105**, 032010 (2022)

Sensitivity of the upgraded T2K Near Detector to constrain neutrino and antineutrino interactions with no mesons in the final state by exploiting nucleon-lepton correlations



Significant decrease of the nuclear effects uncertainties

BACKUP

Electron-nucleon scattering

$$\ell^-(k) + N(p) \rightarrow \ell^-(k') + N(p')$$

Scattering on a point-like spinless target

$$\left(\frac{d\sigma}{d\Omega}\right)_{\text{Mott}} = \frac{\alpha^2}{4E_k^2} \frac{E_{k'}}{\sin^2 \frac{\theta}{2} E_k} \cos^2 \frac{\theta}{2}$$

Scattering on a point-like spin $\frac{1}{2}$ target

$$\left(\frac{d\sigma}{d\Omega}\right) = \left(\frac{d\sigma}{d\Omega}\right)_{\text{Mott}} \left[1 - \frac{q^2}{2M^2} \tan^2 \frac{\theta}{2}\right]$$

Scattering on spin $\frac{1}{2}$ particle with an internal structure (protons and neutrons):
electric and magnetic form factors

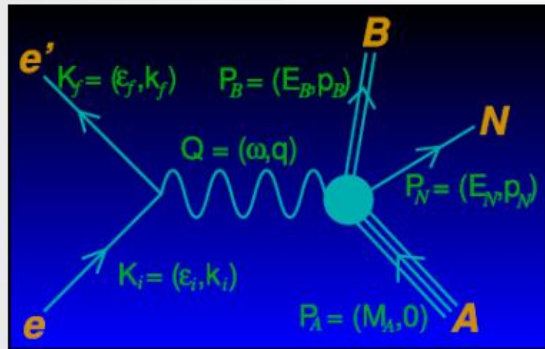
$$\left(\frac{d\sigma}{d\Omega}\right) = \left(\frac{d\sigma}{d\Omega}\right)_{\text{Mott}} \left[\frac{G_E^2 - \frac{q^2}{4M^2} G_M^2}{1 - \frac{q^2}{4M^2}} - \frac{q^2}{2M^2} G_M^2 \tan^2 \frac{\theta}{2} \right]$$

Relativistic scattering: notations and formalism

Four-vectors $A^\mu = (A_0, \vec{A})$

Bjorken&Drell conventions $g^{00} = 1, g^{kk} = -1 (k = 1, 2, 3)$

First Born approximation: one virtual boson exchange



$Q^2 = \omega^2 - q^2 < 0$ space-like virtual boson

$Q^\mu = K^\mu - K'^\mu = P_f^\mu - P_i^\mu$ 4-momentum conservation

$P^2 = M^2$ on-shell condition

$\not{\partial} \equiv \gamma_\mu \partial^\mu$ $\{\gamma^\mu, \gamma^\nu\} = \gamma^\mu \gamma^\nu + \gamma^\nu \gamma^\mu = 2g^{\mu\nu} \mathbb{1}$

$\gamma_5 \equiv i\gamma^0 \gamma^1 \gamma^2 \gamma^3$ $\sigma_{\mu\nu} = \frac{i}{2} [\gamma_\mu, \gamma_\nu]$

Dirac equation and Dirac spinors:

$(i \not{\partial} - M) \Psi = 0$ free particles

$(i \not{\partial} - e \not{A} - M) \Psi = 0$ in presence of e.m. field

$(\not{P} - M) u(\mathbf{p}, s) = 0$

$(\not{P} + M) v(\mathbf{p}, s) = 0$

$\Psi_{\mathbf{p}}^{(+)}(\mathbf{x}, t) = \sqrt{\frac{M}{EV}} u(\mathbf{p}, s) e^{-iP_\mu X^\mu}$ positive energy

$\Psi_{\mathbf{p}}^{(-)}(\mathbf{x}, t) = \sqrt{\frac{M}{EV}} v(\mathbf{p}, s) e^{iP_\mu X^\mu}$ negative energy

$$u(\mathbf{p}, s) = \sqrt{\frac{E+M}{2M}} \begin{pmatrix} \chi_s \\ \frac{\boldsymbol{\sigma} \cdot \mathbf{p}}{E+M} \chi_s \end{pmatrix}, \quad v(\mathbf{p}, s) = \sqrt{\frac{E+M}{2M}} \begin{pmatrix} \frac{\boldsymbol{\sigma} \cdot \mathbf{p}}{E+M} \xi_s \\ \xi_s \end{pmatrix}$$

Dirac spinology

Normalization condition and Dirac adjoint operators: $[\bar{u} \equiv u^\dagger \gamma^0 \text{ \& } \bar{v} \equiv \gamma^0 v^\dagger \gamma^0]$

$$\bar{u}(\mathbf{p}, s)u(\mathbf{p}, s) = 1, \quad \bar{v}(\mathbf{p}, s)v(\mathbf{p}, s) = -1$$

Projection operators:

Energy $\hat{\Lambda}_\pm(\mathbf{p}) = \left(\frac{\pm \not{p} + M}{2M} \right) = \sum_{\pm s} u(\mathbf{p}, s)\bar{u}(\mathbf{p}, s)$

Spin $\hat{P}(\pm s) = \frac{1}{2}(\mathbf{1} \pm \gamma_5 \not{S})$ *Four-spin $S^\mu = (s^0, \mathbf{s})$ satisfies: $S^2 = S_\mu S^\mu = -1$ and $P_\mu S^\mu = 0$*

Bilinear covariants and their properties under Lorentz transformations

$$\bar{\Psi}\Psi \text{ (scalar), } \bar{\Psi}\gamma^5\Psi \text{ (pseudoscalar), } \bar{\Psi}\gamma^\mu\Psi \text{ (vector), } \bar{\Psi}\gamma^5\gamma^\mu\Psi \text{ (pseudovector),}$$

Trace theorems:

$$\text{Tr}(A B) = 4A \cdot B, \quad \text{Tr}(\gamma^5) = 0, \quad \text{Tr}(\gamma^5 A B) = 0$$

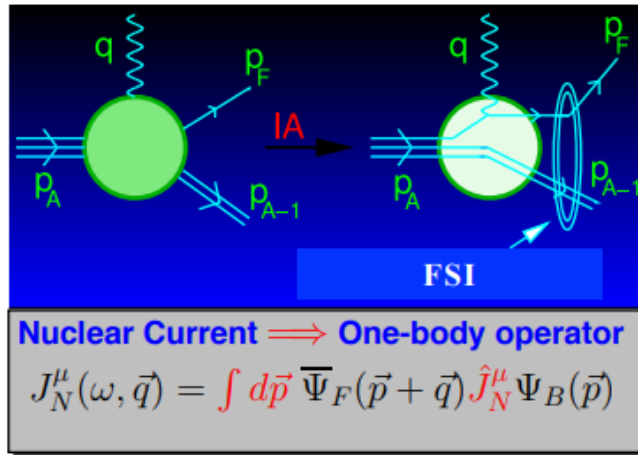
$$\text{Tr}(A B C D) = 4[A \cdot B C \cdot D + A \cdot D B \cdot C - A \cdot C B \cdot D]$$

$$\text{Tr}(\gamma^5 A B C D) = 4i\epsilon_{\alpha\beta\gamma\delta}A^\alpha B^\beta C^\gamma D^\delta$$

Relativistic Mean Field Model

The RMF model is based on the **impulse approximation (IA)**:

scattering off a nucleus = incoherent sum of single nucleon scattering processes.



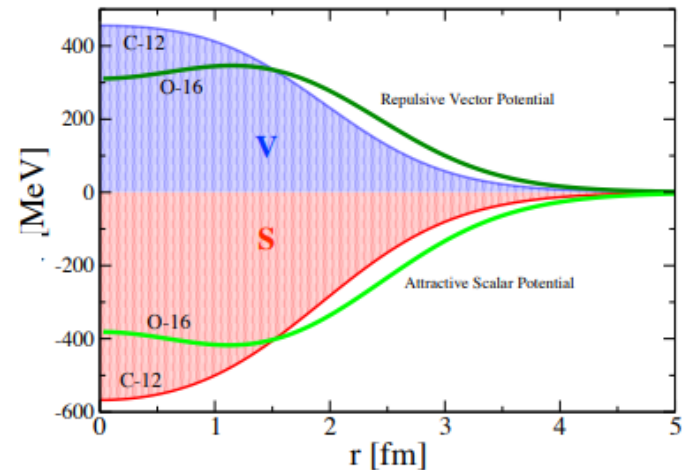
Bound wave function

$$\Psi_B = \begin{pmatrix} \phi^{up} \\ \phi^{down} \end{pmatrix} = \begin{pmatrix} \phi^{up} \\ \frac{\sigma \cdot \mathbf{p}}{E + M + S - V} \phi^{up} \end{pmatrix} = \alpha u + \beta v$$

Scattered wave function

The nucleon wave functions are finite nucleus solutions of the Dirac equation with phenomenological **relativistic scalar and vector potentials** obtained from a Walecka-type Lagrangian fitted to properties of nuclear radii and masses:

$$(i\gamma^\mu \partial_\mu - M - S + V) \psi(\vec{r}, t) = 0$$



The ejected nucleon wave function is distorted by **Final State Interactions (FSI)** with the residual nucleus. In the RMF model it is a scattering solution of the same Dirac equation used to describe the bound state. **Orthogonality is preserved:** the initial and final nucleon wave functions are eigenstates of the same Hamiltonian.

Scattered Nucleon Description

Regarding the scattered nucleon, we can consider several situations:

- **Relativistic Plane-Wave Impulse Approximation (RPWIA)**: the ejected nucleon is considered a plane-wave (i.e, there are not final state interactions)
- **Energy-Dependent Relativistic Mean Field (ED-RMF)**: W.F. solution of the Dirac equation in the continuum using the same RMF potential that describes the initial state times a phenomenological function that weakens the potentials at high energies
- **Relativistic Optical Potential (ROP)**: The scattered nucleon travels under the influence of a phenomenological relativistic optical potential fitted to reproduce elastic proton scattering data. Keeping only the real part of the OP (**rROP**) is an effective way to take into account all the channels (elastic and inelastic)

$$\Psi_{s_N}(\mathbf{r}, \mathbf{p}_N) = 4\pi \sqrt{\frac{E_N + m_N}{2E_N}} \sum_{\kappa, m_l, m_j} e^{-i\delta_\kappa^*} i^l \langle l m_l 1/2 s_N | j m_j \rangle Y_{l m_l}^*(\Omega_N) \psi_\kappa^{m_j}(\mathbf{r})$$

$$\psi_\kappa^{m_j}(\mathbf{r}) = \begin{pmatrix} g_\kappa(r) \phi_\kappa^{m_j}(\Omega_r) \\ i f_\kappa(r) \phi_{-\kappa}^{m_j}(\Omega_r) \end{pmatrix}$$

$$\frac{dg_\kappa}{dr} = -\frac{\kappa}{r} g_\kappa + [E_N + S(r, E_N) - V(r, E_N)] f_\kappa$$

$$\frac{df_\kappa}{dr} = -\frac{\kappa}{r} f_\kappa + [E_N - S(r, E_N) - V(r, E_N)] g_\kappa$$

5

Electromagnetic 2p-2h MEC response

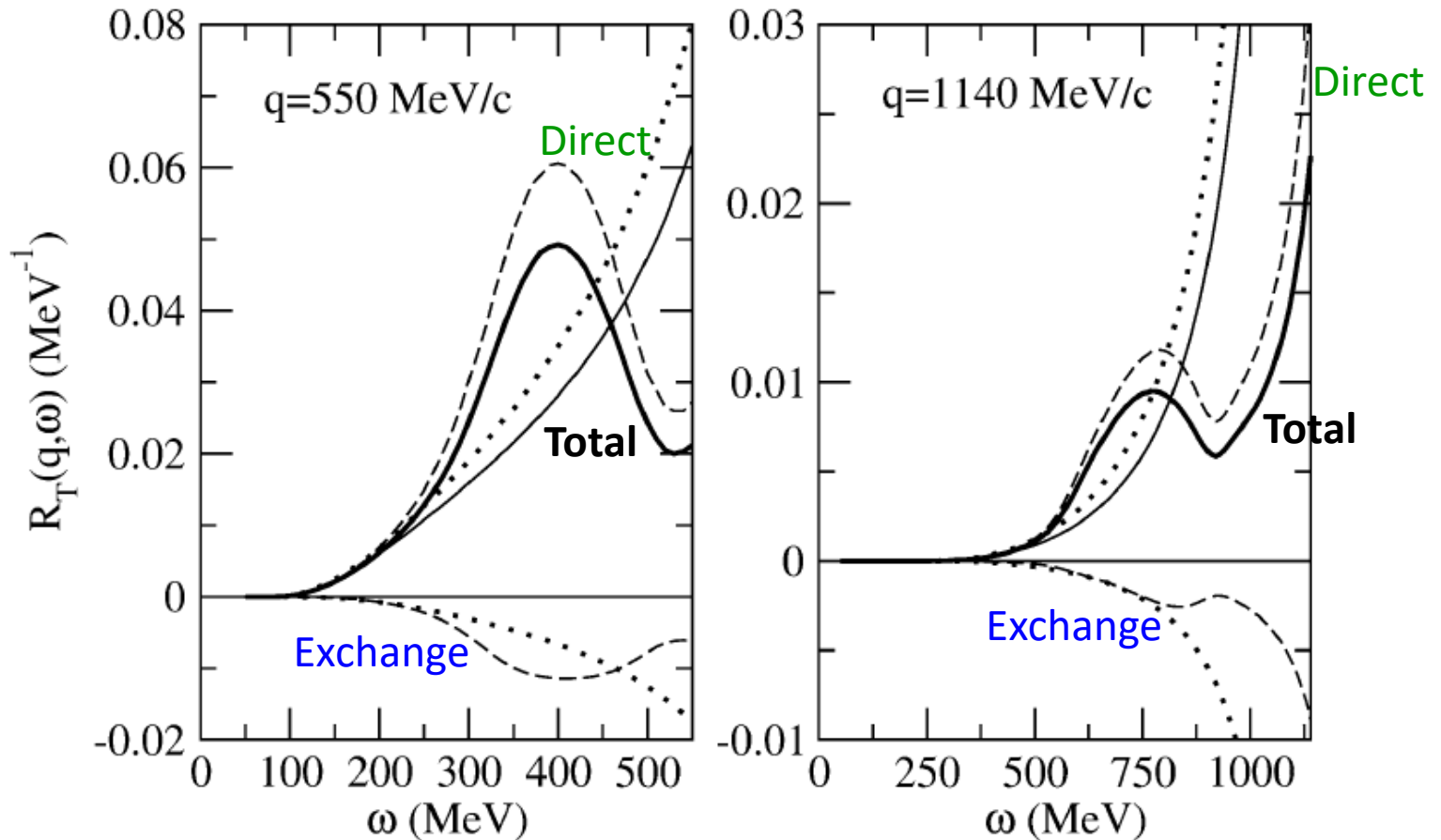


Fig. 12. The transverse response function $R_T(q, \omega)$ at $q = 550 \text{ MeV}/c$ and $q = 1140 \text{ MeV}/c$ including the exchange contributions: non-relativistic direct (positive dotted), non-relativistic exchange (negative dotted), non-relativistic total (light solid), relativistic direct (positive dashed), relativistic exchange (negative dashed) and relativistic total (heavy solid). In all instances $\bar{\epsilon}_2 = 70 \text{ MeV}$ and $k_F = 1.3 \text{ fm}^{-1}$.

De Pace, Nardi, Alberico, Donnelly, Molinari, Nucl. Phys. A741, 249 (2004)

2p-2h phase space integral

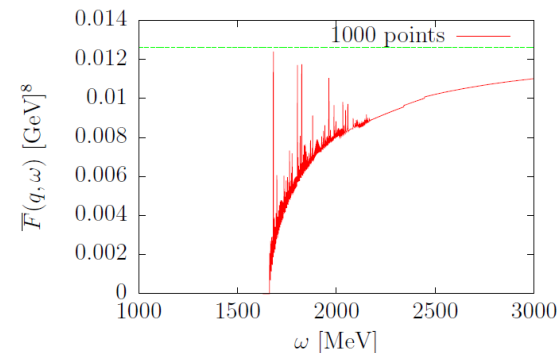
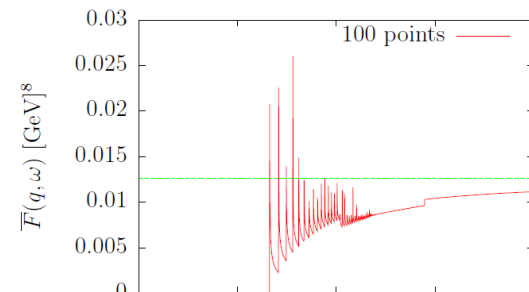
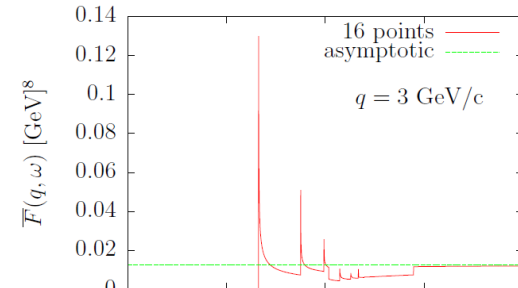
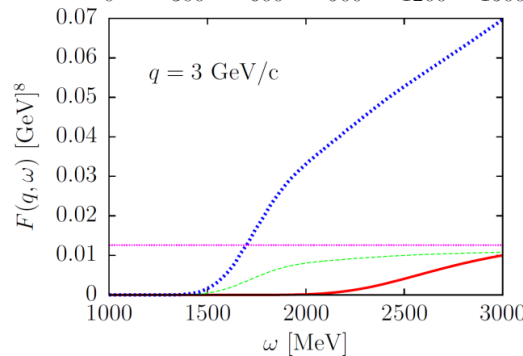
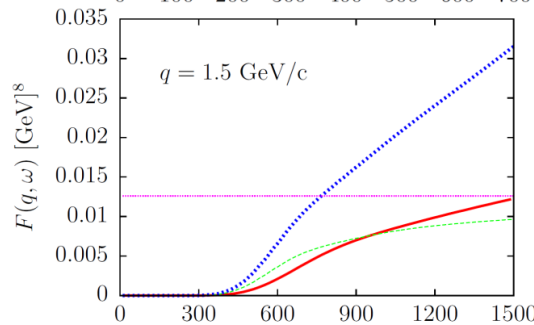
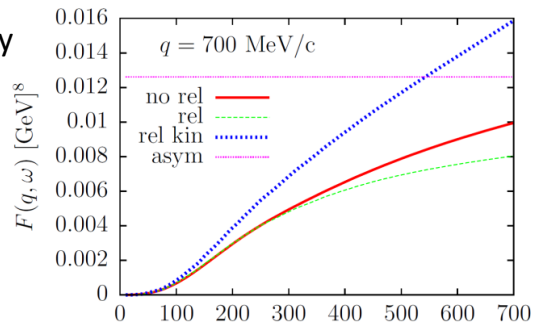
$$F(\omega, q) \equiv \int d^3 h_1 d^3 h_2 d^3 p'_1 \frac{m_N^4}{E_1 E_2 E'_1 E'_2} \Theta(p'_1, p'_2, h_1, h_2) \delta(E'_1 + E'_2 - E_1 - E_2 - \omega)$$

$$\bar{F}(\omega, q) = \left(\frac{4}{3} \pi k_F^3 \right)^2 \int d^3 p'_1 \delta(E'_1 + E'_2 - \omega - 2m_N) \Theta(p'_1, p'_2, 0, 0) \frac{m_N^2}{E'_1 E'_2}$$

Ruiz Simo, Albertus, Amaro, Barbaro, Caballero, Donnelly

Phys. Rev. D 90 033012 (2014)

Phys. Rev. D 90 053010 (2014)



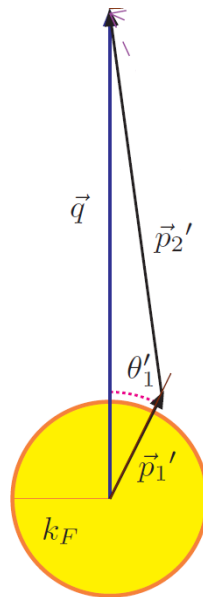
Angular distribution of ejected nucleons

$$\bar{F}(\omega, q) = \left(\frac{4}{3} \pi k_F^3 \right)^2 2\pi \int_0^\pi d\theta'_1 \Phi(\theta'_1)$$

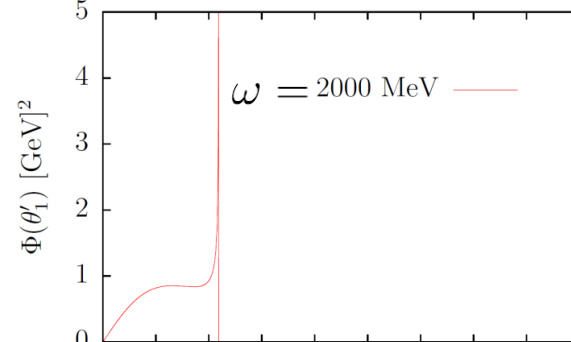
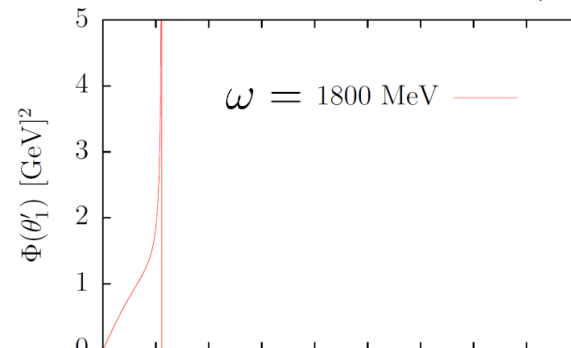
$$\Phi(\theta'_1) = \sin \theta'_1 \int p_1'^2 dp_1' \delta(E_1 + E_2 + \omega - E_1' - E_2')$$

$$\times \Theta(p_1', p_2', h_1, h_2) \frac{m_N^4}{E_1 E_2 E_1' E_2'}$$

$$= \sum_{\alpha=\pm} \frac{m_N^4 \sin \theta'_1 p_1'^2 \Theta(p_1', p_2', h_1, h_2)}{E_1 E_2 E_1' E_2' \left| \frac{p_1'}{E_1} - \frac{p_2'}{E_2} \right|} \Big|_{p_1'=p_1'^{(\alpha)}}$$



$q = 3 \text{ GeV}/c$

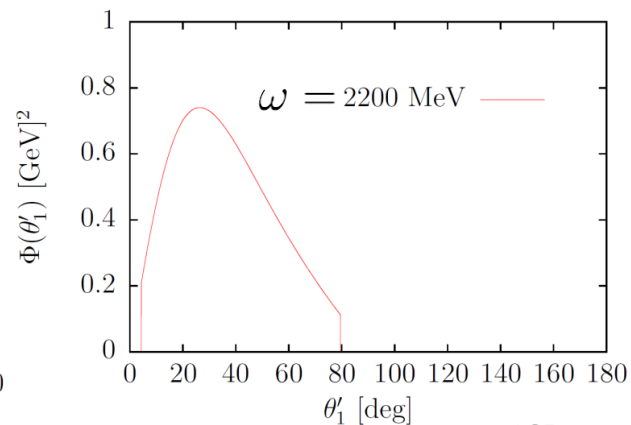
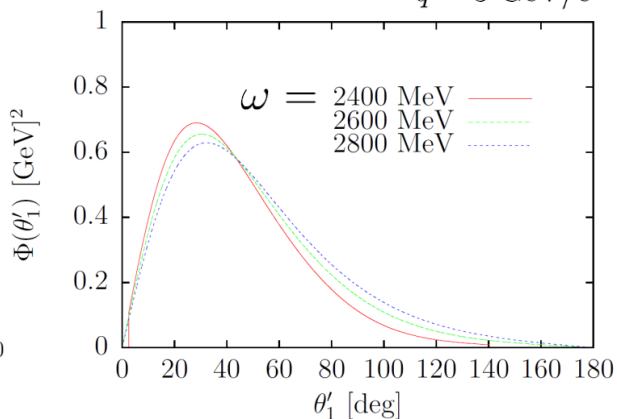
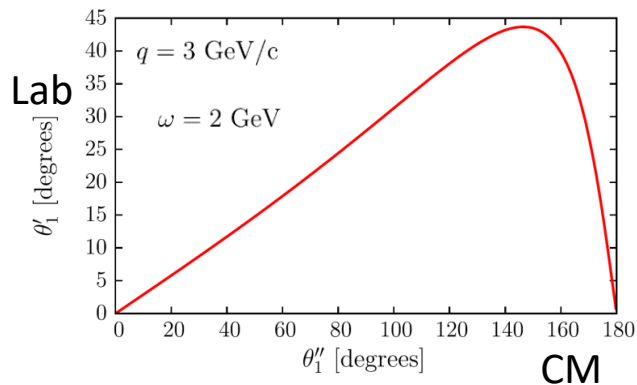


Ruiz Simo, Albertus, Amaro, Barbaro, Caballero, Donnelly

Phys. Rev. D 90 033012 (2014)

Phys. Rev. D 90 053010 (2014)

$q = 3 \text{ GeV}/c$



Difference of ν and $\bar{\nu}$ cross sections and the VA interference term

$$d\sigma \sim d\sigma_L + d\sigma_T \pm d\sigma_{VA}$$

$$d\sigma_\nu - d\sigma_{\bar{\nu}} \overset{?}{\leftrightarrow} 2d\sigma_{VA}$$

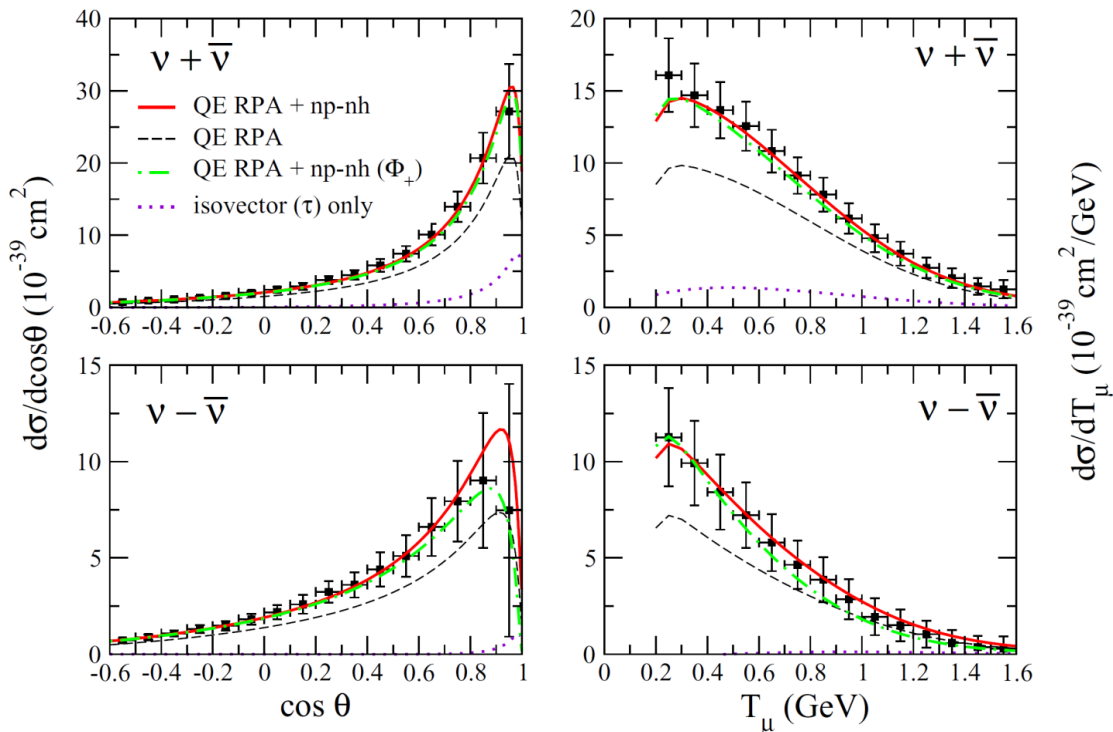
Difference gives only the VA term for identical ν and $\bar{\nu}$ flux

Problem: flux dependence of $d\sigma$ $\frac{d^2\sigma}{dE_\mu d\cos\theta} = \int dE_\nu \left[\frac{d^2\sigma}{d\omega d\cos\theta} \right]_{\omega=E_\nu-E_\mu} \Phi(E_\nu)$

We introduce the **mean flux** $\Phi_+ = 1/2[\Phi_\nu + \Phi_{\bar{\nu}}]$

We calculate the sum and the difference using **real** and **mean** MiniBooNE fluxes results

M. Ericson, M. Martini Phys. Rev. C 91 035501 (2015)



The mean flux contribution is dominant

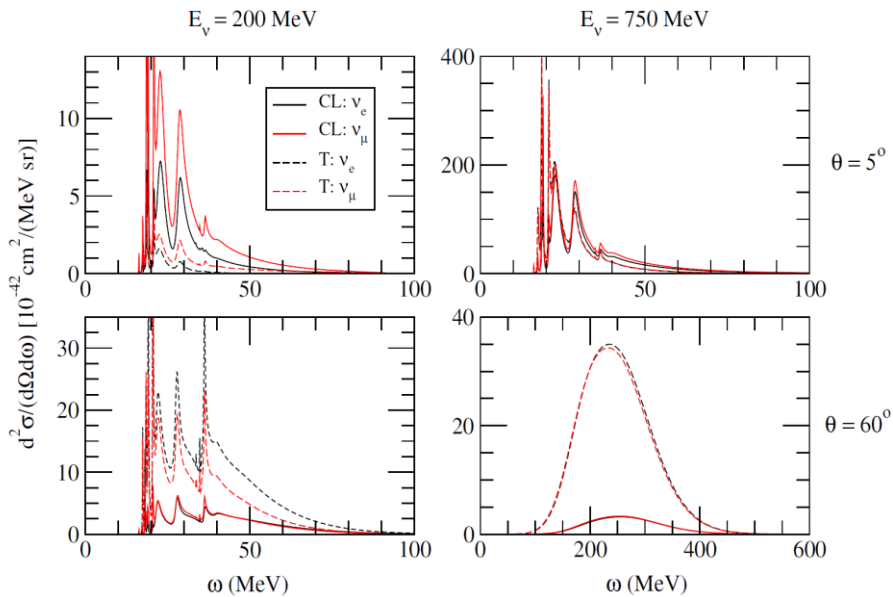
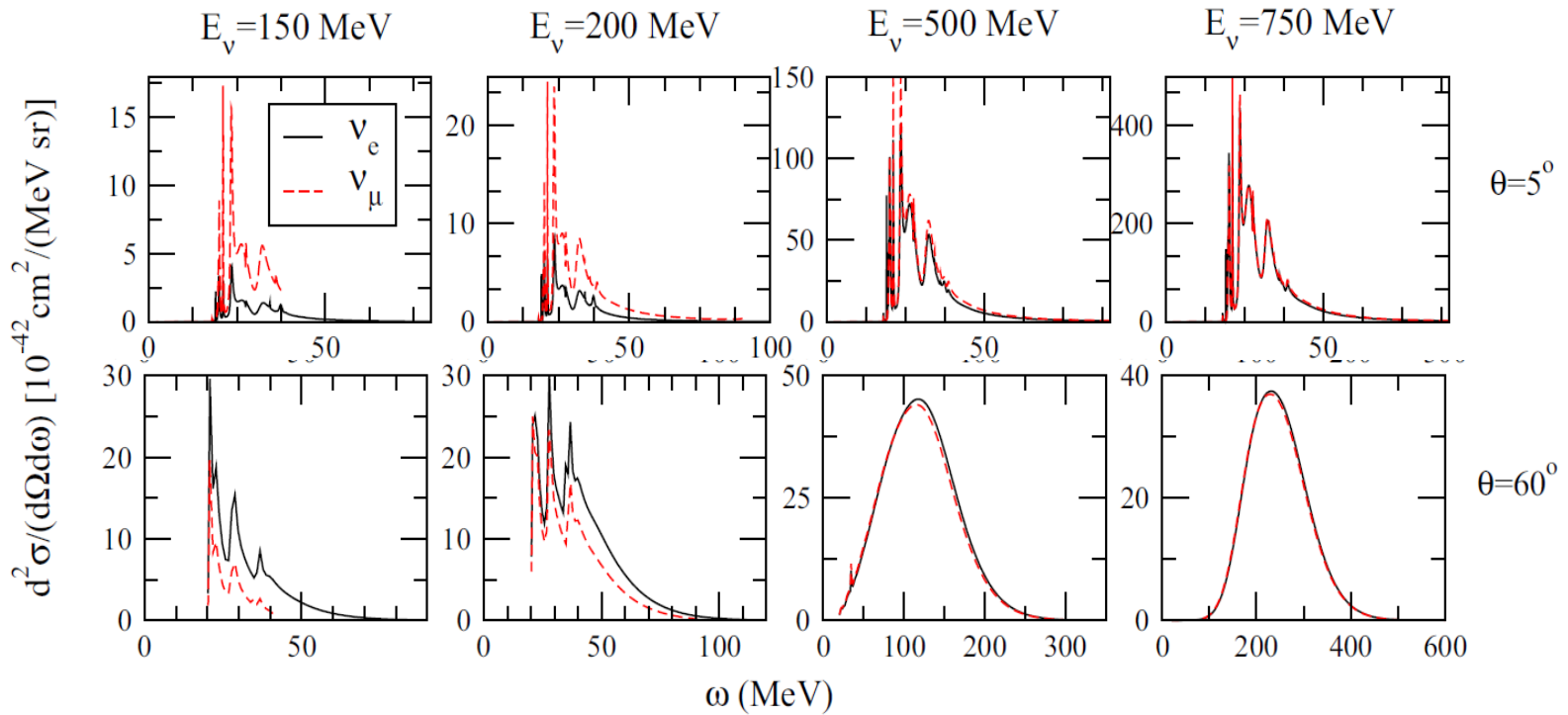


The VA interference term is experimentally accessible in MBdata



Need for the multinucleon component in the VA interference

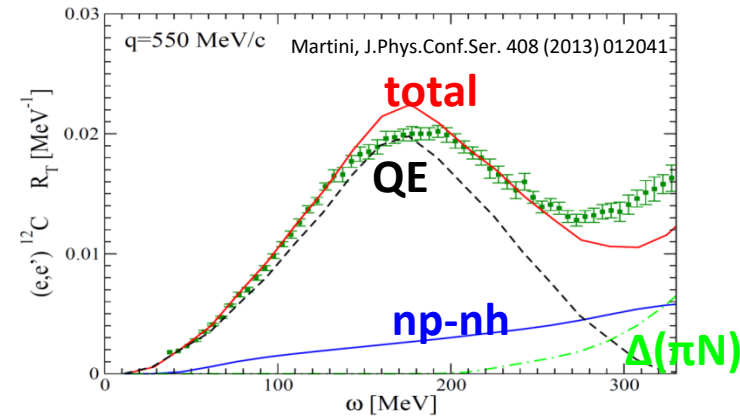
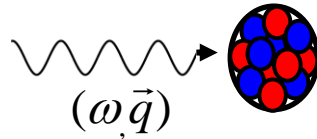
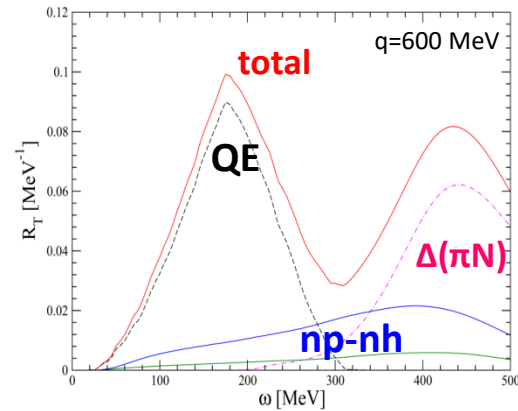
ν_μ and ν_e CCQE $d^2\sigma$ in CRPA



M. Martini et al., Phys. Rev. C 94 015501 (2016)

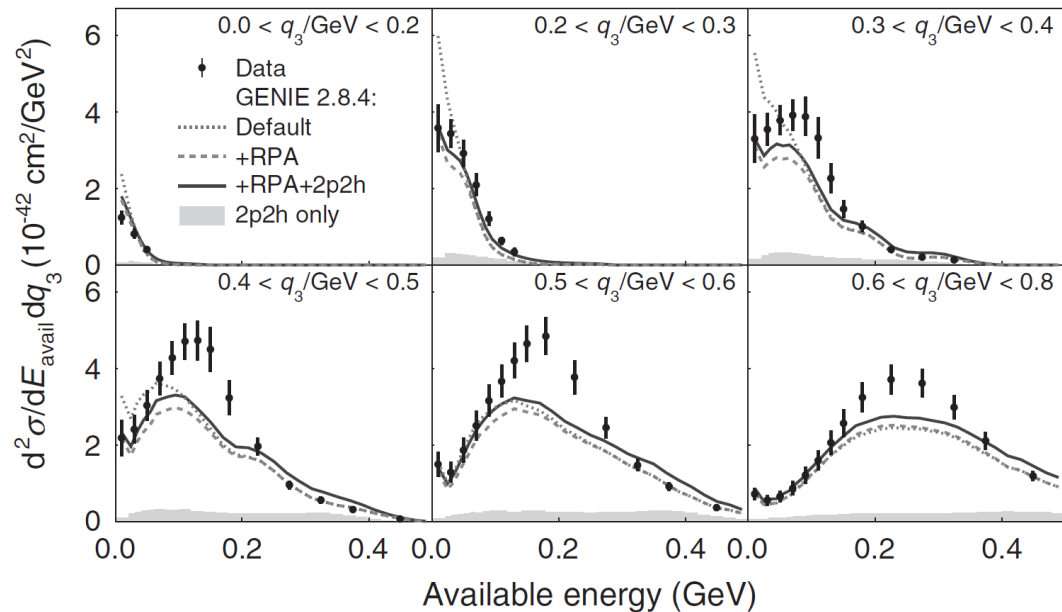
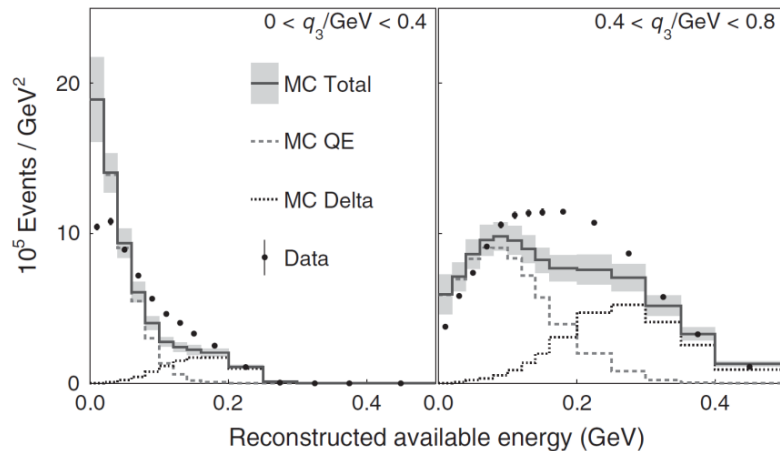
MINERvA “calorimetric” measurement

Aim: isolate the different contributions (in particular np-nh) in the (ω, q) phase space, as in (e, e') scattering



$$E_{\text{avail}} = \sum (\text{Proton and } \pi^{\pm} \text{ KE}) + (\text{Total E of other particles except neutrons})$$

P. A. Rodrigues et al., PRL 116, 071802 (2016)

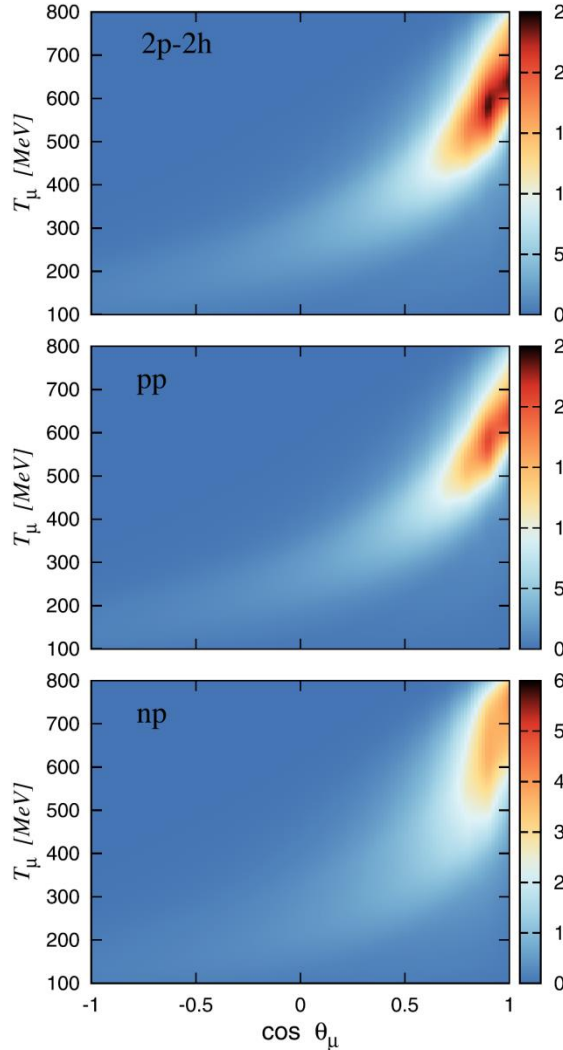
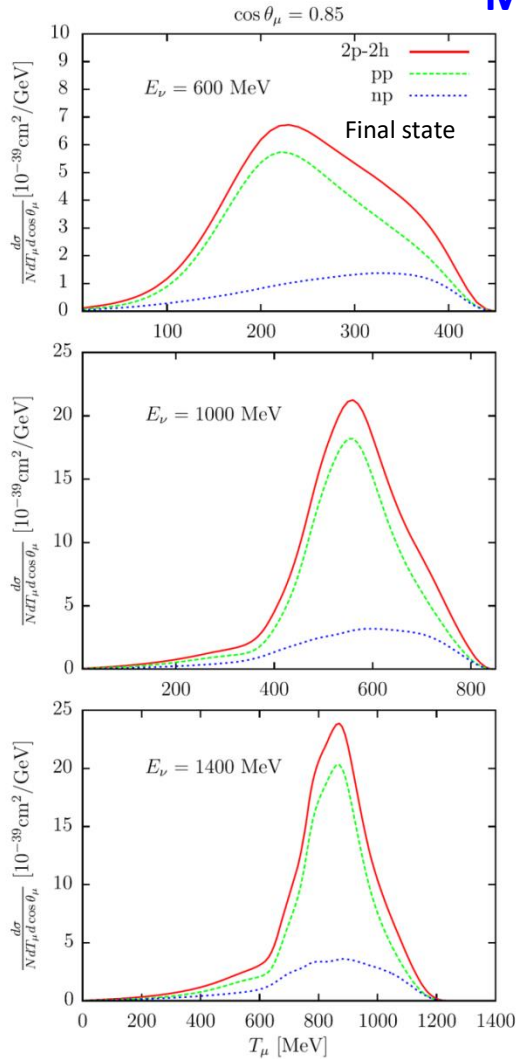


The addition of np-nh excitations via a GENIE implementation of the model of Nieves et al. reduces the discrepancy between simulation and data in the dip region, but more np-nh events would further improve the agreement with data

Theoretical studies on hadron information – Isospin content

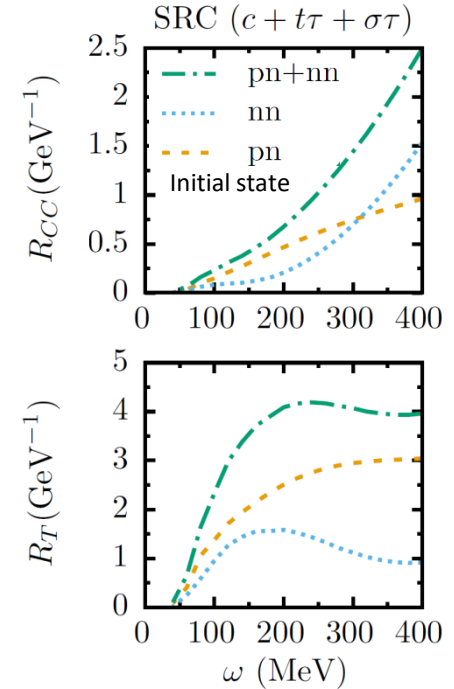
I. Ruiz Simo et al. Phys. Lett.B762, 124 (2016)

MEC



T. Van Cuyck et al. PRC 94, 024611(2016)

NN SRC

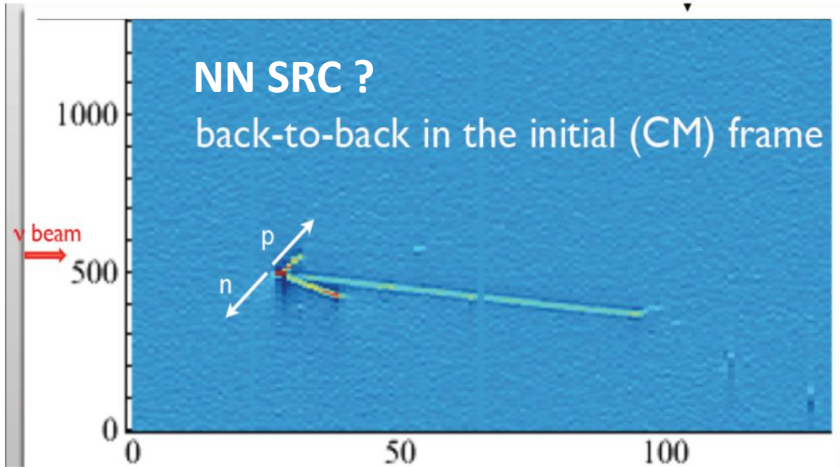


- The **pp** channel final state (**np** in the initial state) dominates in MEC and SRC
- The **pp/np** ratio depends on the kinematics

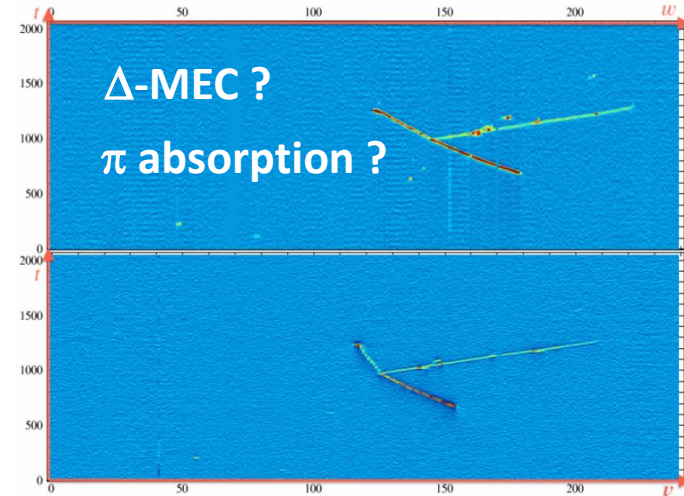
Exclusive processes ($\nu_\mu, \mu^- + 2p$)

ArgoNeut

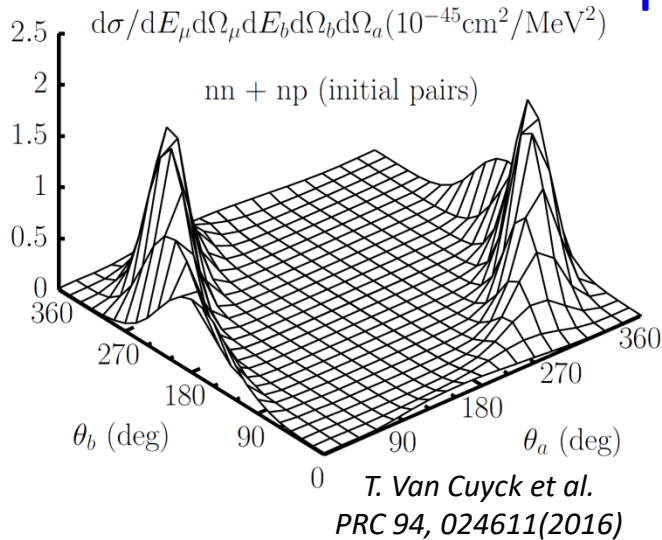
Acciari et al. Phys.Rev. D90 (2014) 012008



Hammer events

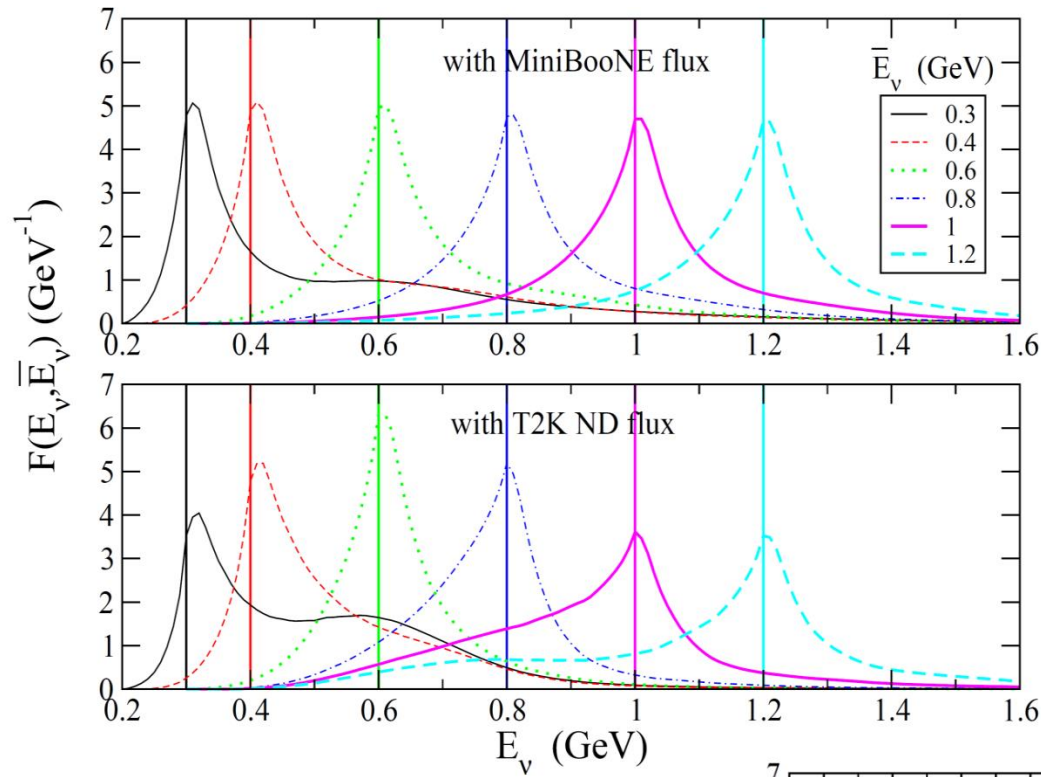


Theoretical studies



- Modeling the coincidence reactions is in demand by the experimental community but it is a very challenging task
- Many models used up to now to compare with the neutrino flux-integrated differential cross sections function of the charged lepton variables are not applicable for exclusive studies. More nuclear response functions contribute to the cross section

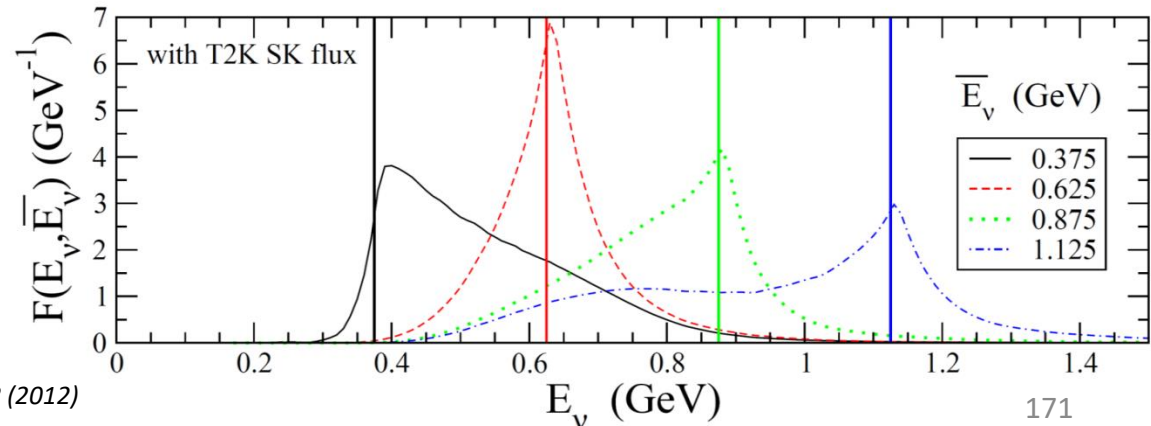
Energy reconstruction: Probability distributions $F(E_\nu, \bar{E}_\nu)$ for several \bar{E}_ν using three different neutrino fluxes



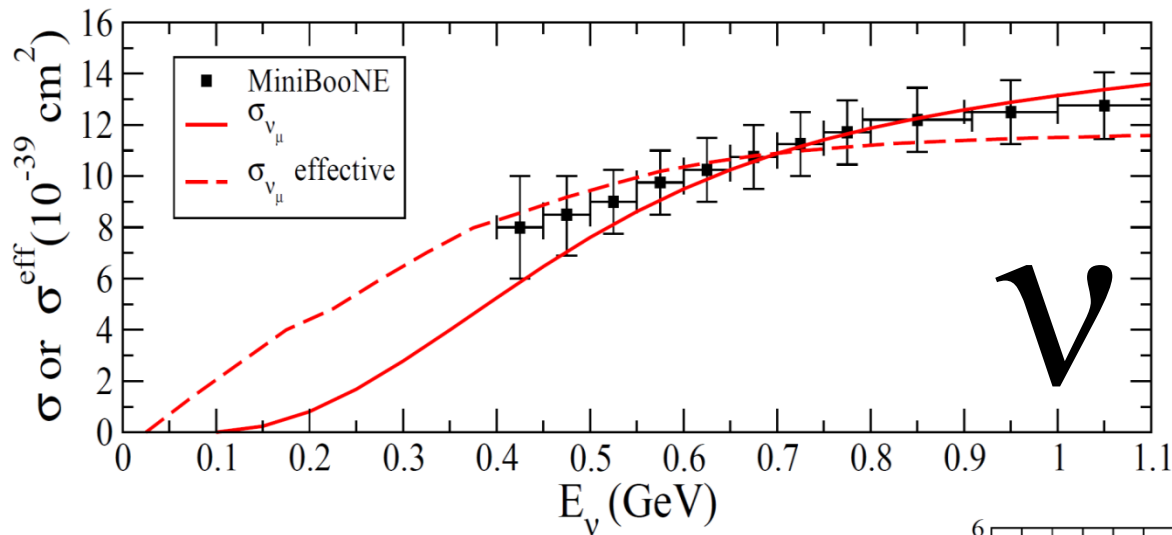
The distributions are not symmetrical around \bar{E}_ν .

The asymmetry favors higher energies at low \bar{E}_ν and smaller energies for large \bar{E}_ν .

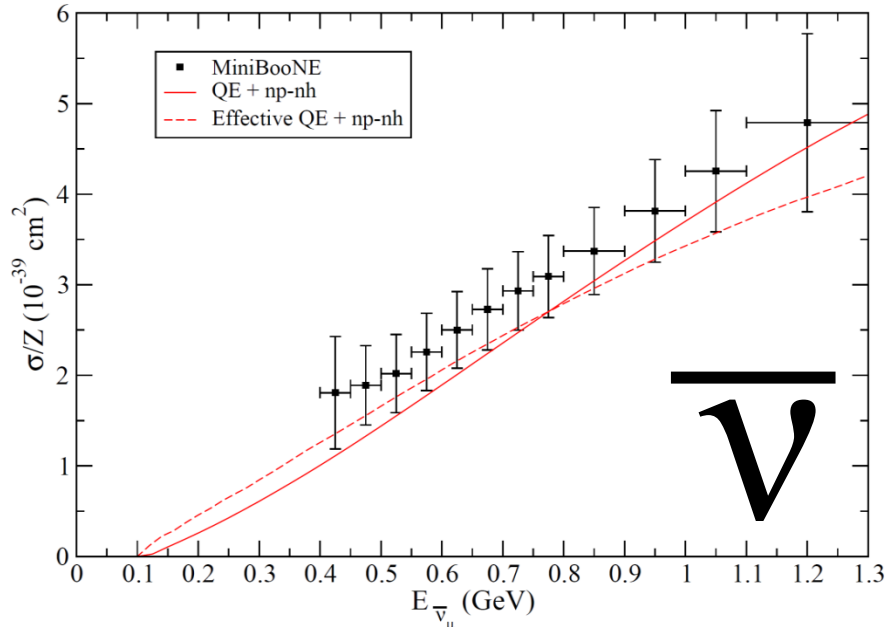
Crucial role of neutrino flux.



CCQE-like cross sections as a function of real (continuous line) and reconstructed (dashed line) neutrino energy



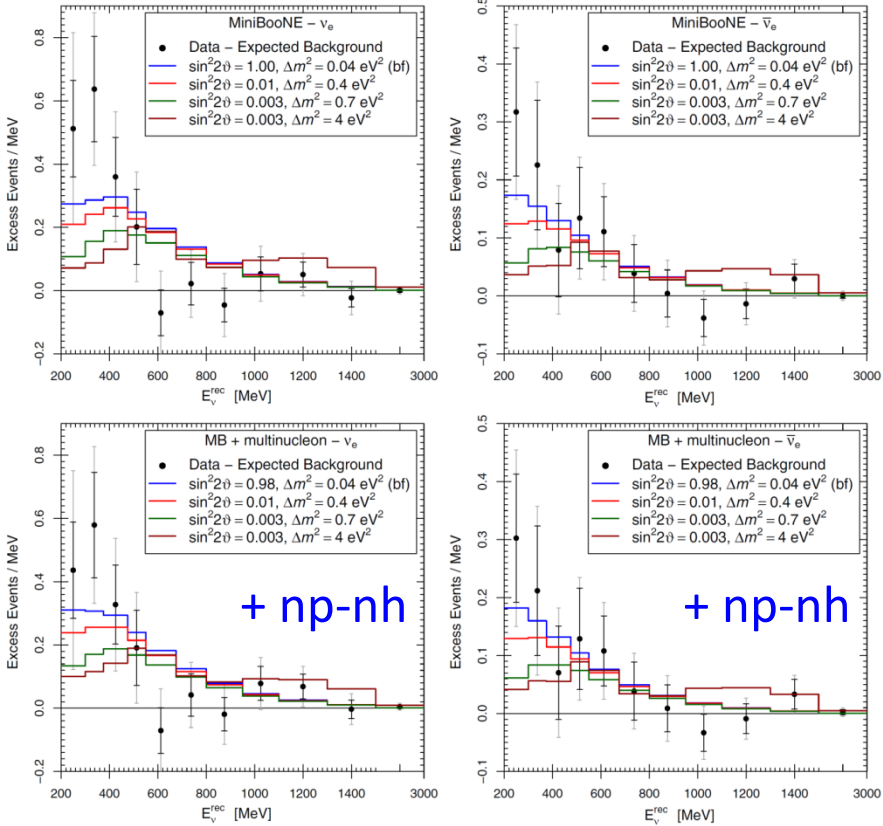
M. Martini, M. Ericson, G. Chanfray, *Phys. Rev. D* 87 013009 (2013)



Martini, Ericson, *Phys. Rev. C* 87 065501 (2013)

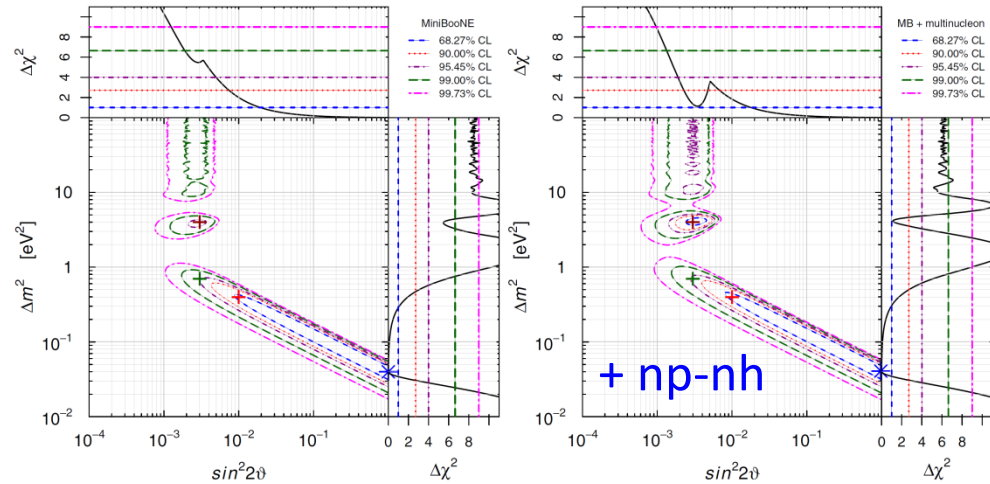
The role of np-nh in the $\nu_\mu \rightarrow \nu_e$ MiniBooNE low-energy anomaly

Quantitative analysis

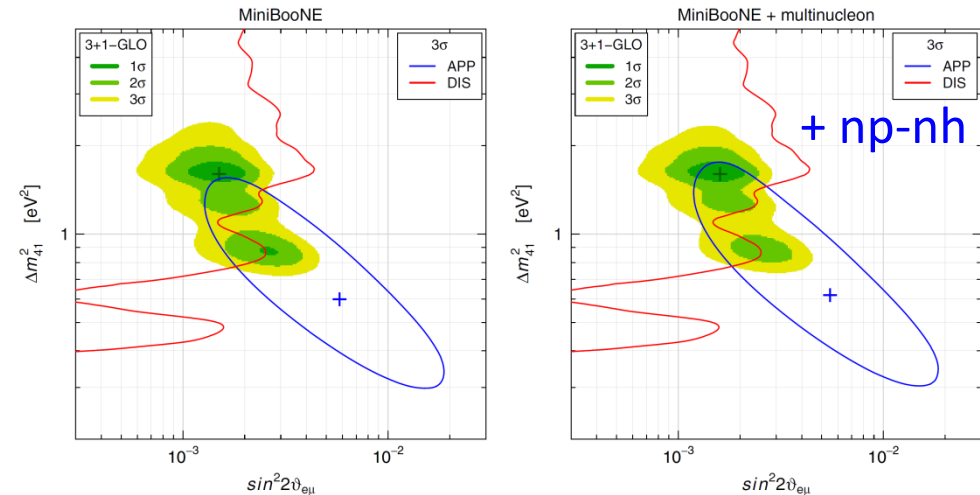


Taking into account np-nh allows a slightly better fit of the MiniBooNE low-energy excess

M.Ericson, M.V.Garzelli, C.Giunti, M.Martini, Phys. Rev. D 93, 073008 (2016)



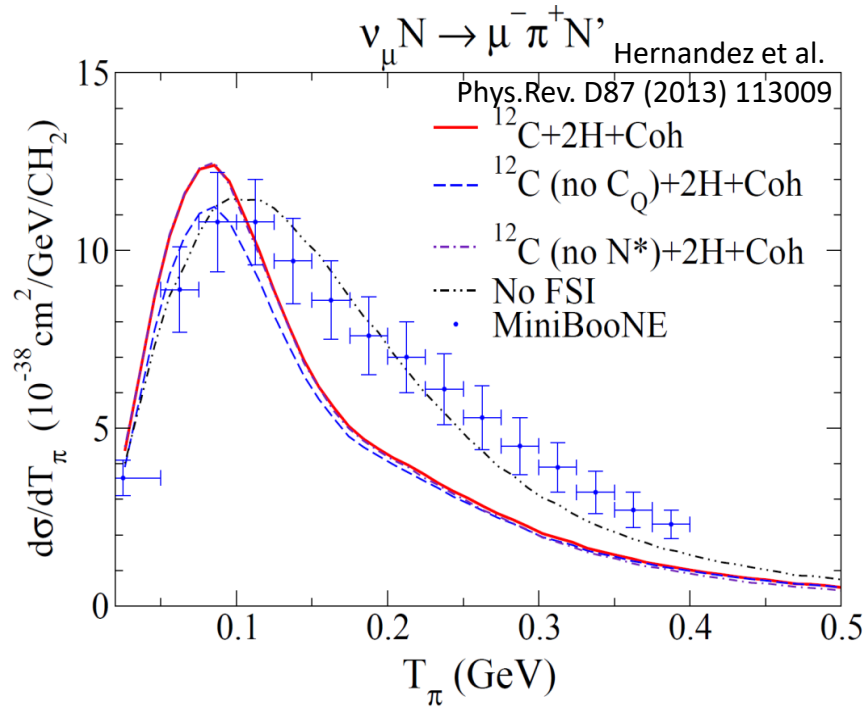
Taking into account np-nh induces a shift of the allowed region towards smaller values of $\sin^2 2\theta$ and larger values of Δm^2 in the framework of 2ν oscillations



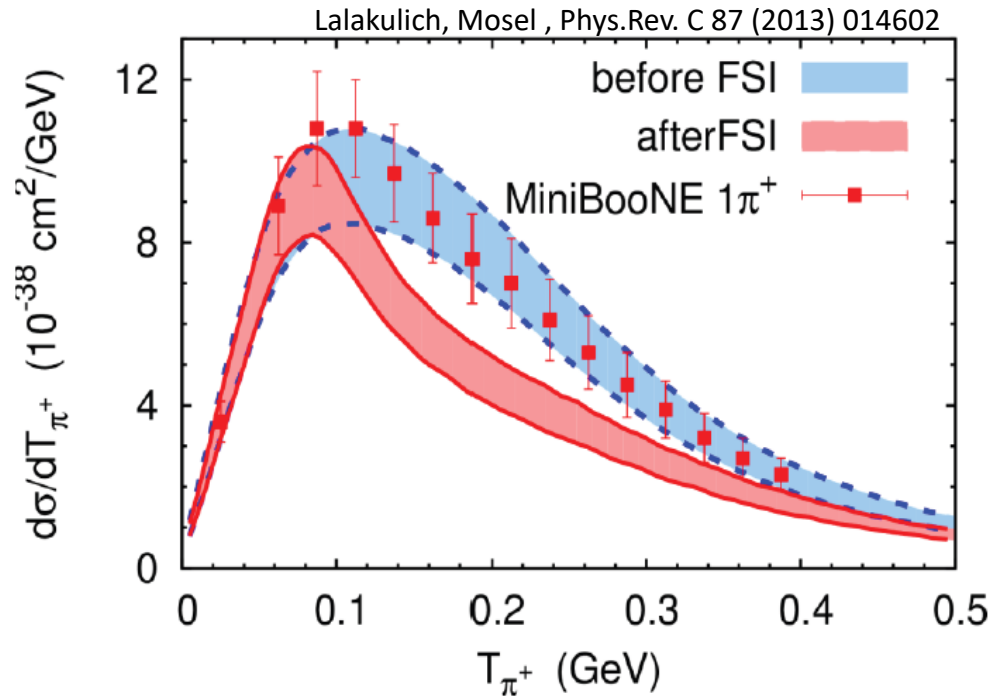
Taking into account np-nh leads to a decrease of the appearance-disappearance tension but not enough to solve the problem in the global fit of short-baseline ν oscillation data

1 Pion production controversy

Best theories (with Δ medium effects and pion rescattering) do not agree with pion KE spectrum



Valencia



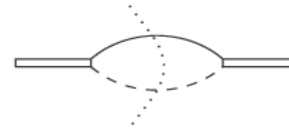
GiBUU

Data prefer calculations with no Final State Interaction for the pion

Delta in the nuclear medium

Mass

$$\tilde{M}_\Delta = M_\Delta + 40(\text{MeV}) \frac{\rho}{\rho_0}$$



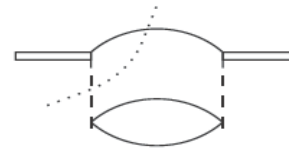
$\Delta \rightarrow \pi N$



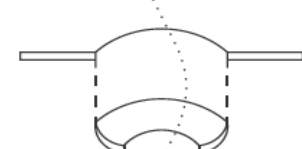
Pauli correction (F_P)

Width

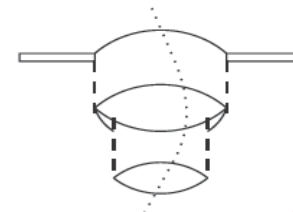
$$\tilde{\Gamma}_\Delta = \Gamma_\Delta F_P - 2\text{Im}(\Sigma_\Delta)$$



Pion distortion (C_Q)



2p-2h



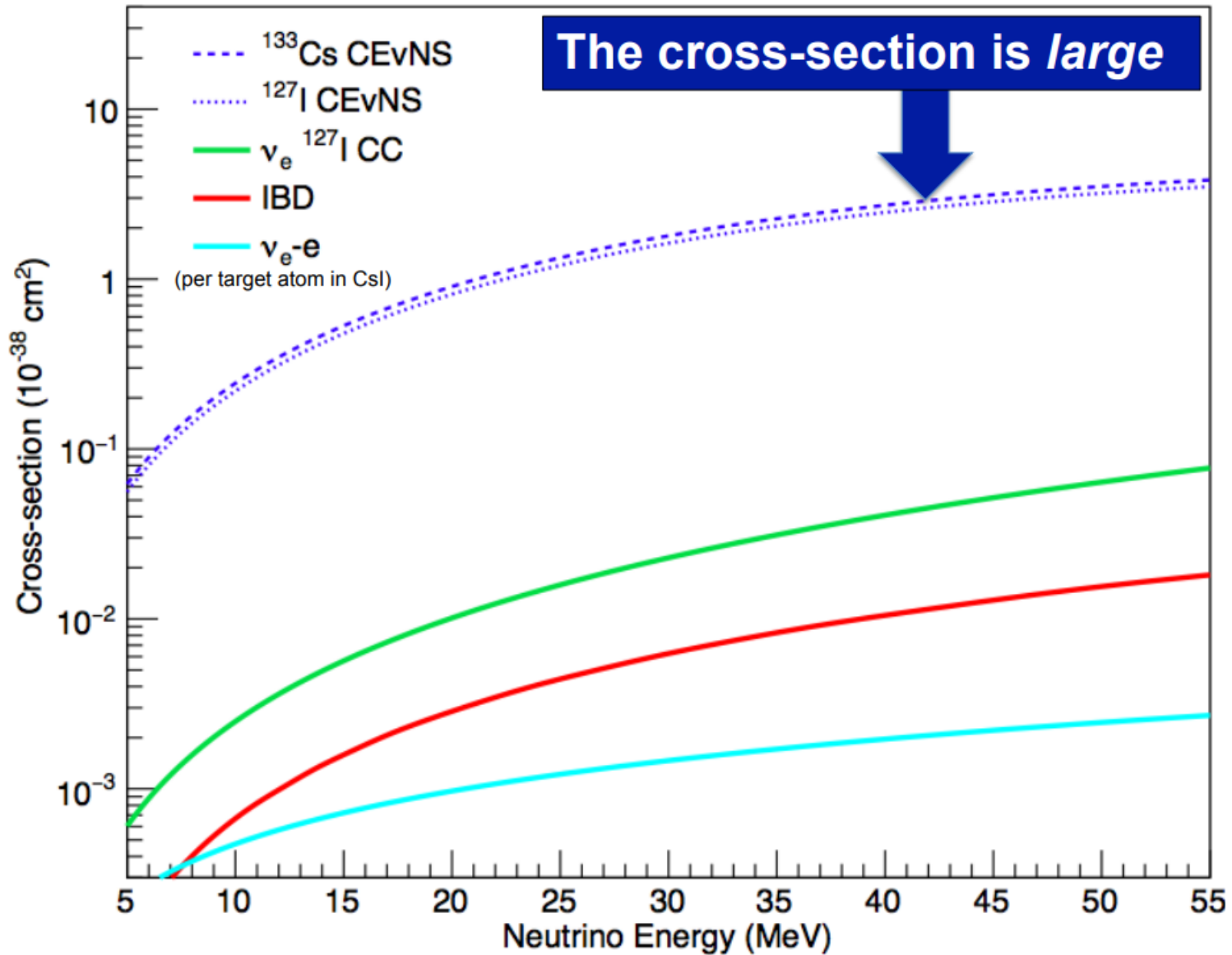
3p-3h

Self energy

$$\text{Im}(\Sigma_\Delta(\omega)) = - \left[C_Q \left(\frac{\rho}{\rho_0} \right)^\alpha + C_{2p2h} \left(\frac{\rho}{\rho_0} \right)^\beta + C_{3p3h} \left(\frac{\rho}{\rho_0} \right)^\gamma \right]$$

E. Oset and L. L. Salcedo, Nucl. Phys. A 468, 631 (1987)

Coherent Elastic neutrino Nucleus Scattering (CEvNS)



CEvNS and Parity Violating Electron Scattering

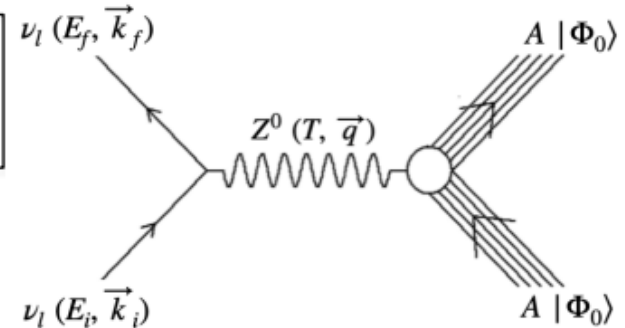
CEvNS cross section:

$$\frac{d\sigma}{dT} = \frac{G_F^2}{\pi} M_A \left[1 - \frac{T}{E_i} - \frac{M_A T}{2E_i^2} \right] \frac{Q_W^2}{4} F_W^2(q)$$

$$Q_W F_W(q) \approx \langle \Phi_0 | \hat{J}_0(q) | \Phi_0 \rangle$$

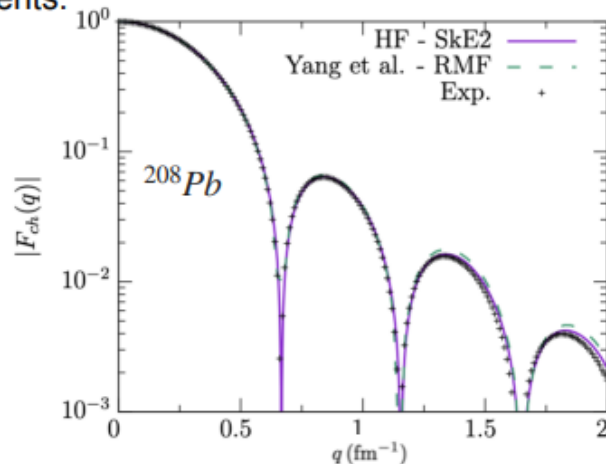
$$\approx (1 - 4 \sin^2 \theta_W) Z F_p(q) - N F_n(q)$$

$$\approx 2\pi \int d^3r \left[(1 - 4 \sin^2 \theta_W) \rho_p(r) - \rho_n(r) \right] j_0(qr)$$



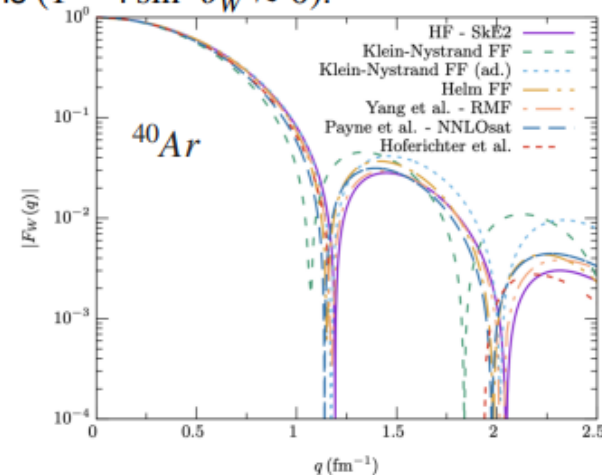
N. Van Dessel, V. Pandey, H. Ray, N. Jachowicz, arXiv:2007.03658 [nucl-th]

Charge density and charge form factor: proton densities and charge form factors are well known through decades of elastic electron scattering experiments.



Data: H. De Vries, et al., *Atom. Data Nucl. Data Tabl.* 36, 495 (1987)

Neutron densities and neutron form factor: neutron densities and form factors are poorly known. Note that CEvNS is primarily sensitive to neutron density distributions ($1 - 4 \sin^2 \theta_W \approx 0$).



Fermilab